

HETEROAROTINOIDS WITH TWO- AND THREE-
ATOM LINKERS AS POTENTIAL
ANTICANCER AGENTS

By

CHAD WAYNE BROWN

Bachelor of Science

University of Central Oklahoma

Edmond, Oklahoma

1996

Submitted to the Faculty of the
Graduate College of the
Oklahoma State University
in partial fulfillment of
the requirements for
the Degree of
DOCTOR OF PHILOSOPHY
August, 2001

COPYRIGHT

By

Chad Wayne Brown

August, 2001

HETEROAROTINONDS WITH TWO- AND THREE-
ATOM LINKERS AS POTENTIAL
ANTICANCER AGENTS

Thesis Approved:

K. D. Berlin

Thesis Advisor

Eldon C. Nelson

Richard A. Bruce

Neil Rendell

Alfred Sarkys
Dean of the Graduate College

ACKNOWLEDGEMENTS

First, I would like to extend my sincere thanks to Dr. Berlin for being a wonderful advisor throughout my studies at Oklahoma State. I thank you Dr. Berlin for your advice, encouragement and support through my time in graduate school. I also thank you for your patience with me as I have learned over these past few years. With your guidance I have certainly become a better scientist and hopefully a better writer.

I also wish to thank Dr. Bunce, Dr. Nelson, and Dr. El Rassi for being members of my advisory committee. I especially thank you Dr. Bunce for the helpful advice on reaction conditions and spectra work, and I express my special thanks to Dr. Nelson and Dr. El Rassi for writing so many letters of recommendation.

My gratitude is also extended to Dr. James Blair and the Department of Biochemistry and Molecular Biology for the Minorities in Biomedical Research Fellowship, which helped fund early work for this thesis. I also gratefully acknowledge the National Institutes of Health for the financial support of this work through the Minorities Access to Research Careers (MARC) Fellowship Program.

Special thanks is extended to my friends and colleagues in the Chemistry Department. My thanks goes out to Joe Klucik and Kevin Tran for their conversation and advice in the lab, and certainly to Dr. Liu for the help and advice as I was getting started on my research project. Tony Tegeler, thanks for the encouragement through the ever-dreaded quantum mechanics as well as the help with so many computer controversies. I wish to

thank Lara, Eric, and especially Darin for the friendship, encouragement, and help through the good and bad times. I also thank all of the secretaries and staff of the Chemistry Department for their help and support.

I would like to express my deepest gratitude and love to all of the members of the Oakwood Church of Christ at Edmond, Oklahoma. Although you may not have known, without your influence I could not have finished graduate school.

I certainly would like to express my deepest and most sincere love and appreciation to my mom and dad, Holly and Glen Brown. Thank you so much for the endless encouragement, support, and patience with me, and I thank you most of all for teaching and showing me God's Word. I love you both dearly.

Finally, I would thank my wonderful and loving wife Heather and our beautiful son Evan. Thank you Heather so much for your patience and love through it all. You have been so kind and supportive through so many trials and difficult times. I love you and respect you more than you could ever know, and without your love and encouragement I certainly could not have completed graduate school.

TABLE OF CONTENTS

Chapter	Page
I. HISTORICAL.....	1
Introduction.....	1
Retinoid Receptors.....	4
Distribution of Retinoid Receptors in Organ Tissues.....	16
Metabolism and Action of Retinoids through Interaction and Activation of Retinoid Receptors.....	17
Classification of Retinoids Based on Their Interaction with Retinoid Receptors.....	27
Measurement of Retinoid Biological Activity.....	36
Toxicity of Retinoids.....	38
Heteroarotinoids and Other Reduced Toxicity Retinoids.....	40
II. RESULTS AND DISCUSSION.....	44
Modified Oxygen and Sulfur Heteroarotinoids.....	44
Synthesis of Key Intermediates.....	46
Synthesis of Heteroarotinoids Possessing Two-Atom Linker Groups.....	51
Synthesis of Heteroarotinoids Possessing Three- or Four-Atom Linker Groups.....	54
Synthesis of Heteroarotinoids Possessing a 4-Hydroxyphenyl Amide Moiety.....	57
NMR Analysis of Select 8-isomer Oxygen Heteroarotinoids.....	62
Biological Activity.....	67
Summary.....	83
Suggestions for Future Work.....	84
III. EXPERIMENTAL SECTION.....	92
General Information.....	92
Methyl 4-{[(2,2,4,4-Tetramethyl-3,4-dihydro-2 <i>H</i> -chromen-6-yl)amino]carbonyl}benzoate (32).....	93
4-{[(2,2,4,4-Tetramethyl-3,4-dihydro-2 <i>H</i> -chromen-6-yl)amino]carbonyl}benzoic acid (33).....	94
Methyl 4-{[(2,2,4,4-Tetramethyl-3,4-dihydro-2 <i>H</i> -chromen-8-yl)amino]carbonyl}benzoate (34).....	95

4-{{(2,2,4,4-Tetramethyl-3,4-dihydro-2 <i>H</i> -chromen-8-yl)amino}- carbonyl}benzoic acid (35).....	96
2,2,4,4-Trimethyl-2 <i>H</i> -chromen-7-yl 4-(methoxycarbonyl)benzoate (36).....	97
[(2-Methoxy-4-nitrophenyl)amino][(2,2,4,4-tetramethylthiochroman-6- yl)amino]methane-1-thione (37).....	98
[(4-Nitrobenzoyl)amino][(2,2,4,4-tetramethylthiochroman-6-yl)amino]- methane-1-thione (38).....	99
Ethyl 4-{{ <i>N</i> -(2,2,4,4-Tetramethylchroman-6-yl)carbamoyl}amino}- benzoate (39).....	99
Ethyl 4-{{ <i>N</i> -(2,2,4,4-Tetramethylchroman-6-yl)thiocarbamoyl}amino}- benzoate (40).....	100
[(4-Nitrophenyl)amino][(2,2,4,4-tetramethylchroman-6-yl)amino]- methane-1-thione (41).....	101
Ethyl 4-{{ <i>N</i> -(2,2,4,4-Tetramethylchroman-8-yl)carbamoyl}amino}- benzoate (42).....	102
Ethyl 4-{{ <i>N</i> -(2,2,4,4-Tetramethylchroman-8-yl)thiocarbamoyl}amino}- benzoate (43).....	103
[(4-Nitrophenyl)amino][(2,2,4,4-tetramethylchroman-8-yl)amino]- methane-1-thione (44).....	104
Ethyl 4-[(2,2,4-Trimethyl-2 <i>H</i> -chromen-7-yloxy)carbonylamino]- benzoate (45).....	104
{4-[[<i>N</i> -(4-Hydroxyphenyl)carbamoyl]phenyl]- <i>N</i> -(2,2,4,4-tetramethyl(3 <i>H</i> - benzo[3,4- <i>e</i>]thian-6-yl))carboxamide (46).....	105
{4-[[<i>N</i> -(4-Hydroxyphenyl)carbamoyl]phenyl]- <i>N</i> -(2,2,4,4-tetramethyl- chroman-6-yl)carboxamide (47).....	106
2,2,4,4-Tetramethyl-6-aminochroman (48a).....	108
2,2,4,4-Tetramethyl-8-aminochroman (48b).....	109
2,2,4-Trimethyl-2 <i>H</i> -1-benzopyran-7-ol (49).....	110
2,2,4,4-Tetramethyl-6-aminothiochroman (50a).....	111
2,2,4,4-Tetramethyl-8-aminothiochroman (50b).....	113
4-(2-Hydroxyphenyl)-2,4-dimethyl-2-pentanol (52).....	114
2,2,4,4-Tetramethylchroman (53).....	115
2,2,4,4-Tetramethyl-6-nitrochroman (54a) and	
2,2,4,4-Tetramethyl-8-nitrochroman (54b).....	116
2,2,4,4-Tetramethyl-6-nitrothiochroman (57a) and	
2,2,4,4-Tetramethyl-8-nitrothiochroman (57b).....	117
<i>Mono</i> -Methyl terephthaloyl chloride (58).....	118
Determination of MICs.....	119

BIBLIOGRAPHY.....	206
-------------------	-----

LIST OF TABLES

Table		Page
1.	Growth Inhibition Against Various Cancerous Cell Types by Heteroarotinoids.....	68
2.	Anti-Bacterial Activity of Heteroarotinoids Against <i>M. bovis</i>	80

LIST OF FIGURES

Figure	Page
1. Schematic representation of mouse Retinoic Acid Receptor (RAR) isoforms.....	6
2. Schematic representation of the P-Box and D-Box of the RAR DNA-binding domain (DBD).....	7
3. The human RAR- γ ligand-binding domain (LBD) crystallographic structure [co-crystallized with <i>t</i> -RA (3)].....	9
4. Schematic representation of mouse Retinoid X Receptor (RXR) isoforms.....	12
5. Schematic relationship between the human retinoid receptors RAR- α RXR- α	12
6. The human RXR- α ligand-binding domain (LBD) crystal structure.....	14
7. Schematic representation of the human Retinoid Orphan Receptor (ROR) isoforms.....	15
8. Schematic representation of dietary retinoid metabolism.....	18
9. Schematic representation of retinoid metabolism within target cells.....	21
10. Schematic representation of dimers and their corresponding response element direct repeats (DRs).....	24
11. Schematic representation of the RXR/RAR heterodimer with DNA and its transcriptional machinery.....	26
12. Schematic representation of minimum energy conformations of <i>t</i> -RA (3) and 9- <i>c</i> -RA (4) within the RAR ligand-binding pockets.....	30
13. Schematic representation of a reporter plasmid for measuring transcriptional activity of a RAR or RXR after activation by a ligand....	37
14. ¹ H NMR spectra sections from spectroscopic experiments on 44	64

LIST OF PLATES

Plate		Page
I.	IR Spectrum of 32	120
II.	¹ H NMR Spectrum of 32	121
III.	¹³ C NMR Spectrum 32	122
IV.	IR Spectrum of 33	123
V.	¹ H NMR Spectrum of 33	124
VI.	¹³ C NMR Spectrum 33	125
VII.	IR Spectrum of 34	126
VIII.	¹ H NMR Spectrum of 34	127
IX.	¹³ C NMR Spectrum 34	128
X.	IR Spectrum of 35	129
XI.	¹ H NMR Spectrum of 35	130
XII.	¹³ C NMR Spectrum 35	131
XIII.	IR Spectrum of 36	132
XIV.	¹ H NMR Spectrum of 36	133
XV.	¹³ C NMR Spectrum 36	134
XVI.	IR Spectrum of 37	135
XVII.	¹ H NMR Spectrum of 37	136
XVIII.	¹³ C NMR Spectrum 37	137
XIX.	IR Spectrum of 38	138

Plate		Page
XX.	¹ H NMR Spectrum of 38	139
XXI.	¹³ C NMR Spectrum 38	140
XXII.	IR Spectrum of 39	141
XXIII.	¹ H NMR Spectrum of 39	142
XXIV.	¹³ C NMR Spectrum of 39	143
XXV.	IR Spectrum of 40	144
XXVI.	¹ H NMR Spectrum of 40	145
XXVII.	¹³ C NMR Spectrum of 40	146
XXVIII.	IR Spectrum of 40	147
XXIX.	¹ H NMR Spectrum of 41	148
XXX.	¹³ C NMR Spectrum of 41	149
XXXI.	IR Spectrum of 42	150
XXXII.	¹ H NMR Spectrum of 42	151
XXXIII.	¹³ C NMR Spectrum of 42	152
XXXIV.	IR Spectrum of 43	153
XXXV.	¹ H NMR Spectrum of 43	154
XXXVI.	¹³ C NMR Spectrum of 43	155
XXXVII.	IR Spectrum of 44	156
XXXVIII.	¹ H NMR Spectrum of 44	157
XXXIX.	¹³ C NMR Spectrum of 44	158
XL.	2D NOESY NMR Spectrum of 44	159
XLI.	2D DQCOSY NMR Spectrum of 44	160

Plate		Page
XLII.	IR Spectrum of 45	161
XLIII.	¹ H NMR Spectrum of 45	162
XLIV.	¹³ C NMR Spectrum of 45	163
XLV.	IR Spectrum of 46	164
XLVI.	¹ H NMR Spectrum of 46	165
XLVII.	¹³ C NMR Spectrum of 46	166
XLVIII.	IR Spectrum of 47	167
XLIX.	¹ H NMR Spectrum of 47	168
L.	¹³ C NMR Spectrum of 47	169
LI.	IR Spectrum of 48a	170
LII.	¹ H NMR Spectrum of 48a	171
LIII.	¹³ C NMR Spectrum of 48a	172
LIV.	IR Spectrum of 48b	173
LV.	¹ H NMR Spectrum of 48b	174
LVI.	¹³ C NMR Spectrum of 48b	175
LVII.	IR Spectrum of 49	176
LVIII.	¹ H NMR Spectrum of 49	177
LIX.	¹³ C NMR Spectrum of 49	178
LX.	IR Spectrum of 50a	179
LXI.	¹ H NMR Spectrum of 50a	180
LXII.	¹³ C NMR Spectrum of 50a	181
LXIII.	IR Spectrum of 50b	182

Plate		Page
LXIV.	^1H NMR Spectrum of 50b	183
LXV.	^{13}C NMR Spectrum of 50b	184
LXVI.	IR Spectrum of 52	185
LXVII.	^1H NMR Spectrum of 52	186
LXVIII.	^{13}C NMR Spectrum of 52	187
LXIX.	IR Spectrum of 53	188
LXX.	^1H NMR Spectrum of 53	189
LXXI.	^{13}C NMR Spectrum of 53	190
LXXII.	IR Spectrum of 54a	191
LXXIII.	^1H NMR Spectrum of 54a	192
LXXIV.	^{13}C NMR Spectrum of 54a	193
LXXV.	IR Spectrum of 54b	194
LXXVI.	^1H NMR Spectrum of 54b	195
LXXVII.	^{13}C NMR Spectrum of 54b	196
LXXVIII.	IR Spectrum of 57a	197
LXXIX.	^1H NMR Spectrum of 57a	198
LXXX.	^{13}C NMR Spectrum of 57a	199
LXXXI.	IR Spectrum of 57b	200
LXXXII.	^1H NMR Spectrum of 57b	201
LXXXIII.	^{13}C NMR Spectrum of 57b	202
LXXXIV.	IR Spectrum of 58	203
LXXXV.	^1H NMR Spectrum of 58	204

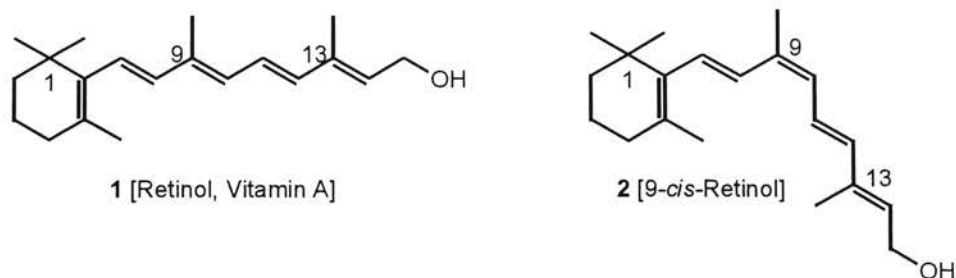
Plate	Page
LXXXVI. ^{13}C NMR Spectrum of 58	205

CHAPTER I

HISTORICAL

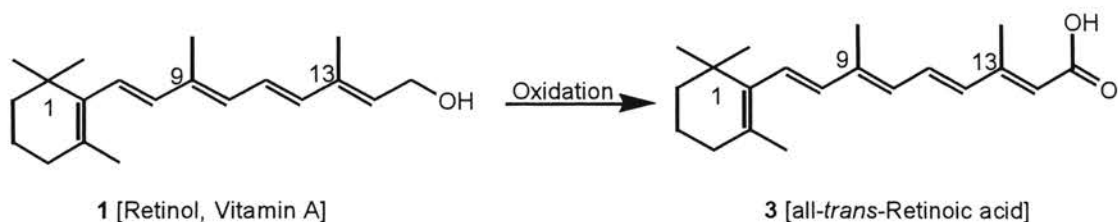
Introduction

Retinoids can be described as a group of compounds, whether natural or synthetic, that are structurally similar to retinol (**1**, vitamin A) or 9-*cis*-retinol (**2**) and that “can elicit

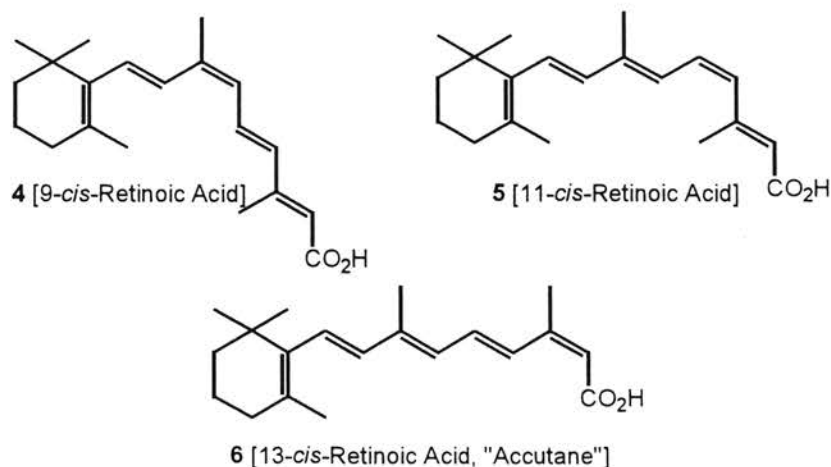


specific biological responses by binding to and activating a specific receptor or set of receptors”.¹ Many retinoids have been produced and studied extensively for various therapeutic uses.¹

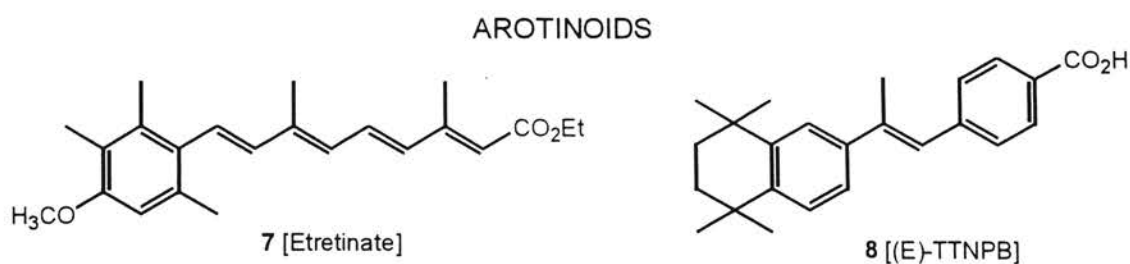
Vitamin A (**1**) deficiency has been known to cause epithelial defects since the early 1800’s.² However, in the 1960’s Saffiotti and co-workers, as well as Chu and Malmgren, noted that vitamin A (**1**) had an inhibitory effect on the development of various carcinomas.³ Observations such as these have subsequently led to an explosion of research efforts. It has been found that all-*trans*-retinoic acid (**3**, *t*-RA), an oxidized



vitamin A, was probably responsible for much of the anti-cancer activity. Since that time, the term “retinoid” has been used to describe any analog of vitamin A regardless of the observed biological activity. All-*trans*-retinoic acid (**3**, *t*-RA), 9-*cis*-retinoic acid (**4**, 9-*c*-RA), 11-*cis*-retinoic acid (**5**, 11-*c*-RA), and 13-*cis*-retinoic acid (**6**, 13-*c*-RA) are some examples of naturally occurring retinoids.¹



Intense studies of the natural retinoids spawned molecular modification thereof, which has ultimately led to the birth of a wide variety of synthetic retinoids including arotinoids and heteroarotinoids (for more on heteroarotinoids, see the section on Heteroarotinoids and Other Reduced Toxicity Retinoids). Arotinoids, such as Etretnate (**7**)⁴ and TTNPB (**8**),⁵ received the name ‘arotinoids’ because they have at least one aryl group in the basic structure. Several other types of retinoids are known.¹



Early examples of synthetic retinoids, such as **7** and **8**, have been the progenitors of a very large number of molecules that are now being synthesized and screened for potential pharmaceutical use. Natural and some synthetic retinoids are both powerful regulators of cell growth, differentiation, and homeostasis (relative state of equilibrium) in embryos and adult animals of several vertebrate species.⁶ Epidemiologic studies have suggested an inverse correlation between the development of cancer and dietary consumption of vitamin A (**1**) or beta-carotene.^{7,8} Histologic similarities between the epithelium of vitamin A-deficient organs and neoplastic tissue was first noted by Wolbach and Howe.⁷ In 1955, Lasnitski demonstrated that a pre-malignant phenotype of mouse prostate cancer that had had been induced with the carcinogen 3-methylcholanthrene could be altered by retinoid treatment.⁸ It was shown that in prostate cell cultures retinoid treatment caused the disappearance of atypical epithelial cells that had been induced by the carcinogen, and that the atypical cells were replaced by cells with a more normal morphology. Such epidemiologic studies and animal experiments have thus prompted researchers to test the efficacy of retinoids in the prevention and treatment of cancer in various organ tissues, including skin, stomach, lung, and breast, among several others.⁹

Retinoids have also been employed clinically for the treatment of various skin disorders such as acne, photo-damaged skin, hyperpigmentation, rosacea, actinic keratoses, wrinkles, superficial scarring, and epidermal atrophy.¹⁰⁻¹² In addition, retinoids have found use in the treatment of acute promyelocytic leukemia,^{13,14} in the management of central nervous system tumors,¹⁵ and in the treatment of AIDS-related cutaneous Kaposi's sarcoma.¹⁶ Furthermore, retinoids may find use in proper immune system functioning,¹⁷ as anti-inflammatory agents for dealing with rheumatoid arthritis,¹⁸

and/or as an improved treatment for emphysema.¹⁹ In light of these studies and the ability of retinoids to regulate proliferation and differentiation in both normal and malignant cells *in vitro* and *in vivo*, future investigations and therapeutic applications of retinoids promises to be significant.

Retinoid Receptors

The activity of retinoids is thought to be due, at least in part, to the interaction with and activation of a group of nuclear receptors termed “retinoid receptors”.²⁰ Retinoid receptors were identified as being in cell nuclei in 1987,²¹ and there are now known two distinct subfamilies of retinoid receptors, namely Retinoic Acid Receptors²² (RARs—RAR- α , RAR- β , and RAR- γ) and Retinoid X Receptors²³ (RXRs—RXR- α , RXR- β , and RXR- γ), totaling six retinoid receptors. These receptors act as ligand-inducible, transcriptional regulators that transduce the effects of retinoids on cell growth, differentiation, and homeostasis during embryonic development and adult life.²¹ The discovery of the retinoid receptors has thus allowed for an intense investigation to elucidate their structure. Perhaps more importantly, it has provided an essential means that can provide insight into the complex molecular mechanisms by which retinoids influence developmental control of genes and cell differentiation.

Retinoic Acid Receptors (RARs). Chimeric-screening assays of orphan receptors allowed the functional identification of the first retinoic acid receptor, RAR- α , which is a polypeptide composed of 462 amino acid residues.^{22d} In 1987, Petkovich and co-workers,^{21a} as well as Giguere and co-workers,^{22d} independently isolated a human orphan receptor complementary DNA (cDNA) and were able to show that it encoded the first

known retinoic acid-activated transcription factor. This human retinoic acid (RA) receptor was called RAR- α , and its discovery was pivotal to understanding the action of *t*-RA (3) because it simultaneously provided a mechanistic pathway for the activity of *t*-RA (3), as well as a potential way to identify a set of downstream developmental control genes.

The discoveries of the several loci present in the human genome related to RAR- α , along with the discovery of a family of RAR- α -related genes, provided evidence that other subtypes of the RAR might exist.²⁴ Subsequently, in 1988 a second receptor was found which responded to retinoic acid, and it was called RAR- β .²⁵ Furthermore, in 1989, Chambon and co-workers²⁶ reported the discovery of the third subtype of the RAR and named it RAR- γ . The genes encoding these three highly related RARs map on distinct chromosomes 17q21.1, 3p24, and 12q13 in the human genome.²⁷ Each RAR gene generates multiple isoforms of the receptors, which differ from each other in the number of amino acids that constitute their amino-terminal region (Figure 1).²⁸ Thus, RAR- α has isoforms – RAR- α_1 and RAR- α_2 ,^{28b} RAR- β has four isoforms – RAR- β_1 , RAR- β_2 , RAR- β_3 , and RAR- β_4 ,^{28c} and RAR- γ has two isoforms – RAR- γ_1 and RAR- γ_2 .^{28a} Each isoform of the RARs has a modular structure which can be divided into five distinct domains (A/B-F):

- 1) (domain A/B) – ligand-independent activation function (AF-1),
- 2) (domain C) DNA-Binding Domain (DBD),
- 3) (domain D) hinge,
- 4) (domain E) ligand-binding domain (LBD) which contains the ligand-dependent activation function (AF-2), and

5) (domain F) C-terminus (functionally undefined).²⁹

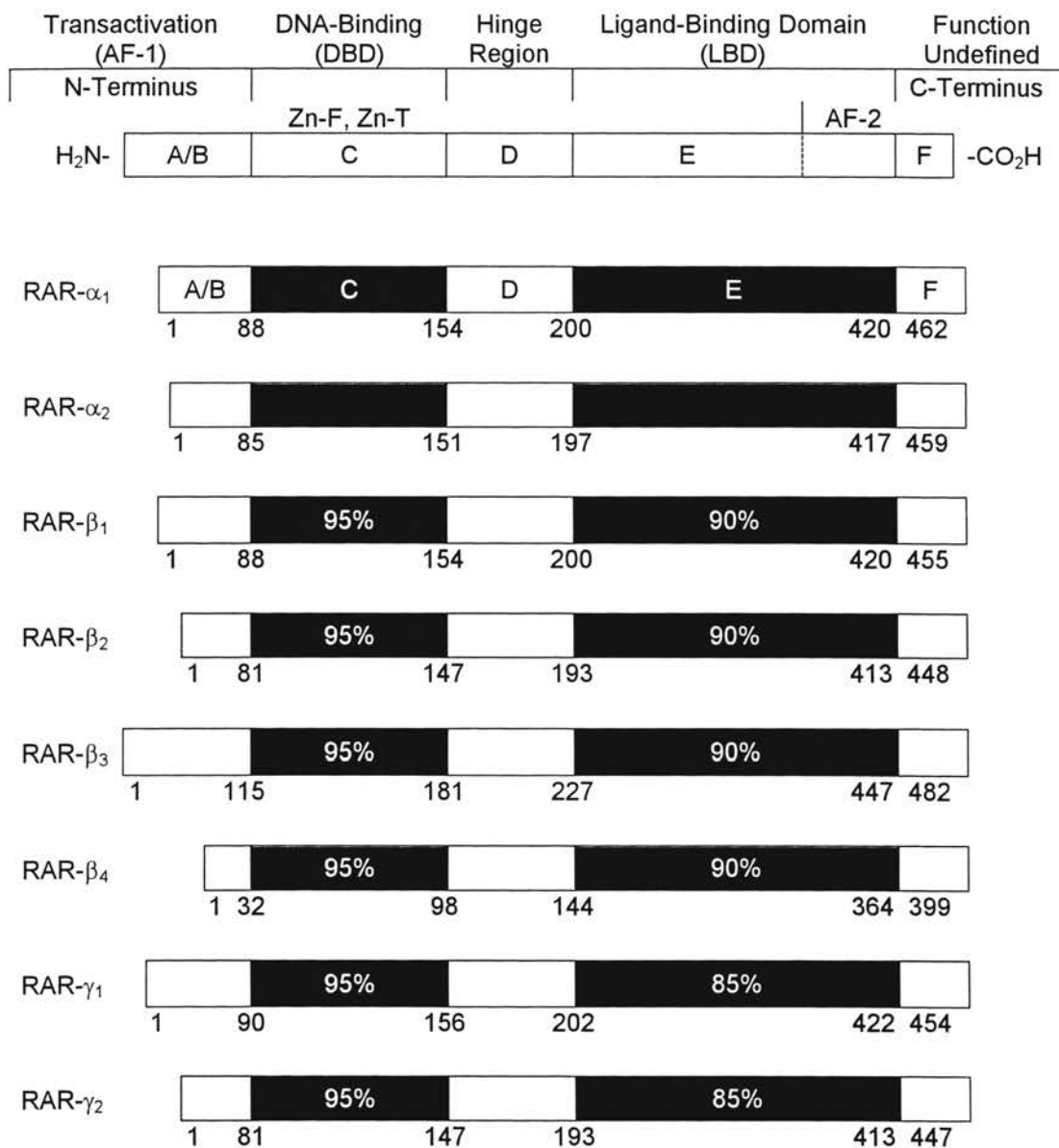


Figure 1. Schematic representation of mouse Retinoic Acid Receptor (RAR) isoforms. The DNA-binding domains (DBD, domain C) and the ligand-binding domains (LBD, domain E) are shown by shaded boxes to denote the highest conserved regions. The percentages within the shaded boxes specify the percent amino acid identity as compared to RAR-α. The numbers below the diagrams indicate domain length as well as the total length of the receptor in terms of amino acid residues.²⁸

The N-terminal A/B domain is rich in proline, serine, and threonine (non-acidic amino acid residues) and is important for transcriptional regulation.³⁰ The number and sequence of the amino acid residues within the A/B domain vary in each RAR isoform, and the A/B domain is one of the lowest conserved regions of the receptor (Figure 1).²⁹

Domain C of the RARs is the DNA-binding region, which is responsible for specific recognition of a DNA sequence called the hormone response element [HRE, or for retinoic acid-response element (RARE)].³¹ This domain is comprised of two features called the ‘zinc finger’³² and the ‘zinc twist’ (Figure 2).³³ The P-Box (‘zinc finger’) is

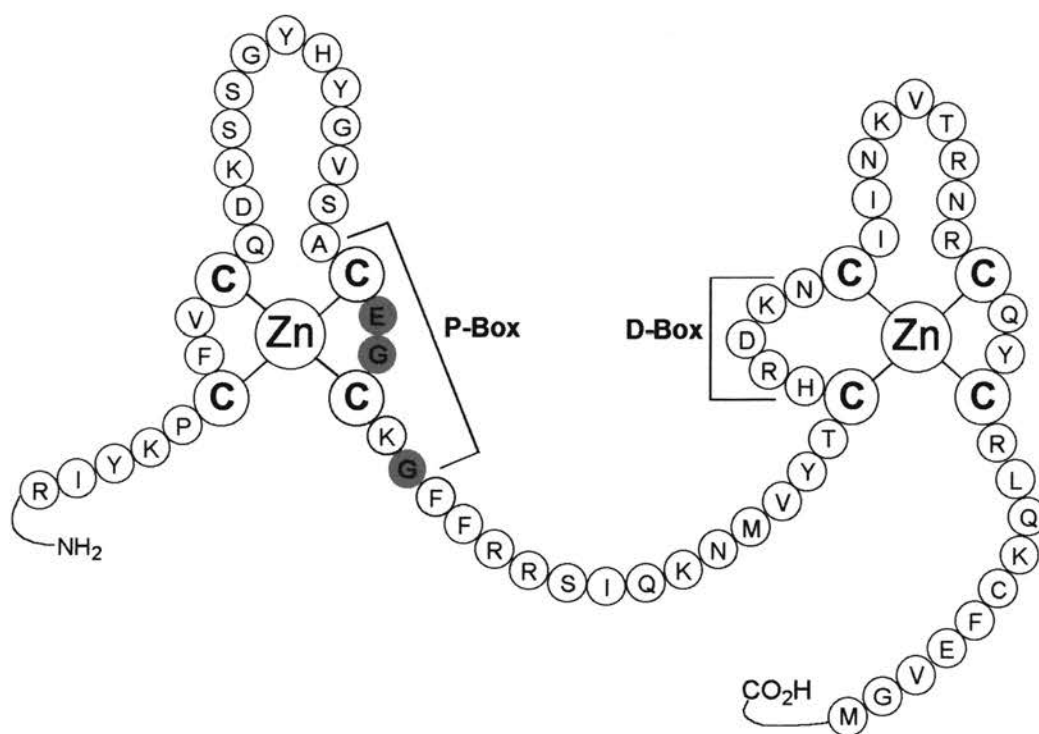


Figure 2. Schematic representation of the P-Box and D-Box of the RAR DNA-binding domain (DBD). The red-colored circles represent the amino acid residues that are thought to be responsible for specificity of binding to DNA hormone response element RARE.³³

closest to the N-terminus and contains three amino acid residues, which are different in all isoforms of the RARs, and are responsible for the recognition and specificity of

binding the RAR to the RARE³⁴ by making contact with DNA through insertion within the major groove of the DNA double helix.³⁵ The ‘zinc twist’ (D-Box) is responsible for the formation of homo- or heterodimers with other nuclear receptors³⁶ and determines the number of nucleotides which are allowed to separate the two half-sites of RARE.^{31b,37} These fascinating characteristics of the RARs and other DNA-binding receptors are due to the interaction of two zinc ions with eight cysteine residues.^{32,33b} The coordination of each zinc with a separate set of four highly conserved cysteine residues^{32,33b} forms such ‘zinc clusters’ as illustrated in Figure 2. Domain D has been termed a hinge and contains a nuclear translocation signal.^{29,38}

The E domain is the ligand binding domain (LBD) which contains an overlapping functional domain called the ligand-dependent transactivation function (AF-2).^{21,29} The LBD of the RARs resides at the C-terminus, spans approximately 220 amino acid residues,²⁹ and fulfills multiple functions,³⁹ one of which is to interact with retinoids, such as endogenous ligands *t*-RA (**3**) or 9-*c*-RA (**4**). The latter “activates” the receptor (for more information about the interaction of retinoids with the LBD and the resulting activity, see the section on Metabolism and Action of Retinoids).

The human RAR- γ_2 holo-LBD (receptor with ligand bound) crystal structure has been elucidated by Renaud and co-workers (Figure 3).⁴⁰ The LBD of RAR- γ is made up of 220 amino acid residues, which comprise nine α -helical structures in helices 1-12 (H1 to H12), two omega (Ω) loops, and two beta (β) sheets (B1 and B2).⁴⁰ This numbering system was continued from the crystal structure of apo-RXR- α (receptor without ligand bound)⁴¹ which was reported shortly prior to that of RAR- γ . The α -helices were numbered by their resemblance in comparison to RXR- α , but not sequentially. For

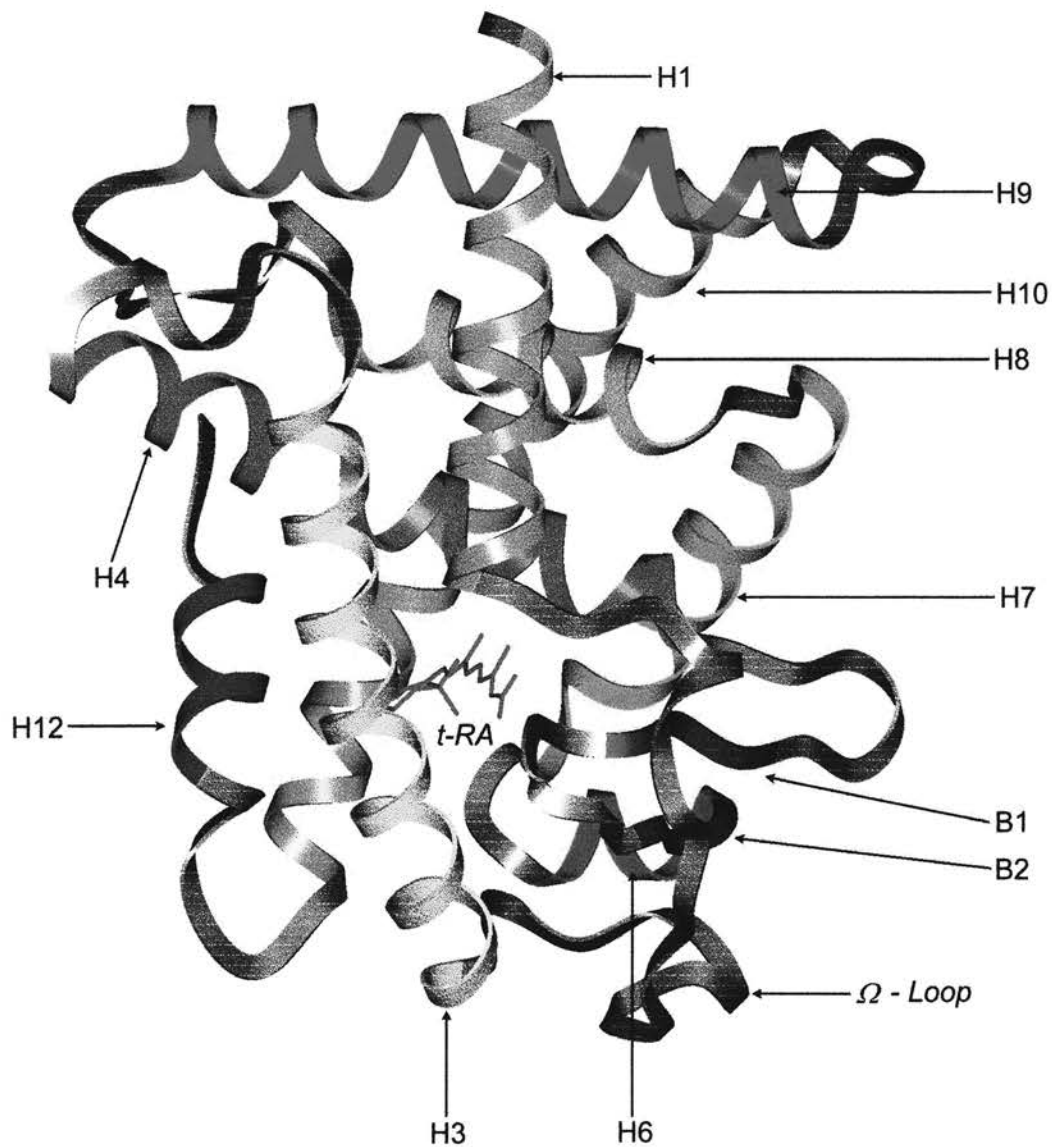


Figure 3. The human RAR- γ ligand-binding domain (LBD) crystallographic structure [co-crystallized with *t*-RA (**3**)].⁴⁰

instance, helices H2, H5, and H11 are omitted from the holo-LBD of the RAR- γ crystal structure because those helices do not exist within the structure after the receptor is bound to a ligand.⁴⁰ The nine α -helices are organized in a three-layer structure with H4, H5, H6, H8, and H9 sandwiched between H1 and H3 on one side and H7, H10, and H11 on

the other.⁴⁰ Two topologically conserved β -strands (B1 and B2) form a β -turn inserted between loop 1-3 (connecting H1 to H3) and H3.⁴⁰

Twenty four amino acid residues of the LBD make up what is referred to as the ligand-binding pocket (LBP).⁴⁰ These residues include Phe201, Thr227, Phe230, Ser231, Leu233, Ala234, Lys236, Cys237, Leu271, Met272, Arg274, Ile275, Arg278, Phe288, Ser289, Gly303, Phe304, Ala394, Arg396, Ala397, Leu400, Met408, Ile412, and Met415.⁴⁰ A sequence alignment of RAR- α , RAR- β , and RAR- γ was also done by Renaud and co-workers⁴⁰ which, interestingly, showed that only three residues in the LBPs were variable. Variations were A234 for RAR- γ (S232 in RAR- α and A225 in RAR- β), M272 in RAR- γ (I270 in RAR- α and I263 in RAR- β), and A397 in RAR- γ (V395 in RAR- α and V388 in RAR- β). These different residues are certainly candidates that could potentially provide receptor isoform selectivity (for more information on receptor selectivity see the section on Toxicity of Retinoids).

The LBD not only contains the essential LBP, but it also contains the functionally important ligand-dependent transactivation function (AF-2, Figure 1) which is located at the C-terminal in α -helix 12 (H12)⁴² of the ligand-binding domain. In addition, the LBD has a structural theme spanned by the amino terminal of H7, the amino terminal of H10, the loop between H9 and H10, and the carboxyl terminal of H9 which provides a dimerization surface for the formation of homo- or heterodimers with other nuclear receptors including the vitamin D₃ receptor, the thyroid hormone receptor, the RXRs, and others.⁴³

Retinoid X Receptors (RXRs). Through further screening assays of orphan receptors, another class of retinoid-responsive transcription factors was discovered, and it

was referred to as retinoid X receptors (RXRs).⁴⁴ The family of RXRs consists of three subtypes, RXR- α , RXR- β , and RXR- γ , as does the RAR group, and the RXRs are approximately 46 kDa in size and display the same structural organization as found in the RARs, that is, the former have a domain comprised of domains A/B-F.⁴⁵ The RXRs even have a 'zinc finger, zinc twist' feature as do the RARs.^{33a} However, a striking observation that came from the cloning of RXR is the apparent dissimilarity of its sequence to that of the RARs.⁴⁴ In fact, RAR is more similar to the thyroid hormone receptor than it is to RXR.^{21b}

As is also true with the RAR family, the RXR proteins are closely related to each other in both their DNA-binding and ligand-binding domains and are encoded by separate genes at distinct chromosomal loci.^{21b,46} The RXR- α , RXR- β , and RXR- γ proteins map on chromosomes 9q34.3, 6p21.3, and 1q22-23, respectively, in the human genome,^{21b,47} and have sequence alignment homologies for DBDs of 92% and 95%, and LBDs of 89% and 86% for RXR- β and RXR- γ , respectively, as compared to RXR- α (Figure 4).^{46,48} In addition, each subtype of the RXR family has two isoforms, namely RXR- α_1 , RXR- α_2 , RXR- β_1 , RXR- β_2 , and RXR- γ_1 and RXR- γ_2 .⁴⁸

Because of the low degree of homology between RARs and RXRs over their entire protein sequences, 61% in the DBDs (the highest similarity) of RAR- α and RXR- α and 27% in their LBDs (Figure 5),⁴⁶ activation of the RXR family of receptors by *t*-RA (**3**) has not been observed.⁴⁹ However, it was discovered that 9-*c*-RA (**4**) was a natural ligand for the RXRs⁴⁹ and that 9-*c*-RA (**4**) could also activate the RARs with potencies comparable to that of *t*-RA (**3**).⁵⁰ Thus, 9-*c*-RA (**4**) has been termed a *pan* agonist, because of this ability to bind to more than one type of receptor subtype.⁴⁶

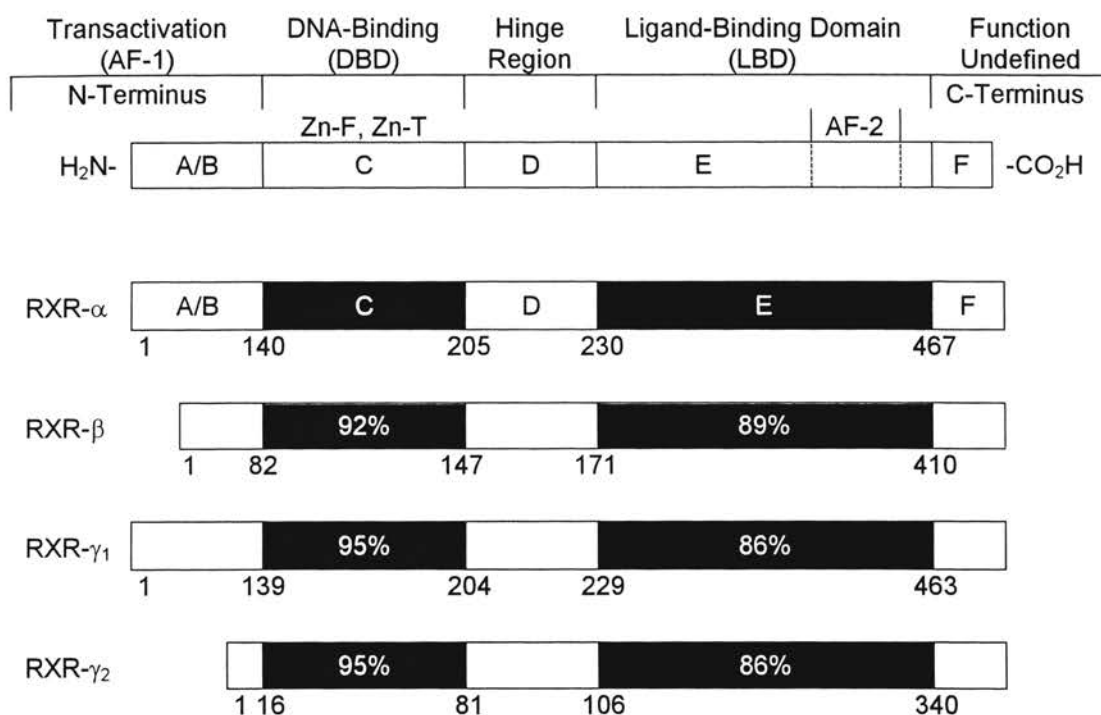


Figure 4. Schematic representation of mouse Retinoic X Receptor (RXR) isoforms. The DNA-binding domains (DBD, domain C) and the ligand-binding domains (LBD, domain E) are shown by shaded boxes to denote the highest conserved regions. The percentages within the shaded boxes specify the percent amino acid identity as compared to RXR-α. The numbers below the diagrams indicate domain length in terms of amino acid residues.⁴⁶

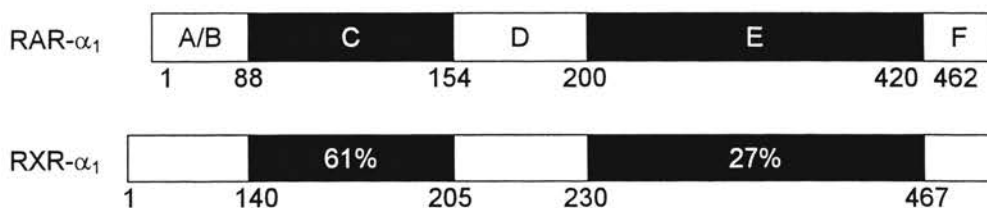


Figure 5. Schematic relationship between the human retinoid receptors RAR-α and RXR-α. The DNA-binding domains (DBD, domain C) and the ligand-binding domains (LBD, domain E) are shown by shaded boxes to denote the highest conserved regions. The percentages within the shaded boxes specify the percent amino acid identity as compared to RAR-α. The numbers below the diagrams indicate domain length in terms of amino acid residues.⁴⁶

The crystallographic structure of the human apo-ligand-binding domain (apo-LBD, no ligand bound) of RXR- α has been reported by Bourget and co-workers^{41a} and is shown in Figure 6. The RXR- α LBD has been described as an antiparallel α -helical sandwich with dimensions of 38 x 74 x 25 Å organized in a three-layered structure.^{41a} Twelve α -helices account for 65 % of the domain, with helices H4-H5, H8, H9, H11, and the N-terminal of H12 sandwiched between H1, H2 and H3 on one side and H6, H7 and H10 on the other.^{40,41a} Two short β -strands (B1 and B2) form a β -hairpin and constitute the only β -structure of the domain. The domain of RXR- α also has a dimerization surface comprised of helices H10, H5, and H8, the C-terminal activation function AF-2 sequence (450-FLMEMLE-458), and two proposed ligand binding pocket locations.^{40,41a} More recently, Egea and co-workers^{41b} reported the crystal structure of the human RXR- α ligand-binding domain (holo-LBD) bound to its endogenous ligand 9-*c*-RA (**4**). It was reported that 9-*c*-RA (**4**) was buried in an essentially hydrophobic pocket formed by residues located on helices H3, H5, H7, H11, and the β -turn (see Figure 6). These residues are conserved in all three RXR subtypes, suggesting difficulty in finding RXR- α , RXR- β , or RXR- γ subtype selective ligands.^{41b}

Retinoid Orphan Receptors. When ligands for receptor-like proteins are initially unknown, the receptors are referred to as “orphan” receptors. Studies of orphan receptors led to the discovery of the two retinoid receptor families RAR and RXR.^{21b} A novel family of steroid hormone nuclear receptor superfamily related to the retinoic acid receptors have been identified by Giguere and co-workers.⁵¹ This family has been termed the ROR- α s. Three isoforms, namely ROR- α_1 , ROR- α_2 , and ROR- α_3 have been

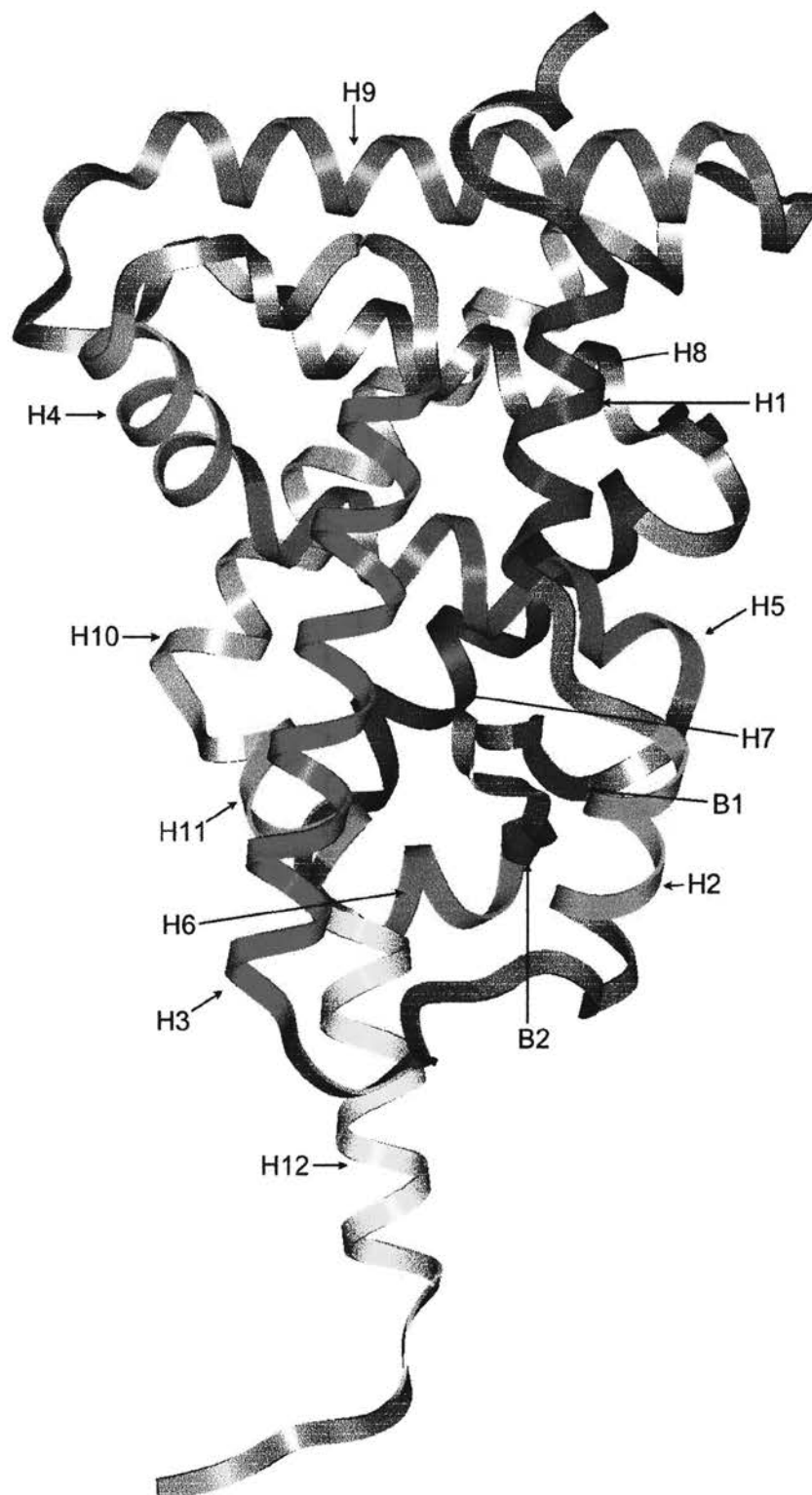


Figure 6. The human RXR- α ligand-binding domain (LBD) crystal structure.^{41a}

reported as sharing common DNA- and putative ligand-binding domains, but are characterized by distinct amino-terminal domains (Figure 7).⁵¹ Distinct DNA-binding properties were observed for each of these isoforms, and these properties were governed by the specific amino-terminal domains.⁵¹ It is believed that the amino-terminal domain and the 'zinc finger' region in the DBD work concurrently to impart high affinity and

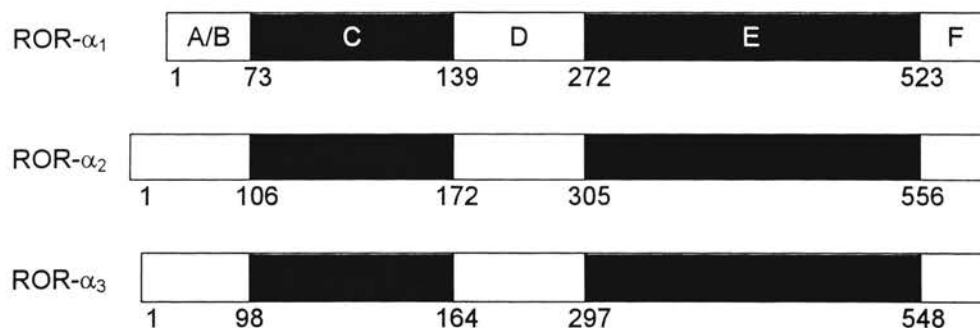


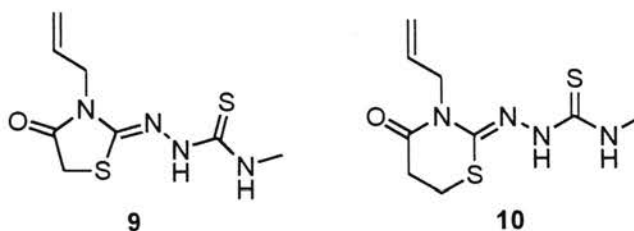
Figure 7. Schematic representation of the human Retinoid Orphan Receptor (ROR) isoforms. The DNA-binding domains (DBD, domain C) and the ligand-binding domains (LBD, domain E) are shown by shaded boxes to denote the highest conserved regions. The numbers below the diagrams indicate domain length in terms of amino acid residues.⁵¹

specific DNA-binding characteristics.⁵¹ Both ROR- α_1 and ROR- α_2 activate transcription and bind to DNA as monomers to the ROR hormone response elements (ROREs).⁵¹

Melatonin has been suggested as a natural ligand for the RORs because it is bound to and activates the RORs via concentrations in the low nanomolar range.⁵² Furthermore, melatonin has been shown to exhibit anti-stress and anti-aging properties, and influences various immunological and endocrinological functions.^{52b} The RORs have also been implicated in cholesterol homeostasis⁵³ and bone metabolism.⁵⁴

More recently, another retinoid-related orphan receptor has been reported (ROR- γ), and it has been suggested as being essential for lymphoid organogenesis and controlling

apoptosis (programmed cell death) during thymopoiesis.⁵⁵ In addition, a retinoid-related orphan receptor called RZR, whose name was given arbitrarily by its discoverers Carlberg and co-workers,⁵⁶ has been identified. The RZR exhibits a highly restricted brain-specific expression pattern,⁵⁷ and the exact role and function of the RZR has not been determined.⁵⁶ Due to a high expression of RZR in the pineal, thalamus, and hypothalamus glands, it has been suggested that RZR is important for physiological and developmental regulation of the central nervous system and for possible regulation of the circadian rhythm.^{52b} No natural ligand for RZR has yet been identified, but the synthetic thiazolidine diones **11** and **12** have proven to be RZR specific ligands and have shown potent antiarthritic activity.⁵⁸



Distribution of Retinoid Receptors in Organ Tissues

The vast utility of retinoids in biological activities is partially due to the diverse expression of these RAR and RXR genes. The RAR- α isoform is found in most tissues,²¹ but has a major concentration in brain tissue, primarily in the hippocampus and cerebellum, indicating a possible importance in the development and maintenance of the central nervous system.²⁴ RAR- β expression has been found predominantly in the kidney, spinal cord, prostate, pituitary gland, and adrenal gland,^{46,52b} but small concentrations of RAR- β have been detected in the liver, spleen, brain, and genital tract.^{52b} The RAR- γ isoform has been found in high concentration in skin and lung

tissue^{46,59} and in modest concentration in cardiovascular tissue.⁶⁰ As a whole, the RXRs are widely expressed in the adult organism.⁴⁸ RXR- α is abundant in the liver, kidney, spleen, and a variety of visceral tissues.⁴⁸ RXR- β , like RAR- α , is expressed to some extent in nearly all tissues.^{1,25,46} RXR- γ has a more restricted expression, being present most abundantly in muscle and brain tissue.²¹ However, RXR- γ has been found to be co-expressed with RAR- β in the pituitary gland,^{21,46} suggesting a potential role for retinoids in the regulatory cascade associated with hypophyseal differentiation.²¹

Metabolism and Action of Retinoids through Interaction and Activation of Retinoid Receptors

Vitamin A (Retinol, **1**) has no known biological activity, but rather serves as a source substrate for the biosynthesis of functional retinoids.⁶¹ Metabolism of β -carotene (**11**, Figure 8) or hydrolysis of retinyl esters obtained through dietary sources (both occur in the small intestine)⁶¹ provides endogenous retinol which is then shuffled through the living system by various binding proteins and enzymatic conversions to target cells, where it is ultimately oxidized to retinoic acid and other functional metabolites that are utilized and elicit various useful biological responses.

This metabolic pathway (Figure 8) begins with the central cleavage of β -carotene (occurs in the small intestine) which produces retinaldehyde (**12**, or simply retinal, Figure 8) that is then bound by cellular retinol-binding protein (CRBP-II) and thus protected from oxidation to retinoic acid [*t*-RA (**3**)].⁶² However, as Kakkad and Ong have shown,⁶² when bound to CRBP-II, retinal (RCHO) is readily reduced to retinol (ROH) by the

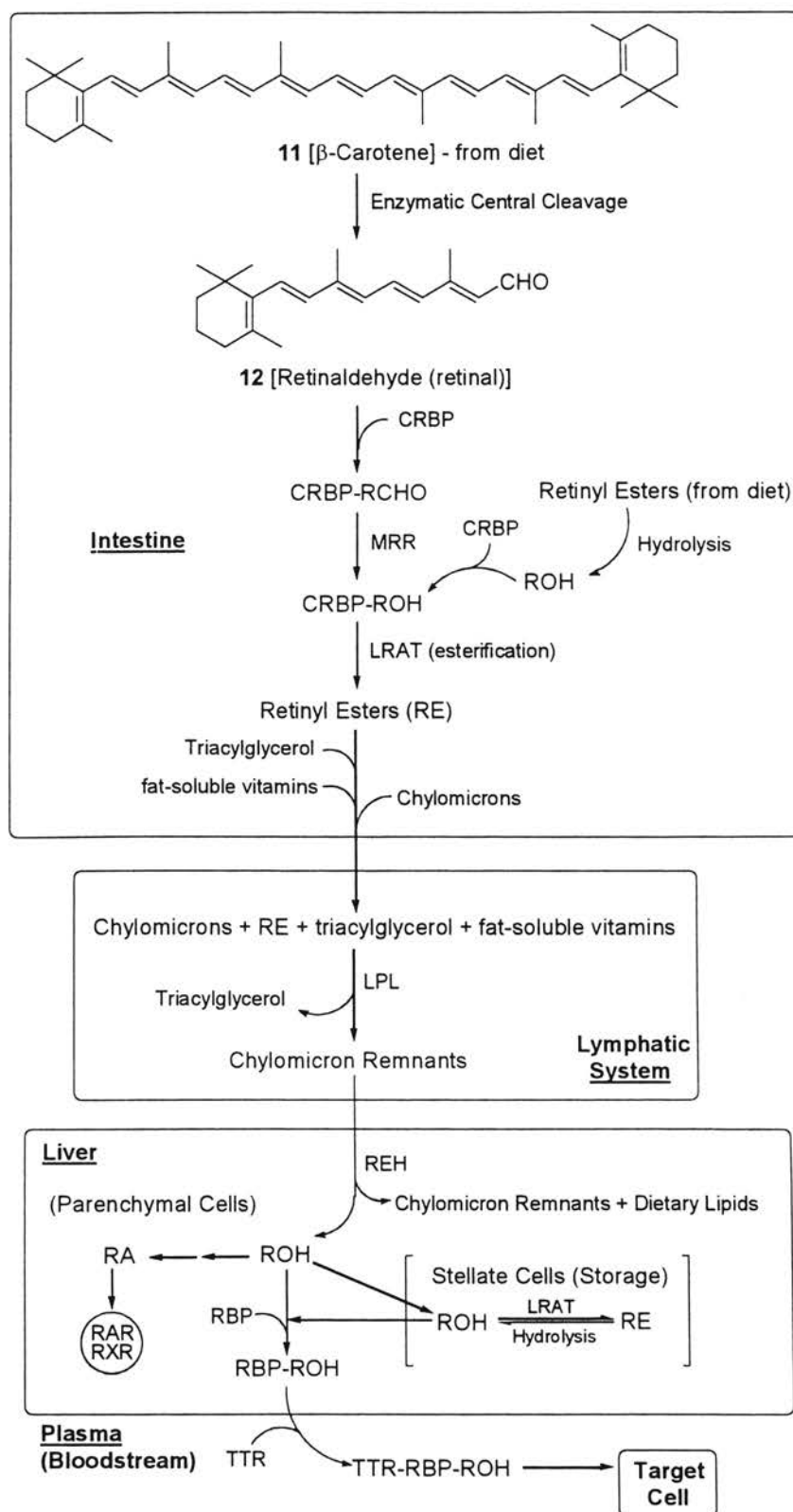


Figure 8. Schematic representation of dietary retinoid metabolism (see text for details).⁶²⁻⁶⁹

mucosal enzyme retinaldehyde reductase (MRR). Both retinol formed from the reduction of retinaldehyde and retinol absorbed as such by the intestinal mucosa is then converted to a retinyl ester [RE, (retinyl palmitate)] for storage in nascent chylomicrons.⁶³ The esterification is accomplished by lecithin:retinol acyltransferase (LRAT), which requires retinol bound to CRBP as a substrate for the esterification reaction.^{63,64} The retinyl esters are then packaged in chylomicrons, along with triacylglycerol and other fat-soluble vitamins, and secreted into the lymphatic system,⁶⁵ where the chylomicrons undergo lipolysis, catalyzed by lipoprotein lipase (LPL).⁶⁶ This lipolysis removes triacylglycerol and gives rise to chylomicron remnants, where the retinyl esters remain to be delivered to the liver.⁶²

In the liver, two different cell types are important for retinoid storage and metabolism, namely the parenchymal cells and the stellate cells.⁶⁷ Parenchymal cells are responsible for the uptake, processing, and secretion of retinoids, while stellate cells store retinoids as retinyl esters (RE).⁶⁷ After arriving at the liver, the chylomicron remnants initially undergo uptake by parenchymal cells, and the retinyl esters are quickly hydrolyzed to retinol by a bile-salt-insensitive retinyl ester hydrolase (REH, this hydrolase may likely provide support in separating the dietary retinoids from the remainder of the dietary lipids being internalized with the chylomicron remnant).⁶⁸ Depending on the dietary needs of the body, some of the dietary retinoid internalized by the parenchymal cells may be secreted directly into the circulation [bound to a retinol-binding protein (RBP), which is produced by parenchymal cells] or transferred to stellate cells for storage.^{62,67} For transport to stellate cells, the retinoid is transferred in the form of retinol and then re-esterified (by LRAT) to be stored for future use.⁶² Retinol (ROH), produced from retinyl

ester hydrolysis, is bound to a retinol-binding protein (RBP - which protects ROH from oxidation and isomerization) in parenchymal cells, which is the major site for synthesis of RBP.⁶⁹ This RBP-ROH complex is then secreted into the plasma where it further complexes with transthyretin (TTR, a plasma transport protein), thus protecting retinol from degradation in the kidney⁶² and providing delivery support to target cells for utilization.

The exact mechanism of uptake of retinol (**1**) by a target cell is yet unknown, and is a matter of some controversy.⁷⁰ The published work on this topic can be divided into two opposing views. One view and its supporting data proposes the involvement of a cell-surface receptor for RBP in the cellular internalization of retinol. The other, and more convincing argument, lies in the theory that a cell-surface receptor for RBP does not exist to assist the uptake of retinol (**1**) by cells (Figure 9).⁷⁰ It is believed that as the TTR-RBP-ROH complex moves in the blood circulation past the plasma membrane of a cell, retinol (**1**) dissociates from RBP and enters the membrane bilayer (Figure 9).⁷⁰ Thus, this process is considered a “passive transport system”. Once inside the bilayer, the retinol rapidly equilibrates between the outer and inner leaflets of the bilayer (“flip-flop”). Apo-CRBP (cellular retinol-binding protein with no bound ligand) may then associate with the retinol in the inner leaflet of the plasma membrane, and, through mass action, may pull additional retinol from the TTR-RBP-ROH complex into the membrane. As retinol is extracted into the cell, it is bound by apo-CRBP (Figure 9), which is specific for retinol (**1**) and retinal (**12**) only, and a holo-CRBP-ROH complex is formed.⁷¹ The ratio of holo-CRBP/apo-CRBP controls the conversion of retinol to either retinoic acid or to a cellular retinyl ester via the inhibition of enzyme LRAT by apo-CRBP and the subsequent

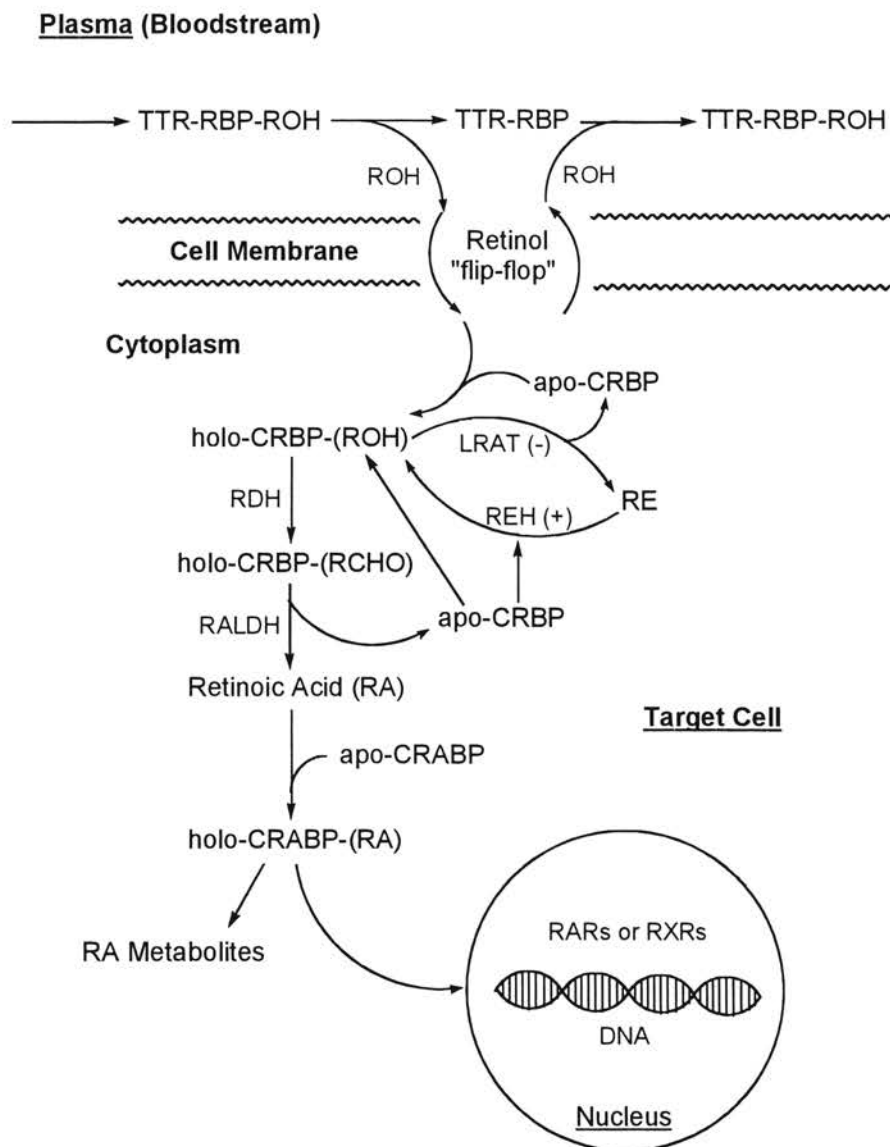


Figure 9. Schematic representation of retinoid metabolism within target cells.⁷⁰⁻⁸⁰

activation of retinyl ester hydrolase (REH).^{72,73} The holo-CRBP also serves as a substrate for microsomal retinol dehydrogenase (RDH) which oxidizes the retinol to retinal (**12**), that remains bound to CRBP, albeit with less affinity.⁷⁴ It is thought that CRBP also mediates the transfer of retinal from RDH to retinal dehydrogenase (RALDH), which then converts retinal to *trans*-retinoic acid (*t*-RA, **3**).⁷⁵ The newly formed *t*-RA (**3**) is

then bound by cellular apo-retinoic acid-binding protein (apo-CRABP), resulting in holo-CRABP, and the resulting complex has a major role in metabolism of retinoic acid and its delivery to the cell nucleus.⁷⁶ Retinoic acid is metabolized oxidatively through dehydrogenation resulting in the formation of 4-oxo-retinoic acid or 18-hydroxyretinoic acid, which may then undergo further degradation (for more information on retinoic acid metabolites, see the section on Toxicity of Retinoids).⁷⁷

All of the endogenous retinoic acids, *t*-RA (3), 9-*c*-RA (4), 11-*c*-RA (5), and 13-*c*-RA (6), arrive at cell nuclei via a similar route just described (Figures 8 and 9). That is, they originate from their corresponding dietary retinol or from the conversion of all-*trans*-retinyl esters.⁷⁸ Although certain studies have suggested that *t*-RA (3) may be enzymatically isomerized to 9-*c*-RA (4) in certain cells,^{49,79} later studies have illustrated that this likely is not the case.^{38b} Rather it is thought that 9-*c*-RA (4) originates from dietary 9-*cis*-retinol (2) or from the conversion of all-*trans*-retinyl esters, as was just described.⁷⁸

The retinoic acids transported to the nucleus dissociate from CRABP and bind to one of the retinoid receptors [RARs or RXRs – with *t*-RA (3), binding is restricted to the RAR isoforms, but with 9-*c*-RA (4), a *pan* agonist, binding can occur to RAR and RXR].^{79,80} In RARs and RXRs that have no ligand bound, helix 12 (H12) of the LBD points away from the core of the LBD, thus forming an entry by which the ligand (retinoic acid) may enter the ligand-binding pocket (LBP) of the ligand-binding domain (LBD).^{40,41} It is thought that the carboxylate group of the retinoic acids enter the pocket first, being drawn in via an electrostatic field gradient induced by basic amino acid residues in the LBP.⁴⁰ These residues and the carboxylate end are anchored together by

hydrophobic interactions of the ligand and receptor induced by a bend of H11, creating a continuous loop between H10 and H12 and drawing the hydrophobic part of the ligand into the LBP.⁴⁰ Helix H12 then swings in and covers the ligand in the LBP through a “mouse trap” like mechanism, which also involves the formation of a salt bridge ($\text{CO}_2^- \cdots \text{H-N}^+\text{H}_2$) between glutamic residues of AF-2 (part of H12) and lysine residues in H4.⁴⁰ The concomitant swinging of H12 unleashes the Ω -loop which flips over underneath H6, carrying along the N-terminal part of H3. In its final position, H12 seals as a ‘lid’ or ‘cap’ on the LBP and further stabilizes ligand binding by contributing to the hydrophobic pocket.⁴⁰

After binding the ligand (either retinoic acid or a synthetic retinoid possessing agonistic qualities), the receptors, which exist as tetramers⁸⁰ in the nucleus in the absence of a ligand, dissociate into monomers. Once the tetramers dissociate into monomers due to retinoid binding, the ligand-independent-transactivation function AF-1 (A/B domain) complexes with transcriptional factors that are specific to the promoter of the target gene.⁸¹ In addition, the dissociation prompts dramatic conformational changes throughout the LBD and directs the receptor toward the formation of homo- or heterodimers via the D-Box (located in the DBD, Figures 1 and 2) and the newly formed dimerization surfaces at the LBD.^{37,40,43,82,83}

The DBDs of the RARs and RXRs not only form homo- or heterodimers between themselves but also with the thyroid hormone receptor (THR) and the vitamin D₃ receptor (VD₃R), which are other nuclear hormone receptors (Figure 10).^{21b} The formation of these various homo- or heterodimers allows for their binding to DNA at

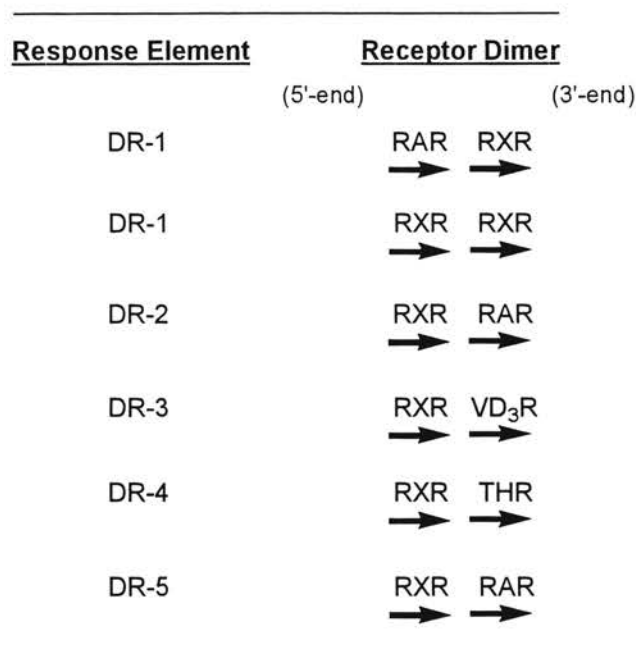


Figure 10. Schematic representation of dimers and their corresponding response element direct repeats (DRs). The arrows below the receptors represent AGGTCA (or related) half-sites.^{21b,31b,46}

specific half-site locations of the promoter region, called hormone response elements (HREs, or this case for retinoic acid, RAREs), thus allowing the mediation of DNA transcription.^{21b,31b} RAREs are nucleotide sequences arranged in direct or inverted repeats spaced by one, two, four, or five nucleotides.^{21b} For instance, a RARE DR-2 designation is assigned to direct polydrome repeats (AGGTCA) spaced by two nucleotides (AA), such as the DNA sequence AGGTC(AA)AGGTCA.⁴⁶ The repeats are well conserved, usually as the sequence AGGTCA or AGTTCA.^{21b} The RAR/RXR heterodimers bind to the direct repeat RAREs in an ordered manner,⁸⁴ such that RXR occupies the 5' (up-stream) half-site and RAR occupies the 3' (down-stream) half-site in DR-2 and DR-5.⁸³ However, the polarity of binding is reversed in the case of the RAR/RXR heterodimer association with DR-1, where the RAR occupies the 5' end and

RXR the 3' end.⁸³ The RXR/RXR homodimer also recognizes DR-1.⁴⁶ The RXR/THR heterodimer recognizes the DR-4,⁸⁵ and the RXR/VD₃R heterodimer recognizes DR-3.⁸⁶

In addition to dimer formation, the agonist-induced conformational change in the transactivation function AF-2 (carboxyl-terminal of the LBD, Figure 1) causes it to bind and form complexes with transcriptional intermediary factors (TIFs), including the estrogen receptor associating protein 160 (ERAP 160),⁸⁷ receptor interacting protein 140 (RIP 140),⁸⁸ TIF 1,^{89,90} unidentified protein profile/thyroid hormone receptor interacting protein 1 (SUG1/TRIP1),⁹¹ and the transcriptional recognition sequence TATA-binding protein (TBP).⁹² As a result of the complex formed between AF-2 and TIFs and the conformational change in the receptor, displacement of transcriptional silencing factors such as nuclear co-repressor (N-Cor),^{38b,93} and silencing mediator of retinoic acid and thyroid hormone receptor (SMRT)⁹⁴ in RARs occurs, which, in the absence of an agonist, are bound to the hinge domain (domain D, Figure 1) of the RAR (but not RXR).⁹⁵ The release of the repressors (N-Cor, SMRT) from the hinge region not only depends upon binding of an agonist to the RAR member of a heterodimeric pair but also upon the binding polarity of the heterodimer to the DNA (if the RAR occupies the 3' end, the repressor is released, and if the RAR member of the dimeric pair occupies the 5' end, the repressor remains bound to the RAR).⁹⁶ Retinoic acid receptor homo- or heterodimers are then directed toward DNA to initiate transcription.^{38b,78}

The homo- or heterodimeric pair of receptors binds to the DNA at the corresponding RARE promoter region, where they may help moderate the transcription process.^{93,94} After binding of the dimeric pair to the RARE, the DNA makes a loop and is positioned in such a manner that interaction of the TIFs bound to RAR or RXR, with transcriptional

machinery (elements needed for initiation and specification of transcription) located up- and down-stream from the TATA box, is possible (Figure 11).^{93,94}

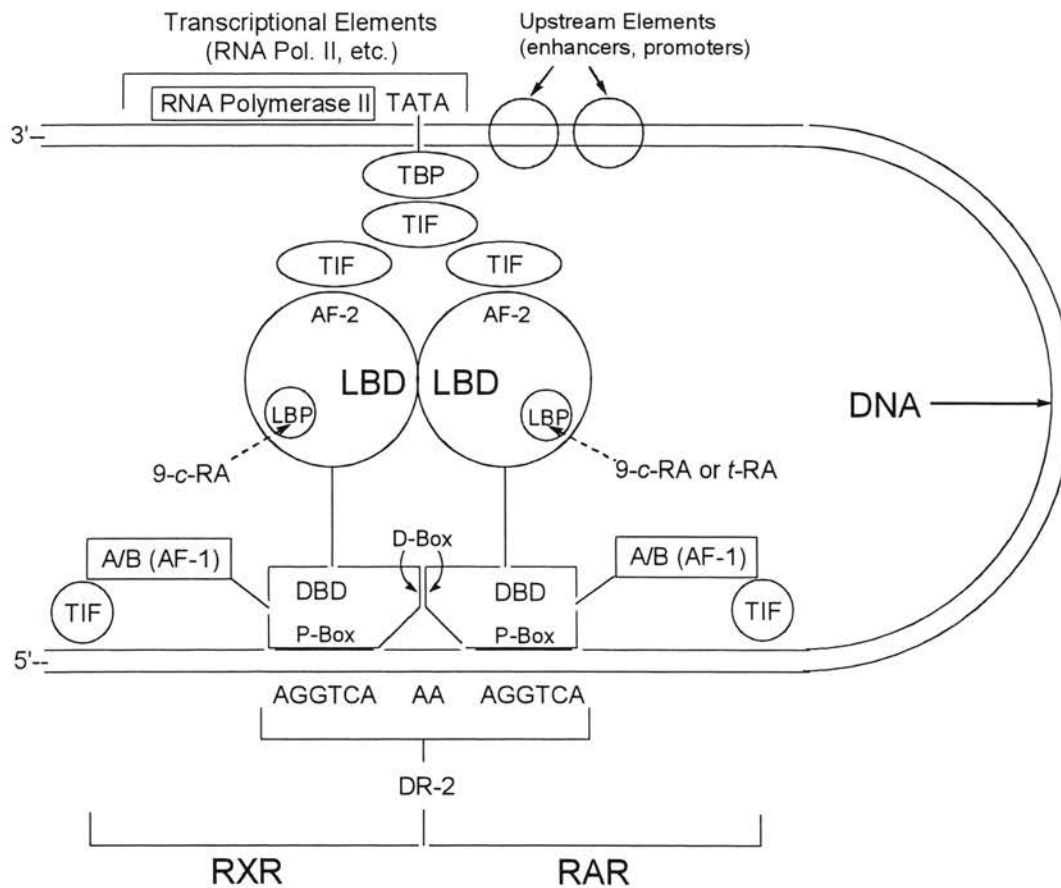


Figure 11. Schematic representation of the RXR/RAR heterodimer with DNA and its transcriptional machinery.^{44,71} After activation of the receptors by a ligand, the newly formed heterodimer binds to the promoter region (RARE), located upstream from the TATA box, via the DNA-binding domains (DBDs). Due to the loop formation assumed by DNA, the transcriptional intermediary factors (TIFs) bound to the ligand-binding domain (LBD) of the heterodimer are able to 'chemically communicate' with transcriptional machinery proteins, such as TATA binding protein (TBP), etc. The A/B domain, which also recruits TIFs, aids in specificity of DNA binding and 'cross-talk' with enhancers of transcription.^{86,93}

In short, retinoids may effect a cell's homeostasis via this process and may interact with retinoid receptors as receptor agonists, inverse agonists, *pan* agonists, antagonists, or

as agents capable of inducing programmed cell death (apoptosis) (for more information on these classifications, see the following section on Classification of Retinoids). Retinoids clearly elicit their biological activities through a very complex pathway consisting of various mechanisms. Some aspects of these mechanisms and pathway are partially understood, but certainly further research is needed to fully comprehend retinoid function and potential medicinal uses.

Classification of Retinoids Based on Their Interaction with Retinoid Receptors

Since the discovery of the retinoid receptors and due to the known therapeutic uses of naturally occurring retinoids,¹⁻¹⁶ and more specifically their anticancer properties,¹³⁻¹⁵ the interest in retinoids has grown astronomically. This interest has spawned the production and study of many new retinoid analogues (synthetic retinoids) to gain further insight into the biological activities manifested by interaction of these compounds with the retinoid receptors.

Synthetic retinoids can be divided into five categories described by their biological activities and interaction with retinoid receptors:

- 1) Agonists,
- 2) Inverse Agonists,
- 3) *Pan* agonists,
- 4) Antagonists, and
- 5) Agents that induce apoptosis (programmed cell death).

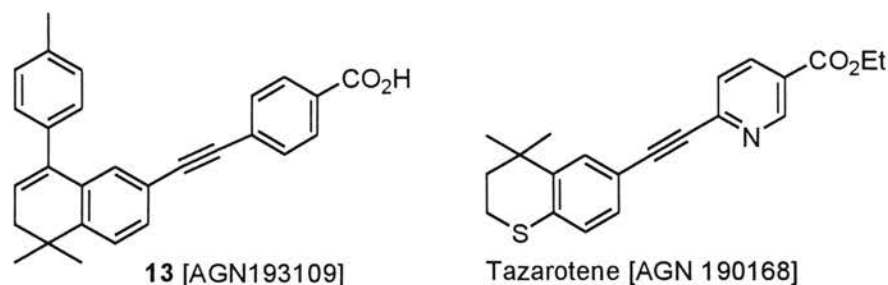
Agonists. Retinoid receptor agonists exhibit their characteristics through interaction and activation of the receptors as is described in the previous section on metabolism and

action of retinoids. Synthetic retinoids in this category act in a similar fashion as *t*-RA (3) by interacting with the LBP of the ligand-binding domain (LBD) and thus causing a conformational change of the receptor such that the transcriptional silencing factors^{38b,93,94} are displaced from the hinge region (domain D, Figures 1 and 2) of retinoic acid receptors (RARs).⁹⁵ The displacement of the silencing factors thus allows the receptor to actively *enhance* DNA transcription.^{38b,78,86}

Synthetic retinoid agonists have likely received more scientific attention than any of the other categories thus far, and a large number of them have been synthesized and studied. Three such agents that are currently employed clinically are 13-*cis*-retinoic acid (6),¹ which is also known as “Accutane” and is a prescription commonly issued by dermatologists for the treatment of severe acne, Etretinate (7),⁴ and TTNPB (8).⁵

Inverse Agonists. Another means by which retinoids can influence cell homeostasis is through inverse agonism.⁸⁶ An inverse agonist has been described as a compound which, upon binding to a RAR, causes a shift of receptor activity toward that of an active repressor, as opposed to an active enhancer of transcription when the receptor is activated by an agonist.⁸⁶ Unlike agonists, the conformational change of the receptor that is induced by an inverse agonist *does not* displace the co-repressor from the hinge region (domain D), and, as a result, the RAR is actively involved in the transcriptional *repression* of target genes.^{31b} Examples of retinoids with inverse agonist properties are AGN193109 (13), which has been reported to exhibit inverse agonist activity in RAR- γ ,^{97a} and Tazarotene (AGN 190168), a RAR- β /RAR- γ selective synthetic retinoid which has demonstrated anti-inflammatory effects^{97b} and has found use in the treatment of facial acne vulgaris and psoriasis.^{97b,c} Because of the transcriptional repression induced by

inverse agonists, these agents may be of value in reducing the propagation of cancerous tissues.



Pan Agonists. A retinoid which possesses agonist qualities is termed a *pan* agonist because of the ability to bind to more than one type of receptor subtype.⁴⁶ A prime example of a *pan* agonist is 9-*c*-RA (**4**), which can bind to both RARs and RXRs.⁵⁰

It is thought that an unusual conformational adaptation of 9-*c*-RA (**4**), along with the spatial arrangement of the RAR's binding pocket, allows for RAR binding of 9-*c*-RA (**4**) (Figure 12).⁴⁰ However, the activation of RAR- γ by 9-*c*-RA (**4**) was less than the activation of this receptor by *t*-RA (**3**), whereas with RAR- α and RAR- β , the activation by 9-*c*-RA (**4**) equaled, or in some instances surpassed, the activation of these two receptors by *t*-RA (**3**).⁹⁸ From the crystallographic structures of RAR- γ [co-crystallized with *t*-RA (**3**) and 9-*c*-RA (**4**)], it was pointed out that a possible reason for the activity difference is that RAR- γ binds 9-*c*-RA (**4**) less favorably than RAR- α and RAR- β due to the interaction of 9-*c*-RA (**4**) with amino acid residue M272 (which is in H5, see Figure 12).⁹⁹ Supporting this view is the data reported by Renaud and co-workers,⁴⁰ who performed energy minimization calculations to generate the most likely confirmation of 9-*c*-RA (**4**) in the LBP of RAR- γ . Renaud also suggested that the lower affinity of 9-*c*-RA (**4**) for RAR- γ (as compared to RAR- α and RAR- β) could be explained by a steric

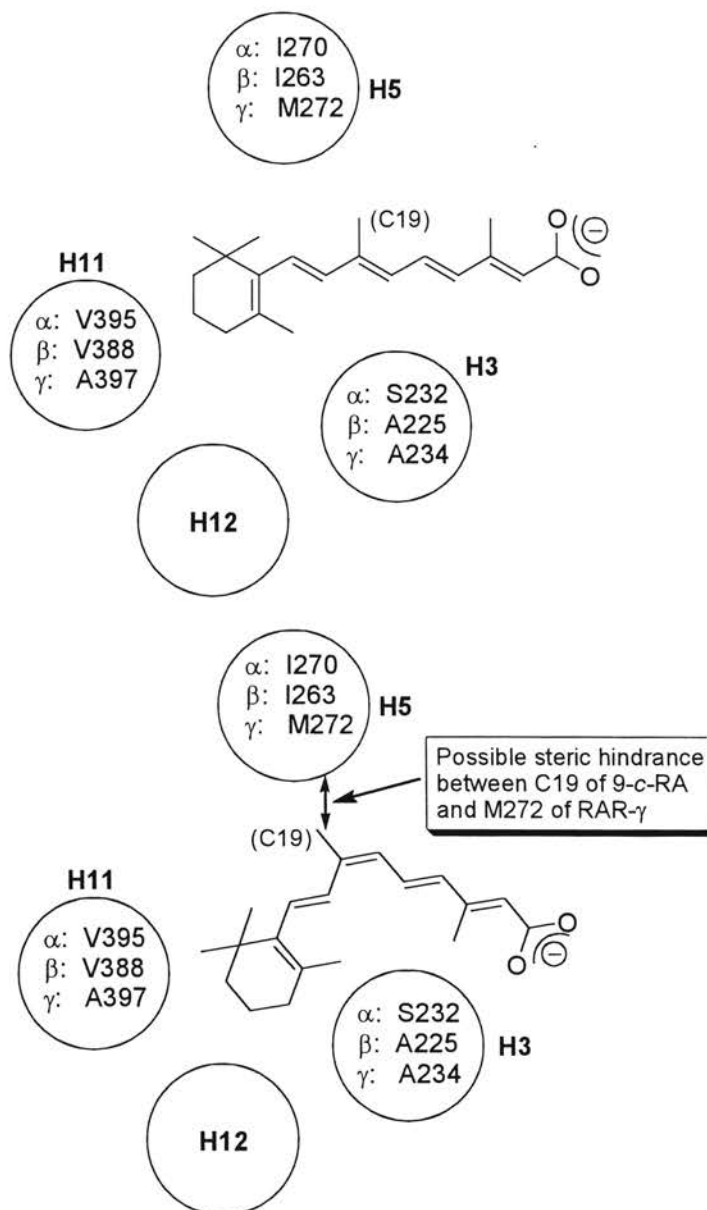


Figure 12. Schematic representation of minimum energy conformations of *t*-RA (3) and 9-*c*-RA (4) within the retinoic acid receptor (RAR) ligand-binding pockets (LBPs).⁴⁰

hindrance between the carbon in the 19 position (C19) of 9-*c*-RA (4) and M272 in H5, which corresponds to an isoleucine residue in RAR-α and RAR-β.⁴⁰ The interaction of the C19 of 9-*c*-RA (4) with less bulky residues in RAR-α (I270) and RAR-β (I263)

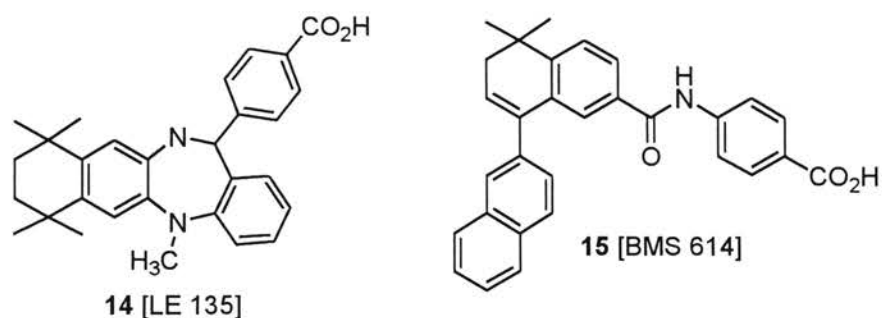
results in a smaller distortion of the “active” conformation of the LBP.⁹⁹ Interestingly, mutation of the amino acid residue phenylalanine 230 (P230) by glycine (P230 to G230) in RAR- γ resulted in the inactivation of the receptor.^{31b} Therefore, P230 may not be important for selectivity of ligand binding, yet it should be taken into consideration because of its function as a “switch” between activity and inactivity of the receptor and its close proximity to A234 and M272.⁵⁰

In contrast, activation of the RXRs by *t*-RA (**3**) has not been observed.^{46,49} One possible explanation for this is that homologues of the A397 (valines in RAR- α and RAR- β) are leucine residues in all RXRs.⁴⁹ In RXRs, it is thought that these leucine residues interact with the C19 methyl group of 9-*c*-RA (**4**) and, as a result, these bulkier residues impose size restrictions on ligands for the receptor.¹⁰⁰ Moreover, isoleucine 275 (I275) in the LBP of RARs corresponds to the phenylalanine 313 (P313) in RXR, and the orientation of P313 sterically interferes with the binding of the more ‘extended’ *t*-RA (**3**). This problem may be overcome by 9-*c*-RA (**4**) because it can adopt a low energy “curved” conformation (Figure 12), which will allow it to fit into the LBP.⁵⁰ Moreover, in contrast to RARs, the amino acid sequence alignment of the LBD of RXRs does not reveal any significant differences within the RXR subtypes.¹⁰⁰ This suggests potential difficulties in designing ligands that are RXR subtype selective.

Antagonists. While agonists *enhance* DNA transcription and inverse agonists *repress* transcription, retinoid antagonists may serve to deactivate certain oncogenic proteins such as activation protein-1 [(AP-1), c-fos and c-jun gene products], nuclear factor-kappaB[(NF- κ B) activator for c-myc, egr-1, LRF-1 cancer genes], and nuclear factor-

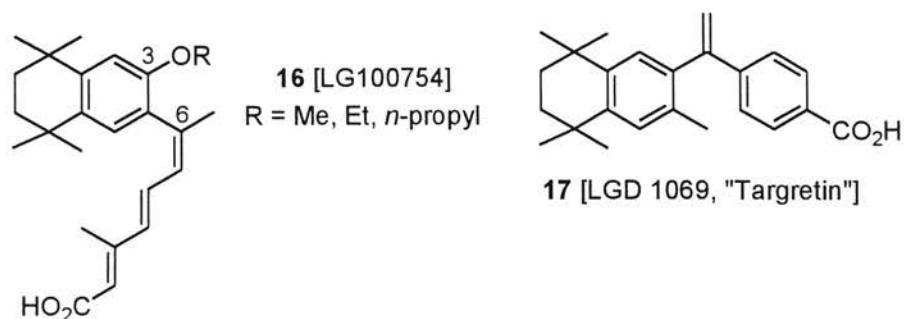
IL6(NF-IL6),⁸² which are all associated with the malignant transformation of cells.¹⁰¹ Deactivation of such cancer genes would thus promote normal cell differentiation.⁸²

The precise mechanism for the binding of an antagonist to the LBP of RARs or RXRs, and the subsequent receptor activity, is not well understood. It has been proposed that an antagonist enters the LBP in the same manner as an agonist.⁹⁹ However, because of structural differences between agonists and antagonists, the AF-2 of the LBD is not able to establish the same salt bridge between H12 and H4. The result is that the receptor undergoes a different conformational change than the one induced by an agonist.^{31b} Induced conformational changes by ligands depend on the structure of the LBP, which in turn suggests that what is perceived as an antagonist in one receptor isoform may be perceived as an agonist in another.^{31b,85} The differences in conformational changes of the receptors' dimeric pair, induced by antagonist binding, may cause the receptors to be incapable of complex formation with RAREs.^{85,86} However, an antagonist-induced conformation of a receptor can bind the AP-1, NF- κ B, or NF-IL6.⁸² The binding of a RAR/RXR heterodimer to AP-1, and/or NF- κ B, and/or NF-IL6, or binding with transcriptional intermediary factors (TIFs), such as cyclic-AMP-binding protein (CBP), and competitively displacing these oncogenic proteins, protects DNA from such influence and essentially silences the activity of AP-1, NF- κ B, or NF-IL6.⁸² Deactivation of oncogenic proteins (such as AP-1 or NF- κ B), or reduction in their activity, reverses the action of the transcriptional machinery, and normal cell differentiation takes place.⁸² Examples of retinoid antagonists include LE 135 (**14**),¹⁰² which has been reported to bind with high affinity to RAR- β and have potent AP-1 activity inhibition, and BMS 614 (**15**),⁹⁹ which was reported to possess highly specific RAR- α antagonistic effects.



In addition, antagonists are also capable of competitively antagonizing both agonists and inverse agonists,¹⁰³ which may provide the reduction of certain toxic side effects associated with high dosages of certain retinoids.¹⁰⁴ For instance, studies have demonstrated¹⁰⁵ that certain retinoid antagonists were not only able to block topical irritation induced by treatment with TTNPB (**8**) and *t*-RA (**3**), but they were also able to inhibit retinoid-induced weight loss.¹⁰⁶ Furthermore, certain retinoid agonists have been shown to enhance replication of several viruses, including HIV-1 and human cytomegalovirus.¹⁰⁷ Therefore, the effects of retinoid antagonists may be utilized as a means of suppressing viral replication.

Koch and co-workers¹⁰⁸ have reported the synthesis and activity of a RXR homodimer antagonist **16** called LG100754. The data presented demonstrated that LG100754 (**16**) displayed high binding affinity for the RXRs and was a potent inhibitor of the known RXR agonist Targretin (**17**, LGD1069) at all three RXR subtypes.¹⁰⁸ The structural

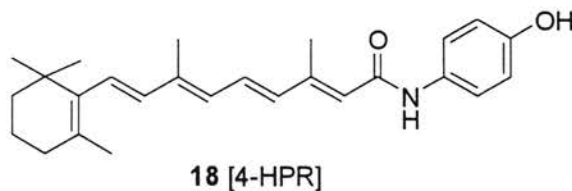


attributes of **16** necessary for RXR homodimer antagonist activity included the size for the 3-alkoxy group on the tetrahydronaphthyl moiety (longer groups providing higher antagonist activity) and the nature of the olefin geometry at C6 (cis geometry being essential for RXR antagonist activity).¹⁰⁸ Such an RXR antagonist could certainly function as a versatile tool for deciphering specific components of transcriptional responses.

Apoptosis. Another use of retinoids in the control of cell homeostasis lies in the ability to induce programmed cell death, or apoptosis.¹⁰⁹ Initiation of this process may be accomplished by the binding of an agonist and/or antagonist to a retinoid receptor and the receptor acting through mechanisms as described above for agonists and antagonists (Figure 11 and related descriptions).^{85,93,94,102} Apoptosis is a part of normal cell differentiation,⁸² and cells from multi-cellular organisms self-destruct when they are no longer needed or have become damaged.¹⁰⁹ Ozato and co-workers¹¹⁰ reported that retinoids cause rapid and extensive apoptosis in P19 EC cells. It was indicated that apoptosis is a receptor mediated process and that RAR binding is essential for the cell death to occur.¹¹⁰ Furthermore, RXR selective ligands alone were unable to induce apoptosis but were cooperative when combined with a RAR specific ligand.¹¹⁰ Retinoids have also been shown by Nagy and co-workers¹¹¹ to induce both differentiation and death

of HL-60 cells. In the study, RAR specific compounds were unable to induce apoptosis, but were able to induce normal cell differentiation.¹¹¹ In contrast, receptor *pan* agonists induced differentiation which was followed by apoptosis of many of the differentiated cells.¹¹¹ A study involving breast cancer cells provided evidence that vitamin D derivatives may promote active cell death, but that 9-*c*-RA (**4**) further enhanced apoptosis induction within this scenario.¹¹² Perhaps this is an indication that the RXR/VD₃R heterodimer is involved in the homeostasis of breast cells.

An example of an agent capable of inducing programmed cell death is the synthetic retinoid *N*-(4-hydroxyphenyl)retinamide (**18**, 4-HPR). Wang and Phang^{112a} found that 4-HPR (**18**) was able to induce apoptosis in breast cancer cells. It was reported that the



addition of 4-HPR (**18**) to cultures resulted in a concentration- and time-dependent decrease in the mRNA level for Bcl-2, an anti-apoptotic protein.¹¹² In addition, studies have shown that 4-HPR (**18**) induced programmed cell death in a variety of human tumor cell types, including melanoma,^{113a} head and neck,^{113b} prostate,^{113c} leukemia,^{113d} and ovarian carcinomas.^{113e} In addition, 4-HPR (**18**) has demonstrated the ability to inhibit cancer cell proliferation in various tissues, including the colon,^{114a} ovary,^{113e,114b} and prostate.^{114c} However, there is some evidence which suggests that 4-HPR (**18**) acts independent of retinoid receptor activation.¹¹⁵ Guruswamy and co-workers^{113e} reported that at lower concentrations ($\leq 1 \mu\text{M}$) 4-HPR (**18**) acted like classic retinoids by inducing cell differentiation through a receptor-dependent mechanism. At higher concentrations

($\geq 1 \mu\text{M}$, concentrations above those achieved in clinical chemoprevention trials) 4-HPR (**18**) appeared to induce apoptosis through retinoic acid, receptor-independent mechanisms.^{113e} Although, the exact mechanism by which 4-HPR (**18**) exhibits its action is a matter of some controversy,^{112b,113e,115,116} the enhanced anti-cancer properties of 4-HPR (**18**), as compared to *t*-RA (**3**), appear to be due to a single structural modification as certain studies suggest.^{112b,113e,115,116} This modification pertains to the presence of a 4-hydroxyphenylamide functionality on the polar end of molecule **18**, which is not found in *t*-RA (**3**). Therefore, this particular functionality may be worth consideration for incorporation into new agents for potential apoptotic qualities.

Certainly there are many more retinoids that can be classified into the categories listed here. Madler¹¹⁷ and Klucik¹¹⁸ have each catalogued a good number of retinoids along with the corresponding retinoid receptor selectivities, biological activities, and toxic properties. These efforts serve to underscore the potential which retinoids have for therapeutic use in a variety of disorders. In addition, such studies illustrate the need for further examination of retinoids, which may help to elucidate structure-activity relationships, the complex mechanistic pathways initiated by retinoids, and ultimately provide more potent and selective treatments for various types of cancer.

Measurement of Retinoid Biological Activity

Several methods exist for the detection of RAR or RXR ligand-induced activities. One of the most frequently employed methods is the use of reporter assays to measure quantitatively the transcriptional activity of RAR and RXR homo- or heterodimers.¹¹⁹ The reporter plasmid construct (Figure 13) is comprised of a reporter gene, such as β -

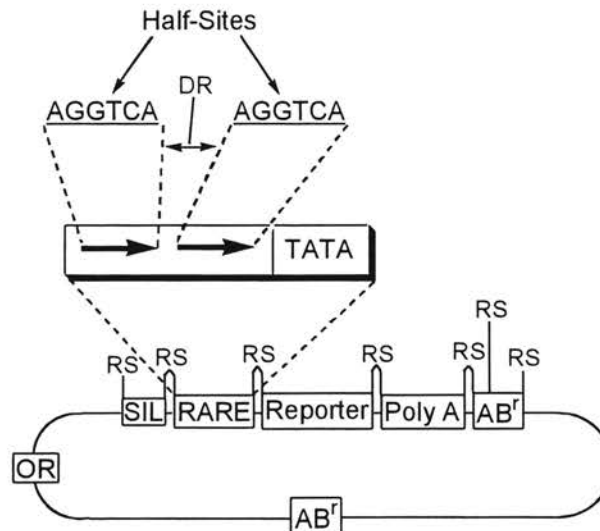


Figure 13. Schematic representation of a reporter plasmid for measuring transcriptional activity of a RAR or RXR after activation by a ligand.¹¹⁹ The arrows represent AGGTCA (or related) half-sites and DR represents the direct repeat nucleotide spacing (see text for details).

galactosidase or luciferase, whose product can easily be detected and measured (detection, and the measurement is usually accomplished via methods such as isotopic labeling or fluorescence).¹¹⁹ The reporter gene is driven by a minimal promoter containing a TATA motif and a RARE.¹¹⁹ At the 5' end immediately upstream from the RARE is a "silencer" (SIL) that acts to dampen spurious transcriptional read-through originating from upstream vector sequences.¹¹⁹ In addition, there are several antibiotic selective genes (AB^r), restriction sites (RS), and an origin of replication (OR) to ensure proper functioning and analysis of the RAREs transcriptional influence on the reporter gene.¹¹⁹ Such assays have the advantage of detecting retinoid transcriptional activity directly after it is initiated, thus avoiding any potential measurement errors that could result from cascade events.

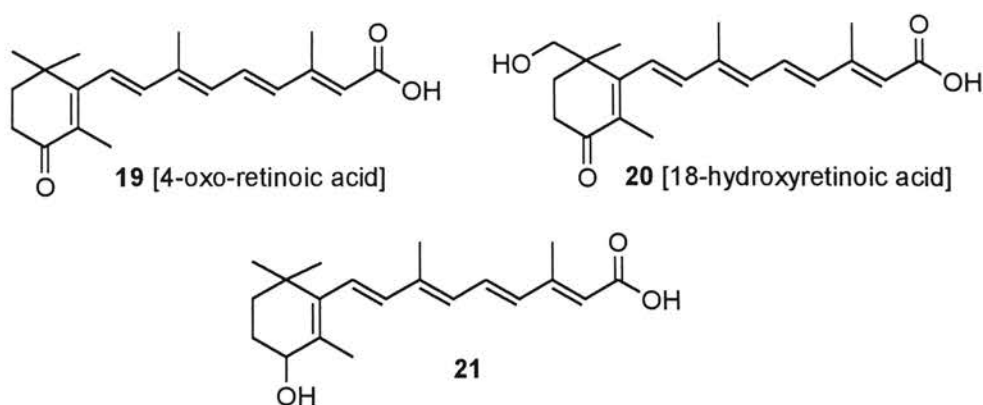
Toxicity of Retinoids

Retinoids do exhibit a variety of useful biological responses. However, certain retinoids can produce severe toxic side effects, and some retinoids are reported as having teratogenic properties (causing birth defects).¹²⁰ The toxicity of retinoids is well documented,^{22a,117,120} and it has proven to be a significant problem following chronic administration of retinoids, resulting in a condition referred to as “hypervitaminosis A” (vitamin A toxicity).¹²⁰ The general signs of hypervitaminosis A include reduced food intake, weight loss, weakness, reduced motor activity, bone and skin lesions, and, in extreme scenarios, possibly death.¹²⁰ Both naturally occurring retinoids, such as *t*-RA (**3**) and 13-*c*-RA (**6**), as well as synthetic retinoids, such as the arotinoids etretinate (**7**) and TTNPB (**8**), have demonstrated at least some toxic and/or teratogenic properties.¹²⁰ For instance, birth malformations in babies born to mothers exposed to isotretinoin (13-*c*-RA, **6**) or etretinate (**7**) during pregnancy have been reported.¹²⁰ The body parts most consistently affected by both drugs are the cranium and face, central nervous system, heart, and thymus.¹²⁰ It is also suspected that 13-*c*-RA (**6**) may effect the intellectual performance of children whose mothers took the drug during pregnancy, even when no structural abnormalities were observed in the children.¹²⁰

TTNPB (**8**), a conformationally restricted aromatic analogue of *t*-RA (**3**), is a more potent inducer of RAR transcriptional activity than *t*-RA (**3**) even though **8** has a binding concentration for RARs that is approximately 10 times lower than that of *t*-RA (**3**).¹²¹ However, TTNPB (**8**) is approximately 1000 times more toxic than *t*-RA (**3**).¹²¹ It has been suggested that the higher activity and toxicity of TTNPB (**8**) is due to an inability to complex with CRABP.¹⁰⁶ CRABP helps regulate the levels of retinoic acid in the cell

and its transport to the nucleus where *t*-RA (**3**) interacts with RARs.¹²¹ Since TTNPB (**8**) is not bound by CRABP as effectively as is *t*-RA (**3**), its concentration is unregulated, and thus its metabolism is slowed. Therefore, TTNPB (**8**) remains in the cell and nucleus for longer periods of time, allowing more interaction with RARs, which may be a contributing factor to the observed toxicity of TTNPB (**8**).¹²¹

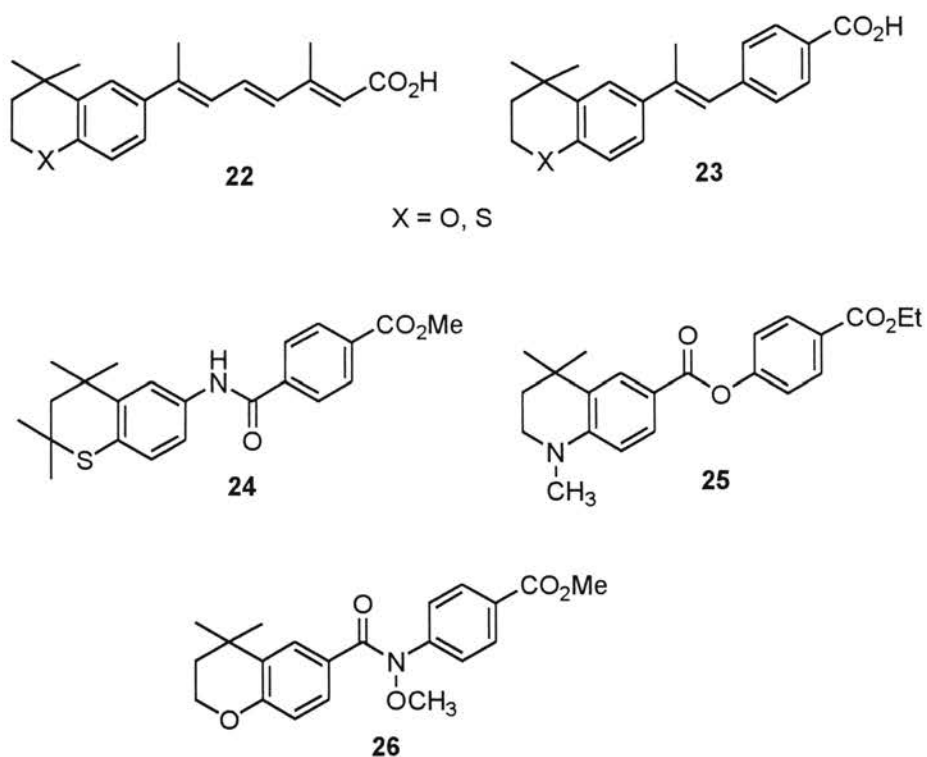
Another factor attributed to retinoid toxicity (especially endogenous retinoids) is the oxidized metabolites resulting from retinoid degradation.¹²⁰ For instance, some oxidized metabolites of *t*-RA (**3**), including **19-21**, have been isolated, studied, and found to be toxic and/or teratogenic.^{120,122}



Although the retinoids mentioned thus far possess toxic properties, they do exhibit quite useful qualities, especially in the treatment of various types of cancer.¹ Furthermore, current studies on heteroarotinoids (another type of synthetic retinoid)^{50,123,113e} and other synthetic retinoids that may prove to be retinoid receptor subtype specific¹²⁴ may help provide future, selective and less toxic treatments for certain types of cancer.

Heteroarotinoids and Other Reduced Toxicity Retinoids

The teratogenicity¹²⁰ and/or toxic manifestations^{120,124} exhibited by endogenous retinoids, such as *t*-RA (**3**) and 9-*c*-RA (**4**), as well as synthetic arotinoids, such as the clinically employed Etreinate (**7**) or TTNPB (**8**), have limited the use of such compounds. Thus, the study of heteroarotinoids originated as an attempt to mimic the anti-carcinogenic action of retinoids while at the same time reducing unwanted side effects. Heteroarotinoids (such as **22-26**) constitute a class of synthetic retinoids that



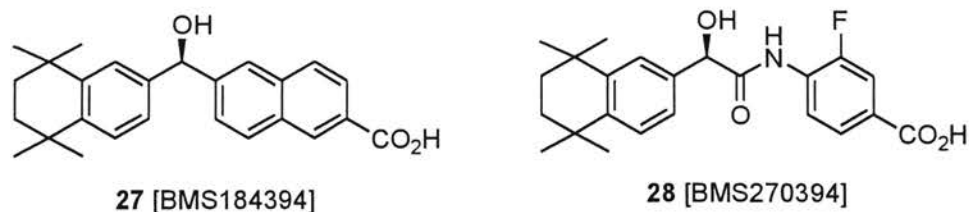
structurally resemble arotinoids (such as **7** and **8**) in that at least one aryl moiety is present within the molecule. However, heteroarotinoids contain an aryl-fused, heterocyclic ring as a modification, and several studies have shown that some heteroarotinoids demonstrate promising inhibition of various cancers as well as reduced toxicity.^{20a,50,123,125,126} For instance, it has been reported that structure **22** (where X = S or

O) demonstrated a toxicity approximately **3-fold less** than that of *t*-RA (**3**) and **3000-fold less** than that of TTNPB (**8**).¹²⁵ In addition, sulfur heterarotinoid **24** has been reported to possess excellent anti-cancer properties as well as reduced toxicity.^{113e,123} Compound **24** appeared to possess *pan*-agonist properties and showed powerful anticancer properties against SCC-38 head and neck squamous cell carcinoma lines in nude mice, as compared to *t*-RA (**3**).¹²³ Complete tumor regression was noted in 3 of 5 mice treated with *t*-RA (**3**) and 4 of 5 mice treated with heteroarotinoid **24**.¹²³

Another approach that can be taken for decreasing the toxicological effect of retinoids is the design of agents that are retinoid receptor subtype selective. As is discussed in a previous section on the distribution of retinoid receptors in organ tissues, the retinoid receptors have a diverse expression pattern throughout the tissues of the body, which may explain the vast array of effects exhibited by retinoids.^{21c,124} This diverse expression pattern may also help explain the various side effects attributed to some retinoids, especially those that are not receptor subtype selective.

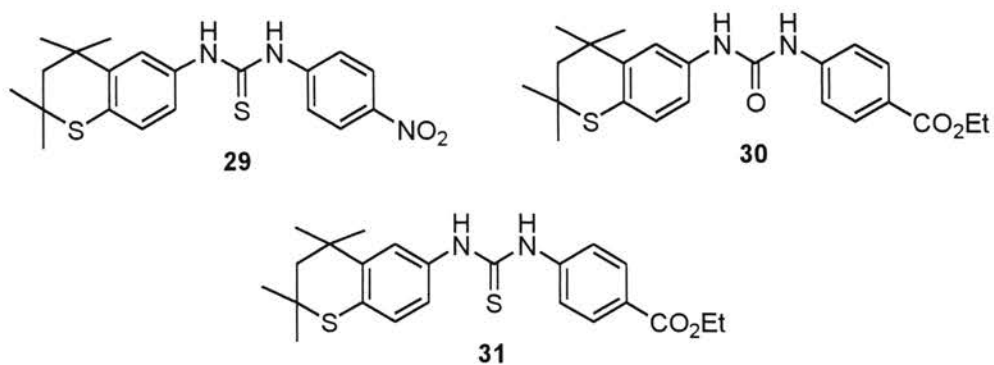
Some studies^{99,124,127} suggest that the presence of a three-atom 'linker' group (a linker group is a moiety connecting the two aryl rings) within an arotinoid may increase specificity for the RARs. Other studies also demonstrated that a linker with an attached, non-bulky functionality capable of hydrogen bonding via proton donation (such as via an -OH) enhances RAR- γ selectivity.^{99,124,127,128} Klaholz and co-workers¹²⁴ have provided strong evidence that may explain RAR- γ selectivity of an agent possessing a linker group with an attached -OH. Through computer aided crystallographic studies, Klaholz and co-workers¹²⁴ have clearly demonstrated that a hydrogen bond may exist between a hydroxyl group attached to the linker of a retinoid and the sulfur atom of M272 on α -helix 5 (H5,

Figure 12 and related text) of RAR- γ . The study was accomplished by separately co-crystallizing RAR- γ -selective agonists, such as BMS184394 (**27**) and BMS270394 (**28**) with the human RAR- γ LBD. It was shown that a hydrogen bond may exist between the hydroxyl group of such agents and M272 of RAR- γ . Thus, the amino acid residue M272 should be considered in designing potential RAR- γ -selective agents. Klaholz¹²⁴ also



noted that steric hindrance involving the hydrophobic region of a ligand with S232 of H3 (Figure 12), which corresponds to A234 in RAR- γ and A225 in RAR- β , may also be considered in designing retinoid receptor subtype-selective compounds. Certainly, an agent with these structural characteristics could be useful for the specific treatment of disorders such as melanoma or vulvarian carcinomas, due to a high expression of RAR- γ in both skin⁵⁹ and urogenital tissues.¹²⁹

By combining these two approaches (heteroarotinoids with a three-atom linker that may aid in receptor subtype selectivity), an agent could potentially be produced that has much reduced toxicity and could be utilized for the treatment of select types of cancer. It is conceivable that by constructing an agent possessing a semi-flexible three-atom linker with self-capability of hydrogen bonding through proton donation, higher RAR- γ specificity may be achieved. This could further reduce the undesired side effects of retinoids. In fact, three heteroarotinoids (**29-31**) possessing a novel urea functionality as



a three-atom linker group were recently produced by this lab and demonstrated potentially useful results.^{113e} The urea group was chosen as a three-atom linker due to its somewhat flexible nature which could accommodate a better fit into the RARs, and therefore enhance activation. Moreover, a urea group provides two –NH– groups capable of hydrogen bonding with the receptor, thus possibly improving RAR- γ selectivity.^{99,124,127,128} All three heteroarotinoids induced apoptosis in both monolayer and organotypic cultures of OVCAR-3, Caov-3, and SK-OV-3 ovarian carcinoma cell lines, with few toxic side effects.^{113e} Moreover, programmed cell death was induced by heteroarotinoids **29-31** at clinically achievable concentrations [$\leq 1 \mu\text{M}$, a trait that *has not* been observed with 4-HPR (**18**) which is employed clinically].^{113e} These results certainly suggest that further investigation of such compounds is warranted and demonstrate promise as effective chemoprevention agents for ovarian cancer.

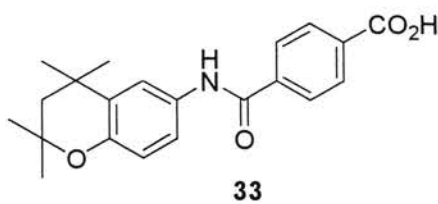
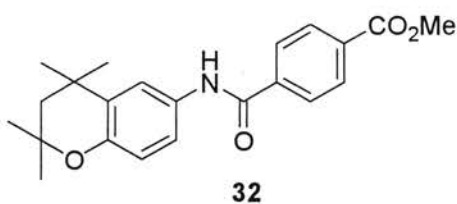
CHAPTER II

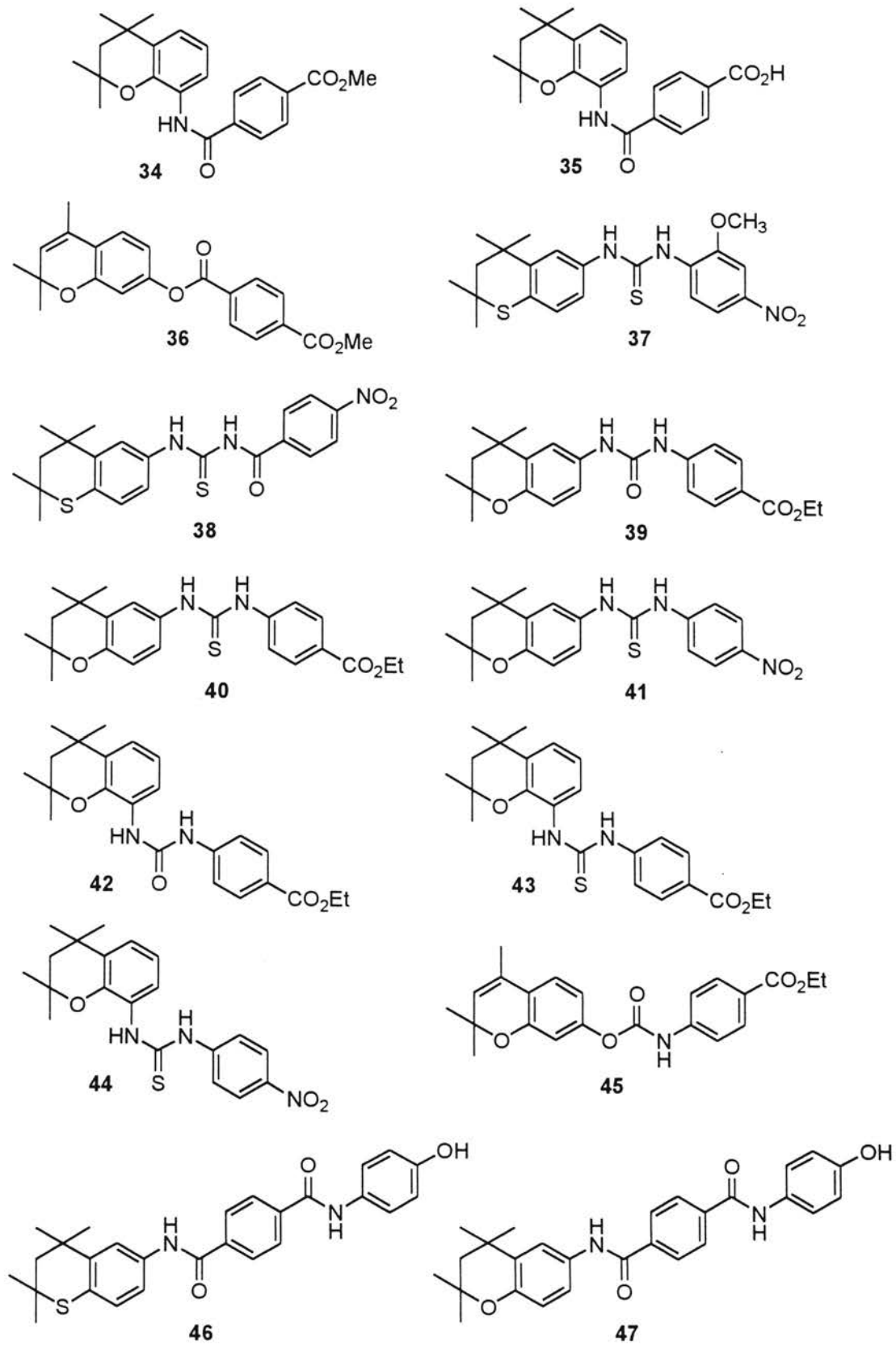
RESULTS AND DISCUSSION

Modified Oxygen and Sulfur Heteroarotinoids

The goal of this project was multi-faceted, being directed toward the production of various sulfur- and oxygen-containing heteroarotinoids, which were designed to be potentially RAR- γ selective, RXR subfamily selective, to possess *pan* agonist qualities, or possess the ability to induce programmed cell death (apoptosis). Heteroarotinoids **32-47** (shown below), containing various structural features, which may provide these characteristics (for details on intended biological characteristics resulting from these structural features see the Biological Activity section in this chapter), were synthesized and have been classified under three categories based on structural similarities of the 'linker' groups between the aryl rings of the compounds:

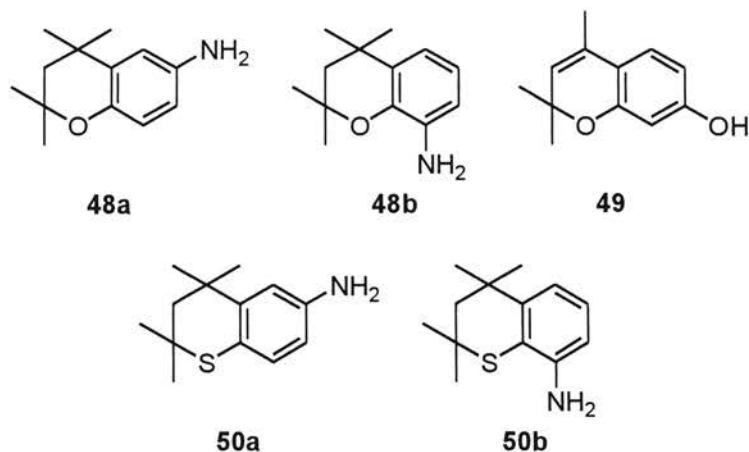
- 1) Heteroarotinoids containing a two-atom linker group (**32-36**),
- 2) Heteroarotinoids containing a three- or four-atom linker group (**37-45**), and
- 3) Heteroarotinoids containing a 4-hydroxyphenylamide moiety as a 'polar tail' group (**46-47**).





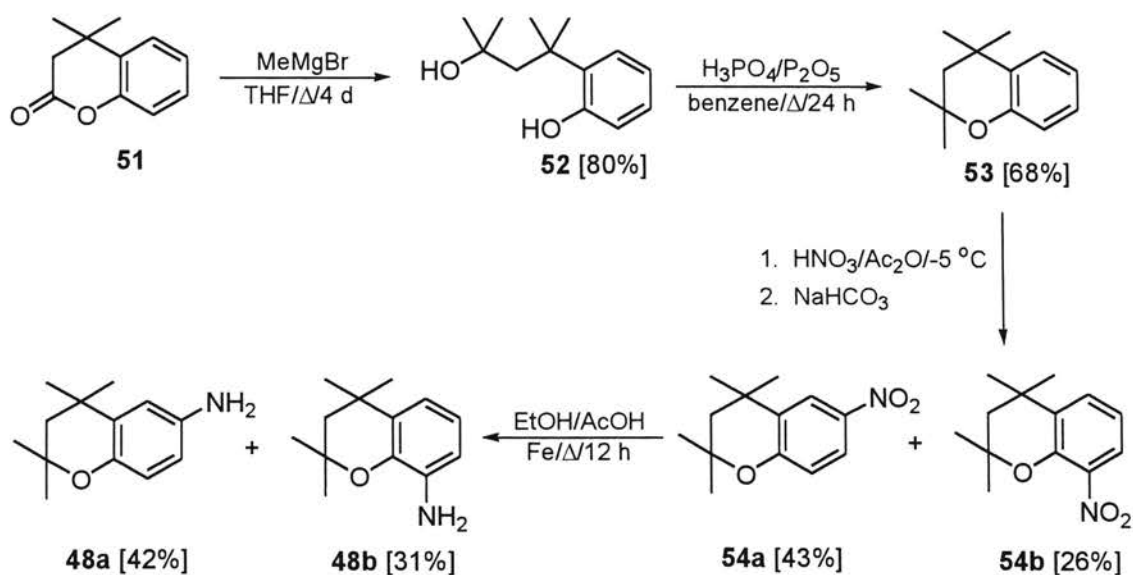
Synthesis of Key Intermediates

Several synthetic intermediates were required for the production of the desired heteroarotinoids **32-47**. Specifically, the target heteroarotinoids were constructed by utilizing four key intermediates **48a,b-50a**, whose synthesis has been described below.



Amines 48a and 48b. It was visualized that the reaction sequence **51**→**52**→**53**→**54a** and **54b**→**48a** and **48b**, as illustrated in Scheme 1, would provide the key intermediate

Scheme 1



amines **48a** and **48b**. The 6-isomer **48a** could then be utilized to obtain the desired heteroarotinioids **32**, **33**, **39-41**, and **47** while the 8-isomer **48b** could be used to synthesize compounds **34**, **35**, and **42-44**. Therefore, lactone **51** was prepared by modification of a known method,¹³⁰ and boiling **51** in dry THF with excess methylmagnesium bromide for 4 days led to crude diol **52** as a clear yellow solid. Upon recrystallization (petroleum ether) of the yellow solid, pure **52** was obtained in excellent yield (80%). Dehydration-cyclization of diol **52** using phosphoric acid and phosphorous pentoxide ($\text{H}_3\text{PO}_4/\text{P}_2\text{O}_5$) resulted in the generation of chroman **53** in reasonable yield (68%) after purification by vacuum distillation. Nitration of **53** using a nitric acid/acetic anhydride ($\text{HNO}_3/\text{Ac}_2\text{O}$) mixture¹³¹ at $-5\text{ }^\circ\text{C}$ afforded the two nitro compound isomers **54a** (6-isomer) and **54b** (8-isomer) in an overall yield of 69% (43% and 26%, respectively). The two resulting isomers (**54a** and **54b**) were partially separable by flash column chromatography using the unusual solvent combination hexanes:ethyl ether (20:1).

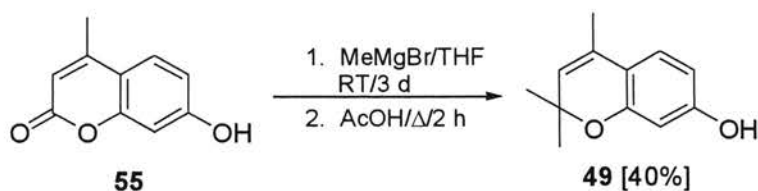
A search for a clean, straightforward reduction procedure to accomplish the conversion of nitro compounds **54a** and **54b** to the corresponding amines **48a** and **48b** was initiated. Reduction of nitroarenes to the corresponding aniline derivatives is a common process and a useful tool for the production of key amines that can be utilized for the generation of a variety of desired products. However, many of the protocols required pressurizing reaction vessels with explosive H_2 gas or employed expensive reagents such as tin/hydrochloric acid or tin (II) chloride/hydrochloric acid.¹³² Furthermore, many of these procedures provided modest yields at best. The reported

procedure for the synthesis of **50a**¹²³ using a solution of titanium (III) chloride in HCl was considered. However, the method required the use of a very large excess of TiCl₃/HCl, which was quite expensive, and the reaction workup was complicated and required the handling of titanium salts.

Finally, an assessment was made of the reduction of nitroarenes published by Owsley and Bloomfield.¹³³ Some modifications of the method were instituted for the conversion of **54a** and **54b** to the desired amines **48a** and **48b** (Scheme 1). The reaction was carried out by boiling a mixture of **54a** or **54b** in absolute EtOH for 12 hours using glacial acetic acid as a proton source and iron powder as the reducing agent. The reaction workup was simple, and the by-products were only H₂O and iron (III) acetate, which were readily soluble in water and easily removed. It was found that the resulting amines **48a** and **48b** could be well separated (substantially better than the precursor nitro compounds) via flash chromatography [hexanes:ethyl ether (1:1)] and thus be obtained in high purity but in somewhat modest yields [6-isomer **48a** (42%) and 8-isomer **48b** (31%)]. Therefore, rather than purifying the nitro compounds **54a** and **54b** individually, immediate reduction of the crude mixture of the two isomers to the corresponding amines **48a** and **48b** was easily accomplished and separation of the latter via chromatography was very facile.

Phenol 49. It was reasoned that the use of known lactone **55**¹³⁴ in the conversion **55**→**49** (Scheme 2) would provide phenol **49** that could be used for the synthesis of

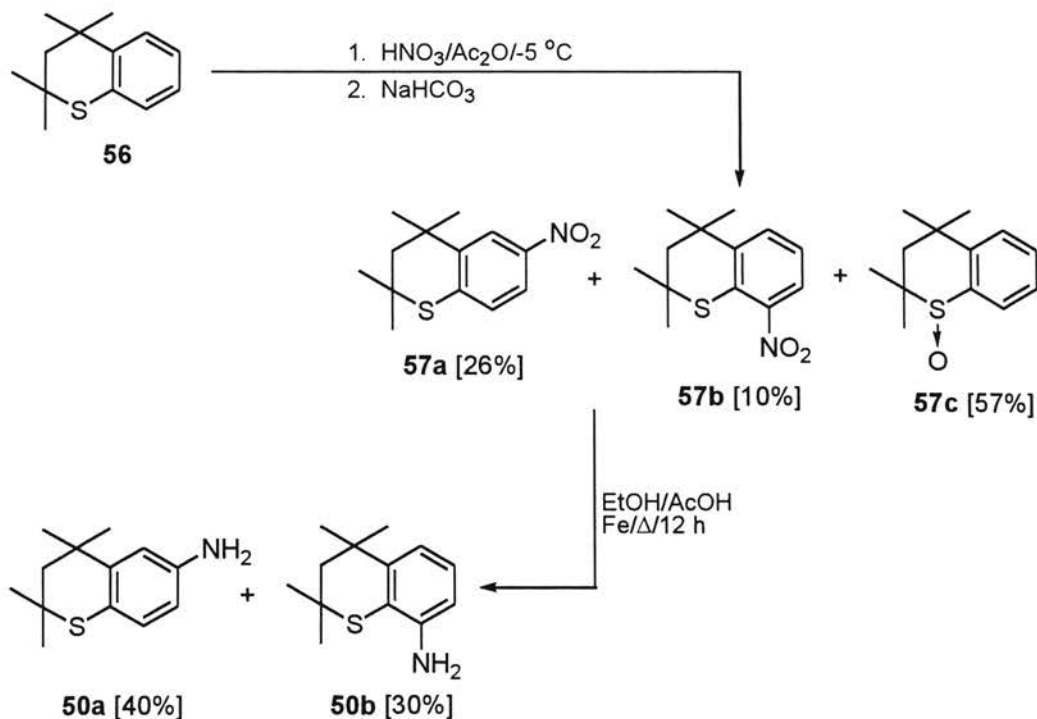
Scheme 2



desired heteroarotinioids **36** and **45**. Lactone **55**¹³⁴ was stirred with excess methylmagnesium bromide in dry THF for 2 days at room temperature. Upon workup of the reaction with saturated, aqueous NH_4Cl , the crude product obtained was then immediately dissolved in glacial acetic acid, and the resulting solution was heated gently with stirring for 2 hours. After aqueous workup, washing with saturated NaHCO_3 solution, and subjecting the crude product to flash chromatography [Et_2O :hexanes (5:1)], pure phenol **49** was obtained (40%).

Amines 50a and 50b. It was envisioned that the reaction sequence **56**→**57a** and **57b**, as illustrated in Scheme 3, would provide the 6- and 8-isomeric nitro compounds **57a** and

Scheme 3



57b, which could be used in the conversions **57a**→**50a** and **57b**→**50b** (Scheme 3) and thus provide key intermediate amines **50a** and **50b**. The 6-isomer **50a** could then be utilized to obtain the desired heteroarotinoids **37**, **38**, and **46**, and **50b** could be used to synthesize other 8-isomer heteroarotinoids. Although the conversion **56**→**57a**→**50a** is known,¹²³ different conditions were employed here.

The reaction sequence (Scheme 3) began with the nitration of known thiochroman **56**^{126a} using a HNO₃/Ac₂O mixture¹³¹ at -5 °C and stirring the reaction mixture for 1.5 hours. The two resulting isomers [**57a** (6-isomer) and **57b** (8-isomer)] were partially separable by flash column chromatography using hexanes:ethyl acetate (5:1) and provided the nitro compounds **57a** and **57b** in modest yields (26% and 10%, respectively). However, in this case only 1 equivalent of the nitrating agent was used, as compared to 2 equivalents in the reported procedure,¹²³ with essentially no reduction in the reaction yield of the desired nitro compound **57a** (27% being reported previously). The reduced yield of **57a** can be partially explained by a competitive side reaction leading to sulfoxide **57c** (the sulfoxide structure was suggested by IR and NMR analyses). The sulfoxide **57c** was also separated from the crude reaction product mixture as a major component (57%).

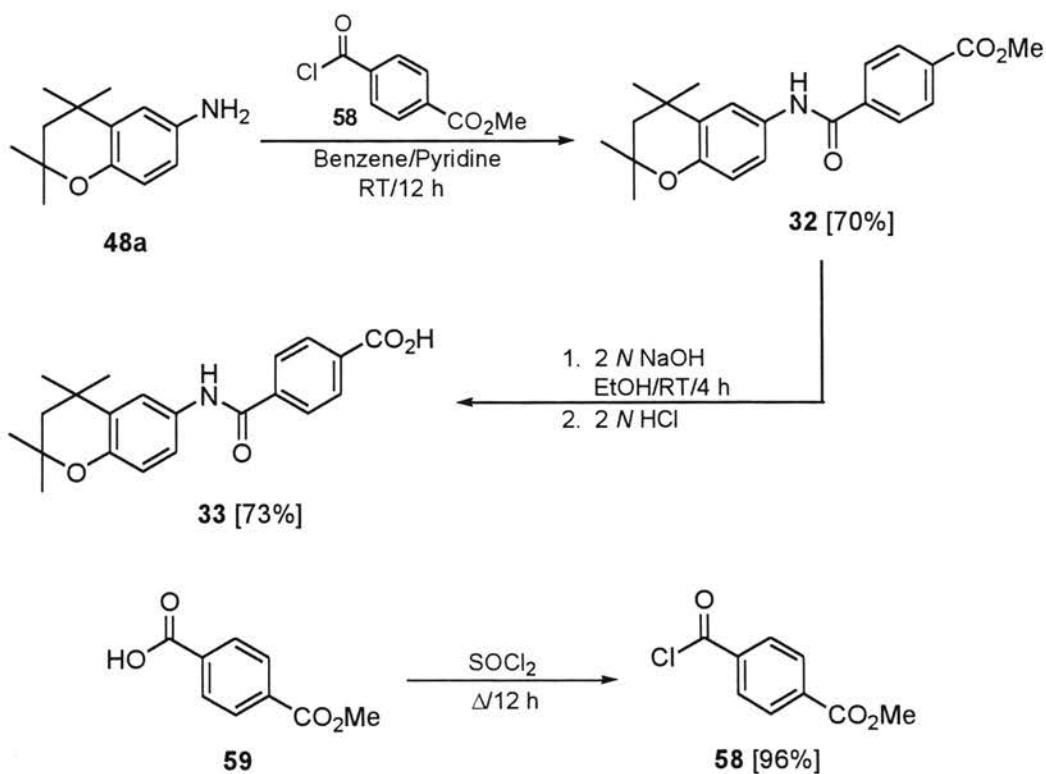
Reduction of the nitro groups in **57a** and **57b** (Scheme 3) was achieved via a modification of the method¹³³ described above (in the conversion **54a** and/or **54b**→**48a** and/or **48b**). The nitro compound **57a** or **57b** was placed in absolute EtOH, along with iron powder and glacial AcOH, and the resulting mixture was stirred at reflux for 12 hours. Again it was noted that the resulting amines **50a** and **50b** could be well separated (substantially better than the precursor nitro compounds, as was the case for **48a** and **48b**)

via flash chromatography [hexanes:ethyl acetate (2:1)] and thus be obtained pure, albeit in somewhat modest yields [6-isomer **50a** (40%) and 8-isomer **50b** (30%)]. Therefore, rather than purifying the nitro compounds **57a** and **57b**, reduction of the crude mixture of these two isomers to the corresponding amines **50a** and **50b** (as in the production of **48a** and **48b** discussed above) was performed and separation of the isomeric amines by flash column chromatography was again accomplished easily. Although the previous method¹²³ reported a yield of 50% for amine **50a** from the reduction of the nitro group in **57a**, our iron/acetic acid approach, provided a low cost and a simple reaction workup and resulted in only a slightly reduced yield.

Synthesis of Heteroarotinoids Possessing Two-Atom Linker Groups

Oxygen Heteroarotinoids with a Linker Group Placed at the 6-Position of a Tetramethylchroman Moiety (32 and 33). Amine **48a** was first employed to produce desired heteroarotinoids **32** and **33** via the conversion **48a**→**32**→**33** as demonstrated in Scheme 4. The conversion of **48a**→**32** was completed by simply adding the *mono*-methyl terephthaloyl chloride (**58**) in one portion to amine **48a** which was dissolved in benzene containing a small amount of pyridine. After purification, amide **32** was thus obtained in reasonable yield (70%). Interestingly, acid chloride **58** was first prepared via a modified procedure developed by this lab.¹³⁵ The procedure required the addition of a large excess of thionyl chloride (SOCl₂), containing a few drops of DMF, to *mono*-methyl terephthalate (**59**) and then stirring the resulting mixture in an ice bath. Continued stirring for an additional 12 hours followed while allowing the reaction mixture to warm slowly to room temperature. However, yields of **58** by this method only

Scheme 4



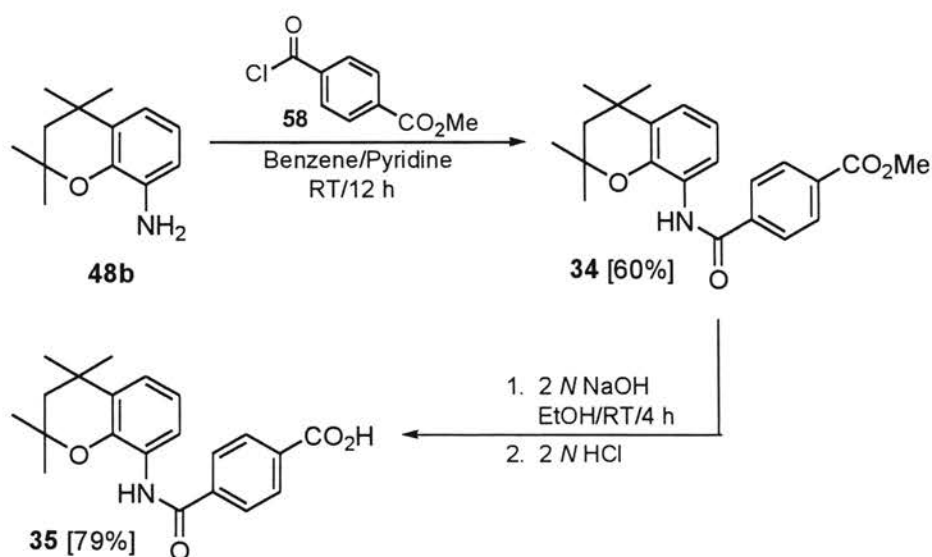
averaged approximately 50%. Therefore, a procedure by Yli-Kauhalouma and co-workers¹³⁶ for synthesizing **58** was employed (Scheme 4) with slight modification. Commercially available *mono*-methyl terephthalate (**59**) was placed in a reaction flask along with an excess of SOCl_2 (~7 eq). The mixture was then stirred at reflux for 12 hours, and excess SOCl_2 was removed under reduced pressure to give the desired acid chloride **58** (96%). Furthermore, **58** could be characterized by IR and NMR analyses which indicated a high purity product.

Compound **33** was produced via a reported method¹³⁵ that involved saponification of ester groups (as has **32**) with 2 N NaOH under mild conditions to avoid cleaving sensitive amide linkages present within the molecule (Scheme 4). Upon acidification of the

reaction mixture (pH~2) using 2 *N* HCl, acid **33** precipitated and was then filtered and recrystallized [ethyl acetate:hexanes (2:1)] to give the pure product **33** (73%).

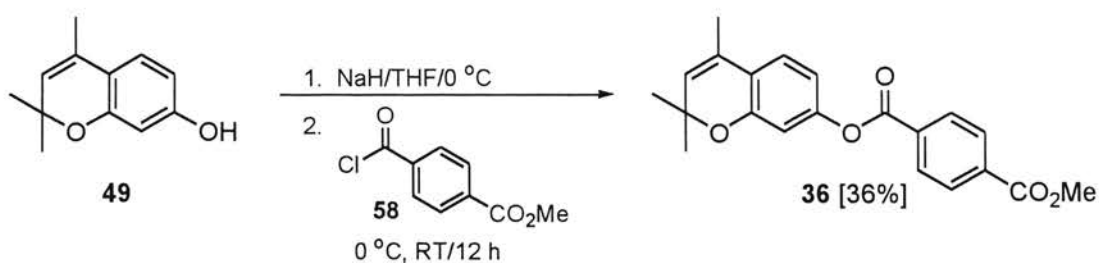
Oxygen Heteroarotinoids with a Linker Group Placed at the 8-Position of a Tetramethylchroman Moiety (34 and 35). Heteroarotinoids **34** and **35** were prepared from amine **48b** in the conversion **48b**→**34**→**35** (Scheme 5), following the same reaction conditions applied for **48a**→**32**→**33** (Scheme 4). Amide **34** was obtained pure in a reasonable yield (60%), and acid **35** was afforded in good yield (79%, Scheme 5).

Scheme 5



Oxygen Heteroarotinoid with a Linker Group Placed at the 7-Position of a Trimethylchromen Moiety (36). Target compound **36** was afforded from key intermediate phenol **49** as demonstrated in Scheme 6. Phenol **49** was first treated with sodium hydride in THF at 0 °C, and then acid chloride **58** was added to the resulting reaction mixture while maintaining the reaction temperature at 0 °C during the addition. After workup of the reaction and evaporation of the solvent, a white solid was obtained

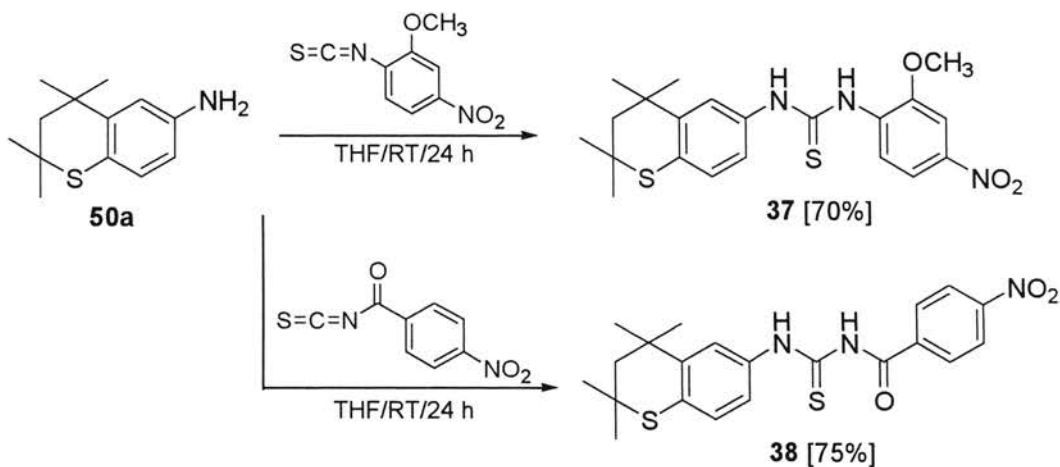
Scheme 6



and recrystallized [HCCl_3 :pentane (1:1)] to provide the desired di-ester **36** (36%). Possibly, conversion of **49** to the intermediate sodium salt was in low yield, resulting in a moderate yield of **36**.

Synthesis of Heteroarotinoids Possessing Three- or Four-Atom Linker Groups
Sulfur Heteroarotinoids with a Linker Group Placed at the 6-Position of a Tetramethylthiochroman Moiety (37 and 38). Amine **50a** was used to synthesize the desired sulfur heteroarotinoids **37** and **38** via the conversion illustrated in Scheme 7.

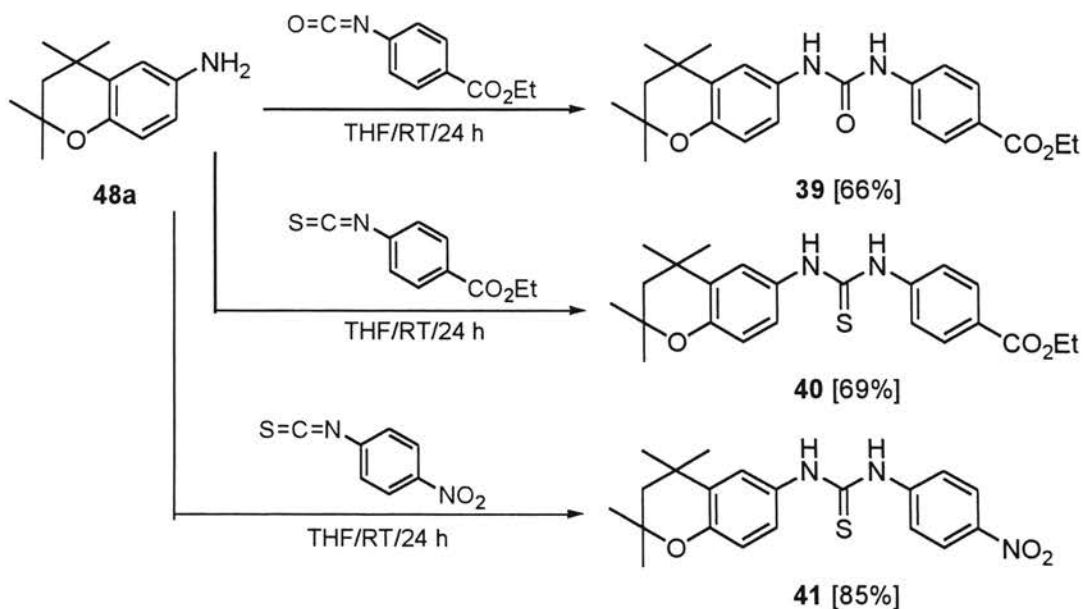
Scheme 7



Compounds **37** and **38** were both prepared in a similar fashion and involved dissolving amine **50a** in dry THF and coupling it with the required, commercially available isothiocyanate at room temperature (Scheme 7). Upon evaporation of the solvent, the crude products were recrystallized from an appropriate solvent system to afford the desired heteroarotinoids **37** and **38** with good yields (70% and 75%, respectively).

Oxygen Heteroarotinoids with a Linker Group Placed at the 6-Position of a Tetramethylchroman Moiety (39-41). Key amine **48a** was also used to synthesize the desired compounds **39-41** in a similar manner as the conversion of **50a**→**37** and **38** (Scheme 7). Amine **48a** was dissolved in dry THF and then coupled with the appropriate, commercially available isocyanate or isothiocyanate at room temperature (Scheme 8) to yield the crude urea/thiourea derivatives **39-41**. Upon evaporation of the solvent, the crude products were purified by flash column chromatography and/or

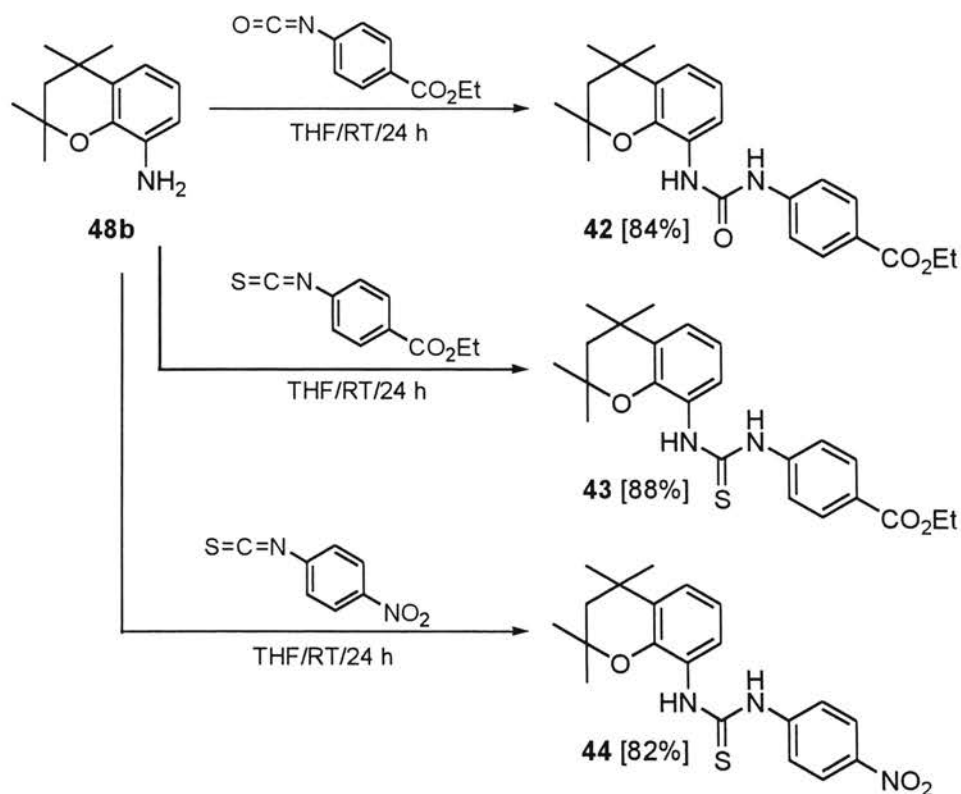
Scheme 8



recrystallization from an appropriate solvent system to afford heteroarotinooids **39-41** in good yields as shown. Of course, one conformation is drawn for **39-41**, but others are possible.

Oxygen Heteroarotinooids with a Linker Group Placed at the 8-Position of a Tetramethylchroman Moiety (42-44). As with amine **48a**, **48b** was further utilized to obtain certain desired heteroarotinooids. Amine **48b** (under similar conditions as in the conversions of **48a**→**39-41**, Scheme 8), dissolved in dry THF, was coupled with the appropriate, commercially available isocyanate or isothiocyanate at room temperature (Scheme 9) to yield the crude compounds **42-44**. Upon evaporation of the solvent, the

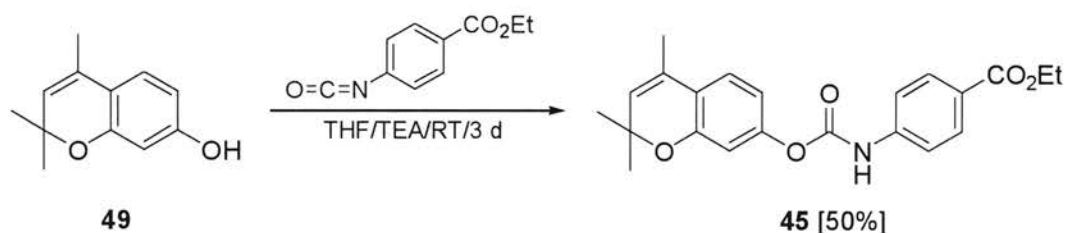
Scheme 9



products were purified by flash column chromatography and/or recrystallization from an appropriate solvent system to afford heteroarotinooids **42-44** in good yields.

Oxygen Heteroarotinoid with a Linker Group Placed at the 7-Position of a Trimethylchromen Moiety (45). The target carbamate-ester **45** was prepared from key phenol **49** via a reaction of **49** with commercially available 4-ethoxycarbonylphenyl isocyanate in THF (Scheme 10). The reactants were stirred at room temperature for 3

Scheme 10



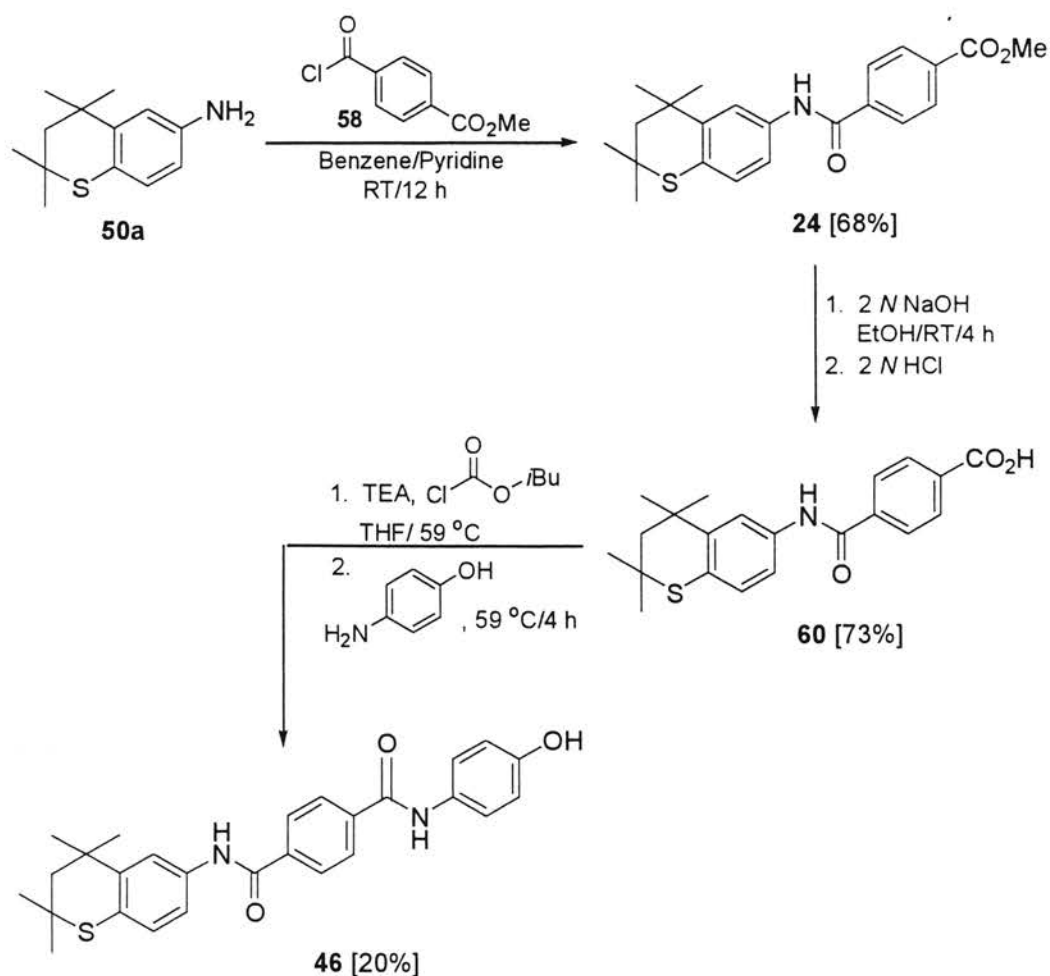
days in the presence of a catalytic amount of triethylamine (TEA). Upon evaporation of the solvent, the resulting crude material was subjected to flash column chromatography [EtOAc:hexanes (2:1)], and the resulting residue was then recrystallized [Et₂O:pentane (1:1)] to yield pure **45** (50%).

Synthesis of Heteroarotinoids Possessing a 4-Hydroxyphenylamide Moiety

Sulfur Heteroarotinoid 46. Amine **50a** was also utilized to produce target heteroarotinoid **46** via the conversion **50a**→**24**→**60**→**46** as illustrated in Scheme 11. The procedure employed in the conversion of **50a**→**24** (Scheme 11) was similar to that used in the preparation of **32** from **48a** (Scheme 4). Acid chloride **58** was added in one portion to amine **50a** (dissolved in benzene containing pyridine). After workup and purification, amide **24**¹²³ was thus obtained in good yield (70%).

Saponification of the ester group of **24**, via the reported method¹³⁵ which employed 2 *N* NaOH at room temperature (similar conditions as in the conversion **32**→**33**), was

Scheme 11



performed to afford structure **60**. Upon acidification of the reaction mixture (pH~2) using 2 N HCl, crude acid **60**¹³⁵ precipitated and was then filtered and recrystallized (EtOAc:hexanes) to yield a pure sample of acid **60** (73%).

As can be noted (Scheme 11), the conversion of **60** to the desired structure **46** essentially involves conversion of a carboxylic acid (**60**) to an amide functionality (**46**). Such conversions are quite common in the literature and provide various useful products. However, this particular case proved to be somewhat problematic. Acid **60** contains functional groups such as the sulfur atom in the fused ring and the amide group

connecting the two aryl rings both of which can be vulnerable to degradation under certain conditions. Thus, several approaches were attempted before a procedure was developed that would successfully effect the desired conversion **60**→**46**.

The first attempt involved the conversion of acid **60** to the corresponding acid chloride (using SOCl₂) which could then be coupled with commercially available 4-aminophenol to produce the desired product **46**. However, the reaction of **60** and SOCl₂ resulted in a complex mixture of products, even at ambient temperatures (this might be expected due to the presence of the amide function connecting the two aryl rings). It has been reported that the conversion of acid groups to the corresponding acid chlorides can be accomplished by the reaction of SOCl₂ with molecules that may be vulnerable to such conditions (such as penicillins) by careful control of the reaction stoichiometry.¹³⁷ However, the procedure¹³⁷ required an addition of precise equivalents of pyridine and then maintaining cold temperatures (-20 °C) over several hours. Therefore, a more straightforward approach was sought to effect the conversion **60**→**46**.

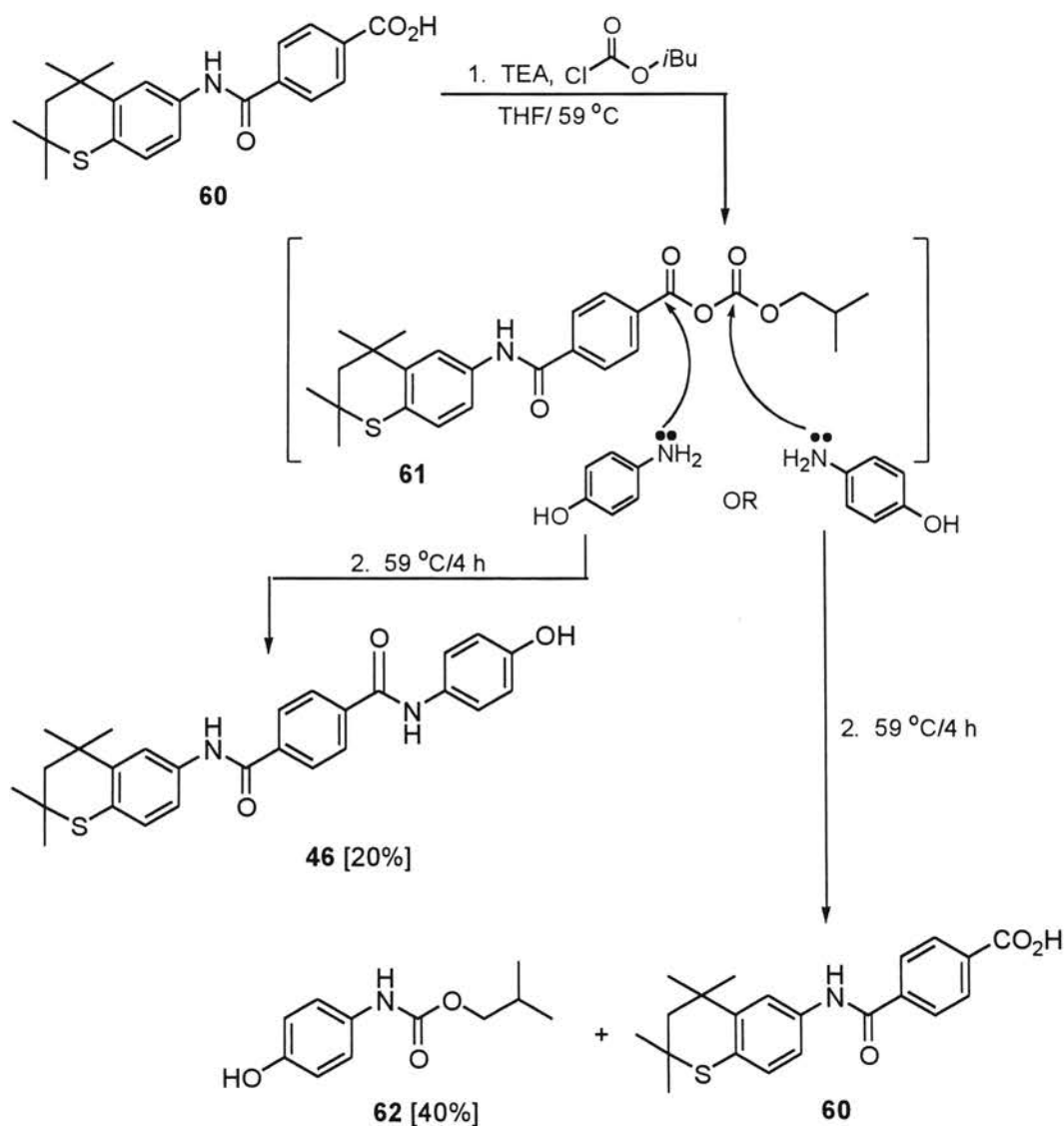
The second approach used in producing **46** from **60** was to form the amide bond of **46** via the reaction of 4-aminophenol with the corresponding acid bromide of **60** (generated *in situ*). Barstow and Hruby¹³⁸ reported the synthesis of various amides from the corresponding amines and acid bromides, generated *in situ* from the actions of Ph₃P and BrCCl₃ on the corresponding carboxylic acid in THF. However, attempts to use this technique resulted in **46** being generated in low yields (<10%), and purification was very difficult by standard procedures.

It was found that isobutyl chloroformate had been employed in a mixed anhydride method to produce amides from the corresponding carboxylic acids containing a variety

of sensitive functional groups.¹³⁹ Acid **60** was placed in dry THF along with triethylamine (TEA), and the resulting mixture was stirred at room temperature for 45 minutes. Isobutyl chloroformate was then added to the reaction mixture at room temperature, and the resulting mixture was heated at 59 °C for 1.5 hours. A solution of 4-aminophenol in pyridine was then added to the new reaction mixture, and the resulting mixture was stirred at 59 °C for 4 hours. After reaction workup, purification by flash column chromatography [ethyl acetate:hexanes (2:1)] and recrystallization [methanol:H₂O (13:8)] provided pure **46**, albeit in modest yield (20%).

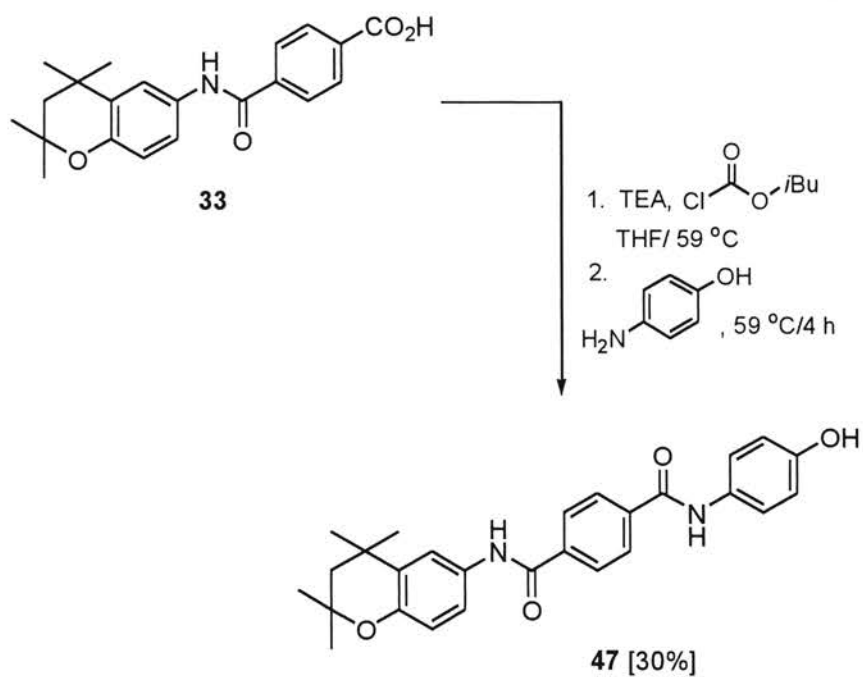
The low yield of this reaction may be due, in part, to two factors, the first of which is the modest solubility of the starting acid **60** in the solvent (THF). The second, and perhaps less obvious reason for the low yield of **46**, may be competitive processes leading to several products (Scheme 12). The reaction of isobutyl chloroformate with the acid group of **60** likely produces the mixed anhydride **61**. The latter has two carbonyls that may undergo nucleophilic attack by the nitrogen atom of 4-aminophenol. If the carbonyl closer to the aromatic ring of the anhydride reacts with 4-aminophenol, then the desired compound **46** is formed. However, if the carbonyl further away from the aromatic ring undergoes nucleophilic attack by 4-aminophenol, then the starting acid **60** is reformed along with the production of a carbamate by-product **62**. The carbonyl closer to the aryl ring should be the more reactive of the two. However, the carbonyl further from the aryl ring is apparently somewhat reactive due to the observed formation of the carbamate by-product **62** (structure suggested by NMR analysis), which was separated from the product mixture in a yield of 40%.

Scheme 12



Oxygen Heteroarotinoid 47. Once a protocol had been developed which provided **46**, the same method was employed to obtain the oxygen analog **47**. Thus, **47** was synthesized (via a method essentially identical to that in the conversion of **60**→**46**) from structure **33** (Scheme 13).

Scheme 13



Acid **33** was placed in a reaction vessel with isobutyl chloroformate (using the mixed anhydride method)¹³⁹ and coupled with commercially available 4-aminophenol. After reaction workup and purification via flash column chromatography [EtOAc:hexanes (2:1)] and recrystallization [MeOH/H₂O (13:8)], pure **47** was obtained (30%). The increased yield of **47** (30%), as compared to that **46** (20%, Scheme 11), may be partially due to the increased solubility of acid **33** (the starting material in the production of **47**) in the solvent (THF) as compared to the solubility of acid **60** (the starting material in the production of **46**) in THF.

NMR Analysis of Select 8-isomer Oxygen Heteroarotinoids

Through ¹H NMR analysis of the target products (**32-47**), an interesting spectral feature was noted in the oxygen-containing heteroarotinoids that have a three-atom linker

attached at the 8-position of the tetramethylchroman group (**42-44**). More specifically, compounds **42-44** have a urea (**42**) or thiourea (**43** and **44**) linker group attached at the 8-position. It was observed that the proton attached to carbon atom 7 (C7) of the tetramethylchroman ring system (Figure 14) in structures **43** and **44** (which both contain a thiourea linker group) demonstrated a broadened peak (see Plates XXXV and XXXVIII – Experimental section), while the same proton in **42** (which contained a urea linker group) showed a very sharp signal (see Plate XXXII – Experimental section). Therefore, further spectral investigation of these compounds was warranted to derive a possible explanation for the observation.

Since both **43** and **44** demonstrated a broadened signal ($\sim \delta$ 7.6), **44** was chosen as a single model for the investigation. First, peak assignments were established for the hydrogen atoms at the C5, C6, and C7 positions of the aromatic ring within the fused ring system via the use of two dimensional NOESY (2D NOESY) and 2D double-quantum COSY (2D DQCOSY) analysis. The 2D NOESY (Plate XL) spectrum showed a cross peak between the geminal dimethyl protons of C4 (δ 1.36) and a proton at δ 7.22, indicating that the signal at δ 7.22 likely corresponded to the aromatic proton attached to C5. In addition, the 2D NOESY spectrum showed a somewhat strong cross peak between the C5 proton (δ 7.22) and the proton signal at δ 6.96, and the 2D DQCOSY (Plate XLI) showed an intense cross peak between the C5 proton (δ 7.22) and the proton signal at δ 6.96, indicating that the signal at δ 6.96 likely corresponded to the proton attached to C6. Furthermore, the 2D DQCOSY demonstrated a cross peak between the C6 proton (δ 6.96) and the broad signal at δ 7.62. Considering each of these pieces of

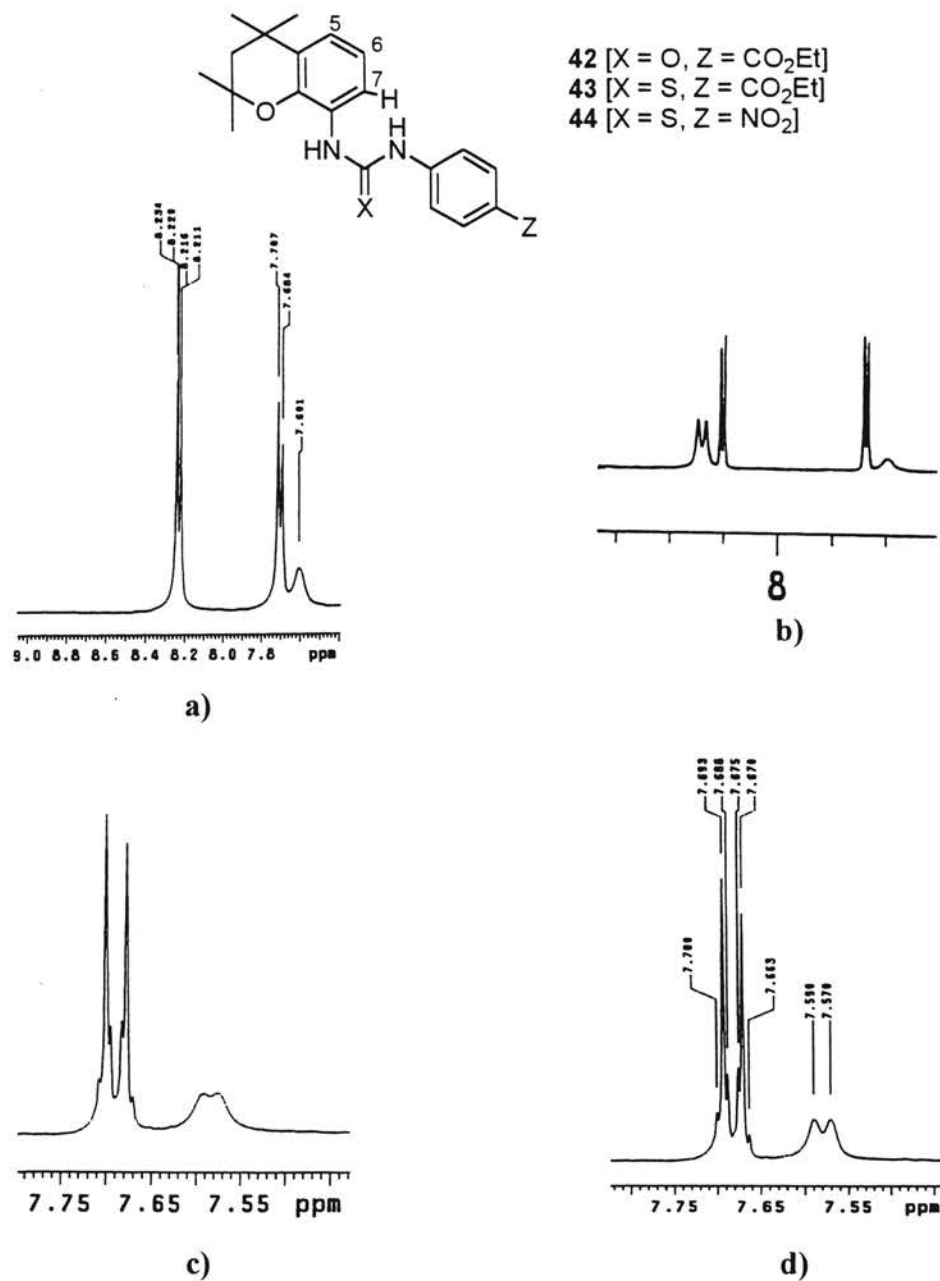


Figure 14. ^1H NMR spectra sections (spectral regions $\sim \delta$ 7.4– δ 9.0) from spectroscopic experiments conducted on heteroarotinoid **44**: (a) D₂O exchange at 22 °C, (b) ^1H NMR at 22 °C, (c) ^1H NMR at 30 °C, (d) ^1H NMR at 40 °C. Spectra were obtained at 400 MHz using DCCl₃ as the solvent and were referenced to TMS.

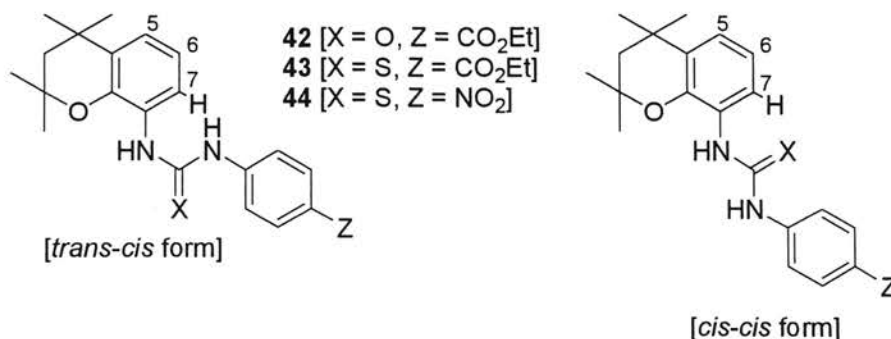
information, it was concluded that the broad signal at δ 7.62 in the ^1H NMR spectrum of **44** likely arose from the hydrogen (H7) attached to C7 of the tetramethylchroman ring system.

To ensure that the signal at δ 7.62 did not correspond to an $-\text{NH}-$ proton, a deuterium exchange NMR experiment was conducted on **44**. It was found that two signals (δ 8.30 and δ 8.34) were greatly reduced in height and the broad signal occurring at 7.62 ppm was not affected. This observation provided further support of the hydrogen atom position assignment established from the 2D NMR experiments by suggesting that the signal occurring at δ 7.62 arose from a hydrogen attached to an aromatic carbon (C7) rather than a nitrogen atom of the thiourea linker group.

Finally an explanation for the H7 signal (δ 6.96) broadening was sought. Structure **44** contains a quadrupole nucleus (^{14}N), and its effect on H7 cannot be eliminated from consideration. The signal broadening may also be due to a dynamic property inherent to the molecular structure of thioureas. Galabov and co-workers¹⁴⁰ demonstrated, through IR and ^1H NMR spectroscopy, that N,N' -diaryl-substituted thioureas in organic solvents (CCl_4 , C_2Cl_4 , CHCl_3 , CH_2Cl_2) at room temperature exist in a complex equilibrium between several rotational conformations of the $-\text{C}(\text{S})-\text{NH}-$ group. In fact, it was reported that the substituted thioureas had several rotational isomers of the type *cis-cis*, *cis-trans*, *trans-cis*, and *trans-trans*, depending on the size of the substituents on the nitrogen atoms. Furthermore, Galabov noted that these various conformations apparently had relatively short lifetimes (and low concentrations), resulting in difficult conformational analysis by ^1H NMR at room temperature.¹⁴⁰

Therefore, a temperature variation ^1H NMR experiment was conducted for **44** in an effort to resolve the rotational isomerism issue, and the results are illustrated in Figure 14. Figure 14 is comprised of small sections (spectral regions ranging $\sim \delta 7.4 - \delta 9.0$) of four distinct spectra (a, b, c, and d) of compound **44**. The spectra listed are a) deuterium exchange, b) ^1H NMR at room temperature (22 °C), c) ^1H NMR at 30 °C, and d) ^1H NMR at 40 °C. Interestingly, as the temperature was increased, the broadened signal ($\delta 7.62$) at 22 °C (Figure 14b) split into two distinct peaks at 40 °C (Figure 14d).

Thus, compounds **43** and **44** may exist in solution as a *trans-cis* form (as was drawn earlier and shown below – left) or as one of the others listed above, including possibly a *cis-cis* form (shown below – right). It is not intuitively obvious why H7 is a more



clearly defined doublet at 40 °C as compared to a broad signal at room temperature. Possibly, the $^3\text{J}_{\text{H6-H7}}$ coupling to H7 at 40 °C results from an average orientation of H6 and H7 which is more nearly a perfect cisoid arrangement. It is also conceivable that the equilibrium of rotational isomers, coupled with further interaction of H7 with the electron orbitals of the bulkier sulfur atom within the thiourea group [as compared to the oxygen atom of the urea group (**42**)], arising due to the various structural conformations, could ultimately lead to broadening of the signal associated with H7 at room temperature.

Biological Activity

Rationale for the Design of Target Heteroarotinoids. Compound **32** has an amide group as a two-atom linker and is an oxygen analog of sulfur heteroarotinoid **24**,¹²³ another compound reported by our lab. As was discussed in Chapter 1 (Heteroarotinoids and Other Reduced Toxicity Retinoids section), structure **24** (Table 1) appeared to possess *pan* agonist properties and showed powerful anticancer properties against head and neck squamous cell carcinoma in nude mice, as compared to *t*-RA (**3**).¹²³ The sulfur atom in the fused ring of **24** was replaced with an oxygen atom in **32**. It was hoped that agent **32** would provide valuable insight into treatment for head and neck carcinomas.

Replacement of the sulfur atom in **24** with the less bulky oxygen atom in compound **32** was initiated because of the reported biological activity of certain oxygen heteroarotinoids.^{20a,123,125} Although heteroarotinoids containing oxygen appear, in general, to exhibit slightly lower biological activity than the sulfur- or nitrogen-containing counterparts,^{123,141} the compounds reported here contain a geminal dimethyl group adjacent to the oxygen atom, unlike those reported previously.^{50,123,125,141} It was conceived that the compact size of oxygen may allow its lone pairs to be somewhat “screened” by the flanking geminal dimethyl group, thus increasing the hydrophobic character of one end of the molecules. Hence, these agents may have improved hydrophobic interaction with the interior of the retinoid receptors,¹¹⁸ thereby increasing receptor activation and ultimately leading to enhanced anti-cancer activity. Studies of compounds with such structural features as these may certainly provide vital information

Table 1. Growth Inhibition Against Various Cancerous Cell Types by Heteroarotinoids^a

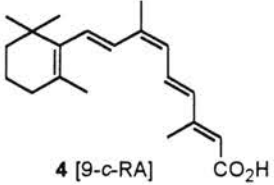
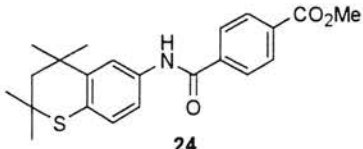
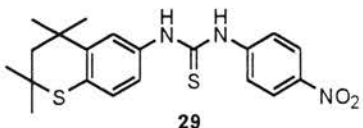
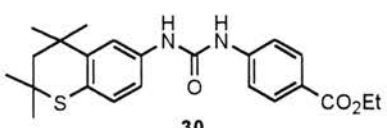
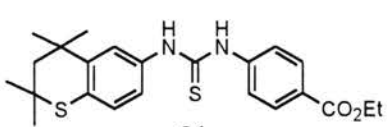
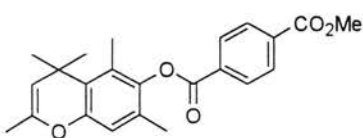
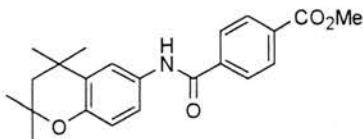
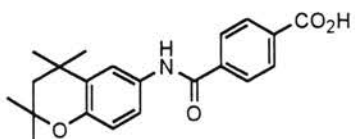
Compound	% Inhibition of Seven Cancerous Cell Types ^b						
	SCC2	UMSC2	UMSC38	SKOV3	CAOV3	SW954	SW962
 4 [9-c-RA]	13	100	100	NA	NA	NA	NA
 24	64	492 ^c	370 ^c	21	24	NA	48
 29	NA	NA	NA	85	98	NA	NA
 30	NA	NA	NA	92	95	NA	NA
 31	NA	NA	NA	94	97	NA	NA
 63	15	115 ^c	-70 ^c	NA	NA	83	84
 32	NA	NA	NA	NA	NA	NA	NA
 33	NA	NA	NA	NA	NA	NA	NA

Table 1. (Continued)^a

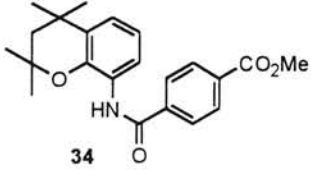
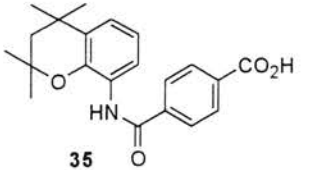
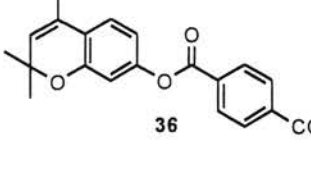
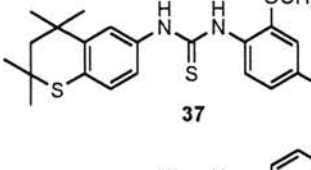
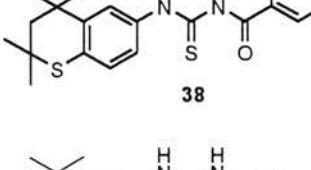
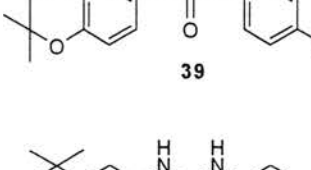
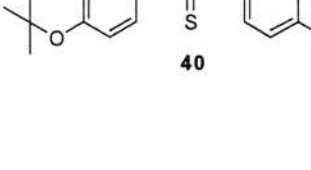
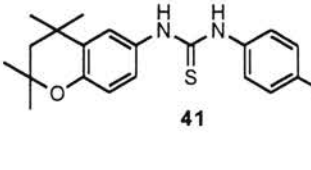
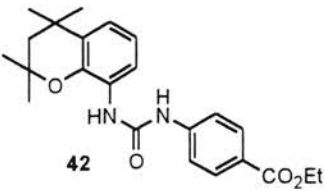
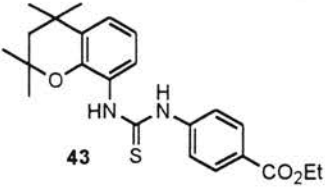
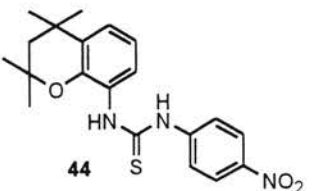
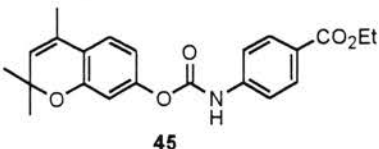
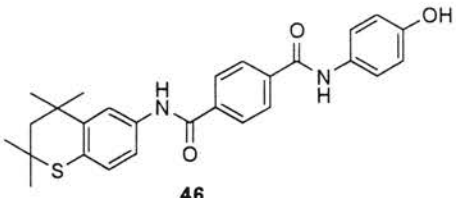
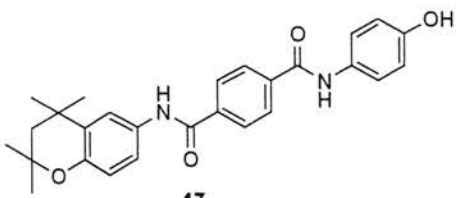
Compound	% Inhibition of Seven Cancerous Cell Types ^b						
	SCC2	UMSC2	UMSC38	SKOV3	CAOV3	SW954	SW962
 34	NA	NA	NA	NA	NA	NA	NA
 35	NA	NA	NA	NA	NA	NA	NA
 36	NA	NA	NA	NA	NA	NA	NA
 37	NA	NA	NA	NA	NA	NA	NA
 38	NA	NA	NA	NA	NA	NA	NA
 39	NA	NA	NA	NA	NA	NA	NA
 40	NA	NA	NA	NA	NA	NA	NA
 41	NA	NA	NA	NA	NA	NA	NA

Table 1. (Continued)^a

Compound	% Inhibition of Seven Cancerous Cell Types ^b						
	SCC2	UMSC2	UMSC38	SKOV3	CAOV3	SW954	SW962
 42	NA	NA	NA	NA	NA	NA	NA
 43	NA	NA	NA	NA	NA	NA	NA
 44	NA	NA	NA	NA	NA	NA	NA
 45	NA	NA	NA	NA	NA	NA	NA
 46	NA	NA	NA	NA	NA	NA	NA
 47	NA	NA	NA	NA	NA	NA	NA

^a The results presented are from biological assays performed by Dr. Doris Benbrook's group (Department of Obstetrics and Gynecology, University of Oklahoma Health Sciences Center, Oklahoma City, Oklahoma). ^b The seven cell types listed are head and neck (SCC2, UMSC2, UMSC38), ovarian (SKOV3, CAOV3), and vulvar (SW954, SW962). ^c Values listed are compared to 9-*c*-RA (**4**, 100%). NA = Not Available at this time.

about the tolerated bulk size within the hydrophobic region of the ligand-binding pocket (LBP) of the retinoid receptors.

Heteroarotinoid **33**, an oxygen analog of known acid **60**,¹³⁵ is similar to **32** but the former contains a carboxylic acid functionality as a polar tail instead of an ester as in **32**. Historically, most retinoids found in the literature contain a carboxylic acid group as a polar tail [such as *t*-RA (**3**) or TTNPB (**8**)]. It is assumed that there are various esterase enzymes within the body that could cleave the ester group, and thus, within living systems, both the acid and ester may be converted to the carboxylate anion. It has been reported that the carboxylate anion (CO_2^-) is required for receptor binding due to a “salt bridge” formation between the carboxylate group and glutamic and lysine amino acid residues of the retinoid receptors.^{40,50,142} Therefore, the carboxylic acid group was incorporated into **33** as a comparison with **32** to determine potency differences, or in the event one of these two polar end groups produced better retinoid receptor activation. In addition, the study of various tail groups, such as those that are non-ionizable, or groups that can or cannot hydrogen bond, may provide valuable insight into structural attributes necessary for reasonable bioavailability.¹⁴³

Due to the large number of pharmaceuticals that are produced and screened today, concern is rising about drugs' bioavailability through intestinal uptake, resulting from oral administration (drugs may be administered via different routes, the oral route generally being the preferred for reasons of ease and compliance by the patient).¹⁴³ It has been noted that factors to be considered in the design of drugs for oral absorption include lipophilicity, molecular size (molecular weights <500 generally having better absorption), and hydrogen-bonding (H-bonding) capability.¹⁴³ Therefore, the study of

heteroarotinoids having tail groups differing in functionality (such as **32** and **33**) may ultimately lead to anticancer agents which could be administered orally.

Compounds **34** and **35**, respectively, are similar to **32** and **33** and have an amide linker and polar end groups. However, the linker is attached to the aryl ring at the C8 position in **34** and **35** rather than at the C6 position as in **32** and **33**. Since **24** had *pan* agonist qualities (was bound by both RARs and RXRs), and **32** may have similar properties, it was conceived that moving the linker moiety from the C6 position to the C8 position may enhance binding affinity for the RXRs over that for the RARs. Movement of the linker from the C6 position to the C8 position could allow the structures to adopt a somewhat “curved” conformation, similar to 9-*c*-RA (**4**),^{40,118} which, in turn, might provide better interaction with the RXRs as compared to the RARs.

Heteroarotinoid **36** has a double bond incorporated into the fused ring. This addition to the heterocyclic ring certainly changes the hydrophobic portion of the ligands as compared to those just described, and therefore the interaction of these compounds with the hydrophobic region in the LBP of the receptors may be altered. It is uncertain what effect the unsaturation will actually produce, but a computer-aided study conducted by Klucik¹¹⁸ also indicated that the presence of such a group may have favorable interaction with the LBP of RAR- γ . Compound **36** contains an ester linker group (two-atom linker) placed in the C7 position of the aryl ring. This placement between the C6 and C8 positions, coupled with the somewhat flexible nature of the linker [which could allow the structure to assume either an ‘elongated’ conformation similar to that of *t*-RA (**3**) or a ‘curved’ conformation similar to that of 9-*c*-RA (**4**)],⁴⁰ may promote interaction with both RARs and RXRs, thus conveying **36** with *pan* agonist qualities, as has 9-*c*-RA (**4**).⁴⁶

Sulfur heteroarotinoids **37** and **38** are a continuation of the study of compounds **29-31** (Chapter 1 - Heteroarotinoids and Other Reduced Toxicity Retinoids section) which were also produced from earlier work in this lab.^{113e} Like **29**, structure **37** possesses a thiourea (three-atom) linker group. However, **37** has a methoxy group attached to the aryl ring containing the polar nitro end group. Such a modification has not been done previously and may help to “map” more accurately the area of the LBP within the receptor that provides H-bonding with the ligand. Compound **38** actually possesses a 4-atom linker rather than a 3-atom linker. The linker was extended one carbon atom by essentially inserting a carbonyl group between the thiourea linker and the second aryl ring. Some molecular modeling studies by Klucik¹¹⁸ have suggested that a 4-atom linker may be slightly too long for receptor activation as agonists, but such agents could be useful as antagonists.

Heteroarotinoids **39-41** are oxygen analogs of compounds **29-31**, which, as was discussed in the previous chapter, showed some profound anticancer characteristics (see Chapter 1, Heteroarotinoids and Other Reduced Toxicity Retinoids section).^{113e} Compounds **39-41** possess a urea functionality as a three-atom ‘linker’ group (as do the reported structures **29-31**). The urea and/or thiourea functionality was selected as a three-atom linker due to its somewhat enhanced flexible nature (compared to a pure amide), which could result in a better fit into the LBP of RARs, and therefore enhance activation. Moreover, a urea function provides two –NH– groups capable of hydrogen bonding with the receptors, which may improve RAR- γ selectivity, possibly via the formation of a hydrogen bond with the sulfur atom of the amino acid residue methionine 272 (M272) in RAR- γ .^{99,124,127,128} Due to the promising activity of heteroarotinoids **29-31**, the study of

the urea group as a three-atom linker has been extended to the oxygen analogs **39-41**, whose synthesis is described within this thesis.

The presence of a sulfur atom within the linker group (thiourea, **40**), as opposed to an oxygen atom (urea, **39**), may provide insight on the influence of size and electronegativity of the carbonyl or thiocarbonyl function within the linker group in terms of influence on receptor activation and/or selectivity. In addition, modulation of the polar “tails” of the compounds [as in the exchange of an ester functionality (**40**) for a nitro group (**41**)] was done to further explore the more polar region of the LBP of the retinoid receptors responsible for H-bonding^{21b,21c,22,23} and to determine potency differences in the event one of these two polar tail groups produced better retinoid receptor activation. It is expected that studies on agents with a urea or thiourea linker, such as **39-41**, may ultimately lead to the production of compounds that are highly RAR- γ selective.

Heteroarotinoids **42-44** are 8-isomer analogs of **39-41** (as **34** and **35** are 8-isomer analogs of **32** and **33**). This alignment of the linker group (attached in the 8 position of the tetramethylchroman group as in **34** and **35**) with respect to the aryl moieties is expected to suppress the binding affinity for the RARs. Again, movement of the linker from the C6 position to the C8 position could allow the structures to adopt a somewhat “curved” conformation, similar to 9-*c*-RA (**4**),^{40,118} and thus compounds **42-44** may be RXR family selective.

Heteroarotinoid **45** (like **36**) has a double bond incorporated into the fused ring system. Unlike **36**, however, **45** possesses a carbamate function as a three-atom linker group. Like the urea group (as in **39-41** or **29-31**), the carbamate linker (as in **45**) also possesses a –NH– group that may provide hydrogen bonding with amino acid residues

within the interior of the retinoid receptors. Furthermore, the carbamate linker group of **45** (like **36**) was placed in the C7 position of the aryl ring, which may promote interaction with both RARs and RXRs, thus endowing **45** with *pan* agonist qualities, as has 9-*c*-RA (**4**).⁴⁶

The unusual heteroarotinoid **46** was produced with the intent of mimicking the apoptotic properties of 4-HPR (**18**). The synthesis of **46** was also spurred by the impressive anticancer properties of compound **24**,¹²³ which is a synthetic precursor of **46** (see Scheme 11). As was discussed in Chapter 1 (Classification of Retinoids – Apoptosis), clinically employed 4-HPR (**18**) is well known for the ability to induce programmed cell death (apoptosis) in a variety of tissues.¹¹³ This quality may be due to the 4-hydroxyphenylamide functionality on the polar end of the molecule's structure, as certain studies suggest.^{112b,113e,115,116} It was originally assumed that a study of heteroarotinoids possessing a 4-hydroxyphenylamide group would have already been performed, but none was found in the literature. Therefore, heteroarotinoid **46**, which possesses a 4-hydroxyphenylamide group, was synthesized for exploration of the therapeutic potential of heteroarotinoids possessing this functionality.

Structure **47** is the oxygen analog of sulfur heteroarotinoid **46**. The replacement of the sulfur atom in **46** by oxygen may aid to elucidate the pathways by which compounds structurally similar to 4-HPR (**18**) could mimic its action and exhibit apoptotic properties. As was discussed in Chapter 1 (Classification of Retinoids – Apoptosis), the exact mechanism by which 4-HPR (**18**) produces its apoptotic effects is a matter of some controversy.^{112b,113e,115,116} Certain studies suggest that 4-HPR (**18**) acts via retinoid receptor-dependent pathway,¹¹⁶ while other studies state that the action of 4-HPR (**18**)

results from retinoid receptor-independent mechanisms.¹¹⁵ Therefore, the study of sulfur and oxygen analogs **46** and **47** could provide valuable information regarding this matter, in the event that one of these compounds (**46** or **47**) demonstrated better apoptotic characteristics than does 4-HPR (**18**).

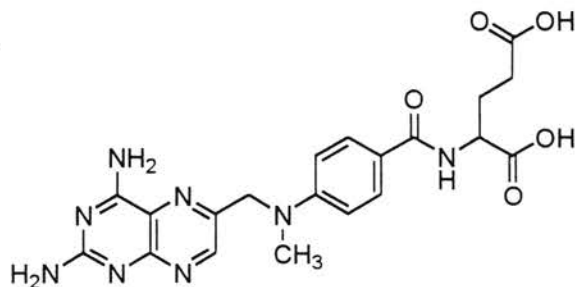
As can be noted in Table 1, compounds **24**, **29-31**, and **63** produced from earlier work by our lab^{113e,123} demonstrated promising inhibition properties against various cancerous cell lines, including ovarian, vulvar, and head and neck carcinomas. Although the compounds reported in this thesis have not yet been tested for anticancer activity, several of the agents structurally resemble heteroarotinoids **24**, **29-31**, and **63**. Thus it is anticipated that a study of such agents reported herein will provide valuable insight on structural characteristics required for optimum anticancer activity in these select types of cancer. Heteroarotinoids **32** and **33** resemble **24**, compounds **39-41** are oxygen analogs of **29-31**, and **36** is slightly similar to **63** (Table 1).

Anti-tuberculin Activity of Heteroarotinoids. *Mycobacterium tuberculosis* (*M. tuberculosis*, or Mtb) is a human pathogen causing tuberculosis (TB), is responsible for the death of millions of people each year, and continues to claim more lives than any other single infectious agent.¹⁴⁴ Its pathogenicity arises from the ability to survive in host cells by colonizing macrophages and remaining quiescent for long periods of time, only to become active decades later.¹⁴⁵ About one-third of the world's population is infected with Mtb, 10% of which will develop the disease at some point in their lives.¹⁴⁶ The current treatment for active TB is a four-drug regimen comprised of isoniazid, rifampin, pyrazinamide, and ethambutol for a period of at least six months.¹⁴⁷ The failure of patients to complete the therapy has led to the emergence of multi-drug-resistant (MDR)

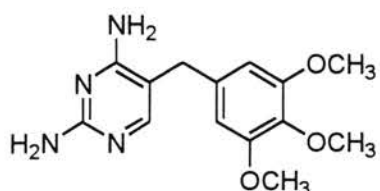
tuberculosis. The growing number of cases of MDR tuberculosis has become such a public health threat that the World Health Organization (WHO) has declared TB a global public health emergency.¹⁴⁸ Thus, greater efforts are needed in investigating the molecular basis of TB pathogenicity and in developing high efficacy drugs as key targets for Mtb treatment.

One approach that has been taken in the fight against TB is the development of drugs that will successfully inhibit the actions of the enzyme Dihydrofolate Reductase (DHFR). DHFR is essential for folate metabolism in both eukaryotic and prokaryotic cells.¹⁴⁹ The enzyme catalyzes the NADPH-dependent reduction of dihydrofolate to tetrahydrofolate which is involved in a variety of biochemical functions involving single-carbon transfers. The reduced form of folate is a precursor of cofactors necessary for the synthesis of thymidylate, purine nucleotides, methionine, serine, and glycine required for DNA, RNA, and protein synthesis. Selective DHFR inhibitors are playing an important role in the treatment of bacterial, protozoal, and fungal infections.¹⁵⁰ In addition, DHFR inhibitors have been shown to be useful in the treatment of patients infected both by HIV and Mtb.¹⁵¹

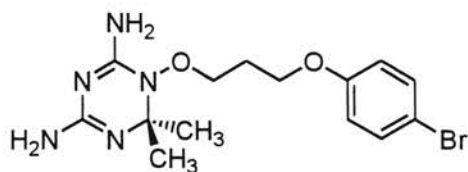
Because rapidly dividing cells have a great demand for DNA and protein synthesis and DHFR promotes such activity, inhibition of this enzyme by methotrexate (MTX, **64**), an anti-inflammatory and immunosuppressive agent, has been exploited in cancer chemotherapy.¹⁵² Trimethoprim (TMP, **65**) is a potent inhibitor of bacterial DHFR, but only a weak inhibitor of mammalian DHFRs.¹⁴⁵ Agent Br-WR99210 (**66**), a bromine analog of Triazine (WR99210), has been instigated in the inhibition of malarial DHFR.¹⁴⁵



64 [Methotrexate, MTX]



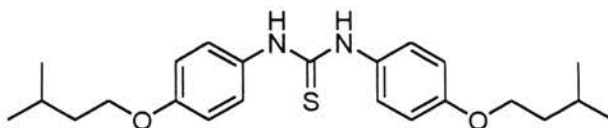
65 [Trimethoprim, TMP]



66 [Br-WR99210]

A structural comparison study of human and tuberculosis DHFRs performed by Hol and co-workers¹⁴⁵ provided some useful observations in the search for new TB drug treatments. Through a sequence alignment of the amino acids in human and Mtb DHFRs, Hol noted only a ~26% sequence identity and indicated key differences that might be considered in the future development of selective Mtb DHFR inhibitors.

Isoxyl (**67**), a powerful inhibitor of bacterial DHFRs, has demonstrated potent activity against various *Mycobacterium* strains, including *Mycobacterium tuberculosis* (Mtb).¹⁵³



67 [Isoxyl]

As can be noted, **67** contains a thiourea group connecting two aryl rings and is somewhat similar in structure to several compounds (such as **39-44**) reported in this thesis. This

striking structural resemblance thus prompted the screening of several heteroarotinioids produced by our lab for use as anti-bacterial agents.

The fifteen heteroarotinioids listed in Table 2 were tested for anti-bacterial activity against *Mycobacterium bovis* (BCG) and compared to that of Isoxyl (**67**). As can be noted in Table 2, the results are listed as MIC values (note the results in Table 2 are listed in order of decreasing activity – read from left to right, top to bottom). The MIC value has been defined as the lowest concentration (in $\mu\text{g/mL}$) of Isoxyl (**67**), or other standard agent, resulting in 99% reduction in the number of bacterial colonies on that plate compared to those on a plate free of the drug at the same suspension of the bacterial culture dilution (for assay details see Determination of MICs, Experimental section – Chapter III).¹⁵³ Isoxyl (**67**) demonstrated a MIC value of 0.5 against BCG (Table 2), indicating potent anti-bacterial activity. Most of the heteroarotinioids in the study demonstrated somewhat weak anti-bacterial activity with MIC values >20.0 . However, compounds **41** and **69** exhibited reasonable activity, each having MIC values of 20.0, while **40** and **68** each displayed somewhat promising activity with MIC values of 10.0. Interestingly, heteroarotinioid **36**, which appears less structurally similar to **67** than other heteroarotinioids tested, such as **31** or **40**, demonstrated the best activity (as compared to the other heteroarotinioids) against BCG with a MIC value of 2.0.

A computer aided crystallographic study conducted by Hol and co-workers¹⁴⁵ may help establish an explanation for the observed potent anti-bacterial activity of **36**. Three crystal structures of *M. tuberculosis* DHFR, an enzyme quite structurally similar to BCG DHFR,¹⁵³ bound to different inhibitors was reported.¹⁴⁵ The three inhibitors of Mtb

Table 2. Anti-Bacterial Activity of Heteroarotinoids Against *M. bovis*^{a,b}

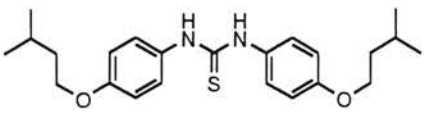
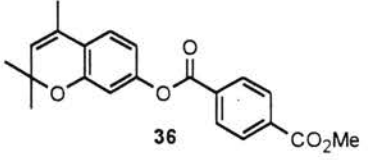
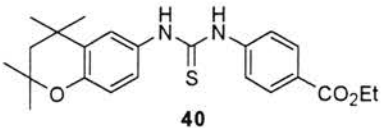
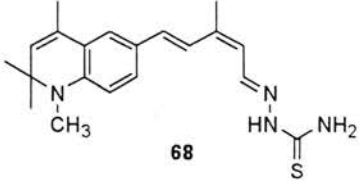
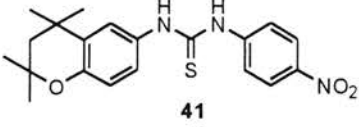
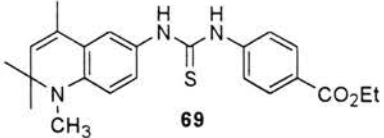
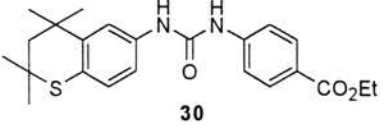
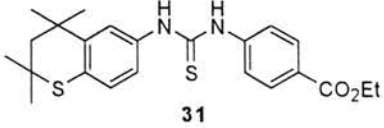
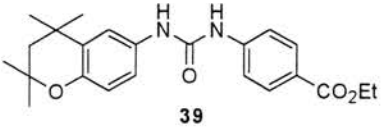
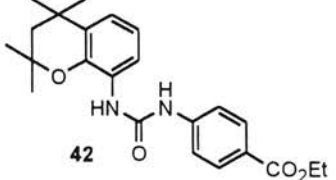
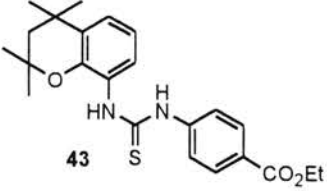
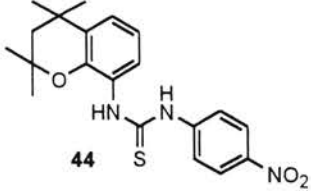
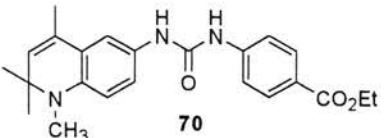
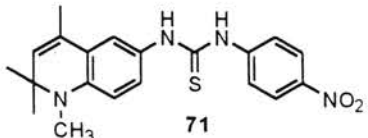
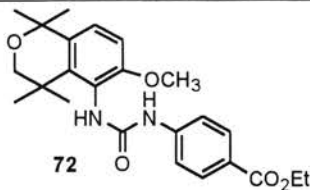
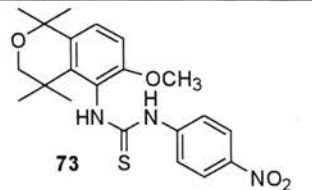
Compound	MIC ^c ($\mu\text{g/mL}$)	Compound	MIC ^c ($\mu\text{g/mL}$)
 67 [Isoxyl]	0.5	 36	2.0
 40	10.0	 68	10.0
 41	20.0	 69	20.0
 30	>20.0	 31	>20.0
 39	>20.0	 42	>20.0
 43	>20.0	 44	>20.0
 70	>20.0	 71	>20.0

Table 2. (Continued)^{a,b}

Compound	MIC ^c ($\mu\text{g/mL}$)	Compound	MIC ^c ($\mu\text{g/mL}$)
 72	>20.0	 73	>20.0

^a Results are from *Mycobacterium bovis* (BCG) being treated with the agents listed. ^b Results listed are from biological assays performed by Dr. Patrick Brennan's group (Department of Microbiology, Colorado State University, Fort Collins, Colorado). ^c MIC is the lowest concentration of the agent (in $\mu\text{g/mL}$) resulting in 99% reduction in the number of colonies on that plate as compared to those on a plate free of the drug at the same suspension of the culture dilution.

DHFR studied were methotrexate (MTX, **64**), trimethoprim (TMP, **65**), and Br-WR99210 (**66**), and Hol noted various structural modifications of the inhibitors which might be exploited to increase affinity and/or selectivity for the bacterial DHFR enzyme. Furthermore, Hol indicated various amino acid residues which appeared to be of some importance for interaction with inhibitors within the binding site of the enzyme. It was observed that all three inhibitors (**64-66**) were involved in hydrogen bond interactions with an aspartate residue (Asp27) and an ordered and conserved water molecule, both within the interior of the enzyme, via the nitrogen 1 (N1) atom of their respective ring systems.¹⁴⁵ In addition, the nitrogen-containing rings of each inhibitor appeared to be situated within a mainly hydrophobic pocket and made Van der Waals contacts with various residues of the pocket, including Ile5, Ile94, Ala6, and Gln28.¹⁴⁵ The aromatic ring of each inhibitor, along with the 1,3-dioxypyropyl linking group of Br-WR99210 (**66**), were observed to engage in hydrophobic interactions with several residues, such as Phe31, Leu50, Thr46, Ile54, and Ile57, which are slightly closer to the protein's surface than the amino acid residues listed above.¹⁴⁵ Finally, it was noted that the α -carboxyl

group of MTX (**64**) engaged in strong “salt bridge” involving -CO_2^- and two positively charged $\text{-}^+\text{NH}_3$ groups of Arg32 and Arg60, which are near the protein’s surface.¹⁴⁵

With these pieces of information, it is conceivable that a reasonable interaction between heteroarotinoid **36** and the bacterial DHFR enzyme could exist. The oxygen atom of the fused heterocyclic ring may engage in hydrogen bonding interactions with Asp27 and/or the conserved water molecule, both of which are toward the interior of the enzyme.¹⁴⁵ In addition, the double bond within the fused aromatic ring system of **36** could allow a unique interaction with Phe31 or one of the other amino acid residues noted to interact with the nitrogen-containing ring systems of **64-66**.¹⁴⁵ The aromatic ring of **36** may also be involved in hydrophobic interactions with the various residues somewhat closer to the protein’s surface, as did **64-66**.¹⁴⁵ Furthermore, if the ester group of **36** is indeed converted to the carboxylate anion within living systems as certain studies suggest,^{40,50,142} then the resulting carboxyl group could certainly be involved in “salt bridge” interactions with Arg32 and Arg60, as was the carboxyl group of MTX (**64**).¹⁴⁵

It was also observed by Hol and co-workers¹⁴⁵ that the three inhibitors (**64-66**) studied all adopted similar, curved, conformations, with the nitrogen-containing ring system oriented toward the interior of the enzyme binding site, and the aromatic ring closer to the surface. As can also be noted, **36** may have a slightly shorter “molecular length” than MTX (**64**) or Br-WR99210 (**66**). Therefore, it is conceivable that **36** may adopt a somewhat more linear conformation between the interior, hydrophobic amino acid residues and the more exterior Arg32 and Arg60 residues of the ligand binding site within the enzyme. Perhaps such a conformation would endow **36** with the observed anti-bacterial qualities. In any case, further research certainly needs to be conducted to

delineate the role of retinoids in the anti-bacterial venue. However, these observations may provide a new avenue for exploration of the therapeutic application of retinoids.

Summary

Sixteen new heteroarotinoids (**32-47**), which include oxygen-containing heteroarotinoids **32-36**, **39-45**, and **47** as well as sulfur-containing heteroarotinoids **37**, **38**, and **46**, have been synthesized. Oxygen and sulfur were chosen as heteroatoms incorporated into the fused ring systems due to the promising anticancer activity of a few reported heteroarotinoids possessing these two heteroatoms.^{20a,113e,123,125} Compounds **32-47** were designed with various structural characteristics, including two-, three-, or four-atom linker groups between the aryl rings, strategic placement of the linker groups relative to the aryl moieties, and varying polar 'tails', which may endow the agents with specific biological qualities, such as potential RAR- γ selectivity, RXR subfamily selectivity, *pan* agonist qualities, or the ability to induce programmed cell death (apoptosis).

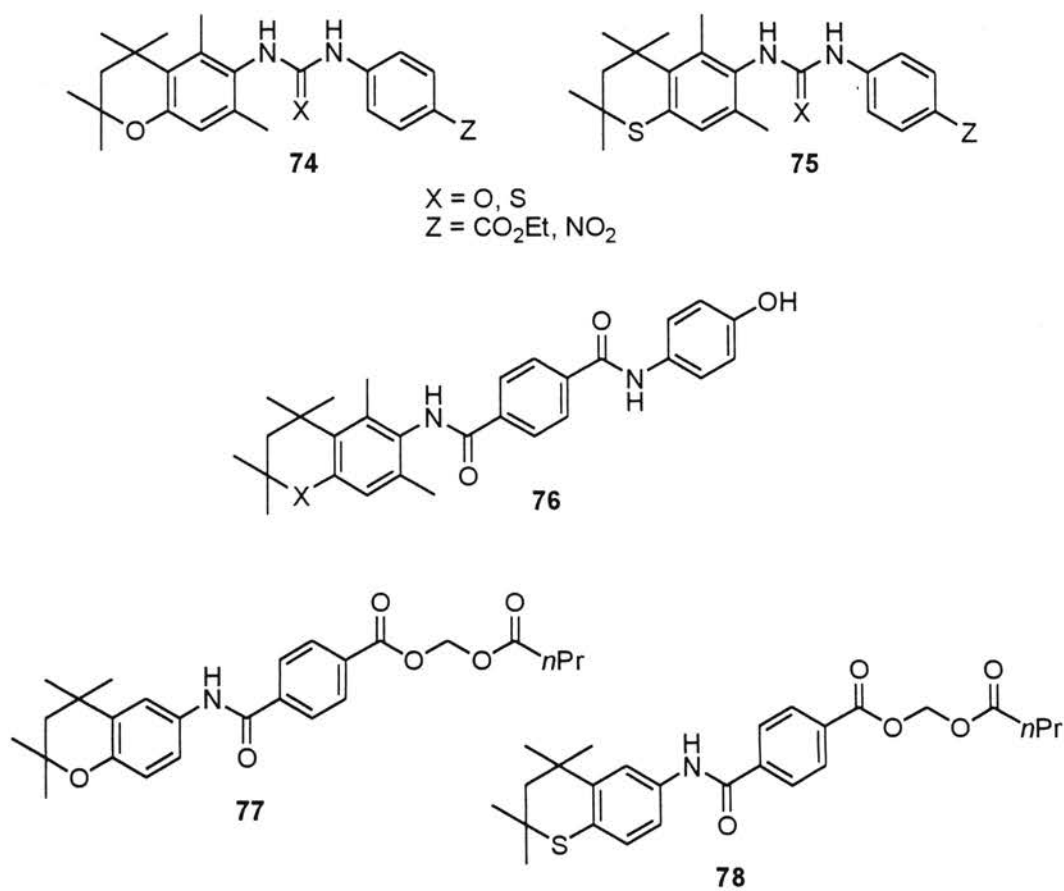
The structures have not yet been tested for their anticancer activities, but it is expected that biological studies of these agents could certainly provide valuable information for the invention of potentially effective anticancer agents possessing high activity and relatively low toxicity. However, several of the heteroarotinoids reported here were tested for antibacterial activity due to their structural resemblance to the potent antibacterial agent Isoxyl (**67**). It was discovered that two heteroarotinoids (**40** and **68**) possessed reasonable antibacterial activities against *Mycobacterium bovis* and that compound **36** possessed promising activity against the same bacteria (Table 2). Of course, more research needs to

be conducted to establish the exact role of retinoids as antibacterial agents, but these observations may ultimately lead to a new therapeutic application of retinoids.

Finally, a new and improved synthetic route to known amine **50a**¹²³ from thiochroman **56**^{126a} was developed. The new method was more straightforward, efficient, and cost-effective than the reported procedure¹²³ for the production of **50a**.

Suggestions for Future Work

Structures **74-77** are suggested as target heteroarotinoids for future synthesis and study as potential anticancer agents. The compound series **74** is similar to **39-41**, whose synthesis is described in this thesis, while the series **75** resembles structures **29-31** which



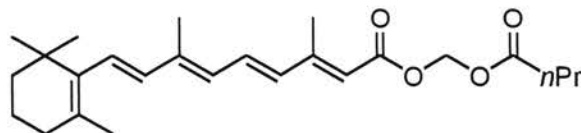
have demonstrated powerful anticancer properties,^{113e} as discussed in Chapter I. Unlike **39-41** and **29-31**, **74** and **75** each contain two methyl groups placed at the C5 and C7 positions of the chroman ring systems. The production of such compounds is encouraged due to the reported success of compounds **63**,¹²³ which contain two methyl groups positioned in the same manner, and the fact that very few compounds of this type are even reported. The study of agents with these characteristics may provide valuable information about the best tolerated bulk within the hydrophobic portion of the LBP of the retinoid receptors. Furthermore, because **39-41** and **29-31** may likely be RAR subtype selective, introducing two methyl groups in the C5 and C7 positions could serve to help “fine tune” the structural features needed for selectivity between the three isoforms (RAR- α , RAR- β , and RAR- γ) of the RAR subtype.

Structure(s) **76** are modified continuations of compounds **46** and **47** (which are reported in this thesis). Addition of the two methyl groups at the C5 and C7 positions may further aid in the delineation of the mechanism by which retinoids that are structurally similar to 4-HPR (**18**) induce apoptosis. The presence of the two methyl groups could help establish how or why compounds similar to 4-HPR (**18**) induce programmed cell death through retinoid receptor-dependent and/or receptor-independent pathways.

Compounds **77** and **78** are methylbutyrate derivatives of acids **33** and **60**, respectively. Structures **77** and **78** are suggested for future study for multiple reasons, including the reported success of compound **24**, which would be a synthetic precursor of **78**. In addition, the incorporation of the methylbutyrate moiety within the heteroarotinoid backbone may endow structures **77** and **78** with enhanced anticancer activity via prodrug

properties, which could arise from the coupled anticancer actions of **33** and/or **60** and butyric acid (BA).¹⁵⁴

Compound BA has been reported as an effective inhibitor of cell proliferation and inducer of cytodifferentiation.¹⁵⁵ In addition, BA is known to inhibit specifically the enzyme histone deacetylase (HDAC), and thus many of its biological effects may be attributed to this activity.¹⁵⁶ Recent studies may have established a link between oncogene-mediated suppression of transcription and recruitment of HDAC into a nuclear complex.¹⁵⁷ Furthermore, it has been suggested that resistance to *t*-RA (**3**) by human acute promyelocytic leukemia (APL) cell lines could be overcome by addition of HDAC inhibitors.¹⁵⁸ The inhibition of HDAC leads to histones hyperacetylation and relaxation of the chromatin structure. The chromatin conformational change allows the access of transcription factors and upregulation of gene expression.¹⁵⁹ Therefore, the combination of BA with a retinoid, such as *t*-RA (**3**), could possibly provide enhanced anticancer activity. However, BA displays low potency *in vivo* due to rapid metabolism.¹⁶⁰ Thus, Nudelman and Raphaeli¹⁵⁴ combined of BA and *t*-RA (**3**) in the form of a prodrug by producing an acyloxyalkyl ester of retinoic acid, all-*trans*-retinoyloxymethyl butyrate (**79**), in hopes of coupling the therapeutic potential of each. Compound **79** was tested for differentiation induction activity in the human myeloid leukemic cell line HL-60.¹⁵⁴ It was observed that the effective dose (ED₅₀) of **79** was 0.031 μM, which was 40-fold



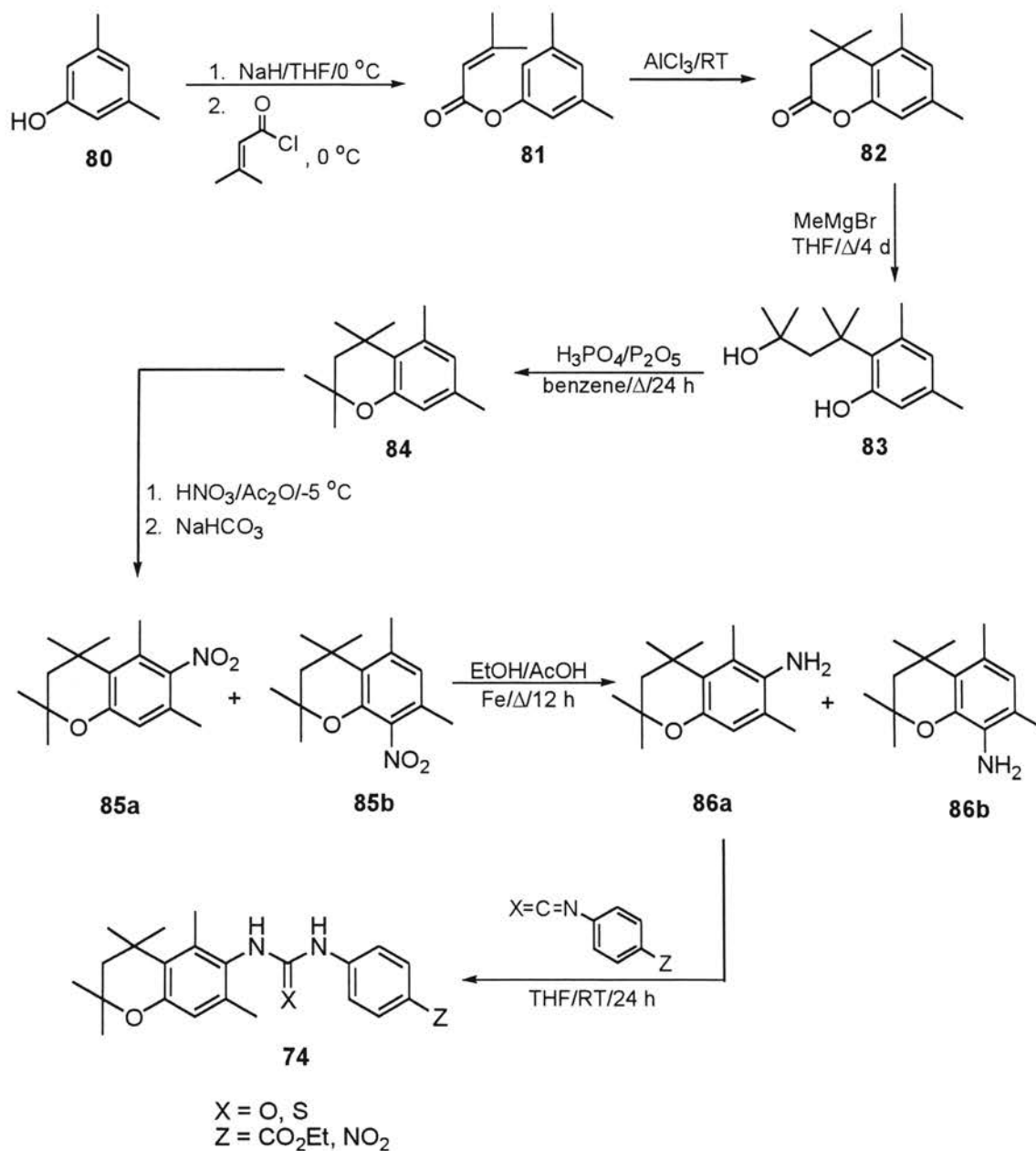
79

lower than that of *t*-RA (**3**) and over 9000-fold lower than that of BA.¹⁵⁴ Therefore, by combining the therapeutic potential of BA and heteroarotinoids through incorporation of BA into the heteroarotinoid backbone in the form of a acyloxyalkyl ester (as in **76** or **77**), an agent possessing a very low ED₅₀ may be produced, thus providing further reduction of unwanted side effects associated with retinoid treatment.

The preparation of compound(s) **74** involves the synthesis of key amine **86a** (Scheme 14). The procedure could start with commercially available 3,5-dimethylphenol (**80**) and follow the steps as shown in Scheme 14 (and described by Dawson and co-workers¹³⁰ in the synthesis of lactone **51**) for the production of intermediate lactone **82**. Once lactone **82** was obtained, the steps illustrated should be similar to those employed in the production of amine **48a** to yield the key amine **86a**. As shown in Scheme 14, an isomeric mixture of nitro compounds **85a** and **85b** is expected [as was the case for **54a** and **54b** (Scheme 1)] from the nitration of chroman **84**. The resulting 8-isomer amine **86b** could also be utilized for the production of various heteroarotinoids. Amine **86a** could be converted to the desired compound(s) **74** (Scheme 14) in a similar fashion as described for the synthesis of **39-41** from amine **48a** (Scheme 8 and related description).

Amine **92a** is needed as a starting material to acquire heteroarotinoid(s) **75**. The reaction sequence could begin with commercially available 3,5-dimethylthiophenol (**87**) and follow the steps outlined in Scheme 15 (the reaction sequence is similar to that reported^{126a} in the synthesis of thiochroman **56**) for the production of unknown thiochroman **90**. Amine **92a** could then be produced from **91a** via a procedure similar to that described for the synthesis of **50a** from **56** (Scheme 3 and related text). Generation

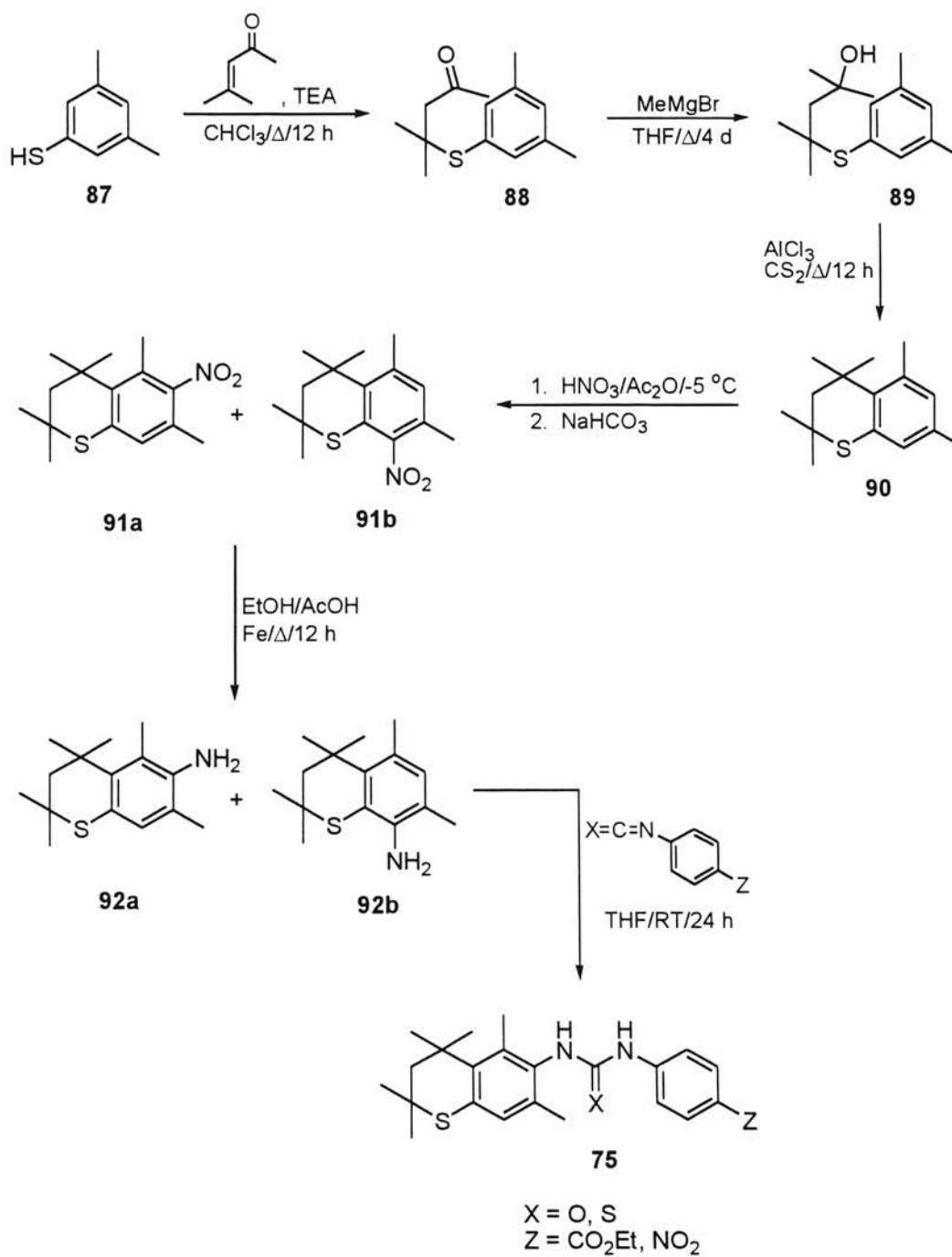
Scheme 14



of the corresponding 8-isomer amine **92b** could also be expected (as was the case with **50a** and **50b**).

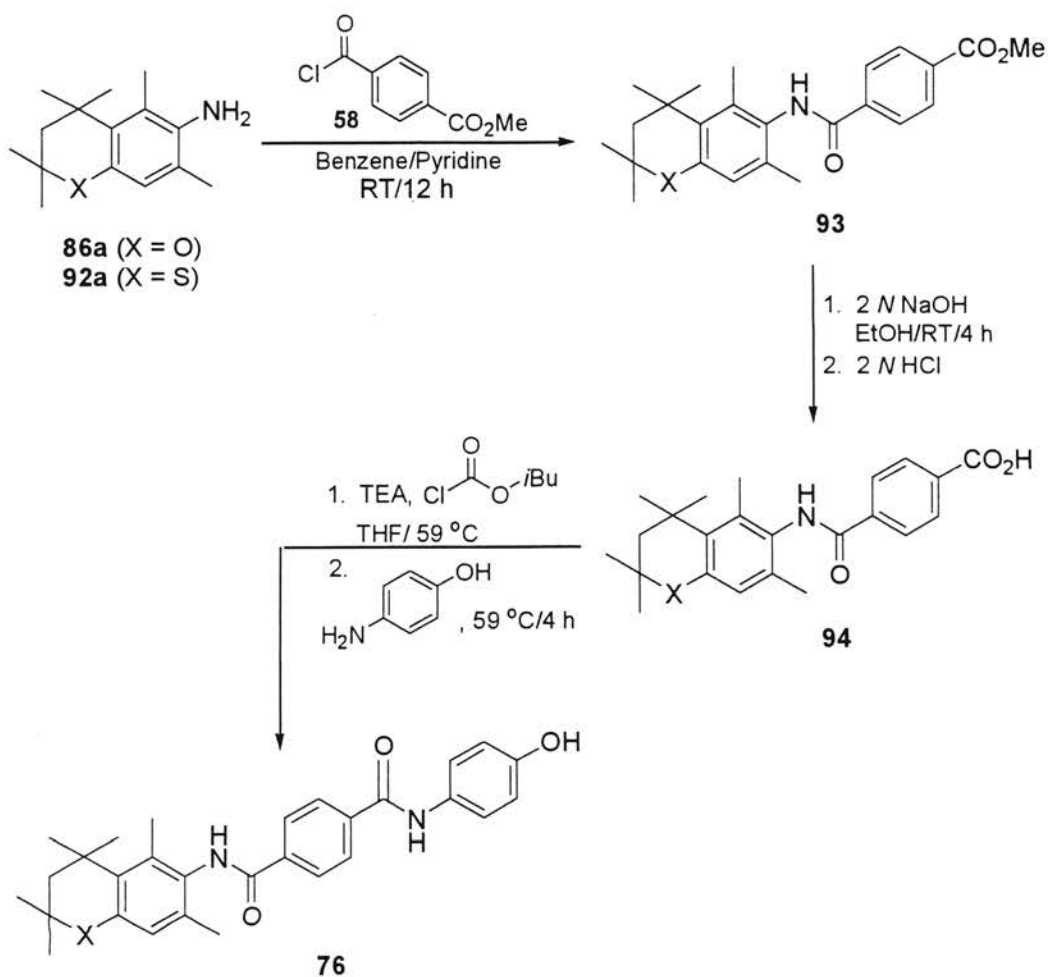
Once amines **86a** and **92a** have been afforded, each may be utilized to obtain heteroarotinoid(s) **76** via a synthetic method as outlined in Scheme 16. The procedure

Scheme 15



should be essentially the same as that employed in the production of compounds **46** and **47**, described above (see Schemes 11 and 13 and related text). As can be noted in Scheme 16, the production of structure(s) **76** would also provide intermediates **93** and **94**,

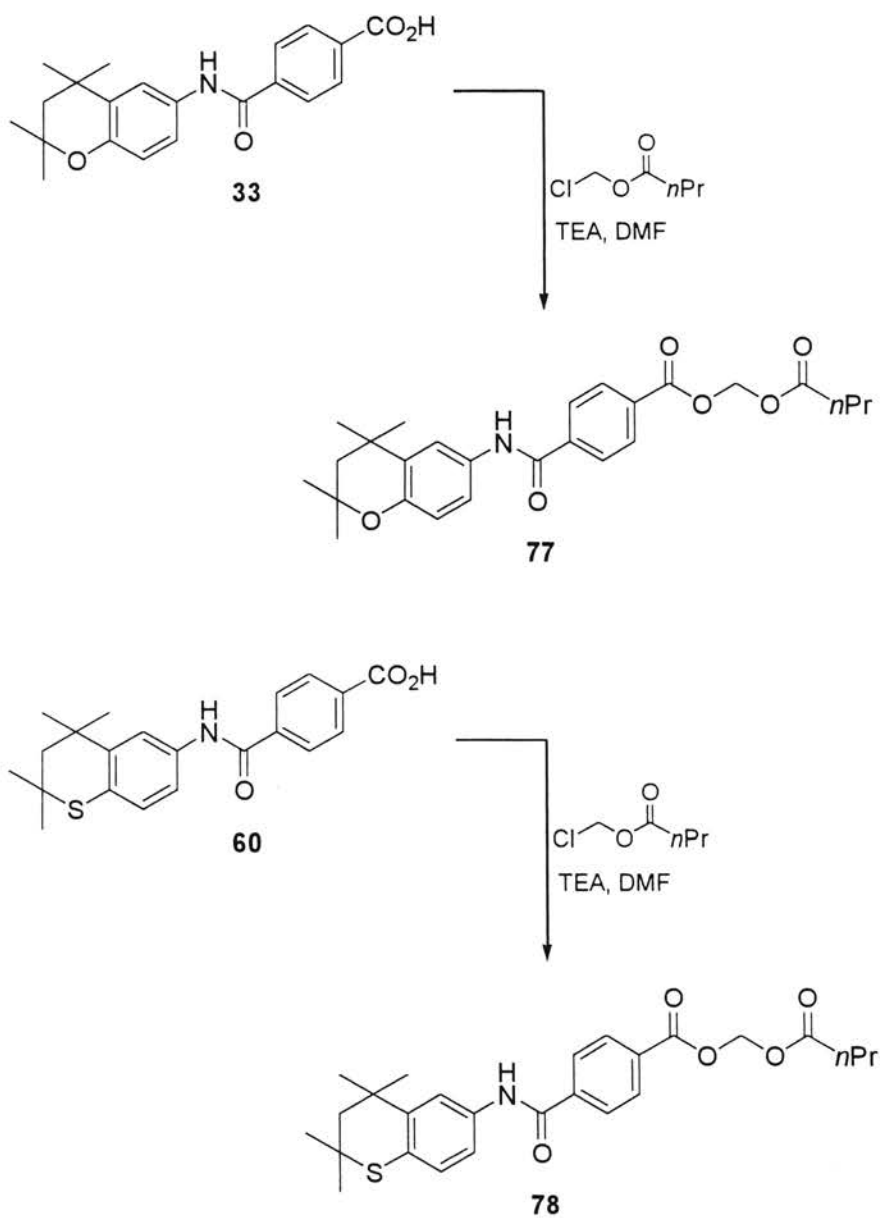
Scheme 16



which are similar in structure to heteroarotinoids **24** and **32** and **33** and **60**, respectively. Hence, **93** and **94** could also be utilized for study as possible anticancer agents, and may provide further insight into structural characteristics required for optimum retinoid receptor interaction.

A possible synthetic route to **77** and **78** is illustrated in Scheme 17. Acids **33** and **60** may be utilized, respectively, for the production of **77** and **78** via a procedure similar to that reported herein and by Nudelman and Raphaeli.¹⁵⁴ The process would involve the

Scheme 17



coupling of acid **33** or **60** with commercially available chloromethyl butyrate in the presence of triethylamine (TEA), using DMF as the solvent.

CHAPTER III

EXPERIMENTAL SECTION

General Information

When performing the synthesis of each of the intermediates and final compounds, various conditions of synthesis and techniques of purification and analysis were used in their production. Each reaction was done using magnetic stirring for thorough mixing of reagents, and each was carried out under N₂ unless otherwise stated. Commercial reagents and solvents were used as received unless otherwise noted, and anhydrous THF was obtained by distillation from a purple solution of sodium and benzophenone. All of the isocyanates and isothiocyanates used were commercially available and were obtained from Carbolabs, Inc., Bethany, CT 06524-3065, Sigma-Aldrich Corporation, Milwaukee, WI 53233, or Transworld Chemicals, Inc., Rockville, MD 20850.

Evaporation of solvents was accomplished *in vacuo* via the use of a BUCHI Rotovapor[®] R-3000 and water aspirator unless otherwise specified. For those intermediates that were liquids and required distillation for purification, vacuum distillation was employed using a Welch[®] Chemstar[™] 1402N vacuum pump with a Thomas[®] Welch vacuum gauge. For those intermediates and compounds that were solids and required purification, in addition to recrystallization, flash column chromatography was used. The chromatography was performed using J. T. Baker flash chromatography silica gel packing, 40 μm mesh.

In addition to the synthesis and purification techniques, each product was analyzed for structure and purity using IR spectroscopy, ¹H NMR spectroscopy, ¹³C NMR

spectroscopy, and TLC. Melting points of all solids were measured using a Thomas-Hoover melting point apparatus and were uncorrected. IR spectra were obtained using a Perkin Elmer 2000 Ft-IR spectrometer as films or KBr pellets, and some ^1H and ^{13}C NMR spectra were obtained using a ^{UNITY}INOVA 400 BB NMR spectrometer operating at 399.99 MHz and 100.01 MHz, respectively. In addition, some ^1H and ^{13}C spectra were recorded using a broadband Gemini 2000 High-Resolution NMR (300 MHz) spectrometer operating at 300.09 MHz and 75.46 MHz, respectively. All NMR signals were referenced to TMS. Furthermore, DCCl_3 was used as the solvent for all NMR spectra unless otherwise stated. Elemental analyses were performed by Atlantic Microlab, Inc., Norcross, GA 30091.

Methyl 4-[(2,2,4,4-Tetramethyl-3,4-dihydro-2H-chromen-6-yl)amino]carbonylbenzoate (32). Amine **48a** (0.350 g, 1.70 mmol), dissolved in dry benzene (20 mL), was placed in a 50-mL, three-necked, round-bottomed flask equipped with an N_2 inlet. To this solution was added dry pyridine (1.75 g, 1.79 mL, 22.16 mmol, 13 eq), and the resulting mixture was stirred at RT (10 min). *Mono*-methyl terephthaloyl chloride (**58**) (0.381 g, 1.82 mmol, 1.07 eq) was then rinsed into the reaction mixture in one portion with dry benzene (14 mL). The resulting reaction mixture was then allowed to stir at RT (12 h), during which time pyridinium hydrochloride precipitated as a flaky white solid. The reaction mixture was then poured into H_2O (85 mL), and the precipitate immediately redissolved in the water layer. The resulting mixture was extracted with EtOAc (4 x 35 mL), and the combined organic layers were washed successively with HCl (2 N, 4 x 35 mL), H_2O (3 x 35 mL), Na_2CO_3 (40%, 35 mL), saturated, aqueous NaHCO_3 (35 mL),

H₂O (35 mL), and brine (35 mL). The organic layer was then dried (Na₂SO₄, 12 h), and the solvent was removed *in vacuo* to give the crude amide-ester **32** as a viscous orange oil. The oil was subjected to flash chromatography [hexanes:EtOAc (3:1)], and, after the solvent was evaporated (rotovap), the pure amide-ester **32** (0.440 g, 70%) was afforded as a bright white solid: mp 148-150 °C; IR (KBr pellet) 3308 [NH], 1727 [C=O], 1650 [HNC=O] cm⁻¹; ¹H NMR (DCCl₃) δ 1.34 [s, 6 H, C(CH₃)₂], 1.35 [s, 6 H, OC(CH₃)₂], 1.83 [s, 2 H, CH₂], 3.94 [s, 3 H, OCH₃], 6.77 [d, *J* = 7.92 Hz, 1 H, Ar-*H*], 7.29 [dd, *J* = 7.91, 2.01 Hz, 1 H, Ar-*H*], 7.63 [d, *J* = 1.99 Hz, 1 H, Ar-*H*], 7.89 [d, *J* = 8.02 Hz, 2 H, Ar-*H*], 8.07 [d, *J* = 8.0 Hz, 2 H, Ar-*H*], 8.12 [s, 1 H, N-*H*]; ¹³C NMR (DCCl₃) ppm 28.38 [C(CH₃)₂], 31.06 [C(CH₃)₂], 32.67 [OC(CH₃)₂], 48.95 [CH₂], 52.38 [OCH₃], 74.54 [OC(CH₃)₂], 118.19-149.75 [Ar-*C*], 164.73 [HNC=O], 166.25 [CO₂Me]. Anal. Calcd for C₂₂H₂₅NO₄: C, 71.91; H, 6.86; N, 3.81. Found: C, 71.73; H, 6.92; N, 3.76.

4-[(2,2,4,4-Tetramethyl-3,4-dihydro-2*H*-chromen-6-yl)amino]carbonyl}benzoic Acid (33**).** Amide-ester **32** (0.270 g, 0.73 mmol), along with 95% EtOH (13 mL), was placed in a 25-mL, three-necked, round-bottomed flask equipped with a spiral condenser. The resulting mixture was stirred vigorously for 10 min, but a small amount of **32** remained undissolved. To the reaction mixture was added, dropwise, 2 *N* NaOH (3.67 mL, 7.35 mmol, 10 eq) at RT, and the resulting mixture was allowed to stir at RT (4 h). After approximately 30 min, the reaction mixture turned from slightly cloudy to completely clear. After stirring 4 h, the reaction mixture was filtered, and the filtrate was chilled to 0 °C (ice bath) and acidified (pH ~ 2) with HCl (2 *N*). At pH ~ 2 a white precipitate formed, which was filtered, washed with cold H₂O (30 mL), dried under

reduced pressure (12 h, 0.75 mm Hg, 80 °C), and recrystallized [EtOAc:hexanes (2:1)] to provide amide-acid **33** (0.190 g, 73%) as a bright white solid: mp 183-185 °C; IR (KBr pellet) 3450 [CO₂H], 3303 [NH], 1701 [C=O], 1686 [HNC=O] cm⁻¹; ¹H NMR (DMSO-*d*₆) δ 1.30 [s, 6 H, C(CH₃)₂], 1.31 [s, 6 H, OC(CH₃)₂], 1.82 [s, 2 H, CH₂], 3.36 [bs, 1 H, O-H], 6.71 [d, *J* = 8.01 Hz, 1 H, Ar-H], 7.50 [dd, *J* = 7.99, 2.03 Hz, 1 H, Ar-H], 7.73 [d, *J* = 1.99 Hz, 1 H, Ar-H], 8.06 [s, 4 H, Ar-H], 10.23 [s, 1 H, N-H]; ¹³C NMR (DMSO-*d*₆) ppm 28.10 [C(CH₃)₂], 30.62 [C(CH₃)₂], 32.65 [OC(CH₃)₂], 48.24 [CH₂], 74.05 [OC(CH₃)₂], 117.23-148.49 [Ar-C], 164.21 [HNC=O], 166.78 [CO₂H]. Anal. Calcd for C₂₁H₂₃NO₄: C, 71.37; H, 6.56; N, 3.96. Found: C, 71.73; H, 6.70; N, 3.89.

Methyl 4-[(2,2,4,4-Tetramethyl-3,4-dihydro-2H-chromen-8-yl)amino]carbonyl-benzoate (34). The amine **48b** (0.770 g, 3.75 mmol) was dissolved in dry benzene (44 mL) and placed in a 100-mL, three-necked, round-bottomed flask equipped with an N₂ inlet. To this solution was added dry pyridine (3.86 g, 3.95 mL, 48.76 mmol, 13 eq), and the resulting mixture was stirred at RT (10 min). *Mono*-methyl terephthaloyl chloride (**58**) (0.840 g, 4.01 mmol, 1.07 eq) was then rinsed into the reaction mixture in one portion with dry benzene (30 mL). The resulting reaction mixture was then allowed to stir at RT (12 h), during which time pyridinium hydrochloride precipitated as a flaky white solid. The reaction mixture was then poured into H₂O (187 mL), and the precipitate immediately dissolved in the water layer. The resulting mixture was extracted with EtOAc (4 x 77 mL), and the combined organic layers were washed successively with HCl (2 N, 4 x 77 mL), H₂O (3 x 77 mL), Na₂CO₃ (40%, 77 mL), saturated, aqueous NaHCO₃ (77 mL), H₂O (77 mL), and brine (77 mL). The organic layer was then dried

(Na₂SO₄, 12 h), and the solvent was removed *in vacuo* to give the crude amide-ester **34** as pink, clumpy solid. The solid was purified by flash chromatography [hexanes:EtOAc (3:1)], and the white solid obtained thereby was recrystallized (hexane) to give the **34** (0.800 g, 60%) as a white solid: mp 124-125 °C; IR (KBr pellet) 3366 [NH], 1713 [C=O], 1668 [HNC=O] cm⁻¹; ¹H NMR (DCCl₃) δ 1.36 [s, 6 H, C(CH₃)₂], 1.41 [s, 6 H, OC(CH₃)₂], 1.89 [s, 2 H, CH₂], 3.96 [s, 3 H, OCH₃], 6.97 [m, 1 H, Ar-H], 7.07 [dd, 8.0, 1.99 Hz, 1 H, Ar-H], 7.94 [d, 7.98 Hz, 2 H, Ar-H], 8.17 [d, 8.0 Hz, 2 H, Ar-H], 8.35 [dd, 8.01, 2.01 Hz, 1 H, Ar-H], 8.70 [s, 1 H, N-H]; ¹³C NMR (DCCl₃) ppm 28.66 [C(CH₃)₂], 31.00 [C(CH₃)₂], 32.52 [OC(CH₃)₂], 48.95 [CH₂], 52.37 [OCH₃], 75.94 [OC(CH₃)₂], 117.05-141.07 [Ar-C], 163.99 [HNC=O], 166.22 [CO₂Me]. Anal. Calcd for C₂₂H₂₅NO₄: C, 71.91; H, 6.86; N, 3.81. Found: C, 72.13; H, 6.95; N, 3.84.

4-[(2,2,4,4-Tetramethyl-3,4-dihydro-2H-chromen-8-yl)amino]carbonyl}benzoic Acid (35). The amide-ester **34** (0.38 g, 1.03 mmol), along with 95% EtOH (17 mL), was placed in a 50-mL, three-necked, round-bottomed flask equipped with a spiral condenser. The resulting mixture was stirred vigorously (10 min), but a small amount of **34** remained undissolved. To the reaction mixture was added, dropwise, 2 N NaOH (5.17 mL, 10.34 mmol, 10 eq) at RT, and the resulting mixture was allowed to stir at RT (4 h). After approximately 30 min, the reaction mixture turned from slightly cloudy to completely clear. After stirring 4 h, the reaction mixture was filtered, and the filtrate was chilled to 0 °C (ice bath) and acidified (pH ~ 2) with HCl (2 N). At pH ~ 2 a white precipitate formed and was filtered, washed with cold H₂O (40 mL), dried under reduced pressure (12 h, 0.75 mm Hg, 80 °C). Thus, amide-acid **35** (0.190 g, 73%) was obtained pure as a white

solid: mp 225-227 °C; IR (KBr pellet) 3415 [NH], 3352 [CO₂H], 1701 [C=O], 1672 [HNC=O] cm⁻¹; ¹H NMR (DMSO-*d*₆) δ 1.32 [s, 6 H, C(CH₃)₂], 1.34 [s, 6 H, OC(CH₃)₂], 1.85 [s, 2 H, CH₂], 3.38 [bs, 1 H, O-*H*], 6.92 [m, 1 H, Ar-*H*], 7.20 [dd, 7.96, 1.91 Hz, 1 H, Ar-*H*], 7.75 [dd, 7.99, 2.0 Hz, 1 H, Ar-*H*], 8.02 [d, 7.96 Hz, 2 H, Ar-*H*], 8.10 [d, 7.99 Hz, 2 H, Ar-*H*], 9.33 [s, 1 H, N-*H*]; ¹³C NMR (DMSO-*d*₆) ppm 27.98 [C(CH₃)₂], 30.67 [C(CH₃)₂], 32.49 [OC(CH₃)₂], 48.30 [CH₂], 75.22 [OC(CH₃)₂], 119.80-143.70 [Ar-C], 164.25 [HNC=O], 166.71 [CO₂H]. Anal. Calcd for C₂₁H₂₃NO₄: C, 71.13; H, 6.56; N, 3.96. Found: C, 70.76; H, 6.58; N, 3.93.

2,2,4-Trimethyl-2*H*-chromen-7-yl 4-(methoxycarbonyl)benzoate (36). In a 25-mL, three-necked, round-bottomed flask, equipped with two addition funnels and a N₂ inlet, was placed NaH (0.054 g, 2.14 mmol, 1.02 eq) and dry THF (1 mL). The resulting suspension was chilled to 0 °C (ice bath), and then the phenol **49** (0.400 g, 2.10 mmol), in THF (3 mL), was added dropwise (5 min). After the addition was complete, the resulting mixture was allowed to stir (5 min), and then acid chloride **58** (0.464 g, 2.33 mmol, 1.1 eq) in THF (2 mL) was added dropwise. The resulting mixture was allowed to warm to RT slowly and was then stirred for an additional 12 h. The final mixture was then poured into H₂O (15 mL) containing 3 drops of glacial acetic acid. Two layers were then separated, and the aqueous layer was extracted with EtOAc (4 x 15 mL). The combined organic layers were washed with 10% NaOH (2 x 15 mL), H₂O (15 mL), and brine (15 mL) and then were dried (Na₂SO₄, 12 h). The solvent was removed *in vacuo* to give a white solid that was recrystallized [HCCl₃:pentane (1:1)] to afford di-ester **36** (0.270 g, 36%) as a shiny white solid: mp 94-95 °C; IR (KBr pellet) 1740 [C=O], 1731 [C=O] cm⁻¹

¹; ¹H NMR (DCCl₃) δ 1.41 [s, 6 H, OC(CH₃)₂], 2.01 [d, *J* = 1.89 Hz, 3 H, HC=C(CH₃)], 3.96 [s, 3 H, OCH₃], 5.41 [m, 1 H, HC=C(CH₃)], 6.68 [d, *J* = 2.0 Hz, 1 H, Ar-*H*], 6.74 [dd, *J* = 7.97, 2.01 Hz, 1 H, Ar-*H*], 7.17 [d, 7.98 Hz, 1 H, Ar-*H*], 8.16 [d, 8.01 Hz, 2 H, Ar-*H*], 8.24 [d, 8.02 Hz, 2 H, Ar-*H*]; ¹³C NMR (DCCl₃) ppm 17.94 [OCH₃], 28.15 [OC(CH₃)₂], 52.46 [HC=C(CH₃)], 76.48 [OC(CH₃)₂], 109.76 [HC=C(CH₃)], 113.25 [HC=C(CH₃)], 121.08-153.94 [Ar-C], 164.17 [C=O], 166.14 [C=O]. Anal. Calcd for C₂₁H₂₀O₅: C, 71.58; H, 5.72. Found: C, 71.61; H, 5.79.

[(2-Methoxy-4-nitrophenyl)amino][(2,2,4,4-tetramethylthiochroman-6-yl)amino]-methane-1-thione (37). Amine **50a** (0.110 g, 0.50 mmol), dissolved in dry THF (3 mL), was placed in a 25-mL, three-necked, round-bottomed flask equipped with an N₂ inlet and addition funnel. The reaction mixture was then cooled to 0 °C (ice bath), and 2-methoxy-4-nitrophenyl isothiocyanate (0.108 g, 0.52 mmol, 1.04 eq) in dry THF (5 mL) was then added dropwise (5 min). After the addition, the reaction mixture was allowed to warm to RT and was then stirred for 24 h. The solvent was removed *in vacuo* to give a yellow solid which was recrystallized [CHCl₃:pentane (1:3)] to give **37** (0.150 g, 70%) as a light yellow solid: mp 155-157 °C; IR (KBr pellet) 3330 [NH], 3190 [NH] cm⁻¹; ¹H NMR (DCCl₃) δ 1.40 [s, 6 H, C(CH₃)₂], 1.45 [s, 6 H, SC(CH₃)₂], 1.99 [s, 2 H, CH₂], 3.82 [s, 3 H, OCH₃], 7.03 [d, *J* = 7.69 Hz, 1 H, Ar-*H*], 7.22 [d, *J* = 7.97 Hz, 1 H, Ar-*H*], 7.35 [s, 1 H, Ar-*H*], 7.69 [s, 1 H, Ar-*H*], 7.89 [d, *J* = 8.38 Hz, 1 H, Ar-*H*], 8.46 [s, 1 H, N-*H*], 8.49 [s, 1 H, N-*H*], 9.09 [d, *J* = 8.79 Hz, 1H, Ar-*H*]; ¹³C NMR (DCCl₃) ppm 31.49 [C(CH₃)₂], 32.48 [SC(CH₃)₂], 35.83 [C(CH₃)₂], 42.45 [SC(CH₃)₂], 53.88 [CH₂], 56.43

[OCH₃], 105.25-148.66 [Ar-C], 179.81 [C=S]. Anal. Calcd for C₂₁H₂₅N₃O₃S₂: C, 58.44; H, 5.84; N, 9.74; S, 14.86. Found: C, 58.20; H, 5.94; N, 9.61; S, 14.99.

[(4-Nitrobenzoyl)amino][(2,2,4,4-tetramethylthiochroman-6-yl)amino]methane-1-thione (38). Amine **50a** (0.110 g, 0.50 mmol), dissolved in dry THF (3 mL), was placed in a 25-mL, three-necked, round-bottomed flask equipped with a N₂ inlet and an addition funnel. The reaction mixture was then cooled to 0 °C (ice bath), and 4-nitrobenzoyl isothiocyanate (0.107 g, 0.52 mmol, 1.04 eq) in dry THF (5 mL) was then added dropwise (5 min). After the addition, the reaction mixture was allowed to warm to RT and was then stirred for 24 h. The solvent was removed *in vacuo* to give a dark orange solid which was recrystallized [HCCl₃:pentane (1:1)] to give **38** (0.160 g, 75%) as a bright orange solid: mp 215-217 °C; IR (KBr pellet) 3289 [NH], 1677 [C=O] cm⁻¹; ¹H NMR (DMSO-*d*₆) δ 1.36 [s, 6 H, C(CH₃)₂], 1.39 [s, 6 H, SC(CH₃)₂], 1.94 [s, 2 H, CH₂], 7.11 [d, *J* = 8.51 Hz, 1 H, Ar-*H*], 7.23 [d, *J* = 8.43 Hz, 1 H, Ar-*H*], 7.86 [s, 1 H, Ar-*H*], 8.15 [d, *J* = 8.65 Hz, 2 H, Ar-*H*], 8.34 [d, *J* = 8.34 Hz, 2 H, Ar-*H*], 11.89 [s, 1 H, N-*H*], 12.18 [s, 1 H, N-*H*]; ¹³C NMR (DMSO-*d*₆) ppm 31.20 [C(CH₃)₂], 32.25 [SC(CH₃)₂], 35.30 [C(CH₃)₂], 42.05 [SC(CH₃)₂], 53.27 [CH₂], 121.12-149.80 [Ar-C], 166.58 [C=O], 178.19 [C=S]. Anal. Calcd for C₂₁H₂₃N₃O₃S₂: C, 58.72; H, 5.40; N, 9.78; S, 14.93. Found: C, 58.50; H, 5.34; N, 9.66; S, 14.70.

Ethyl 4-[[N-(2,2,4,4-Tetramethylchroman-6-yl)carbamoyl]amino]benzoate (39). Amine **48a** (0.150 g, 0.73 mmol), dissolved in dry THF (3 mL), was placed in a 25-mL, three-necked, round-bottomed flask equipped with a N₂ inlet and an addition funnel. The

reaction mixture was cooled to 0 °C (ice bath), and 4-ethoxycarbonylphenyl isocyanate (0.145 g, 0.76 mmol, 1.04 eq) in dry THF (4 mL) was then added dropwise (5 min). After the addition, the reaction mixture was allowed to warm to RT and was then stirred for 24 h. The solvent was removed *in vacuo* to give a clumpy white solid which was recrystallized (EtOAc) to give **39** (0.190 g, 65%) as a bright-white cotton-like solid: mp 234-235 °C; IR (KBr pellet) 3346 [NH], 3195 [NH], 1713 [C=O], 1655 [HNC=O] cm⁻¹; ¹H NMR (DMSO-d₆) δ 1.28 [s, 6 H, C(CH₃)₂], 1.30 [s, 6 H, OC(CH₃)₂], 1.31 [t, 3 H, OCH₂CH₃], 1.80 [s, 2 H, CH₂], 4.29 [q, *J* = 7.09 Hz, 2 H, OCH₂CH₃], 6.65 [d, *J* = 7.99 Hz, 1 H, Ar-*H*], 7.09 [dd, *J* = 7.97, 1.98 Hz, 1 H, Ar-*H*], 7.44 [d, *J* = 2.01 Hz, 1 H, Ar-*H*], 7.58 [d, *J* = 8.08 Hz, 2 H, Ar-*H*], 7.88 [d, *J* = 8.06 Hz, 2 H, Ar-*H*], 8.52 [s, 1 H, N-*H*], 8.99 [s, 1 H, N-*H*]; ¹³C NMR (DMSO-*d*₆) ppm 14.23 [OCH₂CH₃], 28.10 [C(CH₃)₂], 30.61 [C(CH₃)₂], 32.50 [OC(CH₃)₂], 48.35 [CH₂], 60.20 [OCH₂CH₃], 73.84 [OC(CH₃)₂], 117.10-147.48 [Ar-C], 152.33 [C=O], 165.43 [C=O]. Anal. Calcd for C₂₃H₂₈N₂O₄: C, 69.67; H, 7.12; N, 7.07. Found: C, 69.48; H, 7.11; N, 7.05.

Ethyl 4-{{N-(2,2,4,4-Tetramethylchroman-6-yl)thiocarbamoyl}amino}benzoate (40). Amine **48a** (0.150 g, 0.73 mmol), dissolved in dry THF (3 mL), was placed in a 25-mL, three-necked, round-bottomed flask equipped with a N₂ inlet and an addition funnel. The reaction mixture was cooled to 0 °C (ice bath), and 4-ethoxycarbonylphenyl isothiocyanate (0.157 g, 0.799 mmol, 1.04 eq) in dry THF (4 mL) was then added dropwise (5 min). After the addition, the reaction mixture was allowed to warm to RT and was then stirred (24 h). The solvent was removed *in vacuo* to give a tan, viscous oil. The oil was subjected to flash chromatography [Et₂O:hexanes (1:1)], and, after the

solvent was removed *in vacuo*, **40** (0.210 g, 69%) was afforded as a flaky white solid: mp 102-104 °C; IR (KBr pellet) 3351 [NH], 3289 [NH], 1714 [C=O] cm⁻¹; ¹H NMR (DCCl₃) δ 1.34 [s, 6 H, C(CH₃)₂], 1.36 [s, 6 H, OC(CH₃)₂], 1.38 [t, 3 H, OCH₂CH₃], 1.85 [s, 2 H, CH₂], 4.35 [q, *J* = 7.16 Hz, 3 H, OCH₂CH₃], 6.85 [d, *J* = 8.07 Hz, 1 H, Ar-*H*], 7.04 [dd, *J* = 7.98, 2.07 Hz, 1 H, Ar-*H*], 7.24 [d, *J* = 2.04 Hz, 1 H, Ar-*H*], 7.57 [d, *J* = 8.12 Hz, 2 H, Ar-*H*], 7.81 [s, 1 H, N-*H*], 8.01 [d, *J* = 8.05 Hz, 2 H, Ar-*H*], 8.09 [s, 1 H, N-*H*]; ¹³C NMR (DCCl₃) ppm 14.28 [OCH₂CH₃], 28.45 [C(CH₃)₂], 31.06 [C(CH₃)₂], 32.70 [OC(CH₃)₂], 48.47 [CH₂], 60.96 [OCH₂CH₃], 75.09 [OC(CH₃)₂], 119.39-152.35 [Ar-C], 165.85 [C=O], 179.47 [C=S]. Anal. Calcd for C₂₃H₂₈N₂O₃S: C, 66.96; H, 6.84; N, 6.79; S, 7.77. Found: C, 67.24; H, 6.98; N, 6.88; S, 7.73.

[(4-Nitrophenyl)amino][(2,2,4,4-tetramethylchroman-6-yl)amino]methane-1-thione (41). Amine **48a** (0.150 g, 0.73 mmol), dissolved in dry THF (3 mL), was placed in a 25-mL, three-necked, round-bottomed flask equipped with an N₂ inlet and addition funnel. The reaction mixture was cooled to 0 °C (ice bath), and 4-nitrophenyl isothiocyanate (0.137 g, 0.76 mmol, 1.04 eq) in dry THF (4 mL) was then added dropwise (5 min). After the addition, the reaction mixture was allowed to warm to RT and was then stirred for 24 h. The solvent was removed *in vacuo* to give a dark yellow, clumpy solid. The solid was subjected to flash chromatography [Et₂O:hexanes (2:1)], and, after the solvent was evaporated *in vacuo*, **41** (0.240 g, 85%) was obtained as a fluffy, bright-yellow solid: mp 166-168 °C; IR (KBr pellet) 3346 [NH], 3215 [NH] cm⁻¹; ¹H NMR (DCCl₃) δ 1.35 [s, 6 H, C(CH₃)₂], 1.38 [s, 6 H, OC(CH₃)₂], 1.86 [s, 2 H, CH₂], 6.87 [d, *J* = 8.06 Hz, 1 H, Ar-*H*], 7.04 [dd, *J* = 8.01, 2.06 Hz, 1 H, Ar-*H*], 7.23 [d, *J* =

2.01 Hz, 1 H, Ar-*H*], 7.74 [d, $J = 8.03$ Hz, 2 H, Ar-*H*], 7.87 [s, 1 H, N-*H*], 8.18 [d, $J = 8.0$ Hz, 2 H, Ar-*H*], 8.35 [s, 1 H, N-*H*]; ^{13}C NMR (DCCl_3) ppm 28.45 [$\text{C}(\text{CH}_3)_2$], 31.09 [$\text{C}(\text{CH}_3)_2$], 32.72 [$\text{OC}(\text{CH}_3)_2$], 48.38 [CH_2], 75.21 [$\text{OC}(\text{CH}_3)_2$], 119.66-152.71 [Ar-C], 179.15 [$\text{C}=\text{S}$]. Anal. Calcd for $\text{C}_{20}\text{H}_{23}\text{N}_3\text{O}_3\text{S}$: C, 62.32; H, 6.01; N, 10.90; S, 8.32. Found: C, 62.50; H, 6.07; N, 10.63; S, 8.16.

Ethyl 4- $\{[N-(2,2,4,4\text{-Tetramethylchroman-8-yl})\text{carbamoyl}]\text{amino}\}$ benzoate (42).

Amine **48b** (0.130 g, 0.63 mmol), dissolved in dry THF (3 mL), was placed in a 25-mL, three-necked, round-bottomed flask equipped with an N_2 inlet and addition funnel. The reaction mixture was then cooled to 0 °C (ice bath), and 4-ethoxycarbonylphenyl isocyanate (0.26 g, 0.66 mmol, 1.04 eq) in dry THF (3 mL) was then added dropwise (5 min). After the addition, the reaction mixture was allowed to warm to RT and was then stirred (24 h). The solvent was removed *in vacuo* to give a clumpy white solid which was subjected to flash chromatography [Et_2O :hexanes (8:1)], and, after the solvent was evaporated (rotovap), **42** (0.210 g, 84%) was obtained as a fluffy white, cotton-like solid: mp 174-176 °C; IR (KBr pellet) 3348 [NH], 3201 [NH], 1715 [$\text{C}=\text{O}$], 1675 [HNC=O] cm^{-1} ; ^1H NMR (DCCl_3) δ 1.27 [s, 6 H, $\text{C}(\text{CH}_3)_2$], 1.31 [s, 6 H, $\text{OC}(\text{CH}_3)_2$], 1.36 [t, 3 H, OCH_2CH_3], 1.78 [s, 2 H, CH_2], 4.34 [q, $J = 7.21$ Hz, 2 H, OCH_2CH_3], 6.87 [m, 1 H, Ar-*H*], 6.97 [dd, $J = 8.03, 1.98$ Hz, 1 H, Ar-*H*], 7.44 [d, $J = 8.07$ Hz, 2 H, Ar-*H*], 7.74 [s, 1 H, N-*H*], 7.91 [d, $J = 7.98$ Hz, 2 H, Ar-*H*], 7.95 [d, $J = 1.99$ Hz, 1 H, Ar-*H*], 8.03 [s, 1 H, N-*H*]; ^{13}C NMR (DCCl_3) ppm 14.28 [OCH_2CH_3], 28.41 [$\text{C}(\text{CH}_3)_2$], 30.97 [$\text{C}(\text{CH}_3)_2$], 32.53 [$\text{OC}(\text{CH}_3)_2$], 49.02 [CH_2], 60.282 [OCH_2CH_3], 75.45 [$\text{OC}(\text{CH}_3)_2$], 117.31-143.39

[Ar-C], 152.80 [C=O], 166.66 [C=O]. Anal. Calcd for C₂₃H₂₈N₂O₄: C, 69.67; H, 7.12; N, 7.07. Found: C, 69.81; H, 7.18; N, 7.01.

Ethyl 4-{{N-(2,2,4,4-Tetramethylchroman-8-yl)thiocarbamoyl}amino}benzoate (43). Amine **48b** (0.130 g, 0.63 mmol), dissolved in dry THF (3 mL), was placed in a 25-mL, three-necked, round-bottomed flask equipped with a N₂ inlet and an addition funnel. The reaction mixture was then cooled to 0 °C (ice bath), and 4-ethoxycarbonylphenyl isothiocyanate (0.136 g, 0.66 mmol, 1.04 eq) in dry THF (3 mL) was then added dropwise (5 min). After the addition, the reaction mixture was allowed to warm to RT and was then stirred for 24 h. The solvent was removed *in vacuo* to give a tan, viscous oil. The oil was subjected to flash chromatography [Et₂O:hexanes (1:1)], and, after the solvent was removed *in vacuo*, **43** (0.230 g, 88%) was afforded as a fluffy, white solid: mp 56-58 °C; IR (KBr pellet) 3325 [NH], 3199 [NH], 1715 [C=O] cm⁻¹; ¹H NMR (DCCl₃) δ 1.29 [s, 6 H, C(CH₃)₂], 1.34 [s, 6 H, OC(CH₃)₂], 1.39 [t, 3 H, OCH₂CH₃], 1.83 [s, 2 H, CH₂], 4.38 [q, *J* = 7.12 Hz, 3 H, OCH₂CH₃], 6.94 [m, 1 H, Ar-*H*], 7.15 [dd, *J* = 7.91, 1.98 Hz, 1 H, Ar-*H*], 7.51 [d, *J* = 7.99 Hz, 2 H, Ar-*H*], 7.98 [bs, 1 H, Ar-*H*], 8.07 [d, *J* = 8.02 Hz, 2 H, Ar-*H*], 8.30 [s, 1 H, N-*H*], 8.40 [s, 1 H, N-*H*]; ¹³C NMR (DCCl₃) ppm 14.26 [OCH₂CH₃], 28.47 [C(CH₃)₂], 31.02 [C(CH₃)₂], 32.57 [OC(CH₃)₂], 48.71 [CH₂], 61.02 [OCH₂CH₃], 75.98 [OC(CH₃)₂], 120.14-143.91 [Ar-C], 165.73 [C=O], 177.83 [C=S]. Anal. Calcd for C₂₃H₂₈N₂O₃S: C, 66.96; H, 6.84; N, 6.79; S, 7.77. Found: C, 67.34; H, 7.02; N, 6.60; S, 7.50.

[(4-Nitrophenyl)amino][(2,2,4,4-tetramethylchroman-8-yl)amino]methane-1-thione (44). Amine **48b** (0.130 g, 0.63 mmol), dissolved in dry THF (3 mL), was placed in a 25-mL, three-necked, round-bottomed flask equipped with an N₂ inlet and addition funnel. The reaction mixture was then cooled to 0 °C (ice bath), and 4-nitrophenyl isothiocyanate (0.120 g, 0.66 mmol, 1.04 eq) in dry THF (3 mL) was then added dropwise (5 min). After the addition, the reaction mixture was allowed to warm to RT and was then stirred (24 h). The THF was then removed *in vacuo* to give a dark yellow, thick oil. The oil was subjected to flash chromatography [Et₂O:hexanes (2:1)], and, after the solvent was evaporated *in vacuo*, **44** (0.200 g, 82%) was obtained as a fluffy, bright-yellow solid: mp 160-161 °C; IR (KBr pellet) 3327 [NH], 3232 [NH] cm⁻¹; ¹H NMR (DCCl₃) δ 1.35 [s, 6 H, C(CH₃)₂], 1.36 [s, 6 H, OC(CH₃)₂], 1.87 [s, 2 H, CH₂], 6.96 [m, 1 H, Ar-H], 7.22 [dd, *J* = 8.02, 2.04 Hz, 1 H, Ar-H], 7.62 [bs, 1 H, Ar-H], 7.68 [d, *J* = 8.07 Hz, 2 H, Ar-H], 8.21 [d, *J* = 8.07 Hz, 2 H, Ar-H], 8.30 [s, 1 H, N-H], 8.34 [s, 1 H, N-H]; ¹³C NMR (DCCl₃) ppm 28.51 [C(CH₃)₂], 31.09 [C(CH₃)₂], 32.61 [OC(CH₃)₂], 48.67 [CH₂], 76.26 [OC(CH₃)₂], 120.48-144.80 [Ar-C], 178.21 [C=S]. Anal. Calcd for C₂₀H₂₃N₃O₃S: C, 62.32; H, 6.01; N, 10.90; S, 8.32. Found: C, 62.40; H, 5.92; N, 10.84; S, 8.11.

Ethyl 4-[(2,2,4-Trimethyl-2H-chromen-7-yloxy)carbonylamino]benzoate (45). Phenol **49** (0.600 g, 3.15 mmol, 1.05 eq), 4-ethoxycarbonylphenyl isocyanate (0.570 g, 3.00 mmol), and 5 mL of dry THF were placed in a 25-mL, three-necked, round bottomed flask equipped with a N₂ inlet. To this stirred solution was added 4 drops of triethylamine (TEA), and the resulting mixture was stirred (3 days) at RT. The solvent

was then evaporated (rotovap) to give a white, clumpy solid. This solid was subjected to flash column chromatography [EtOAc:hexanes (2:1)]. Upon evaporation of the solvent *in vacuo*, a white solid was obtained which was recrystallized [Et₂O:pentane (1:1)] to afford carbamate-ester **45** (0.560 g, 50%) as a white solid: mp 138.5-140 °C; IR (KBr pellet) 3314 [NH], 1756 [EtOC=O], 1694 [HNC=O] cm⁻¹; ¹H NMR (DCCl₃) δ 1.39 [s, 3 H, OCH₂CH₃], 1.40 [s, 6 H, OC(CH₃)₂], 1.98 [d, *J* = 1.97 Hz, 3 H, HC=C(CH₃)], 4.36 [q, *J* = 7.23 Hz, 2 H, OCH₂CH₃], 5.39 [m, 1 H, HC=C(CH₃)], 6.63 [d, *J* = 1.97 Hz, 1 H, Ar-*H*], 6.69 [dd, *J* = 7.98, 2.01 Hz, 1 H, Ar-*H*], 7.12 [d, *J* = 8.02 Hz, 1 H, Ar-*H*], 7.31 [bs, 1 H, N-*H*], 7.51 [d, *J* = 8.03 Hz, 2 H, Ar-*H*], 8.01 [d, *J* = 8.04 Hz, 2 H, Ar-*H*]; ¹³C NMR (DCCl₃) ppm 14.19 [OCH₂CH₃], 17.81 [HC=(CH₃)], 28.06 [OC(CH₃)₂], 60.81 [OCH₂CH₃], 76.50 [OC(CH₃)₂], 109.80 [HC=C(CH₃)], 113.38 [HC=C(CH₃)], 117.81-151.27 [Ar-C], 154.02 [HNC=O], 166.31 [CO₂Et]. Anal. Calcd for C₂₂H₂₃NO₅: C, 69.28; H, 6.08; N, 3.67. Found: C, 69.31; H, 6.06; N, 3.72.

{4-[*N*-(4-Hydroxyphenyl)carbamoyl]phenyl}-*N*-(2,2,4,4-tetramethyl(3*H*-benzo[3,4-*e*]thian-6-yl))carboxamide (46). Acid **60**¹³⁵ (0.710 g, 1.92 mmol), along with dry THF (8 mL), was placed in a 100-mL, three-necked, round-bottomed flask equipped with a spiral condenser, N₂ inlet, and an addition funnel. To this stirred cloudy, yellow solution was added triethylamine (0.222 g, 2.19 mmol, ~1.14 eq) dropwise, using a pipette for the addition through a sidearm of the flask. The resulting, almost clear mixture was stirred at RT (45 min), and isobutyl chloroformate (0.300 g, 0.28 mL, 2.20 mmol, ~1.14 eq) was added at RT to the reaction mixture through a septum in a sidearm of the flask via a syringe. The resulting yellow, cloudy mixture was then heated to 59 °C via hand control

of the variac, stirred for 1.5 h, and 4-aminophenol (0.356 g, ~1.7 eq) in pyridine (3.5 mL) was added dropwise to the reaction mixture via the addition funnel. During the addition of the aminophenol, the reaction mixture turned to a yellow-orange color, and this resulting solution was stirred (4 h) at 59 °C. The resulting yellowish, cloudy mixture was allowed to cool to RT, and H₂O (65 mL) was added. The resulting cloudy mixture was placed in a separatory funnel and extracted (EtOAc, 4 x 50 mL). The combined organic layers were successively washed with 2 N HCl (2 x 40 mL), H₂O (2 x 50 mL), and brine (40 mL). The organic solution was then dried (Na₂SO₄, 12 h), and the solvent was removed *in vacuo* to give a tan foam. This foam was subjected to flash chromatography [EtOAc:hexanes (2:1)], and, upon removal of the solvent, a yellow solid was obtained, which was then recrystallized [MeOH:H₂O (13:8)] to give **46** (0.177 g, 20%) as a light yellow solid: mp 280-282 °C; IR (KBr pellet) 3405 [OH], 3324 [NH], 1642 [C=O] cm⁻¹; ¹H NMR (DMSO-*d*₆) δ 1.37 [s, 6 H, C(CH₃)₂], 1.38 [s, 6 H, SC(CH₃)₂], 1.93 [CH₂], 6.76 [d, 2 H, *J* = 7.98 Hz, Ar-*H*], 7.05 [d, 1 H, *J* = 7.93 Hz, Ar-*H*], 7.56 [d, 2 H, *J* = 8.0 Hz, Ar-*H*], 7.63 [dd, 1 H, *J* = 8.03, 1.98 Hz, Ar-*H*], 7.91 [d, 1 H, *J* = 2.02 Hz, Ar-*H*], 8.09 [s, 4 H, Ar-*H*], 9.32 [s, 1 H, OH], 10.20 [s, 1 H, NH], 10.32 [s, 1 H, NH]; ¹³C NMR (DMSO-*d*₆) ppm 31.10 [C(CH₃)₂], 32.25 [SC(CH₃)₂], 35.21 [C(CH₃)₂], 41.83 [SC(CH₃)₂], 53.45 [CH₂], 114.92-153.77 [Ar-C], 164.08, 164.47 [C=O]. Anal. Calcd for C₂₇H₂₈N₂O₃S: C, 69.70; H, 6.13; N, 6.08; S, 6.96. Found: C, 69.37; H, 6.19; N, 5.91; S, 6.72.

{4-[N-(4-Hydroxyphenyl)carbamoyl]phenyl}-N-(2,2,4,4-tetramethylchroman-6-yl)carboxamide (47). Acid **33** (0.400 g, 1.13 mmol), along with dry THF (5 mL), was

placed in a 50-mL, three-necked, round-bottomed flask equipped with a spiral condenser, N₂ inlet, and an addition funnel. To this stirred, cloudy yellow solution was added triethylamine (0.131 g, 1.29 mmol, ~1.14 eq) dropwise, using a pipette for the addition through a sidearm. The resulting, almost clear mixture was stirred at RT (45 min), and isobutyl chloroformate (0.177 g, 0.17 mL, 1.29 mmol, ~1.14 eq) was added at RT to the reaction mixture through a septum in a sidearm of the flask, using a syringe. The resulting cloudy, yellow mixture was then heated to 59 °C via hand control of the variac and was stirred for 1.5 h. 4-Aminophenol (0.210 g, ~1.7 eq) in pyridine (2 mL) was added dropwise to the reaction mixture via the addition funnel. During the addition of the aminophenol, the reaction mixture turned to a yellow-orange color, and this resulting solution was stirred (4 h) at 59 °C. The resulting cloudy, yellowish mixture was allowed to cool to RT, and H₂O (39 mL) was added. The resulting cloudy mixture was placed in a separatory funnel and extracted (EtOAc, 4 x 30 mL). The combined organic layers were successively washed with 2 N HCl (2 x 25 mL), H₂O (2 x 30 mL), and brine (25 mL). The organic solution was then dried (Na₂SO₄, 12 h), and the solvent was removed *in vacuo* to give a yellow foam. This foam was subjected to flash chromatography [EtOAc:hexanes (2:1)], and, upon removal of the solvent, a pink solid was isolated and recrystallized [MeOH:H₂O (13:8)] to give **47** (0.150 g, 30%) as a white solid: mp 232-234 °C; IR (KBr pellet) 3431 [OH], 3352 [NH], 1663 [C=O], 1647 [C=O] cm⁻¹; ¹H NMR (DMSO-*d*₆) δ 1.30 [s, 6 H, C(CH₃)₂], 1.32 [s, 6 H, OC(CH₃)₂], 1.82 [CH₂], 6.71 [d, 1 H, *J* = 7.96 Hz, Ar-*H*], 6.76 [d, 2 H, *J* = 8.0 Hz, Ar-*H*], 7.50 [dd, 1 H, *J* = 7.99, 2.01 Hz, Ar-*H*], 7.55 [d, 2 H, *J* = 8.01 Hz, Ar-*H*], 7.74 [d, 1 H, *J* = 2.0 Hz, Ar-*H*], 8.07 [s, 4 H, Ar-*H*], 9.31 [s, 1 H, OH], 10.18 [s, 1 H, NH], 10.20 [s, 1 H, NH]; ¹³C NMR (DMSO-*d*₆) ppm

28.12 [C(CH₃)₂], 30.64 [C(CH₃)₂], 32.62 [OC(CH₃)₂], 48.24 [CH₂], 74.05 [OC(CH₃)₂], 115.02-153.87 [Ar-C], 164.22, 164.26 [C=O]. Anal. Calcd for C₂₇H₂₈N₂O₄: C, 72.85; H, 6.35; N, 6.30. Found: C, 72.50; H, 6.38; N, 6.29.

2,2,4,4-Tetramethyl-6-aminochroman (48a). A mixture of nitro compound **54a** (1.0 g, 4.2 mmol), iron powder (0.850 g, 15.2 mmol, 3.6 eq, Sigma-Aldrich Chemical Co.), glacial acetic acid (1.80 g, 30 mmol, 7 eq), and absolute EtOH (11 mL) was placed in a 25-mL, three-necked, round-bottomed flask equipped with a spiral condenser and N₂ inlet and was stirred at reflux (12 h). Within approximately 15 min, the reaction mixture turned from clear yellow to a dark maroon color. The reaction was allowed to cool to RT and was poured into H₂O (45 mL). The resulting brown emulsion was extracted with Et₂O (2 x 40 mL) and HCCl₃ (3 x 40 mL). The combined organic layers were washed with H₂O (3 x 40 mL), dried (Na₂SO₄, 12 h), and concentrated *in vacuo* to give a dark oil. This crude mixture was then dissolved in Et₂O (30 mL), and the resulting solution was extracted with 2 N HCl (2 x 30 mL). The acid solution was neutralized with 40% Na₂CO₃ (pH ~ 8), and the resulting cloudy solution was extracted (Et₂O, 2 x 30 mL). The combined organic layers were dried (Na₂SO₄, 12 h), and the solvent was removed *in vacuo* to afford amine **48a** as a very light tan oil which solidified upon standing overnight in the freezer. Amine **48a** (0.370 g, 42%) was thus obtained as an off-white solid: mp 40-42 °C. However, it should be noted that it was discovered that a crude mixture of the isomeric nitro-compounds **54a** and **54b**, resulting from the conversion of **53**→**54a** and **54b**, could be co-reduced by this method. The final mixture of amines **48a** and **48b** was more easily separated by flash column chromatography [hexanes:Et₂O (1:1)] than the

corresponding mixture of nitro compounds (fractions 4-10 yielded **48b** and fractions 17-25 yielded **48a**). Data for **48a**: IR (neat) 3433 [NH], 3357 [NH] cm^{-1} ; ^1H NMR (DCCl_3) δ 1.30 [s, 6 H, $\text{C}(\text{CH}_3)_2$], 1.31 [s, 6 H, $\text{OC}(\text{CH}_3)_2$], 1.78 [s, 2 H, CH_2], 3.29 [bs, 2 H, NH_2], 6.46 [dd, $J = 8.03, 1.99$ Hz, 1 H, Ar- H], 6.61 [d, $J = 1.80$ Hz, 1 H, Ar- H], 6.63 [d, $J = 7.89$ Hz, 1 H, Ar- H]; ^{13}C NMR (DCCl_3) ppm 28.35 [$\text{C}(\text{CH}_3)_2$], 30.96 [$\text{C}(\text{CH}_3)_2$], 32.57 [$\text{OC}(\text{CH}_3)_2$], 49.32 [CH_2], 73.81 [$\text{OC}(\text{CH}_3)_2$], 113.41-145.35 [Ar-C]. Data for **48b**: IR (neat) 3455 [NH], 3360 [NH] cm^{-1} ; ^1H NMR (DCCl_3) δ 1.32 [s, 6 H, $\text{C}(\text{CH}_3)_2$], 1.36 [s, 6 H, $\text{OC}(\text{CH}_3)_2$], 1.83 [s, 2 H, CH_2], 3.54 [bs, 2 H, NH_2], 6.54 [dd, $J = 7.94, 2.02$ Hz, 1 H, Ar- H], 6.70 [m, 2 H, Ar- H]; ^{13}C NMR (DCCl_3) ppm 28.63 [$\text{C}(\text{CH}_3)_2$], 30.96 [$\text{C}(\text{CH}_3)_2$], 32.58 [$\text{OC}(\text{CH}_3)_2$], 49.34 [CH_2], 74.48 [$\text{OC}(\text{CH}_3)_2$], 112.37-140.07 [Ar-C]. Amines **48a** and **48b** were used immediately without further purification.

2,2,4,4-Tetramethyl-8-aminochroman (48b). A mixture of nitro compound **54b** (1.60 g, 6.8 mmol), iron powder (1.36 g, 24.3 mmol, 3.6 eq, Sigma-Aldrich Chemical Co.), glacial acetic acid (2.86 g, 47.6 mmol, 7 eq), and absolute EtOH (17 mL) was placed in a 25-mL, three-necked, round-bottomed flask equipped with a spiral condenser and N_2 inlet and was stirred at reflux (12 h). Within approximately 15 min, the reaction mixture turned from clear yellow to a dark maroon color. The reaction was allowed to cool to RT and was poured into H_2O (68 mL). The resulting brown emulsion was extracted with Et_2O (2 x 40 mL) and HCCl_3 (3 x 40 mL). The combined organic layers were washed with H_2O (3 x 65 mL), dried (Na_2SO_4 , 12 h), and concentrated *in vacuo* to give a dark oil. This crude mixture was then dissolved in Et_2O (45 mL), and the resulting solution was extracted with 2 *N* HCl (2 x 55 mL). The acid solution was neutralized with

40% Na₂CO₃ (pH ~ 8), and the resulting cloudy solution was extracted (Et₂O, 2 x 55 mL). The combined organic layers were dried (Na₂SO₄, 12 h), and the solvent was removed *in vacuo* to afford amine **48b** as a light pink oil which crystallized upon standing at RT. Amine **48b** (0.430 g, 31%) was thus obtained as a pink solid: mp 40-42 °C. However, it should be noted that it was discovered that a crude mixture of the isomeric nitro compounds **54a** and **54b**, resulting from the conversion of **53**→**54a** and **54b**, could be co-reduced by this method. The final mixture of amines **48a** and **48b** was more easily separated by flash column chromatography [hexanes:Et₂O (1:1)] than the corresponding mixture of nitro compounds (fractions 4-10 yielded **48b** and fractions 17-25 yielded **48a**). Spectral data for **48b** was the same as stated above (in the description of **48a**). Amines **48a** and **48b** were used immediately without further purification.

2,2,4-Trimethyl-2H-1-benzopyran-7-ol (49). A solution of 3.0 M methylmagnesium bromide in diethyl ether (30 mL, 90.8 mmol, 4 eq), along with dry THF (60 mL), was placed in a 250-mL, three-necked, round-bottomed flask equipped with a spiral condenser, N₂ inlet, and an addition funnel. Known lactone **55**¹³⁴ (4.00 g, 22.7 mmol), dissolved in dry THF (25 mL), was added dropwise, with stirring, to the reaction flask at RT. During the addition, some heat evolved, and a yellow precipitate formed. After the addition was complete, the resulting yellow mixture was stirred (2 days) at RT and the reaction was quenched with saturated NH₄Cl (250 mL). The resulting mixture was placed in a separatory funnel, and the two layers were separated. The aqueous layer was extracted with Et₂O (5 x 50 mL), and the combined organic layers were then dried (Na₂SO₄, 12 h). The solvent was evaporated (rotovap) to give a dark orange oil which

was immediately dissolved in glacial acetic acid (20 mL) and placed in a 50 mL, single-necked, round-bottomed flask equipped with a spiral condenser and N₂ inlet. The resulting solution was stirred and heated gently (2 h-slightly below the boiling point of acetic acid, or at approximately 110 °C). The reaction mixture was allowed to cool to RT and poured into H₂O (100 mL). The resulting dark emulsion was extracted with Et₂O (5 x 50 mL), and the combined organic layers were washed with saturated, aqueous NaHCO₃ (3 x 50 mL) and brine (2 x 50 mL) and were then dried (Na₂SO₄, 12 h). The solvent was removed *in vacuo* to give a dark brown, viscous oil. The oil was subjected to flash column chromatography [Et₂O:hexanes (5:1)], and, upon evaporation of the solvent (rotovap), pure phenol **49** (1.51 g, 40%) was obtained as a white solid: mp 128-130 °C; IR (KBr pellet) 3330 [OH] cm⁻¹; ¹H NMR (DCCl₃) δ 1.38 [s, 6 H, OC(CH₃)₂], 1.96 [d, *J* = 2.09 Hz, 3 H, HC=C(CH₃)], 5.17 [bs, 1 H, O-*H*], 5.28 [m, 1 H, HC=C(CH₃)], 6.32 [d, *J* = 2.01 Hz, 1 H, Ar-*H*], 6.35 [dd, *J* = 8.01, 2.0 Hz, 1 H, Ar-*H*], 6.99 [d, *J* = 8.03 Hz, 1 H, Ar-*H*]; ¹³C NMR (DCCl₃) ppm 17.92 [HC=C(CH₃)], 28.03 [OC(CH₃)₂], 76.38 [OC(CH₃)₂], 103.67 [HC=C(CH₃)], 107.42 [HC=C(CH₃)], 116.62-156.34 [Ar-*C*]. Anal. Calcd for C₁₂H₁₄O₂: C, 75.60; H, 7.42; N. Found: C, 75.30; H, 7.32.

2,2,4,4-Tetramethyl-6-aminothiochroman (50a). A mixture of nitro compound **57a** (1.0 g, 3.97 mmol), iron powder (0.803 g, 14.4 mmol, 3.6 eq, Sigma-Aldrich Chemical Co.), glacial acetic acid (1.67 g, 27.8 mmol, 7 eq), and absolute EtOH (10 mL) was placed in a 25-mL, three-necked, round-bottomed flask equipped with a spiral condenser and N₂ inlet and was stirred at reflux (12 h). Within approximately 15 min, the reaction mixture turned from clear yellow to a dark maroon color. The reaction was allowed to

cool to RT and was poured into H₂O (42 mL). The resulting brown emulsion was extracted with Et₂O (2 x 37 mL) and HCCl₃ (3 x 37 mL). The combined organic layers were washed with H₂O (3 x 37 mL), dried (Na₂SO₄, 12 h), and concentrated *in vacuo* to give a dark oil. This crude mixture was then dissolved in Et₂O (28 mL), and the resulting solution was extracted with 2 N HCl (2 x 28 mL). The acid solution was neutralized with 40% Na₂CO₃ (pH ~ 8), and the resulting cloudy solution was extracted (Et₂O, 2 x 28 mL). The combined organic layers were dried (Na₂SO₄, 12 h), and the solvent was removed *in vacuo* to afford amine **50a** as a tan oil which solidified upon standing at RT. Amine **50a** (0.352 g, 40%) was obtained as an off-white solid: mp 63-65 °C (lit¹²³ mp 57-59 °C). However, it should be noted that it was discovered that a crude mixture of the isomeric nitro-compounds **57a** and **57b**, resulting from the conversion of **56**→**57a** and **57b**, could be co-reduced by this method. The final mixture of amines **50a** and **50b** was more easily separated by flash column chromatography [hexanes:EtOAc (2:1)] than the corresponding mixture of nitro compounds (fractions 11-15 yielded **50b** and fractions 21-28 yielded **50a**). Data for **50a**: IR (KBr) 3450 [NH], 3360 [NH] cm⁻¹; ¹H NMR (DCCl₃) δ 1.35 [s, 6 H, C(CH₃)₂], 1.38 [s, 6 H, SC(CH₃)₂], 1.89 [s, 2 H, CH₂], 3.57 [bs, 2 H, NH₂], 6.45 [dd, *J* = 8.01, 1.97 Hz, 1 H, Ar-*H*], 6.75 [d, *J* = 1.85 Hz, 1 H, Ar-*H*], 6.92 [d, *J* = 7.93 Hz, 1 H, Ar-*H*]; ¹³C NMR (DCCl₃) ppm 31.57 [C(CH₃)₂], 32.25 [SC(CH₃)₂], 35.73 [C(CH₃)₂], 41.90 [OC(CH₃)₂], 54.73 [CH₂], 113.41-144.18 [Ar-C]. Spectral data has been reported for **50a**.¹²³ IR (KBr) 3450, 3360 [NH] cm⁻¹; ¹H NMR (DCCl₃) δ 1.36 [s, 6 H, (CH₃)₂], 1.39 [s, 6 H, SC(CH₃)₂], 1.90 [s, 2 H, CH₂], 3.50 [bs, 2 H, NH₂], 6.44 [d, H, Ar-*H*], 6.75 [s, 1 H, Ar-*H*], 9.92 [d, 1 H, Ar-*H*]. Data for **50b**: IR (neat) 3416 [NH], 3358 [NH] cm⁻¹; ¹H NMR (DCCl₃) δ 1.38 [s, 6 H, C(CH₃)₂], 1.41 [s, 6 H, SC(CH₃)₂], 1.91 [s, 2

H, CH₂], 3.64 [bs, 2 H, NH₂], 6.54 [dd, *J* = 6.18, 1.37 Hz, 1 H, Ar-*H*], 6.85 [dd, *J* = 6.45, 1.37 Hz, 1 H, Ar-*H*], 6.92 [m, 3 H, Ar-*H*]; ¹³C NMR (DCCl₃) ppm 31.95 [C(CH₃)₂], 32.04 [SC(CH₃)₂], 36.11 [C(CH₃)₂], 42.36 [SC(CH₃)₂], 54.46 [CH₂], 112.32-144.35 [Ar-C]. Amine **50a** was used immediately without further purification.

2,2,4,4-Tetramethyl-8-aminothiochroman (50b). A mixture of nitro compound **57b** (1.0 g, 3.97 mmol), iron powder (0.803 g, 14.4 mmol, 3.6 eq, Sigma-Aldrich Chemical Co.), glacial acetic acid (1.67 g, 27.8 mmol, 7 eq), and absolute EtOH (10 mL) was placed in a 25-mL, three-necked, round-bottomed flask equipped with a spiral condenser and N₂ inlet and was stirred at reflux (12 h). Within approximately 15 min, the reaction mixture turned from clear yellow to a dark maroon color. The reaction was allowed to cool to RT and was poured into H₂O (42 mL). The resulting brown emulsion was extracted with Et₂O (2 x 37 mL) and HCCl₃ (3 x 37 mL). The combined organic layers were washed with H₂O (3 x 37 mL), dried (Na₂SO₄, 12 h), and concentrated *in vacuo* to give a dark oil. This crude mixture was then dissolved in Et₂O (28 mL), and the resulting solution was extracted with 2 *N* HCl (2 x 28 mL). The acid solution was neutralized with 40% Na₂CO₃ (pH ~ 8), and the resulting cloudy solution was extracted (Et₂O, 2 x 28 mL). The combined organic layers were dried (Na₂SO₄, 12 h), and the solvent was removed *in vacuo* to afford amine **50b** as a light tan oil which crystallized upon standing overnight in the freezer. Amine **50b** (0.264 g, 30%) was obtained as a cream-colored solid: mp 58.5-60 °C. However, it should be noted that it was discovered that a crude mixture of the isomeric nitro compounds **57a** and **57b**, resulting from the conversion of **56**→**57a** and **57b**, could be co-reduced by this method. The final mixture of amines **50a**

and **50b** was more easily separated by flash column chromatography [hexanes:EtOAc (2:1)] than the corresponding mixture of nitro compounds (fractions 11-15 yielded **50b** and fractions 21-28 yielded **50a**). Spectral data for **50b** was the same as stated above (in the description of **50a**). Amine **50b** was used immediately without further purification.

4-(2-Hydroxyphenyl)-2,4-dimethyl-2-pentanol (52). A solution of 3.0 M methylmagnesium bromide in diethyl ether (121 mL, 363.20 mmol, 4 eq), along with dry THF (240 mL), was placed in a 1-L three-necked, round-bottomed flask equipped with a spiral condenser, N₂ inlet, and an addition funnel. Lactone **51**¹³⁰ (16.00 g, 90.80 mmol), in dry THF (10 mL), was added dropwise to the reaction flask at RT. The resulting mixture was then stirred at reflux (4 days). The reaction mixture was allowed to cool to RT and was then cooled to 0 °C (ice bath). Saturated NH₄Cl solution (820 mL) was then added to the reaction mixture dropwise, via the addition funnel. The resulting mixture was poured into a separatory funnel, and the two layers were separated. The aqueous layer was extracted with Et₂O (4 x 150 mL). The combined organic layers were washed with H₂O (150 mL) and brine (150 mL) and then were dried (Na₂SO₄, 12 h). The solvent was removed *in vacuo* to give a pale yellow oil, which, on standing at RT for ~5 min, crystallized. The resulting yellow solid was recrystallized (petroleum ether) to give diol **52** (16.00 g, 84%) as clear, needle-like crystals: mp 88-90 °C (lit¹⁶¹ mp 91 °C); IR (KBr pellet) 3406 [OH], 1731 [OH] cm⁻¹; ¹H NMR (DCCl₃) δ 1.17 [s, 6 H, C(CH₃)₂], 1.41 [s, 6 H, OC(CH₃)₂], 2.24 [s, 2 H, CH₂], 6.58 [dd, *J* = 7.21, 1.56 Hz, 1 H, Ar-*H*], 6.87 [m, 1 H, Ar-*H*], 7.04 [m, 1 H, Ar-*H*], 7.35 [dd, *J* = 7.18, 1.59 Hz, 1 H, Ar-*H*]; ¹³C NMR (DCCl₃) ppm 30.89 [C(CH₃)₂], 30.94 [OC(CH₃)₂], 37.50 [C(CH₃)₂], 52.31 [CH₂], 73.43

[OC(CH₃)₂], 117.15-155.04 [Ar-C]. The only other information given on **52** was an elemental analysis.¹⁶¹

2,2,4,4-Tetramethylchroman (53). A mixture of diol **52** (45.02 g, 0.22 mol), 85 % H₃PO₄ (21.21 mL, 0.18 mol), and benzene (225 mL) was placed in a 1-L, three-necked, round-bottomed flask equipped with a spiral condenser and N₂ inlet, and was heated (80 °C). After ~5 min, the first of 3 portions of P₂O₅ (25.42 g, 0.54 mol, 2.5 eq of diol 31) was added, all at once via the side arm of the flask with the aid of a funnel. The other 2 portions of P₂O₅ were added at ~7 h intervals for a total of 76.26 g (3 x 25.42 g). From just after the first portion of P₂O₅ was added, the reaction mixture was allowed to stir at reflux for 24 h. The reaction mixture was then allowed to cool to RT and the benzene solution was decanted from a dark, purple residue in the bottom of the flask. The residue was rinsed in the flask with Et₂O (3 x 150 mL), and the ether layers were combined with the benzene solution. The combined organic layers were then washed with 5% NaHCO₃ (3 x 100 mL) and brine (3 x 100 mL), and were then dried (Na₂SO₄, 12 h). The solvent was removed *in vacuo* to give a pale yellow oil, which was subsequently vacuum distilled to afford chroman **53** (21.5 g, 54%) as a colorless oil: bp 69-71 °C/1.5 mm Hg, (lit¹⁶¹ bp 102-104 °C, n^{21.5} 1.5152). ¹H NMR (DCCl₃) δ 1.34 [s, 6 H, C(CH₃)₂], 1.35 [s, 6 H, OC(CH₃)₂], 1.84 [s, 2 H, CH₂], 6.79 [dd, *J* = 7.68, 1.79 Hz, 1 H, Ar-*H*], 6.85 [m, 1 H, Ar-*H*], 7.08 [m, 1 H, Ar-*H*], 7.31 [dd, *J* = 7.76, 1.83 Hz, 1 H, Ar-*H*]; ¹³C NMR (DCCl₃) ppm 28.45 [C(CH₃)₂], 30.74 [C(CH₃)₂], 32.70 [OC(CH₃)₂], 49.20 [CH₂], 74.30 [OC(CH₃)₂], 117.97-152.62 [Ar-C]. The only other information given on **53** was an elemental analysis.¹⁶¹

2,2,4,4-Tetramethyl-6-nitrochroman (54a) and 2,2,4,4-Tetramethyl-8-nitrochroman (54b). A mixture of Ac₂O (4.78 g, 46.8 mmol, 1.6 eq of HNO₃) and HNO₃ (1.89 mL, 30 mmol, 1.1 eq of chroman) was first prepared by chilling Ac₂O to 0 °C (ice bath) and adding HNO₃ to it, dropwise using a pipette. Chroman **53** (5.0 g, 26.3 mmol), dissolved in freshly distilled Ac₂O (5 mL), was then placed in a 50-mL, three-necked, round-bottomed flask equipped with an addition funnel and N₂ inlet. The reaction flask was then chilled to -5 °C (ice/salt bath). The HNO₃/Ac₂O mixture was then added dropwise (5 min), via the addition funnel, and the resulting dark blue reaction mixture was allowed to stir at -5 °C (90 min). The reaction mixture was then poured into saturated, aqueous NaHCO₃ (50 mL), and the resulting dark brown emulsion was extracted with H₂CCl₂ (3 x 30 mL). The combined organic layers were washed with H₂O (45 mL) and brine (45 mL) and were then dried (Na₂SO₄, 12 h). The solvent was removed *in vacuo* to give a dark brown liquid, which was subjected to flash chromatography [hexanes:Et₂O (20:1)] to provide the two isomers **54a** and **54b** (6-isomer **54a** was collected in fractions 5-12, and 8-isomer **54b** was collected in fractions 15-20). The 6-isomer **54a** (2.67 g, 43%) was thus isolated as a pale yellow solid: mp 56-58 °C; spectral data for **54a**: IR (KBr) 1581, 1341 [NO₂] cm⁻¹; ¹H NMR (DCCl₃) δ 1.39 [s, 6 H, C(CH₃)₂], 1.41 [s, 6 H, OC(CH₃)₂], 1.89 [s, 2 H, CH₂], 6.85 [d, *J* = 7.93 Hz, 1 H, Ar-*H*], 7.98 [dd, *J* = 7.01, 1.98 Hz, 1 H, Ar-*H*], 8.22 [d, *J* = 1.97 Hz, 1 H, Ar-*H*]; ¹³C NMR (DCCl₃) ppm 28.48 [C(CH₃)₂], 31.12 [C(CH₃)₂], 32.69 [OC(CH₃)₂], 48.07 [CH₂], 76.39 [OC(CH₃)₂], 118.45-158.46 [Ar-C]. The 8-isomer **54b** (1.61 g, 26%) was thus isolated as a creamy white solid: mp 52-54 °C; spectral data for **54b**: IR (KBr) 1582, 1341 [NO₂] cm⁻¹; ¹H NMR (DCCl₃) δ 1.37 [s, 6 H, C(CH₃)₂], 1.39 [s, 6 H, OC(CH₃)₂], 1.91 [s, 2 H,

CH_2], 6.94 [m, 1 H, Ar-*H*], 7.48 [dd, $J = 7.63, 1.87$ Hz, 1 H, Ar-*H*], 7.57 [dd, $J = 7.59, 1.83$ Hz, 1 H, Ar-*H*]; ^{13}C NMR ($DCCl_3$) ppm 28.35 [$C(CH_3)_2$], 31.30 [$C(CH_3)_2$], 32.55 [$OC(CH_3)_2$], 48.33 [CH_2], 76.86 [$OC(CH_3)_2$], 118.45-146.89 [Ar-*C*]. A melting point of a mixture of the two isomers **54a** and **54b** was measured, and the result was mp 46-48 °C.

2,2,4,4-Tetramethyl-6-nitrothiochroman (57a) and 2,2,4,4-Tetramethyl-8-nitrothiochroman (57b). A mixture of Ac_2O (13.20 g, 0.129 mol, 1.6 eq of HNO_3) and HNO_3 (5.21 mL, 82.9 mmol, 1.1 eq of chroman) was first prepared by chilling Ac_2O to 0 °C (ice bath) and adding HNO_3 to it, dropwise using a pipette. Known thiochroman **56**^{126a} (15.00 g, 72.7 mmol), dissolved in freshly distilled Ac_2O (14 mL), was then placed in a 100-mL, three-necked, round-bottomed flask equipped with an addition funnel and N_2 inlet. The reaction flask was then chilled to -5 °C (ice/salt bath). The HNO_3/Ac_2O mixture was then added dropwise (5 min), via the addition funnel, and the resulting dark blue reaction mixture was allowed to stir at -5 °C (90 min). The reaction mixture was then poured into saturated, aqueous $NaHCO_3$ (140 mL), and the resulting dark brown emulsion was extracted with H_2CCl_2 (3 x 83 mL). The combined organic layers were washed with H_2O (125 mL) and brine (125 mL) and were then dried (Na_2SO_4 , 12 h). The solvent was removed *in vacuo* to give a dark brown liquid, which was subjected to flash chromatography [hexanes:EtOAc (5:1)] to provide isomers **57a** and **57b** (6-isomer **57a** was collected in fractions 8-15, and 8-isomer **57b** was collected in fractions 18-21). The 6-isomer **57a** (4.75 g, 26%) was isolated as a pale yellow solid: mp 64-66 °C (lit¹²³ mp 103-107 °C). The apparent discrepancy between the reported¹²³ mp and the mp measured here is likely because the data reported¹²³ for **50a** corresponded to another compound. As

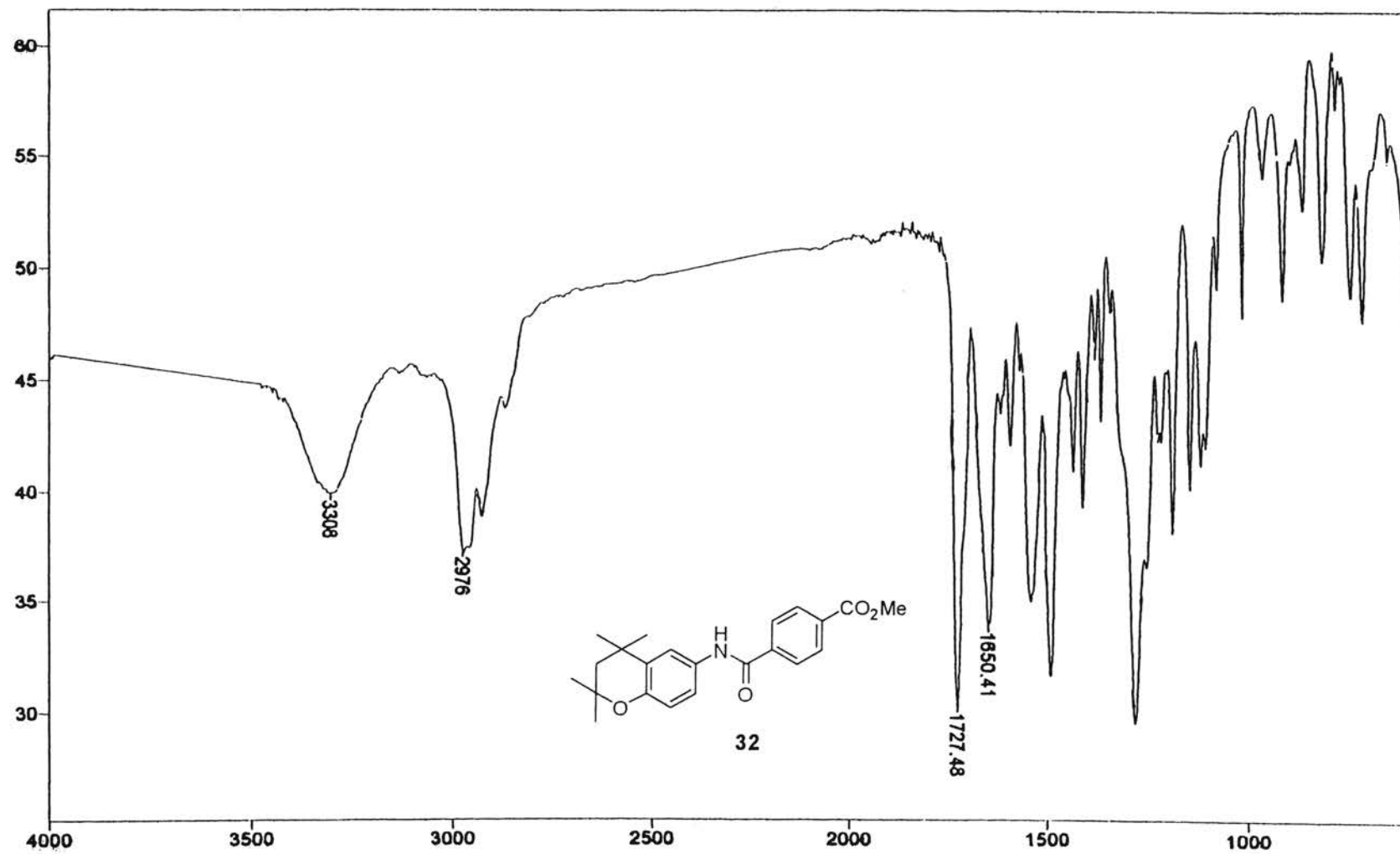
can be seen below, the spectral data for **50a** reported here clearly matches what would be expected, while the data reported¹²³ before does not. Spectral data for **57a**: IR (KBr) 1519, 1345 [NO₂] cm⁻¹; ¹H NMR (DCCl₃) δ 1.45 [s, 6 H, C(CH₃)₂], 1.46 [s, 6 H, SC(CH₃)₂], 2.00 [s, 2 H, CH₂], 7.21 [d, *J* = 8.65 Hz, 1 H, Ar-*H*], 7.88 [dd, *J* = 6.32, 2.33 Hz, 1 H, Ar-*H*], 8.26 [d, *J* = 2.33 Hz, 1 H, Ar-*H*]; ¹³C NMR (DCCl₃) ppm 31.64 [C(CH₃)₂], 32.43 [SC(CH₃)₂], 35.85 [C(CH₃)₂], 43.04 [SC(CH₃)₂], 53.24 [CH₂], 120.90-143.07 [Ar-C]. Spectral data has been reported for **57a**:¹²³ ¹H NMR (DCCl₃) δ 1.10 [s, 3 H, (CH₃)₂], 1.37 [s, 3 H, (CH₃)₂], 1.52 [s, SC(CH₃)₂], 1.56 [s, SC(CH₃)₂], 2.03 [m, 3 H, CH₂], 8.01 [d, 1 H, Ar-*H*], 8.24 [d, 2 H, Ar-*H*]. No further information was provided for **57a**. Previously unknown 8-isomer **57b** (1.83 g, 10%) was isolated as a creamy white solid: mp 105-108 °C; spectral data for **57b**: IR (KBr) 1516, 1338 [NO₂] cm⁻¹; ¹H NMR (DCCl₃) δ 1.37 [s, 6 H, C(CH₃)₂], 1.44 [s, 6 H, SC(CH₃)₂], 2.05 [s, 2 H, CH₂], 7.19 [m, 1 H, Ar-*H*], 7.62 [dd, *J* = 6.89, 1.37 Hz, 1 H, Ar-*H*], 7.87 [dd, *J* = 6.59, 1.51 Hz, 1 H, Ar-*H*]; ¹³C NMR (DCCl₃) ppm 30.64 [C(CH₃)₂], 33.30 [SC(CH₃)₂], 35.91 [C(CH₃)₂], 40.87 [SC(CH₃)₂], 53.89 [CH₂], 123.37-146.20 [Ar-C].

Mono-methyl Terephthaloyl Chloride (58). Commercially available *mono*-methyl terephthalate (**59**, 1.0 g, 5.5 mmol, Sigma-Aldrich Chemical Co.), along with SOCl₂ (4.89 g, 41.1 mmol, 7 eq), was placed in a 25-mL, single-necked, round-bottomed flask equipped with a spiral condenser. The resulting mixture was stirred at reflux (12 h). After approximately 2 h, the white solid dissolved. The resulting solution was allowed to cool to RT, and excess SOCl₂ was removed *in vacuo* to give a white solid which was placed under high vacuum (3 h, RT/0.75 mm Hg) to remove any residual SOCl₂. Acid

chloride **58** (1.06 g, 96%) was obtained as a white solid: mp 53-55 °C (mp 53-55 °C, Acros Organics); IR (KBr pellet) 1773 [C=C=O], 1770 [MeOC=O] cm⁻¹; ¹H NMR (DCCl₃) δ 3.98 [s, 3 H, OCH₃], 8.17 [m, 4 H, Ar-H]; ¹³C NMR (DCCl₃) ppm 52.69 [OCH₃], 129.95-136.59 [Ar-C], 165.56 [C=O], 167.87 [C=O]. ¹H NMR data has been recorded for **58**:¹³⁶ ¹H NMR (300 MHz, DCCl₃) δ 3.98 [s, 3 H], 8.03-8.24 [m, 4 H]. No further data was reported on this compound.

Determination of MICs. The MICs of the agents on solid medium were determined by the microdrop agar proportion test by the method of McClatchy¹⁶² as modified by Phetsuksiri and co-workers.¹⁵³ Briefly, a series of 10-fold dilutions of culture of *Mycobacterium bovis* (BCG) were prepared by using phosphate-buffered saline as a diluent. An aliquot (5 μL) of each dilution was spotted on plates of 7H11 agar (Difco) containing oleic acid-albumin-dextrose-citric acid (OADC) as a supplement and 0.1, 0.5, 1.0, 2.0, 2.5, 5.0, 10.0, and 20.0 μg of each tested drug per mL. The plates were incubated at 37 °C for 14 days, and the number of viable bacteria was scored by counting colonies.

Plate I



IR Spectrum of 32

Plate II

```

amideesters
expl stdih
SAMPLE
date Nov 16 2000 dfrq DEC. & VT 399.918
solvent COCl3 dn H1
file exp dpwr 30
ACQUISITION dof 0
sfrq 399.918 da nnn
tn H1 dm c
at 3.744 dsf 200
np 44028 dsag
sw 6000.6 dres 1.0
fb 3000 homo n
bs 16
tpwr 52 wtfile PROCESSING
pv 6.0 proc ft
dl 0 fn not used f
tof 0 math
nt 16
ct 16 werr
alock n wexp
gain 36 wds
FLAGS wnt
il n
in n
dp y
hs nn
DISPLAY
sp -220.3
wp 4037.1
vs 140
sc 0
wc 250
hzmh 16.15
ls 500.00
rf1 992.3
rfp 0
th 4
ins 25.000
nm cdc ph
    
```

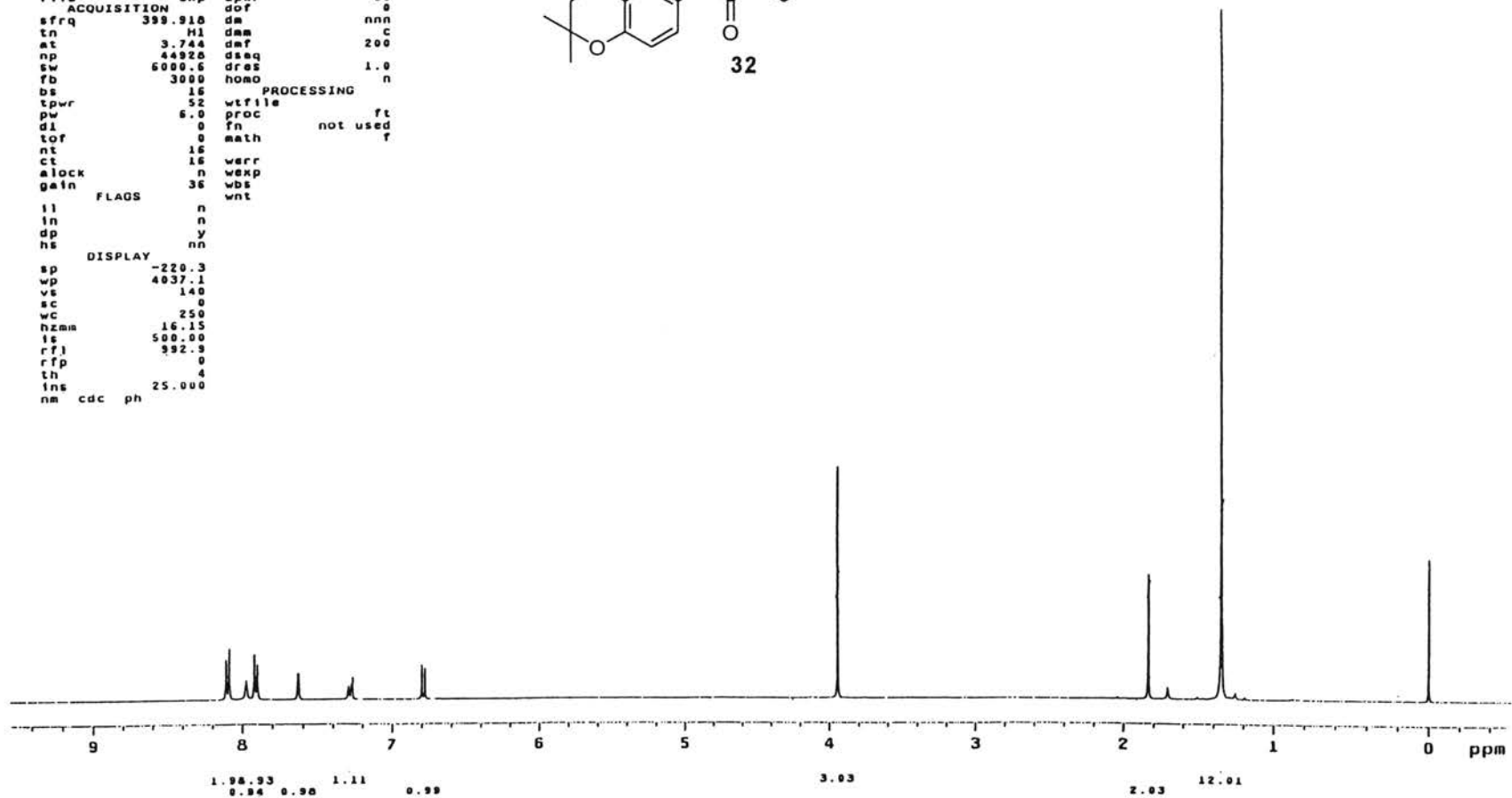
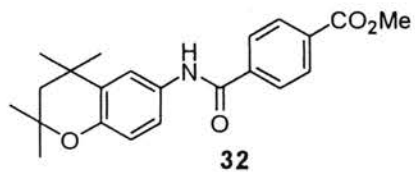
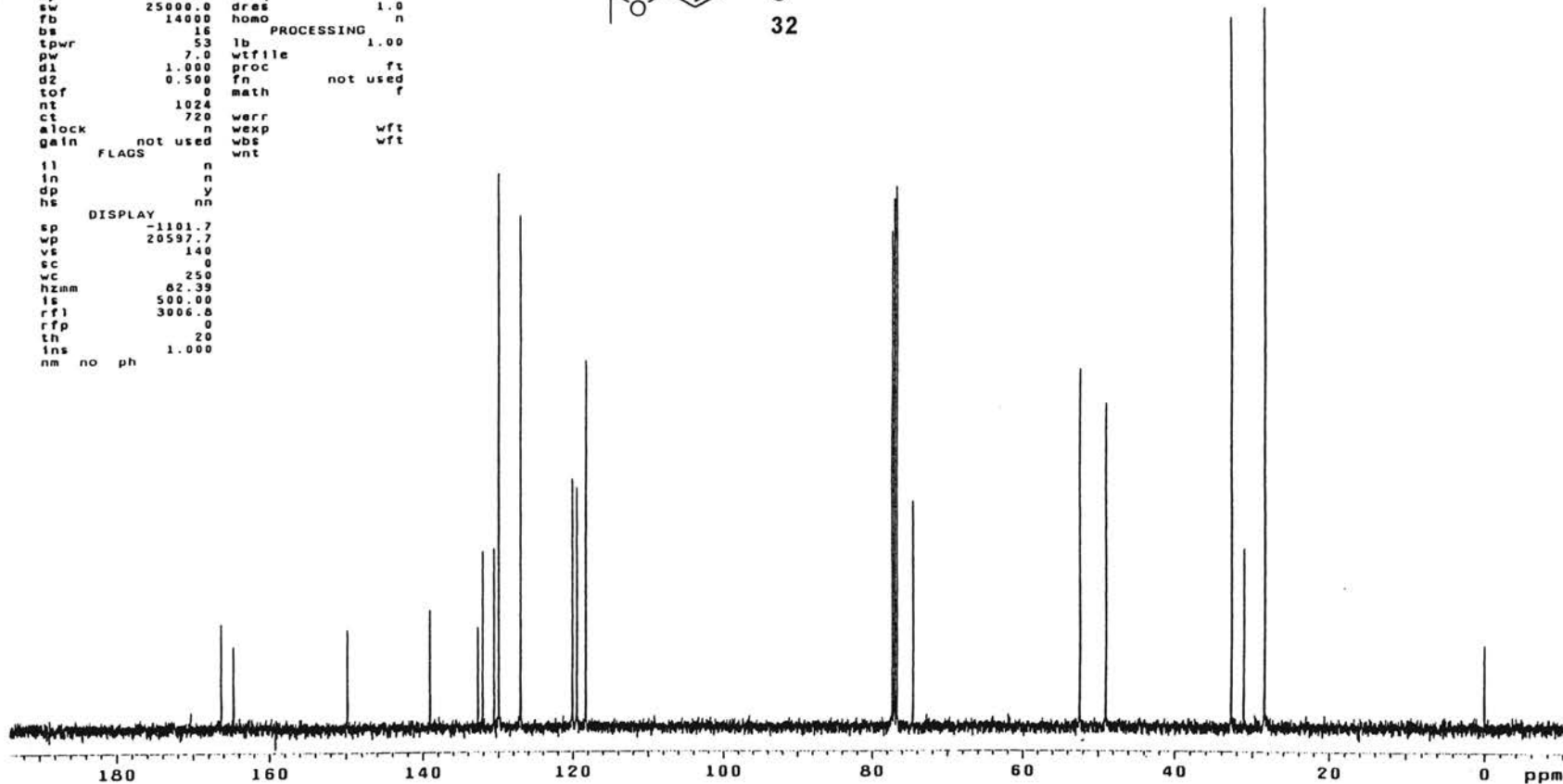
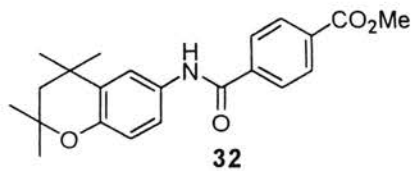


Plate III

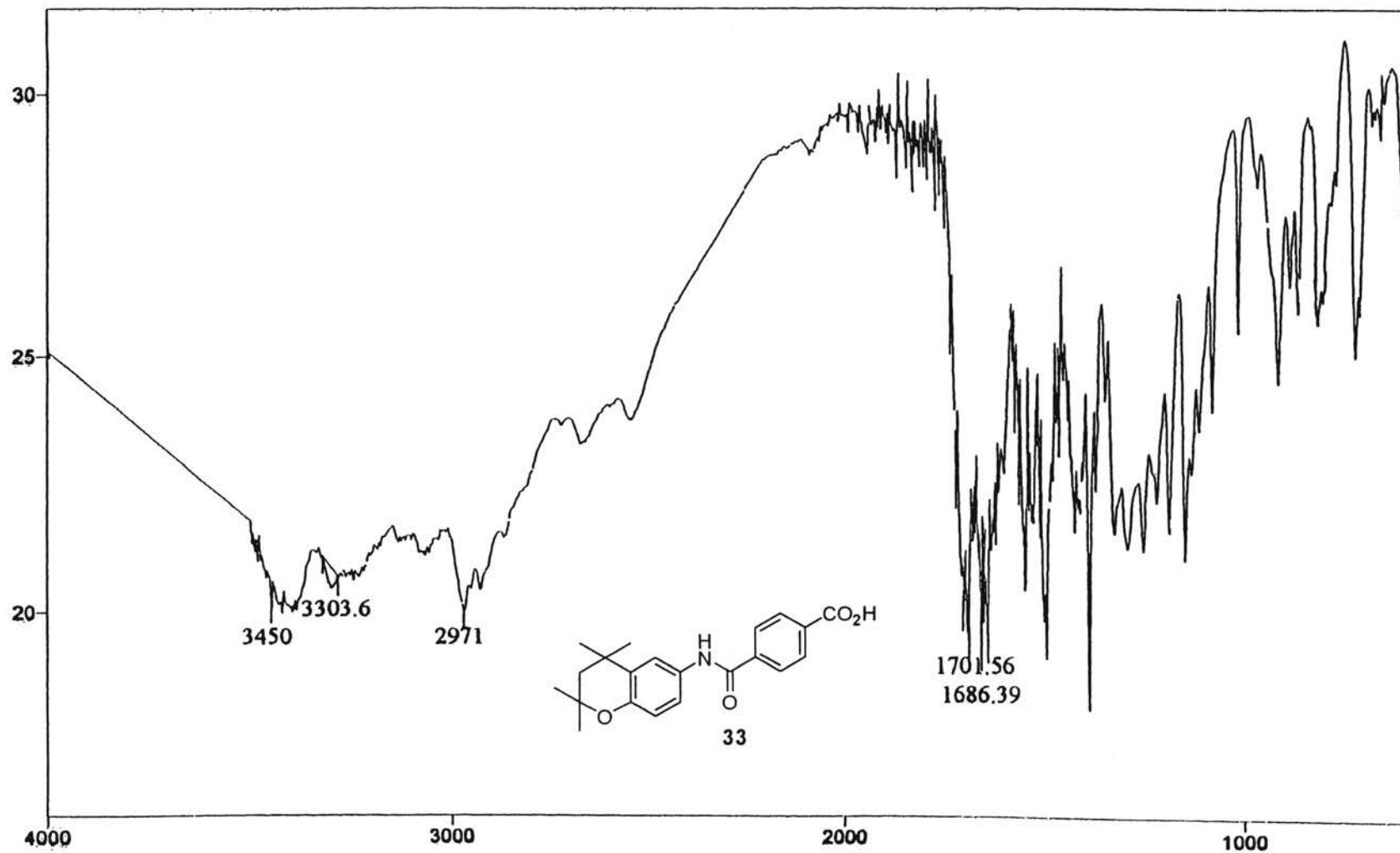
```

amideester6
expi std13c
SAMPLE
date Nov 16 2000 dfrq DEC. & VT 399.915
solvent CDCl3 dn H1
file exp dpwr 40
ACQUISITION exp dof 0
sfrq 100.568 da nyy
tn C13 dam w
at 1.199 dmf 12000
np 59968 dseq
sw 25000.0 dres 1.0
fb 14000 homo n
bs 16 PROCESSING
tpwr 53 lb 1.00
pw 7.0 wtfile
dl 1.000 proc ft
d2 0.500 fn not used
tof 0 math f
nt 1024
ct 720 werr
alock not used n wexp wft
gain not used n wds wft
          FLACS wnt
          n
          n
          y
          nn
DISPLAY
sp -1101.7
wp 20597.7
vs 140
sc 0
wc 250
hzmm 62.39
ls 500.00
rf1 3006.6
rfp 0
th 20
ins 1.000
nm no ph
    
```



¹³C NMR Spectrum of 32

Plate IV

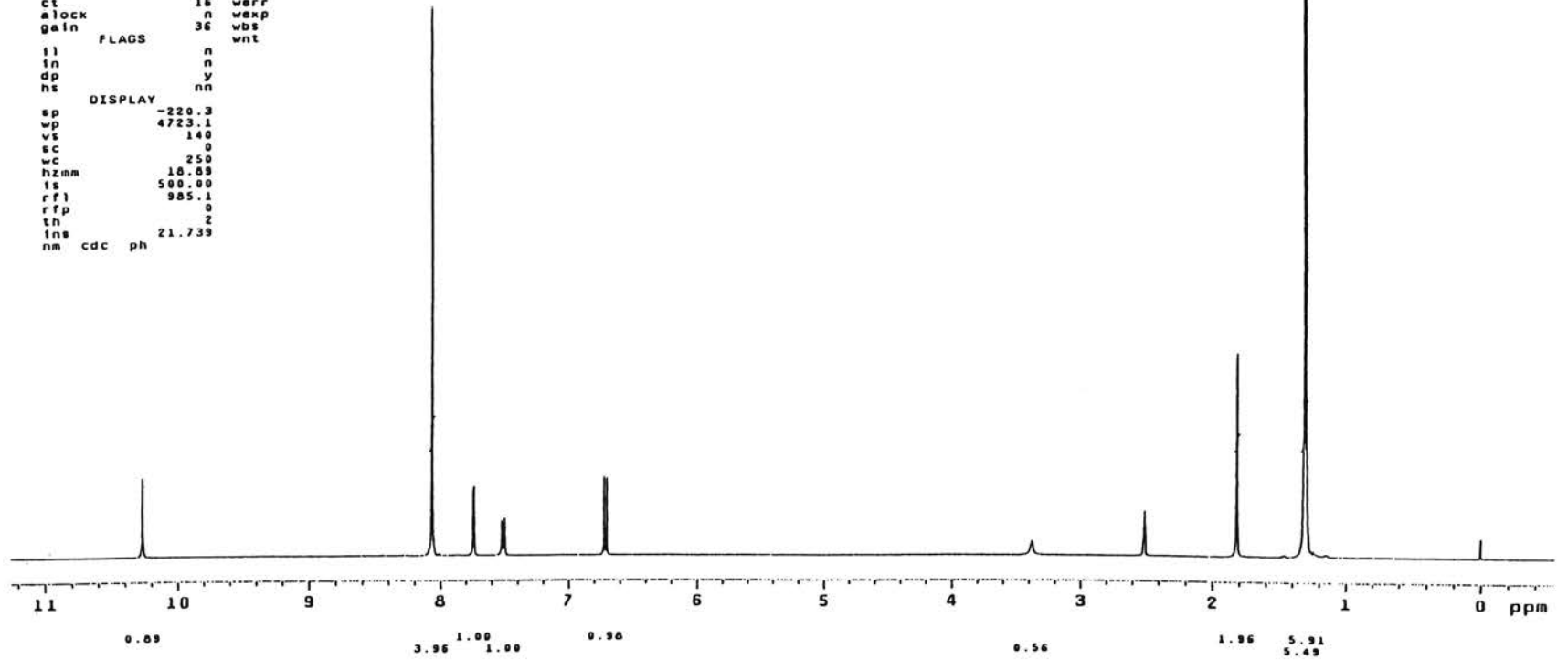
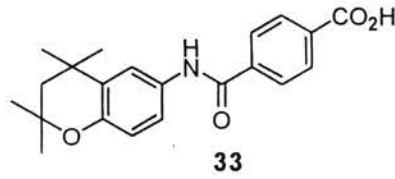


IR Spectrum of 33

Plate V

```

amideacid6
expl std1h
SAMPLE
date Nov 17 2000 dfrq DEC. & VT 399.920
solvent DMSO dn H1
file exp dpwr 30
ACQUISITION dof 0
sfrq 399.920 dm nnn
tn H1 dm c
at 3.744 dmf 200
np 44928 dseq
sw 6000.6 dras 1.0
fb 3000 homo n
bs 16 PROCESSING
tpwr 52 wtfile
pw 6.0 proc ft
dl 0 fn not used
tof 0 math f
nt 16
ct 16 werr
alock n wexp
gain 36 wds
        wnt
        FLAGS
il n
in n
dp y
hs nn
        DISPLAY
sp -220.3
wp 4723.1
vs 140
sc 0
wc 250
hznm 18.69
fs 500.00
rf 985.1
rfp 0
th 2
ins 21.739
nm cdc ph
    
```

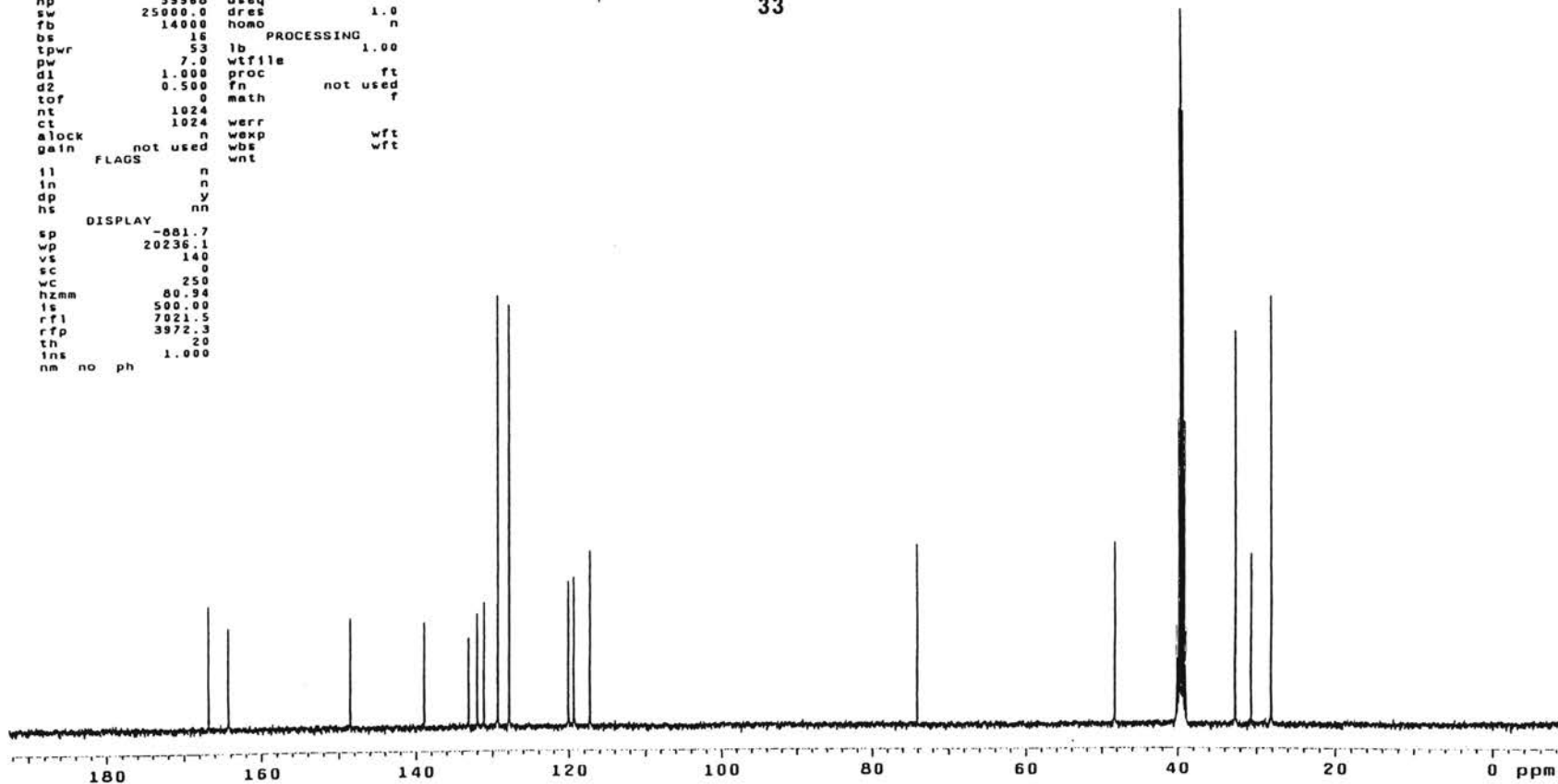
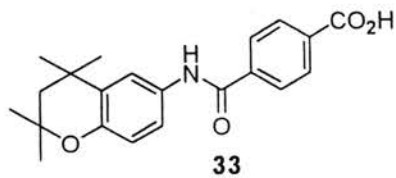


¹H NMR Spectrum of 33

Plate VI

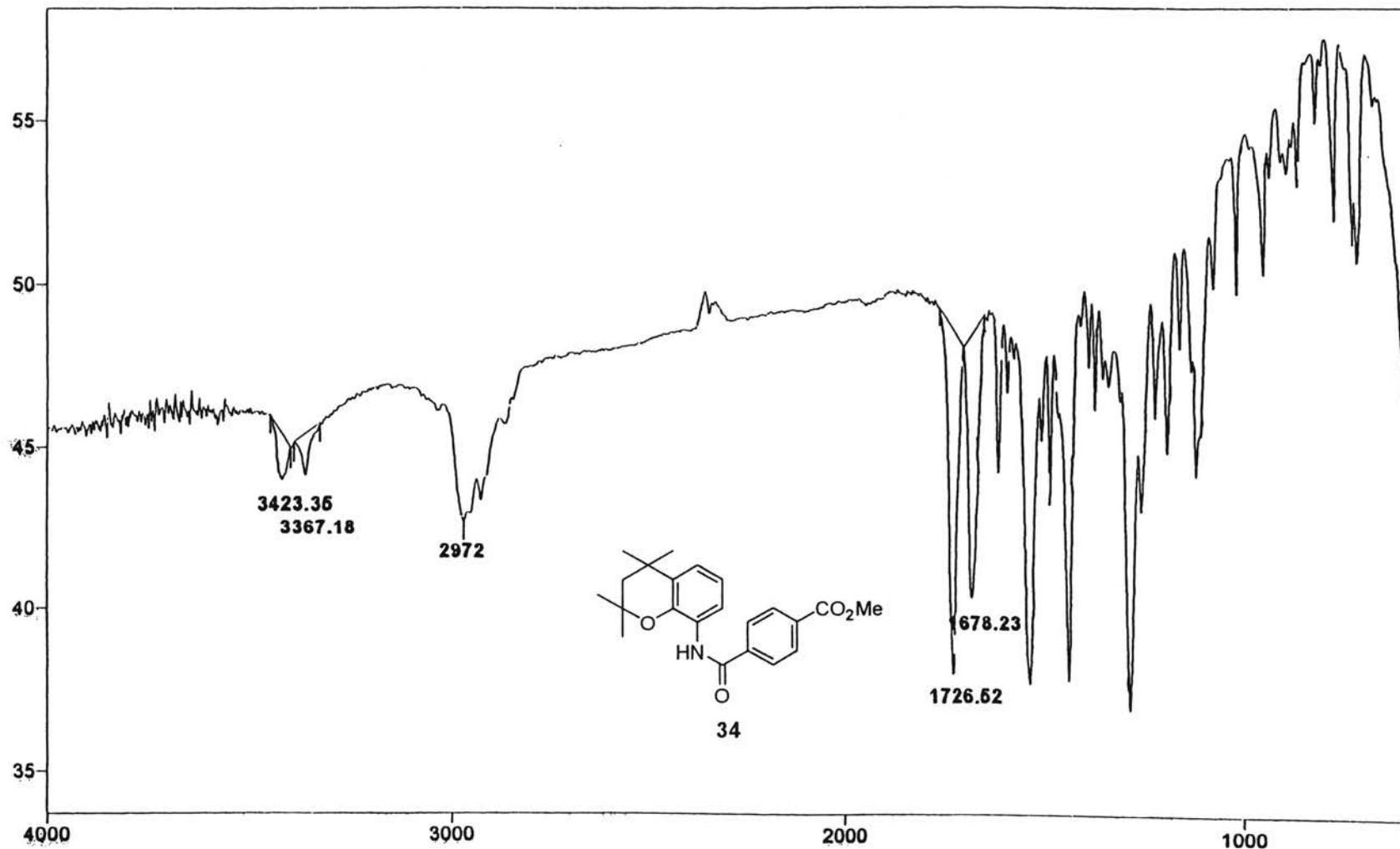
```

amideacid6
expl std13c
SAMPLE
date Nov 17 2000 dfrq DEC. & VT 399.920
solvent OMSD dn H1
file exp dpwr 40
ACQUISITION dof 0
sfrq 100.569 dm nyy
tn C13 dmm w
at 1.199 dmf 12000
np 53960 dseq
sw 25000.0 dres 1.0
fb 14000 homo n
bs 16 PROCESSING
tpwr 53 lb 1.00
pw 7.0 wfile
d1 1.000 proc ft
d2 0.500 fn not used
tof 0 math f
nt 1024
ct 1024 werr
alock n wexp wft
gain not used wbs wft
FLAGS n wnt
il n
in n
dp y
hs nn
DISPLAY
sp -081.7
wp 20236.1
vs 140
sc 0
wc 250
hzmm 80.94
fs 500.00
rf1 7021.5
rfp 3972.3
th 20
ins 1.000
nm no ph
    
```



¹³C NMR Spectrum of 33

Plate VII

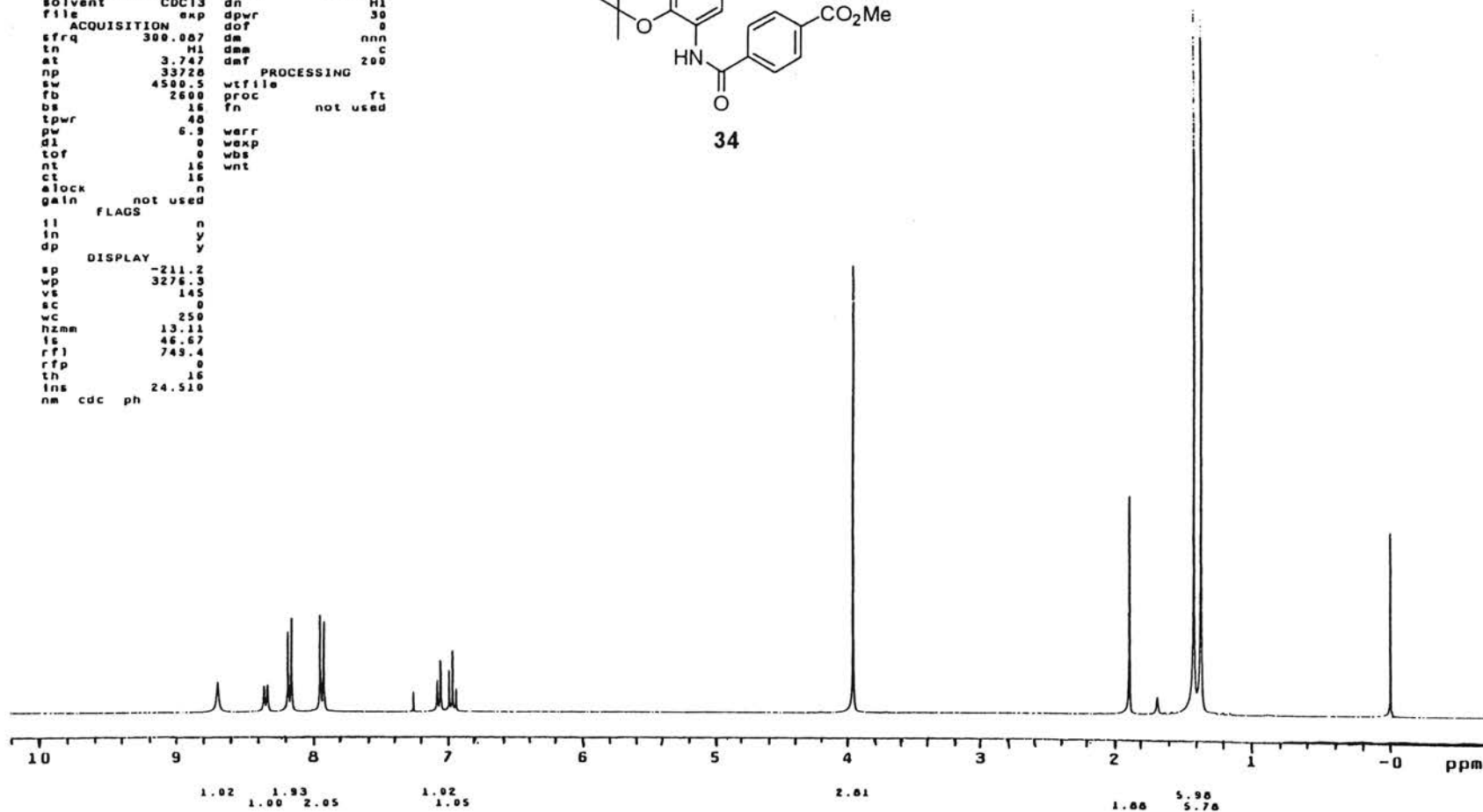
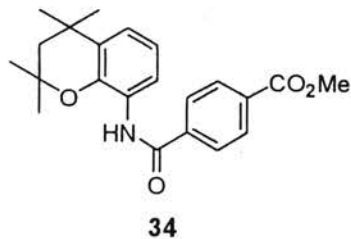


IR Spectrum of 34

Plate VIII

```

amidesters
expl stdih
date Aug 22 2000 dfrq DEC. & VT 300.087
solvent CDC13 dn H1
file exp dpwr 30
ACQUISITION dof 0
sfrq 300.087 dm nnn
tn H1 dnm C
at 3.747 dmf 200
np 33728 PROCESSING
sw 4500.5 wtfile
fb 2600 proc ft
bs 15 fn not used
tpwr 48
pw 6.9 werr
dl 0 wexp
tof 0 wbs
nt 16 wnt
ct 15
elock n
gain not used
FLAGS
il n
in y
dp y
DISPLAY
sp -211.2
wp 3276.3
vs 145
sc 0
wc 250
hzmm 13.11
fs 46.67
rf1 749.4
rfp 0
th 16
ins 24.510
nm cdc ph
    
```

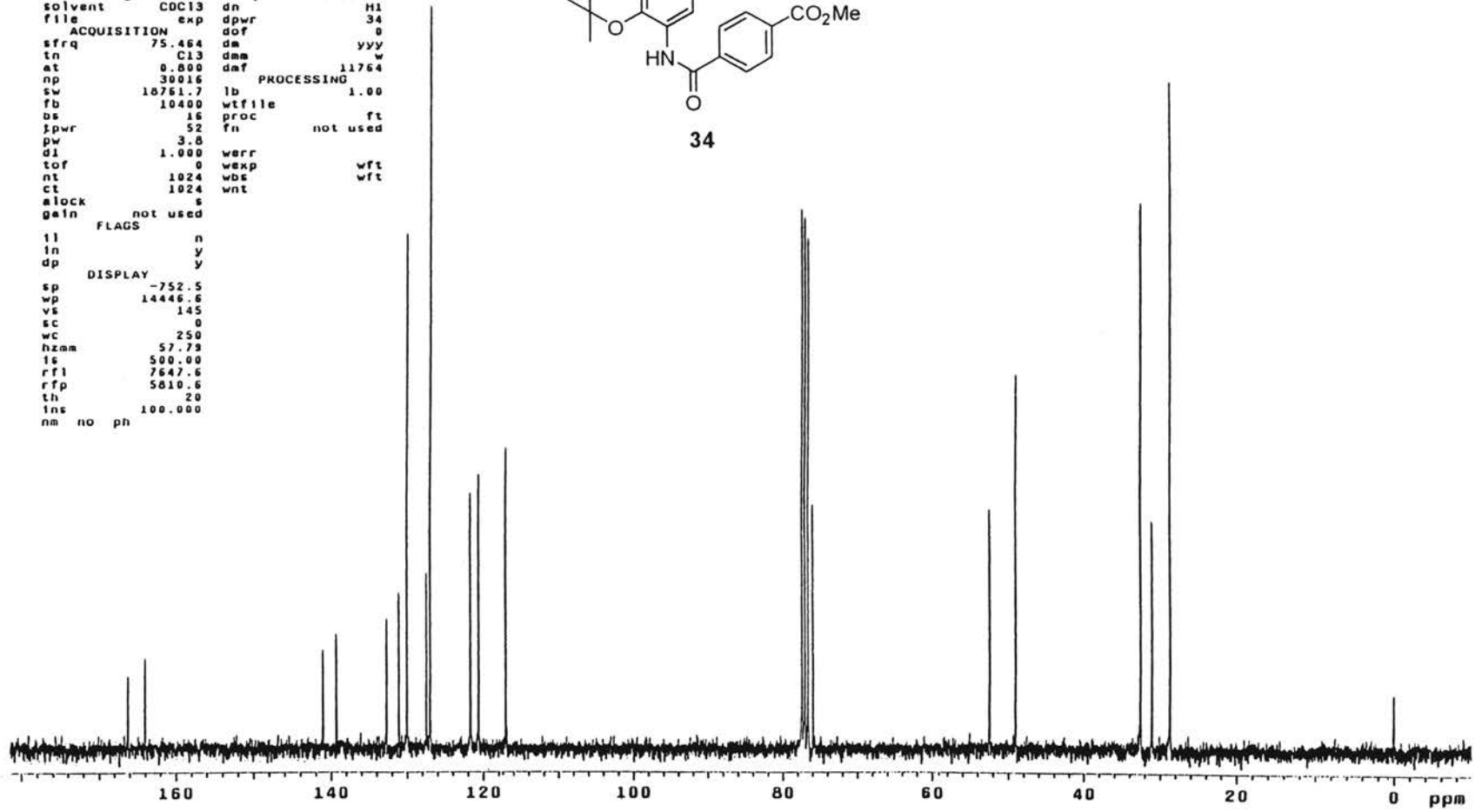
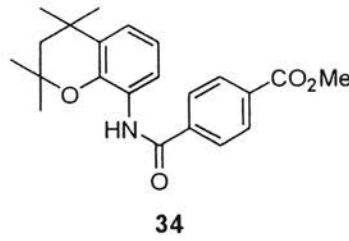


¹H NMR Spectrum of 34

Plate IX

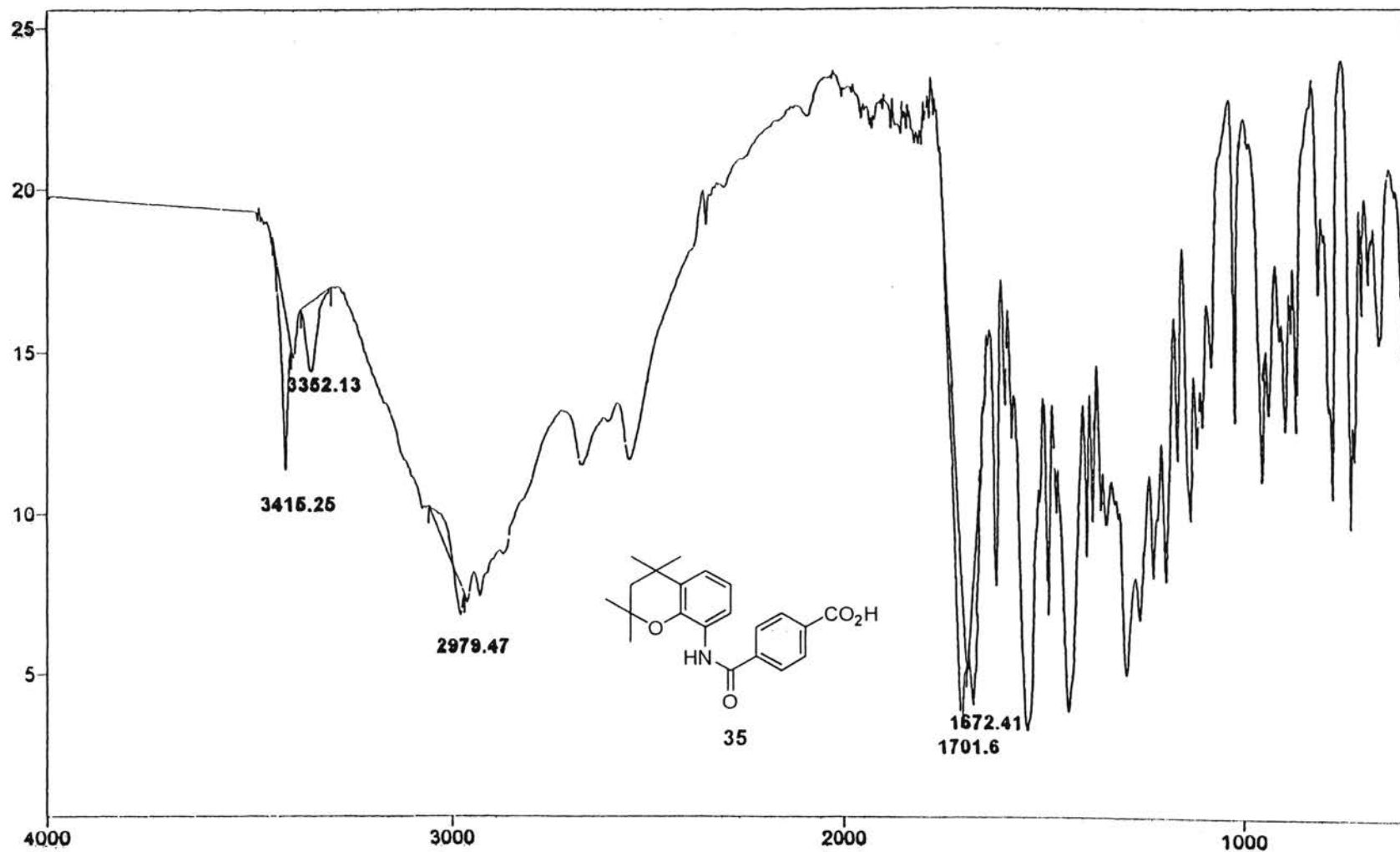
```

amideester0
expl std13c
SAMPLE
date Aug 22 2000 dfrq DEC. & VT 300.087
solvent CDCl3 dn M1
file exp dpwr 34
ACQUISITION dof 0
sfrq 75.464 dm yyy
tn C13 dnm w
at 0.800 daf 11764
np 3016 PROCESSING 1.00
sw 10761.7 lb
fb 10400 wfile ft
bs 16 proc ft
lpwr 52 fn not used
pw 3.8
dl 1.000 werr
tof 0 wexp wft
nt 1024 wds wft
ct 1024 wnt
aLOCK s
gain not used
FLAGS
tl n
ln y
dp y
DISPLAY
sp -752.5
wp 14446.6
vs 145
sc 0
wc 250
hzmm 57.73
fs 500.00
rf1 7647.5
rfp 5010.6
th 20
ins 100.000
nm no ph
    
```



¹³C NMR Spectrum of 34

Plate X

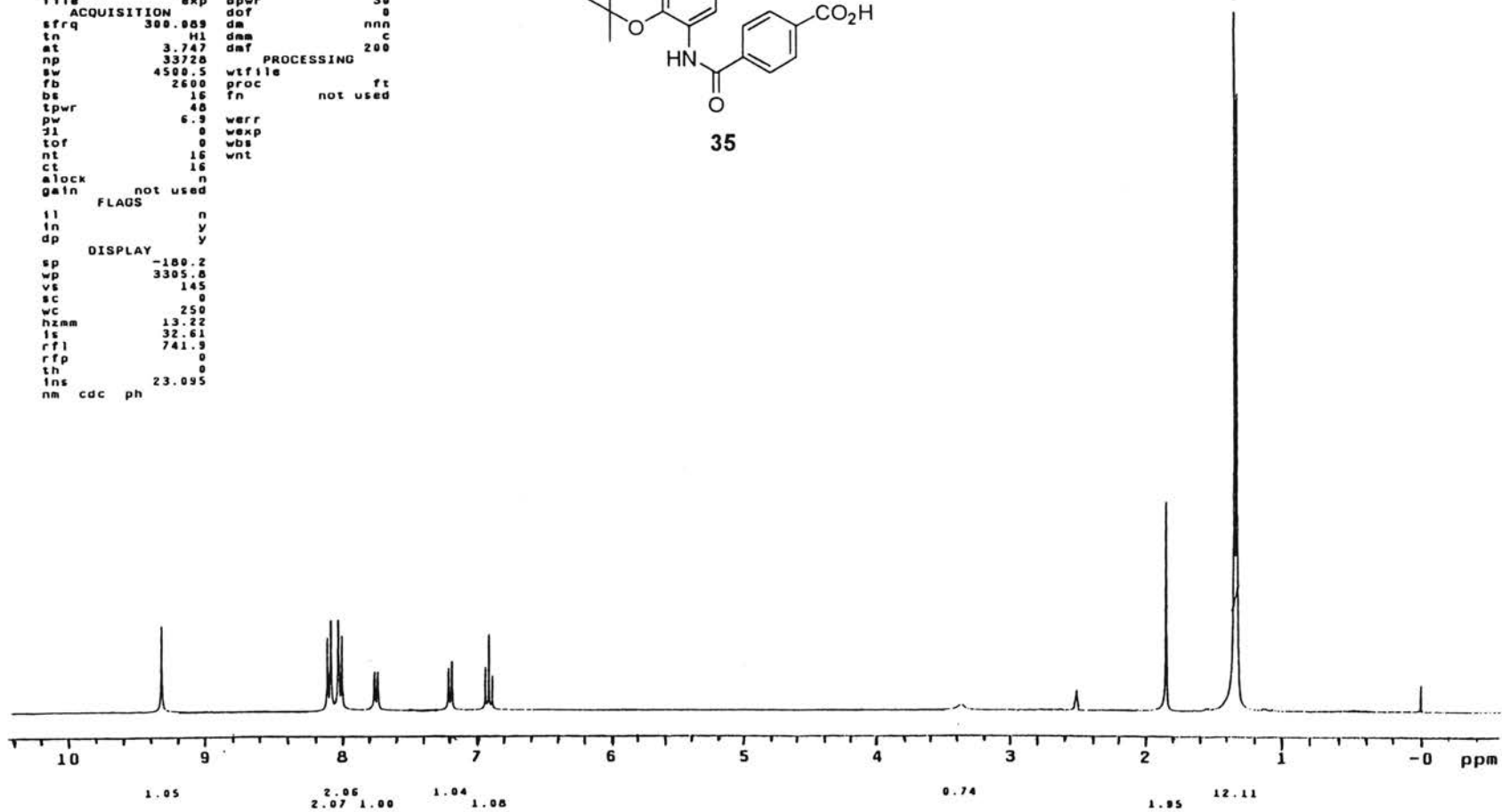
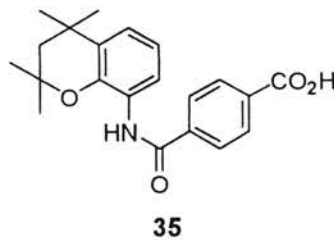


IR Spectrum of 35

Plate XI

```

amideacide8
expi stdih
SAMPLE
date Aug 24 2000 dfrq DEC. & VT 300.000
solvent DMSO dn H1
file exp dpwr 30
ACQUISITION dof 0
sfrq 300.000 dm nnn
tn H1 dm c
at 3.747 daf 200
np 33728
sw 4500.5 wfile
fb 2600 proc ft
bs 16 fn not used
tpwr 48
pw 6.9 werr
jl 0 wexp
tof 0 wds
nt 16 wnt
ct 16
alock n
gain not used
FLAOS
il n
in y
dp y
DISPLAY
sp -180.2
wp 3305.8
vs 145
sc 0
wc 250
hzmm 13.22
fs 32.61
rf1 741.3
rfp 0
th 0
fns 23.095
nm cdc ph
    
```

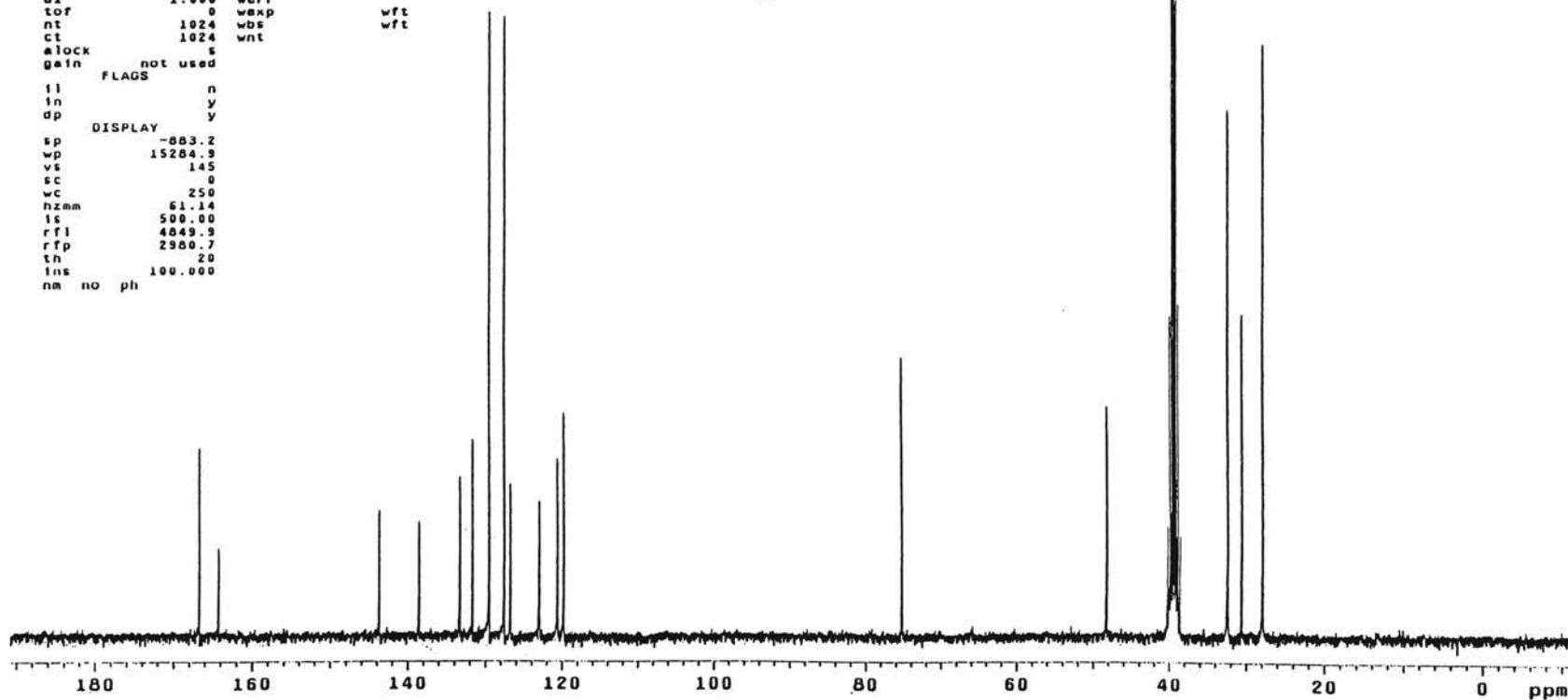
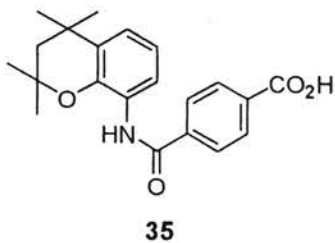


¹H NMR Spectrum of 35

Plate XII

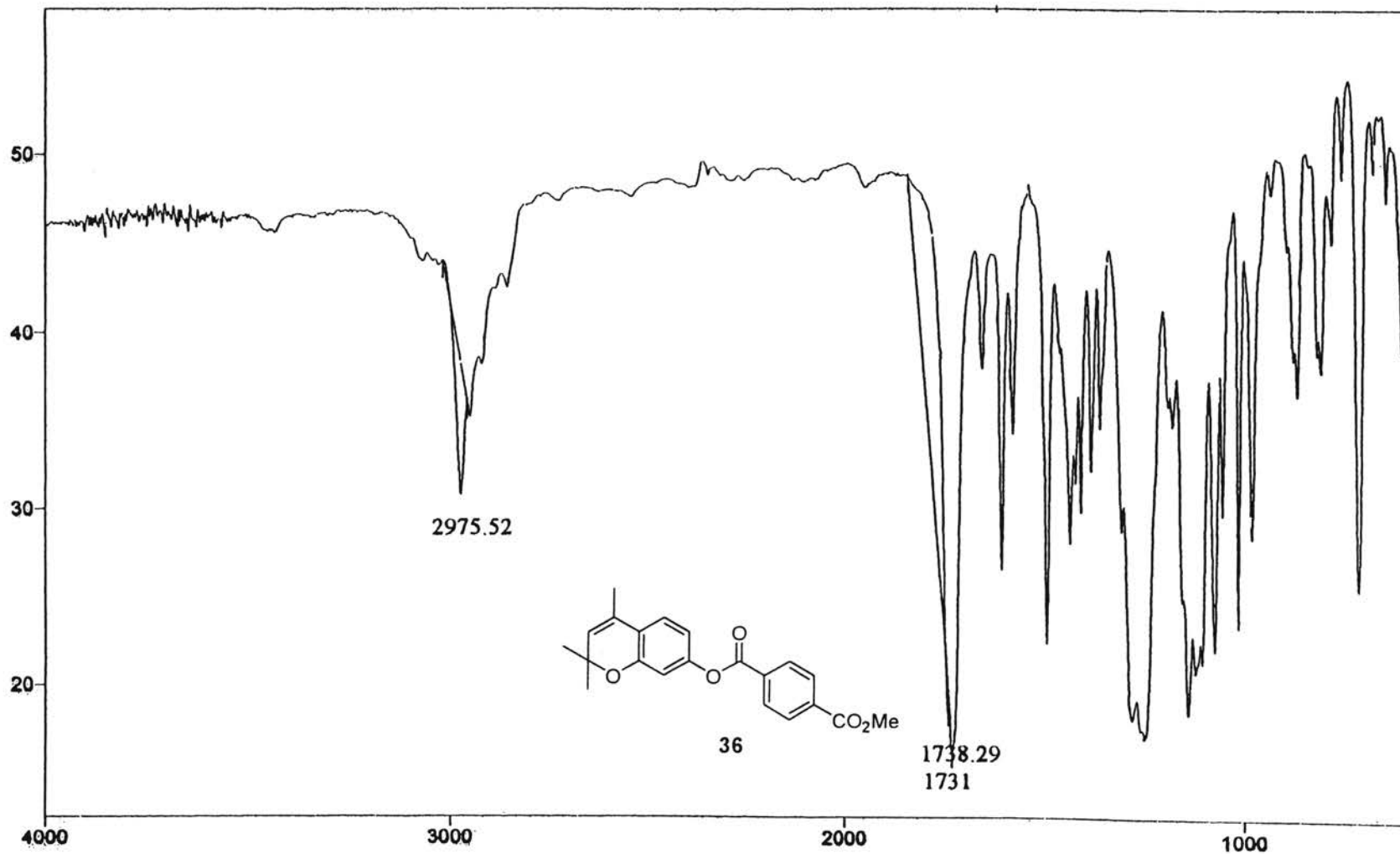
```

amideacid8
expl std13c
SAMPLE DEC. & VT
date Aug 23 2000 dfrq 300.089
solvent DMSO dn H1
file exp dpwr 34
ACQUISITION dot 9
sfrq 75.464 dm yyy
tn C13 dma w
at 0.800 dmf 11764
np 30016 PROCESSING
sw 18761.7 lb 1.00
fb 10400 wtfile
bs 16 proc ft
tpwr 52 fn not used
pw 3.8
d1 1.000 werr
tor 0 wexp wft
nt 1024 wbs wft
ct 1024 wnt
alock s
gain not used
FLAGS
ll n
ln y
dp y
DISPLAY
sp -883.2
wp 15284.3
vs 145
sc 0
wc 250
hzmm 61.14
ls 500.00
rf1 4849.3
rfp 2980.7
th 20
int 100.000
na no ph
    
```



¹³C NMR Spectrum of 35

Plate XIII



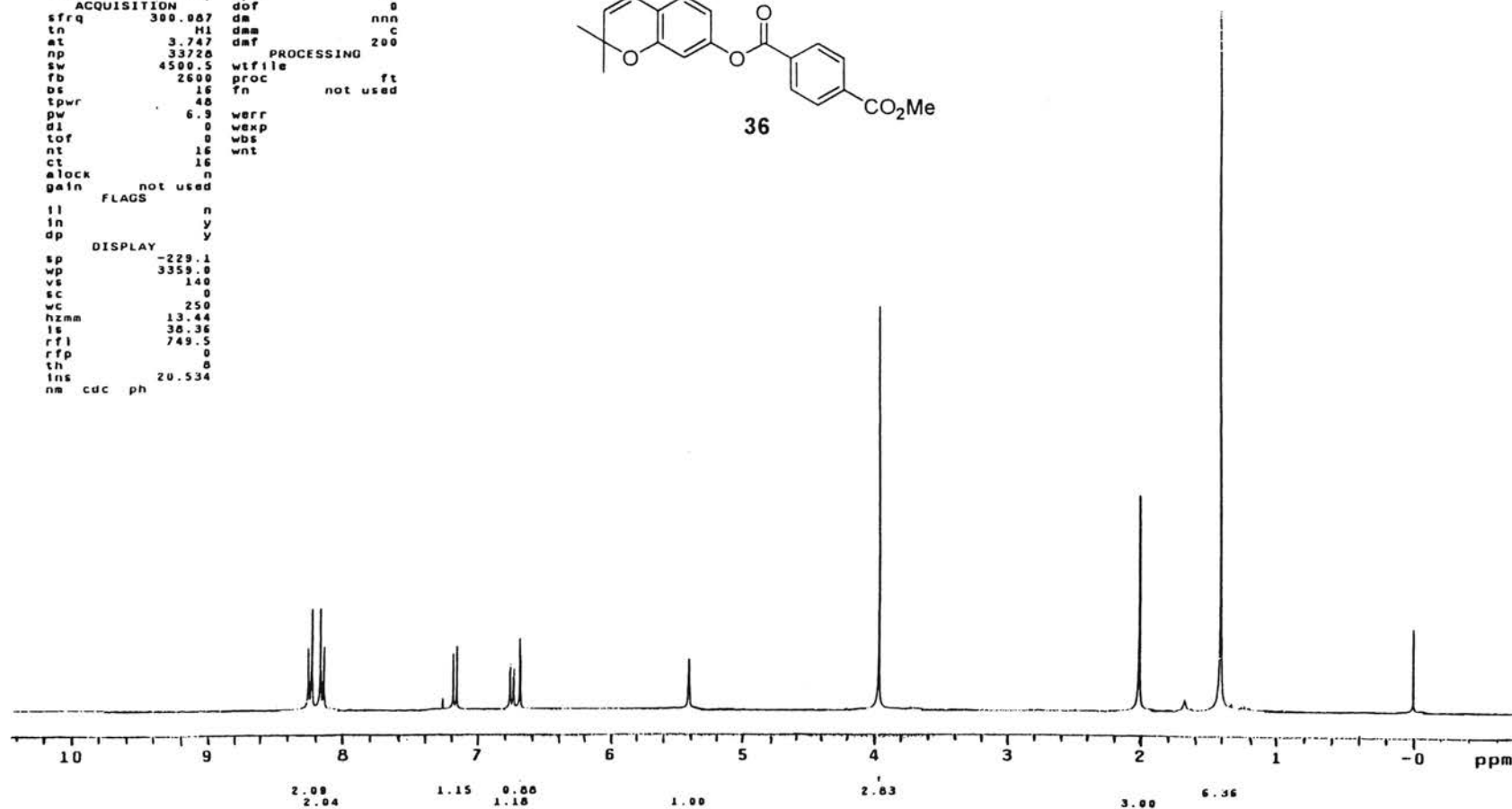
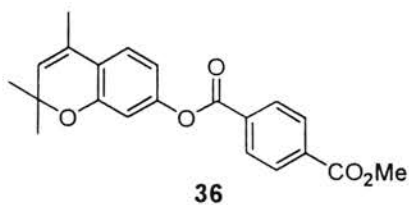
IR Spectrum of 36

Plate XIV

7ester_methylester_chromen

expt stdih

date	Aug 11 2000	dfrq	DEC. & VT	300.007
solvent	CDCl3	dn	H1	
file	exp	dpwr	30	
ACQUISITION				
sfrq	300.007	ds	nnn	0
tn	H1	dsm	C	
at	3.747	daf	200	
np	33720	PROCESSING		
sw	4500.5	wtfile	ft	
fb	2000	proc	not used	
bs	15	fn		
tpwr	40	werr		
pw	6.3	wexp		
di	0	wbs		
tof	0	wnt		
nt	16			
ct	16			
elock	n			
gain	not used			
FLAGS				
il	n			
in	y			
dp	y			
DISPLAY				
sp	-229.1			
wp	3359.0			
vs	140			
sc	0			
wc	250			
hzmm	13.44			
ls	30.36			
rfl	749.5			
rtp	0			
th	0			
ins	20.534			
nm	cdc ph			



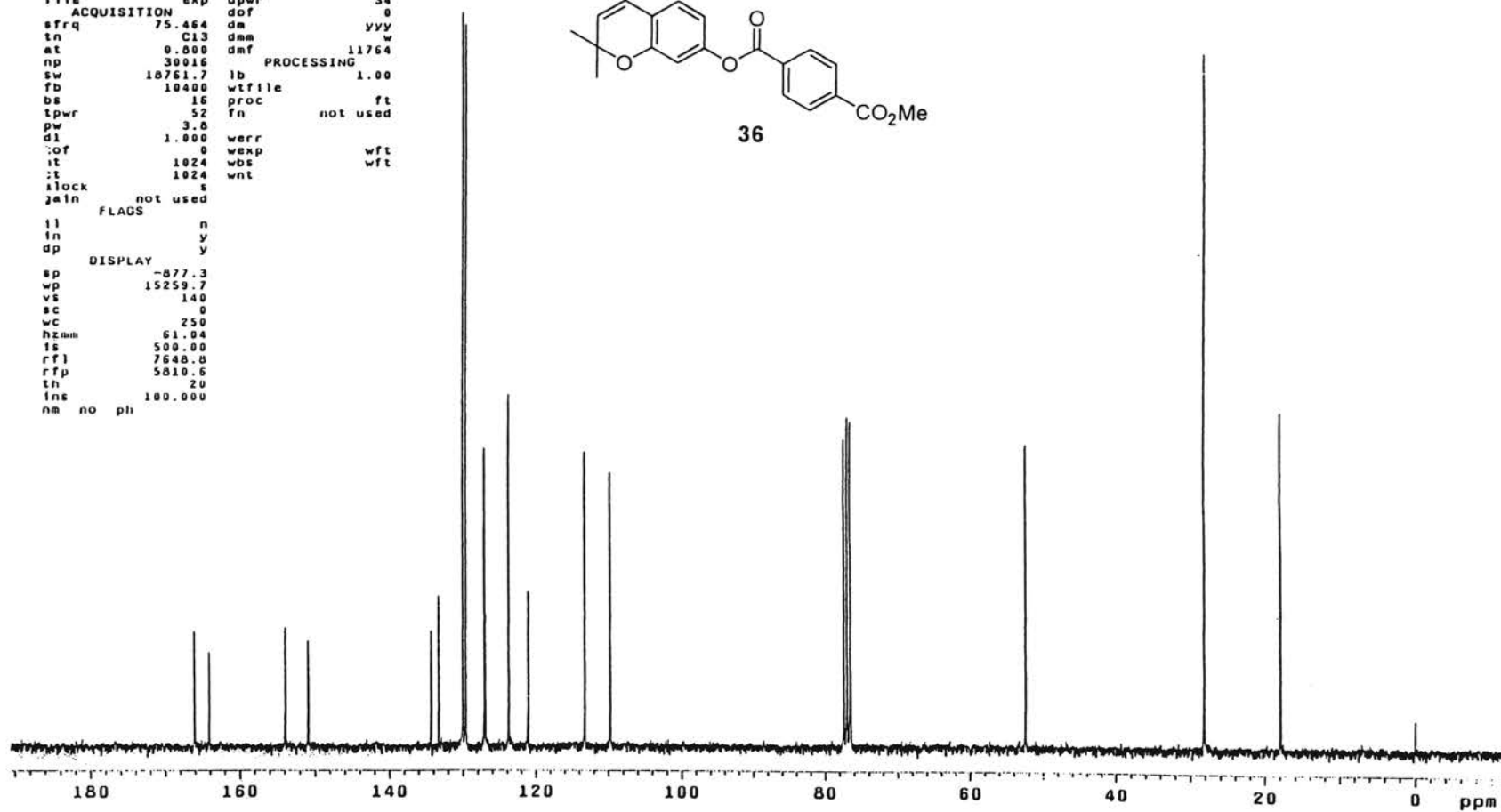
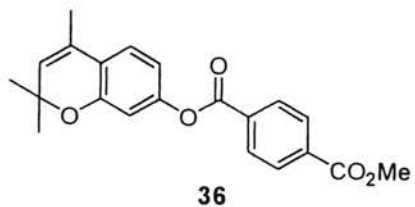
¹H NMR Spectrum of 36

Plate XV

7ester_methyl ester_chromen

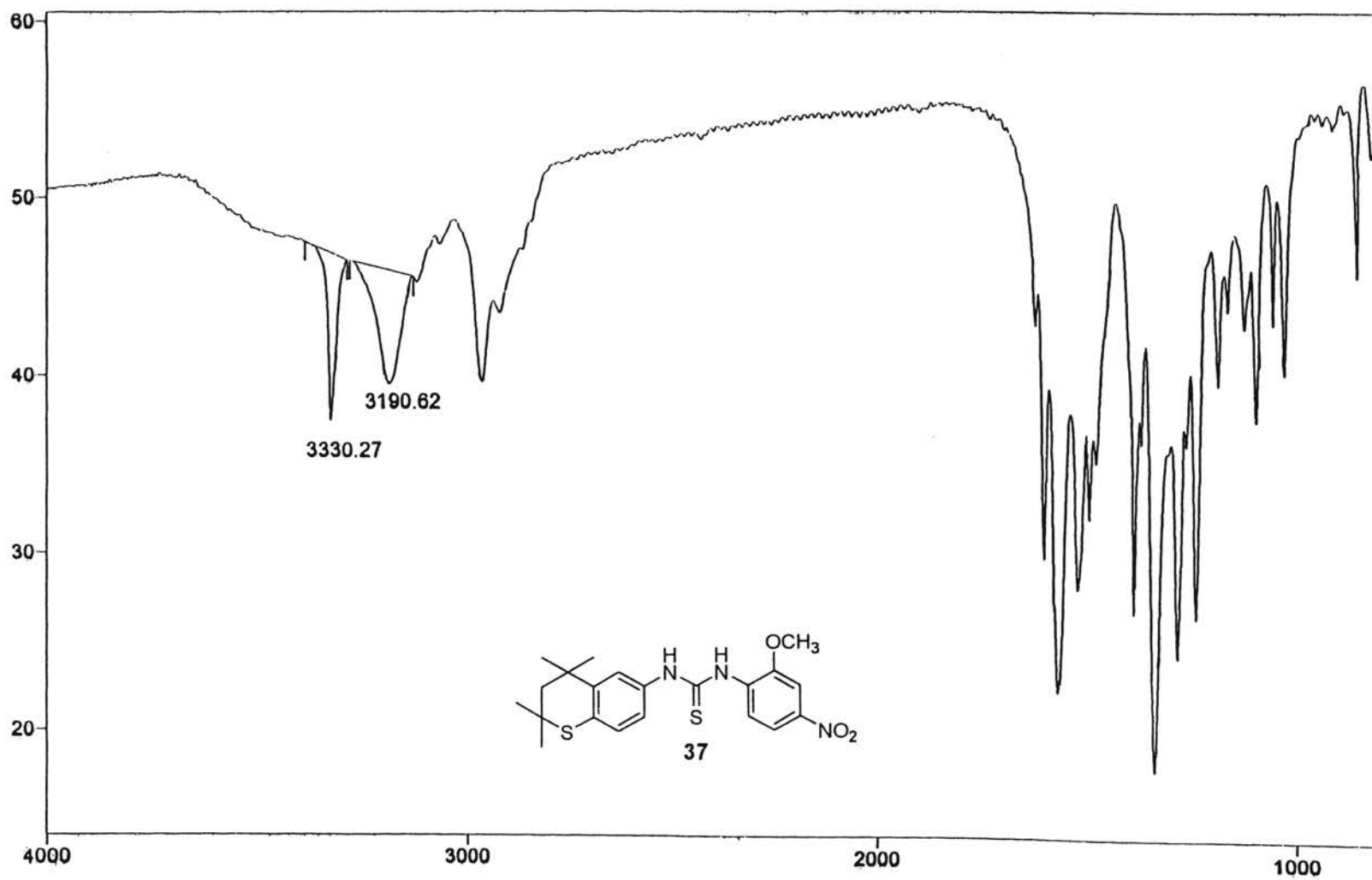
expl std13c

date	Aug 11 2000	dfrq	300.007
solvent	CDC13	dn	H1
file	exp	dpwr	34
ACQUISITION	exp	dof	0
sfrq	75.464	dm	yyy
tn	C13	dmm	w
at	0.000	dmf	11764
np	30016	PROCESSING	
sw	10761.7	lb	1.00
fb	10400	wtfile	
bs	16	proc	ft
tpwr	52	fn	not used
pw	3.0		
d1	1.000	werr	
cor	0	wexp	wft
it	1024	wbs	wft
st	1024	wnt	
ilock	s		
zain	not used		
il	FLAGS	n	
in		y	
dp		y	
DISPLAY			
sp	-077.3		
wp	15259.7		
vs	140		
sc	0		
wc	250		
hzmm	61.04		
fs	500.00		
rfl	7648.0		
rtp	5810.6		
th	20		
lms	100.000		
nm	no	ph	



¹³C NMR Spectrum of 36

Plate XVI



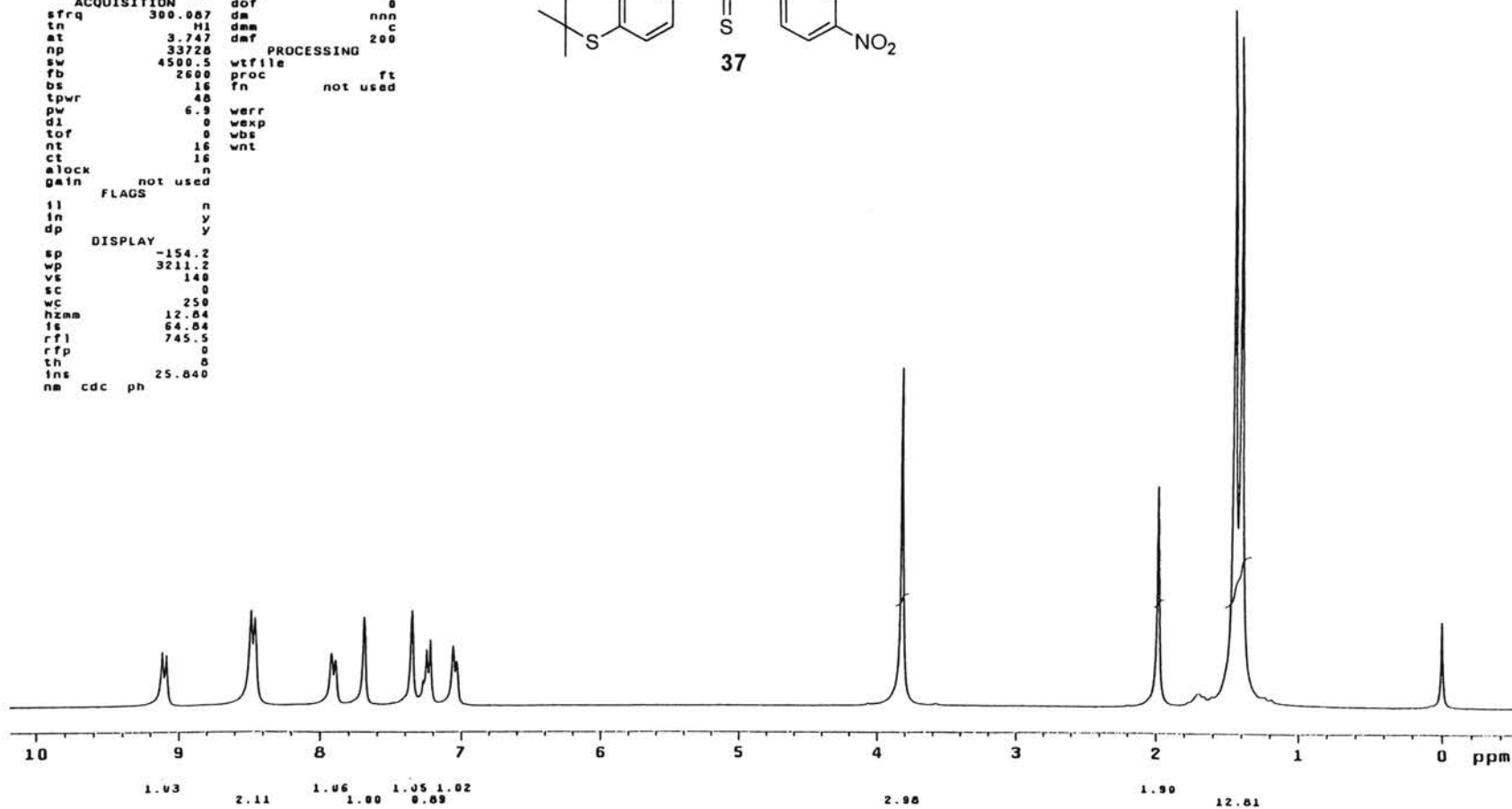
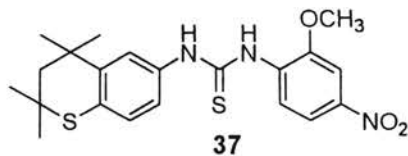
IR Spectrum of 37

Plate XVII

sulfur-methoxy-6-thiourea

expl stdih

date	Apr 20 2001	dfrq	DEC. & VT	300.087
solvent	CDCl3	dn	H1	
file	exp	dpwr	30	
ACQUISITION				
sfrq	300.087	ds	nn	c
tn	H1	dsm		
at	3.747	daf	200	
np	33728	PROCESSING		
sw	4500.5	wtfile	ft	
fb	2600	proc	fn	not used
bs	16			
tpwr	48			
pw	6.9	werr		
dl	0	wexp		
tof	0	wbs		
nt	16	wnt		
ct	16			
alock				
gain	not used			
FLAGS				
il	n			
in	y			
dp	y			
DISPLAY				
sp	-154.2			
wp	3211.2			
vs	140			
sc	0			
wc	250			
hznm	12.84			
fs	64.84			
rfl	745.5			
rtp	0			
th	8			
ins	25.840			
nm	cdc ph			



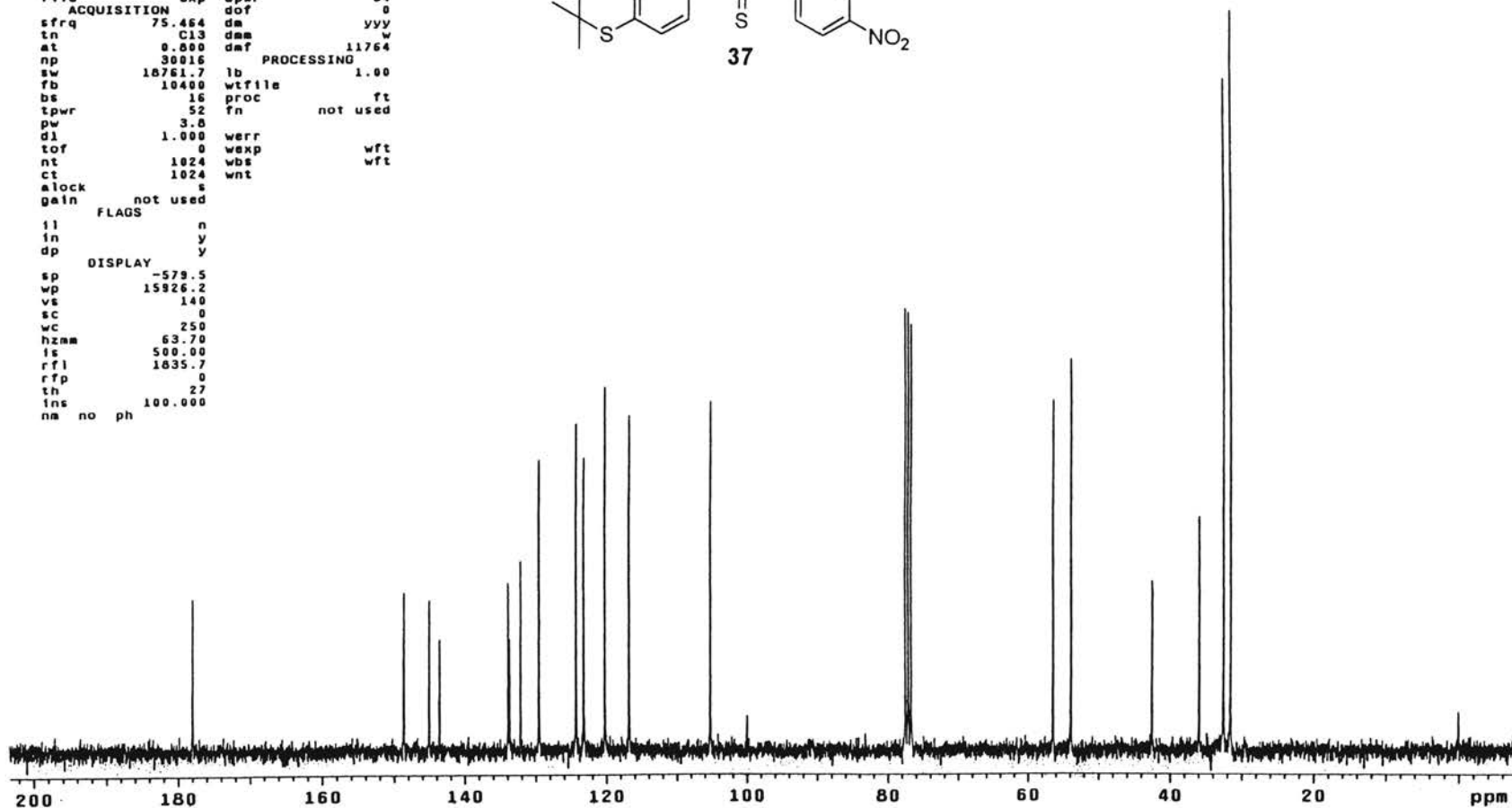
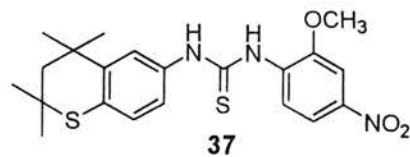
¹H NMR Spectrum of 37

Plate XVIII

sulfur-methoxy-6-thiourea

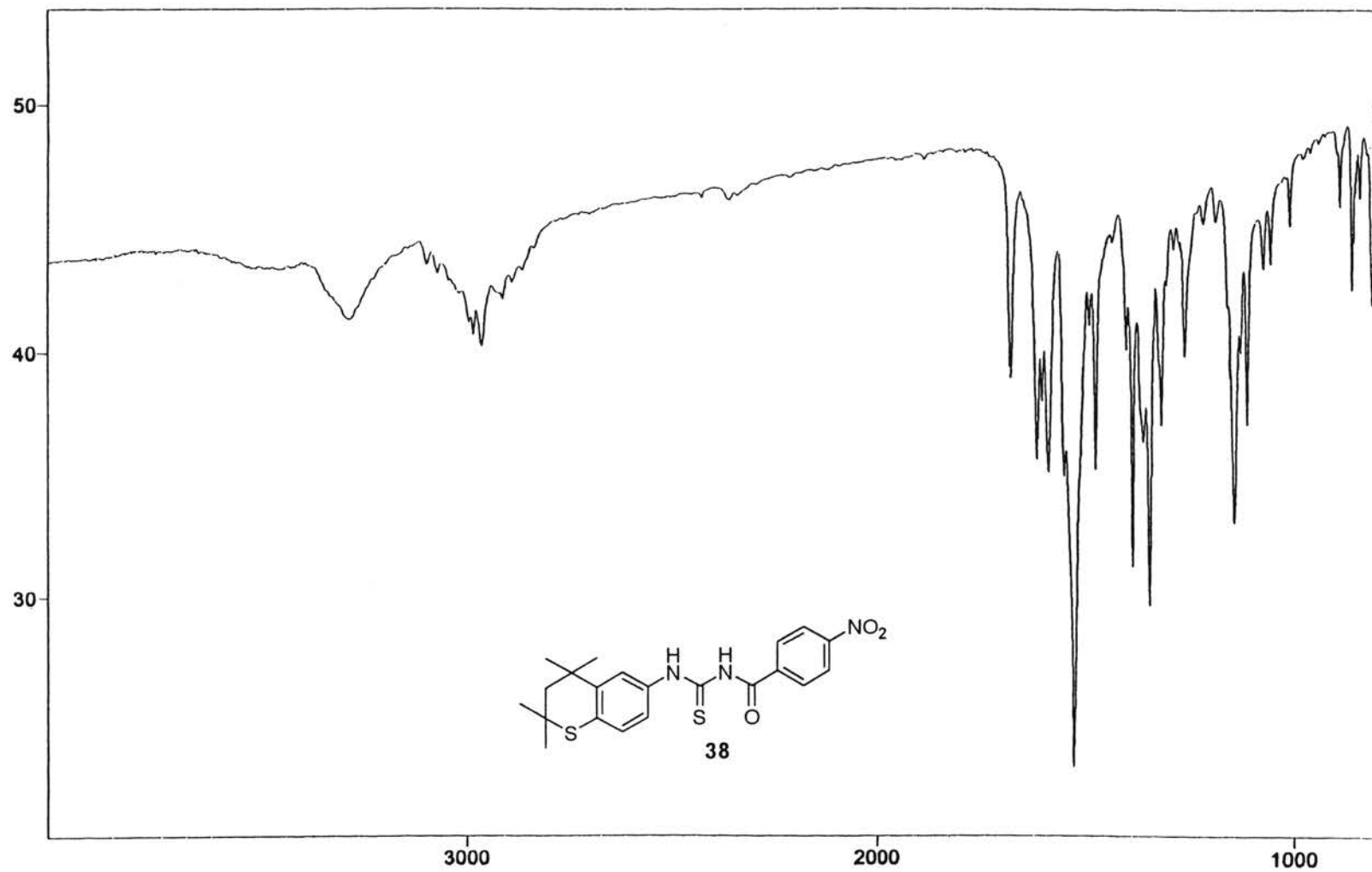
expl std13c

date	Apr 20 2001	dfrq	300.067
solvent	CDC13	dn	H1
file	exp	dpwr	34
ACQUISITION			
exp		dof	0
sfrq	75.464	dm	yyy
tn	C13	dmm	w
at	0.000	dmf	11764
np	30016	PROCESSING	
sw	18761.7	lb	1.00
Tb	10400	wtfile	
bs	16	proc	ft
tpwr	52	fn	not used
pw	3.0		
dl	1.000	werr	
tof	0	wexp	wft
nt	1024	wbs	wft
ct	1024	wnt	
alock	s		
gain	not used		
FLAGS			
ij	n		
in	y		
dp	y		
DISPLAY			
sp	-579.5		
wp	15926.2		
vs	140		
sc	0		
wc	250		
hzmm	63.70		
is	500.00		
rfl	1035.7		
rfp	0		
th	27		
ins	100.000		
nm	no	ph	



¹³C NMR Spectrum of 37

Plate XIX



IR Spectrum of 38

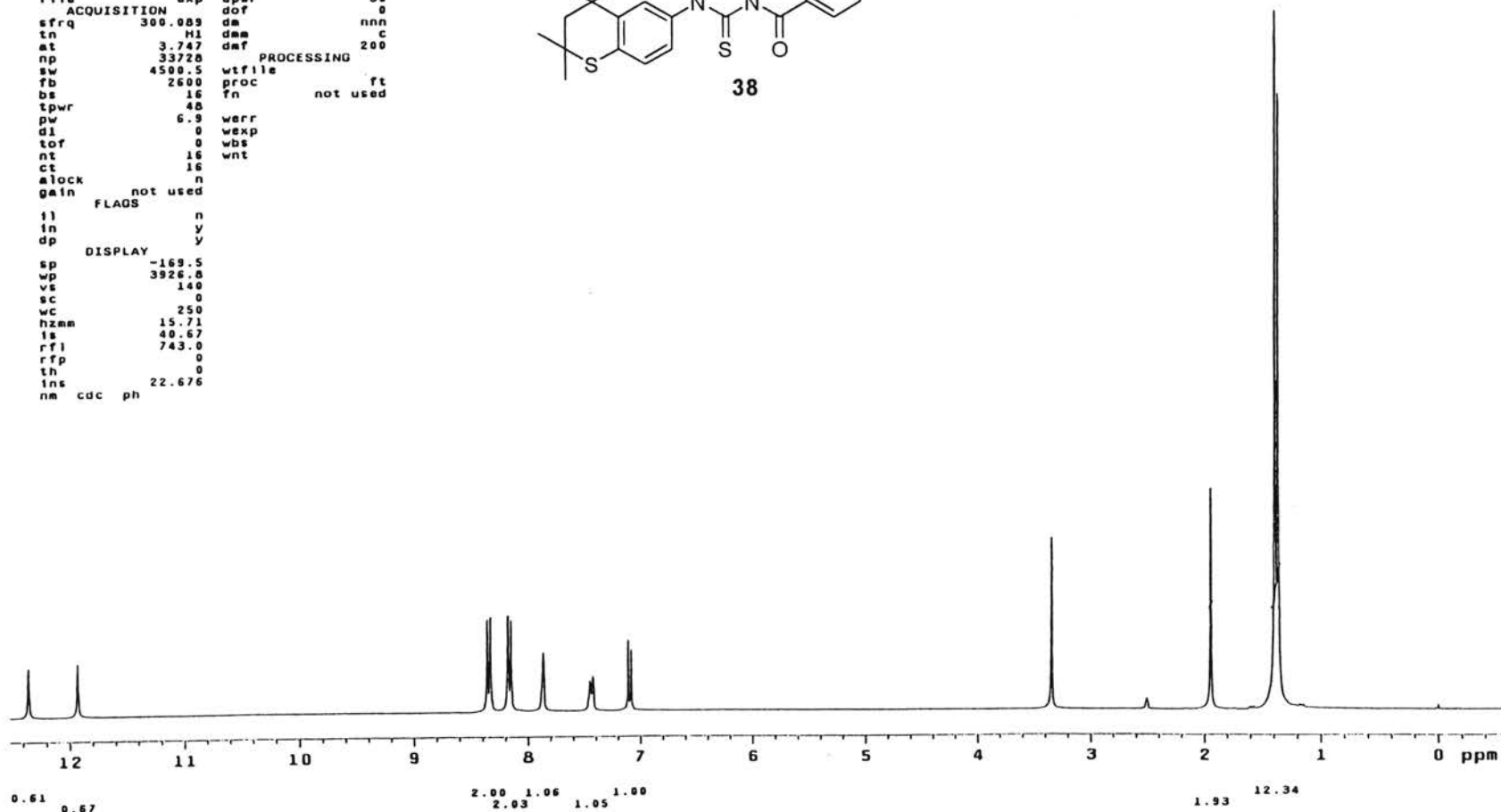
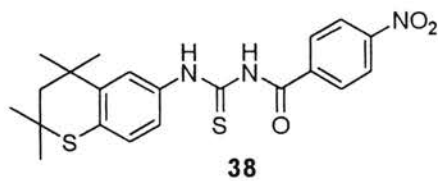
Plate XX

sulfur-4-nitrobenzoylthiourea

expl stdih

```

SAMPLE          DEC. & VT
date  Apr 20 2001  dfrq  300.089
solvent  DMSO      dn      H1
file      exp      dpwr   30
          ACQUISITION  dof      0
sfrq     300.089  da      nnn
tn        H1      dm      C
at        3.747  dmf     200
np        33728  PROCESSING
sw        4500.5  wtfile
fb        2600  proc      ft
bs        16     fn      not used
tpwr      48
pw        6.9   verr
dl        0     wexp
tof       0     wbs
nt       16    wnt
ct       16
alock    n
gain     not used
          FLAGS
il        n
in        y
dp        y
          DISPLAY
sp       -169.5
wp       3926.8
vs       140
sc        0
wc       250
hzmm    15.71
ls       40.67
rf1     743.0
rfp      0
th       0
ins     22.676
nm  cdc  ph
    
```



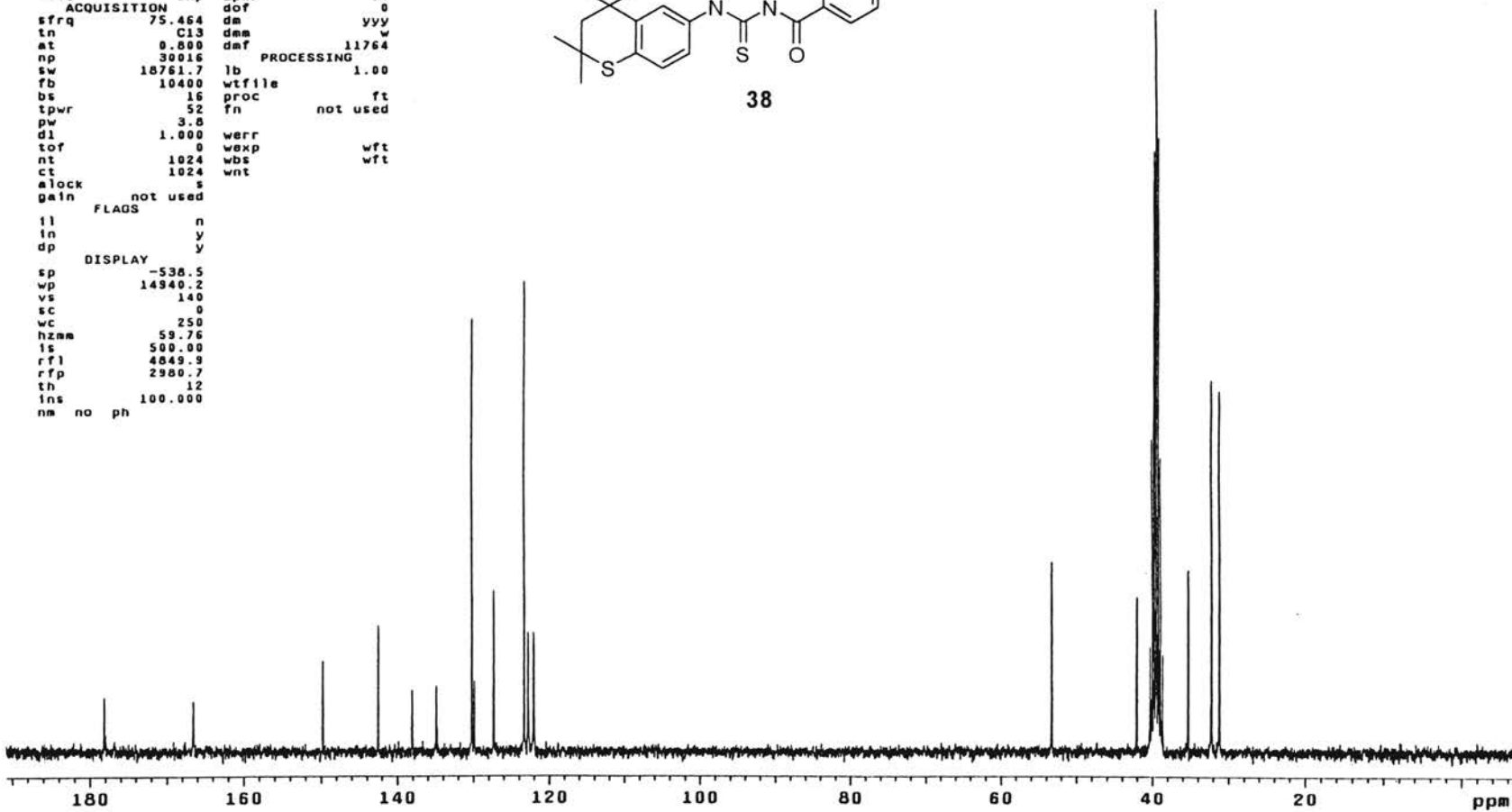
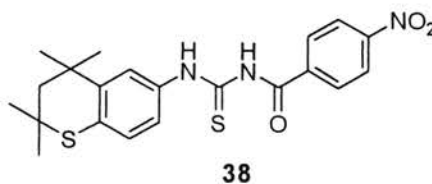
¹H NMR Spectrum of 38

Plate XXI

4-nitrobenzoylthiourea

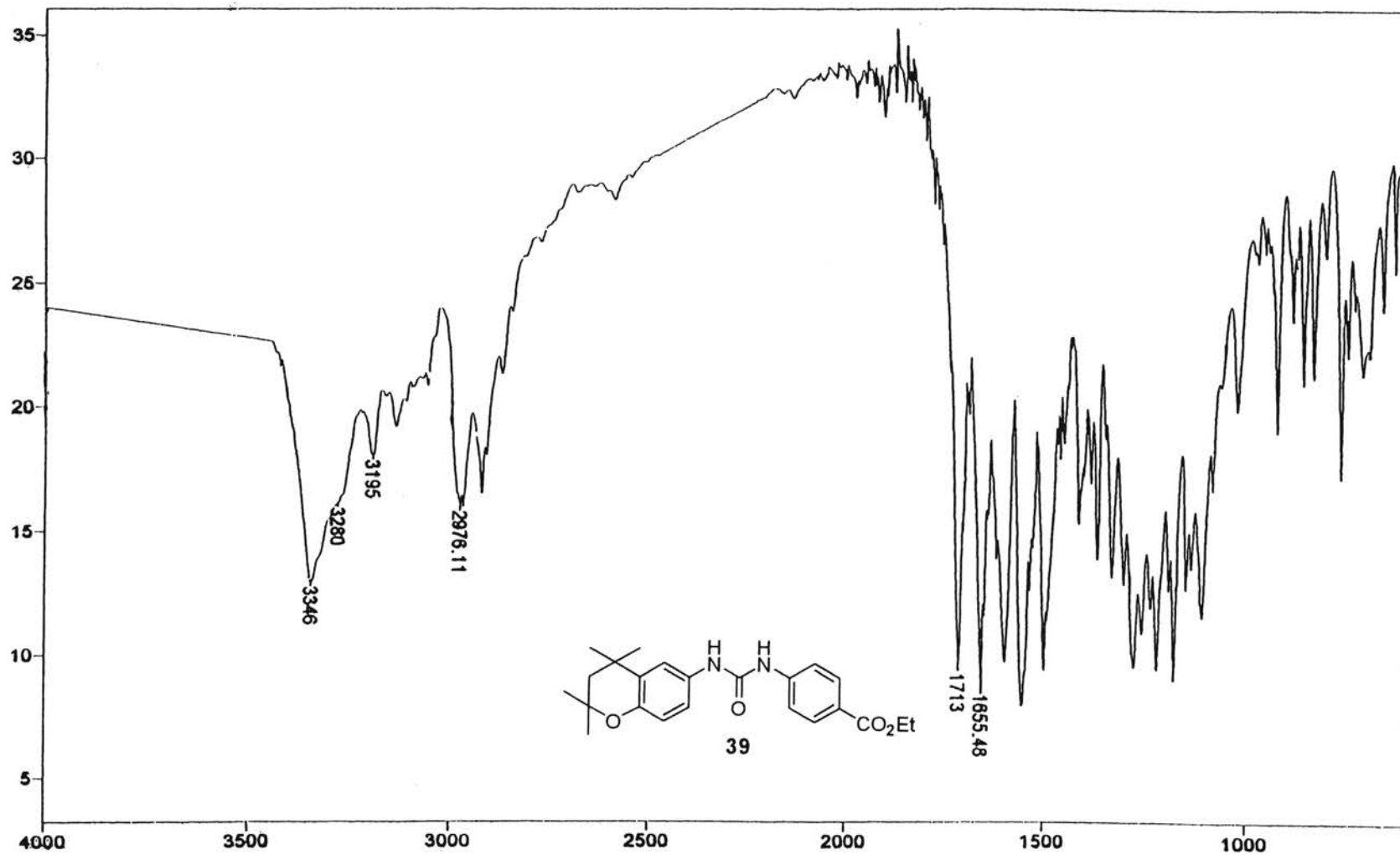
exptl std13c

date	Apr 20	2001	dfrq	300.089
solvent	DMSO		dn	H1
file	exp		dpwr	34
ACQUISITION				
sfrq	75.464		dof	0
tn	C13		dm	yy
at	0.800		dmf	11764
np	30016		PROCESSING	
sw	18761.7		lb	1.00
fb	10400		wtfile	
bs	16		proc	ft
tpwr	52		fn	not used
pw	3.8			
d1	1.000		warr	wft
tof	0		wexp	wft
nt	1024		wbs	wft
ct	1024		wnt	
alock			s	
gain			not used	
FLAGS				
fl			n	
fn			y	
dp			y	
DISPLAY				
sp		-538.5		
wp		14940.2		
vs		140		
sc		0		
wc		250		
hzmm		59.76		
ls		500.00		
rfl		4849.9		
rfp		2980.7		
th		12		
ins		100.000		
nm	no	ph		



¹³C NMR Spectrum of 38

Plate XXII



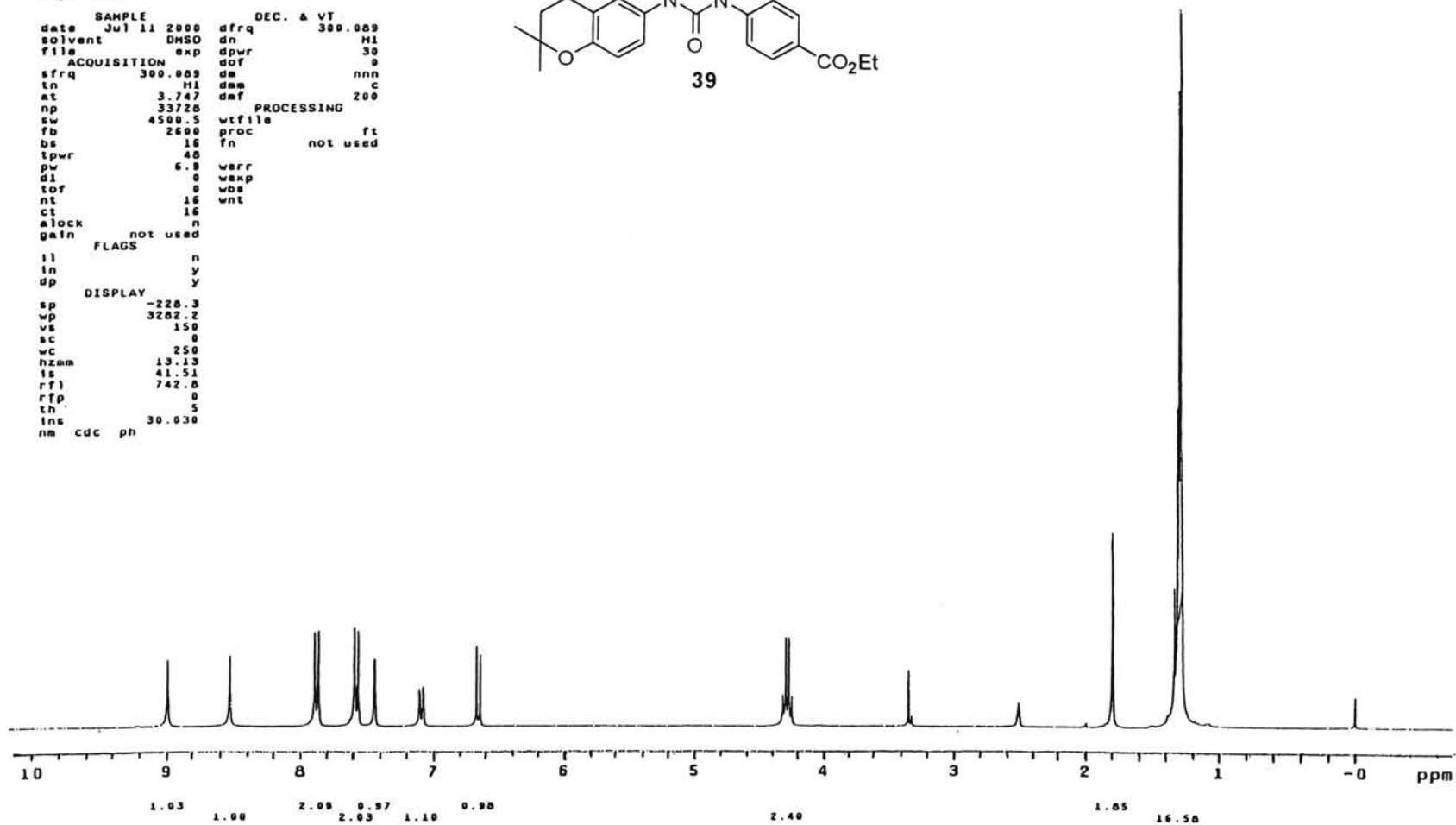
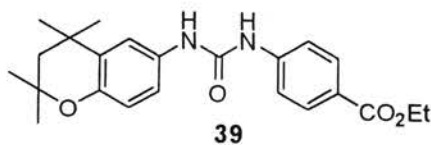
IR Spectrum of 39

Plate XXIII

STANDARD 1H OBSERVE

```

expt stdih
SAMPLE
date Jul 11 2000 dfrq DEC. A VT 300.009
solvent DMSO dn H1
file exp dpwr 30
ACQUISITION dof 0
sfrq 300.009 da nnn
ln H1 daa c
at 3.747 daf 200
np 33728 PROCESSING
sw 4500.5 wtfile
fb 2600 proc ft
bs 16 fn not used
tpwr 40
pw 6.0 werr
d1 0 wexp
tof 0 wba
nt 16 wnt
ct 16
alock n
gain not used
FLAGS
il n
in y
dp y
DISPLAY
sp -228.3
wp 3282.2
vs 150
sc 0
wc 250
hzam 13.13
ls 41.51
rf1 742.0
rfp 0
th 5
ins 30.030
nm cdc ph
    
```



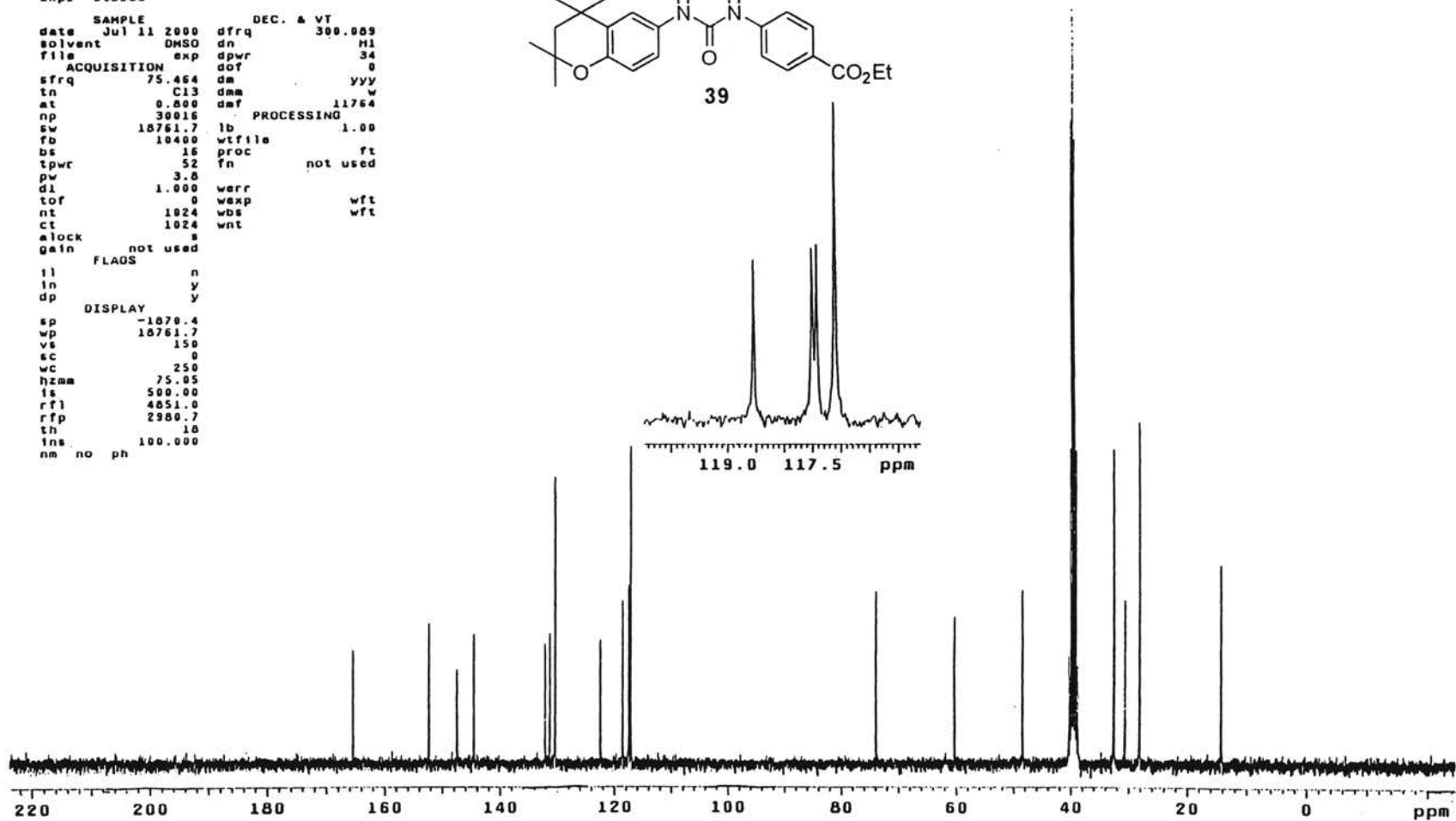
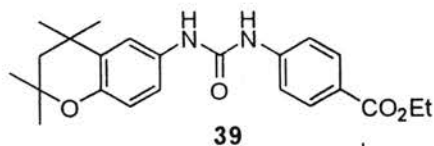
¹H NMR Spectrum of 39

Plate XXIV

13C OBSERVE

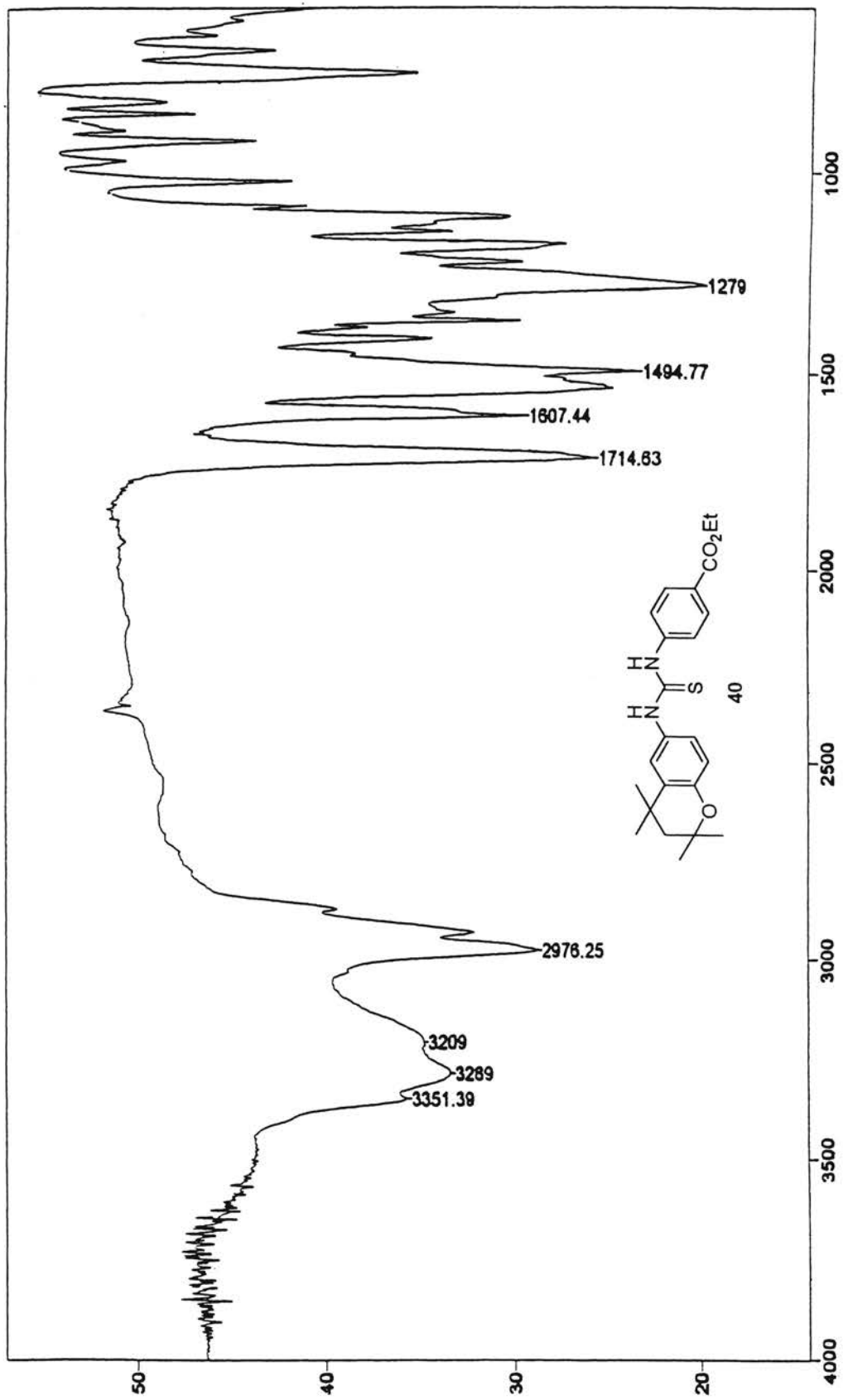
expi std13c

date	SAMPLE	DEC. & VT
Jul 11 2000		300.000
solvent	DMSO	dn
file	exp	dpwr
		34
	ACQUISITION	dot
		0
sfrq	75.464	dm
tn	C13	dmm
at	0.800	daf
np	30016	
sw	18761.7	lb
fb	10400	wf
bs	16	proc
tpwr	52	fn
pw	3.8	
di	1.000	werr
tof	0	wexp
nt	1024	wbs
ct	1024	wnt
alock		
gain	not used	
	FLAQS	
il	n	
in	y	
dp	y	
	DISPLAY	
sp	-1070.4	
wp	10761.7	
vs	150	
sc	0	
wc	250	
hzmm	75.05	
ls	500.00	
rfl	4051.0	
rff	2900.7	
th	10	
ins	100.000	
nm	no	ph



¹³C NMR Spectrum of 39

Plate XXV



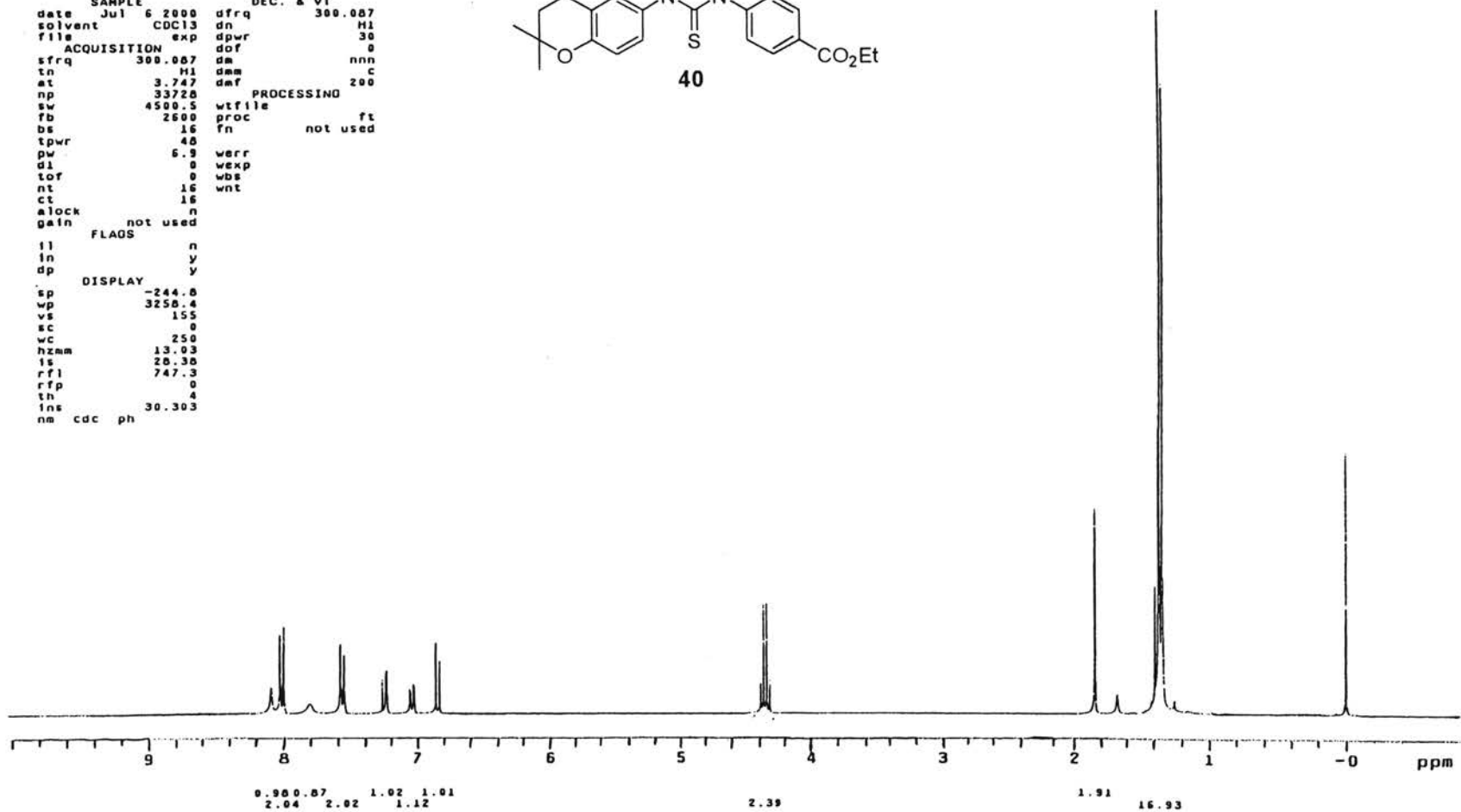
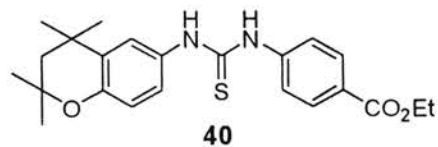
IR Spectrum of 40

Plate XXVI

STANDARD IH OBSERVE

```

expi stdih
SAMPLE
date Jul 6 2000 dfrq DEC. & VT 300.007
solvent CDC13 dn HI
file exp dpwr 30
ACQUISITION dof 0
sfrq 300.007 dm nnn
tn HI dam c
at 3.747 dmf 200
np 33720 PROCESSING
sw 4500.5 wtfile
fb 2500 proc ft
bs 16 fn not used
tpwr 40
pw 6.9 werr
d1 0 wexp
tof 0 wbs
nt 16 wnt
ct 16
alock n
gain not used
FLAOS
il n
in y
dp y
DISPLAY
sp -244.0
wp 3256.4
vs 155
sc 0
wc 250
hzmm 13.03
fs 20.30
rfl 747.3
rfp 0
th 4
ins 30.303
nm cdc ph
    
```



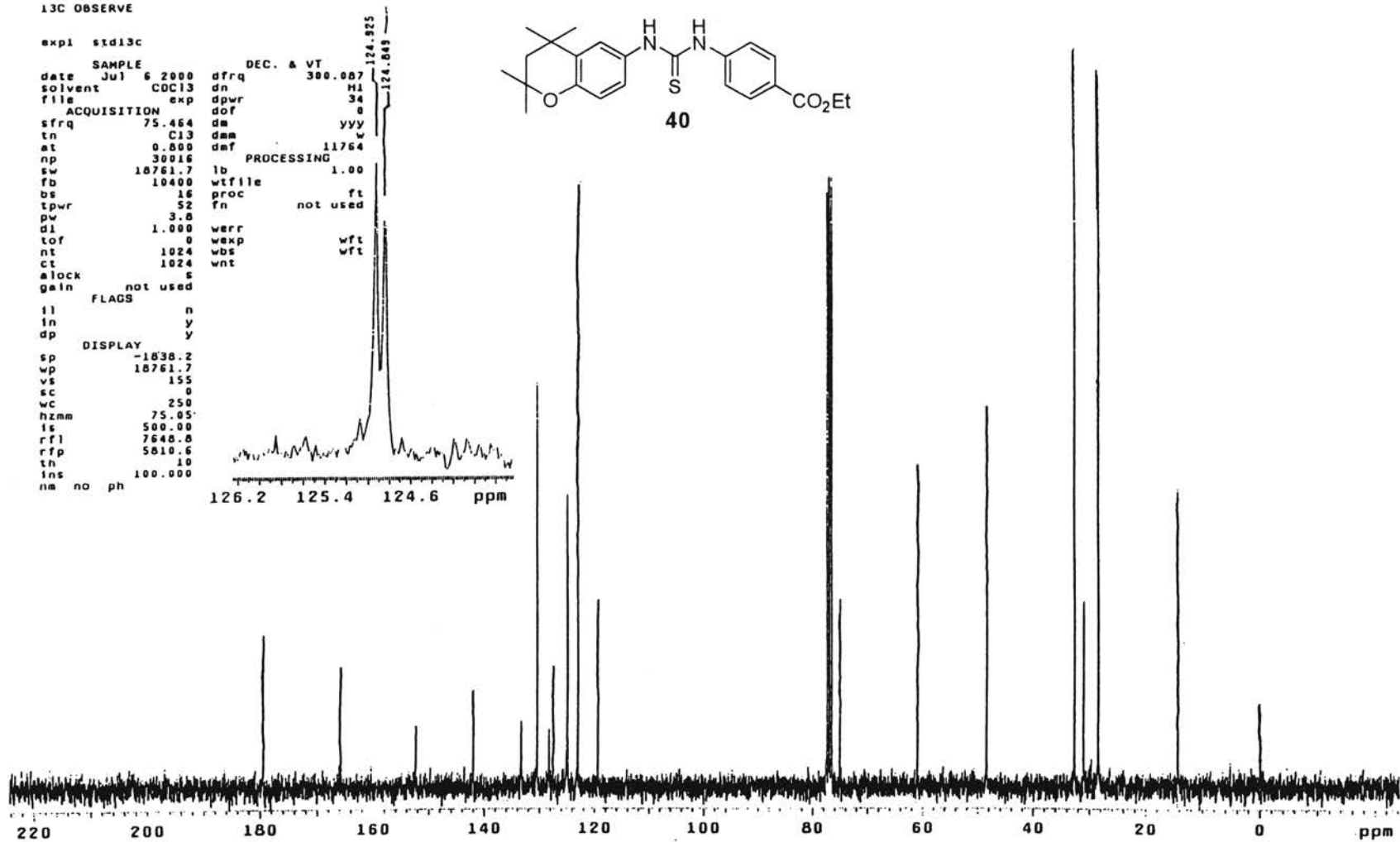
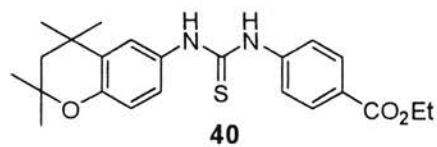
¹H NMR Spectrum of 40

Plate XXVII

13C OBSERVE

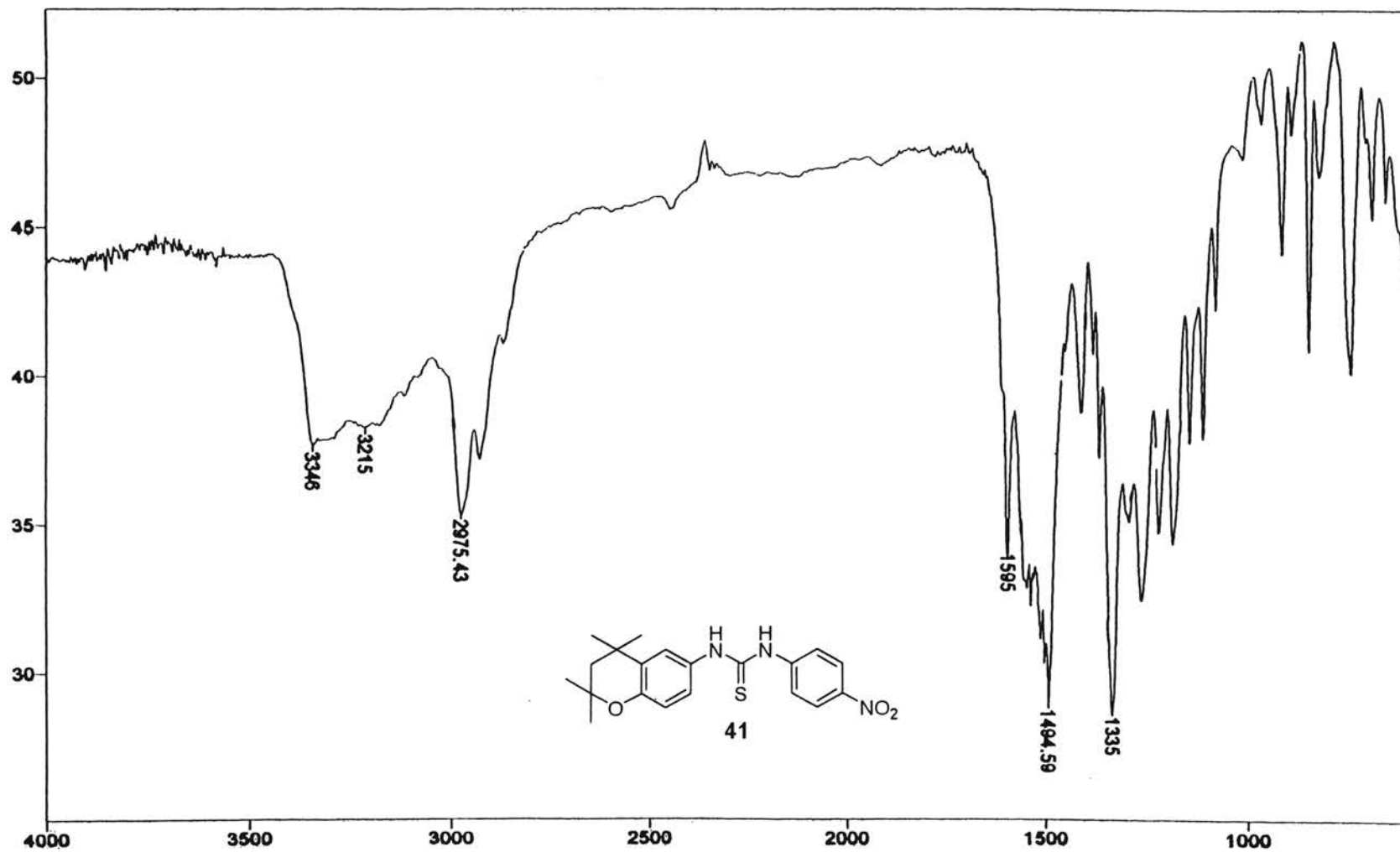
```

expt  std13c
date  Jul 6 2000  dfrq  300.007
solvent  CDCl3  dn  H1
file  exp  dpwr  34
ACQUISITION  exp  dof  6
sfrq  75.464  dm  yyy
tn  C13  dam  11764
st  0.800  dmf  11764
np  30016  PROCESSING
sw  18761.7  lb  1.00
fb  10400  wtfile
bs  16  proc  ft
tpwr  52  fn  not used
pw  3.8
d1  1.000  werr
tof  0  wexp
nt  1024  wbs
ct  1024  wnt
alock  s
gain  not used
FLAGS
il  n
in  y
dp  y
DISPLAY
sp  -1838.2
wp  18761.7
vs  155
sc  0
wc  250
hzmm  75.05
ls  500.00
rfl  7848.8
rfp  5810.6
th  10
ins  100.000
nm  no  ph
    
```



¹³C NMR Spectrum of 40

Plate XXVIII



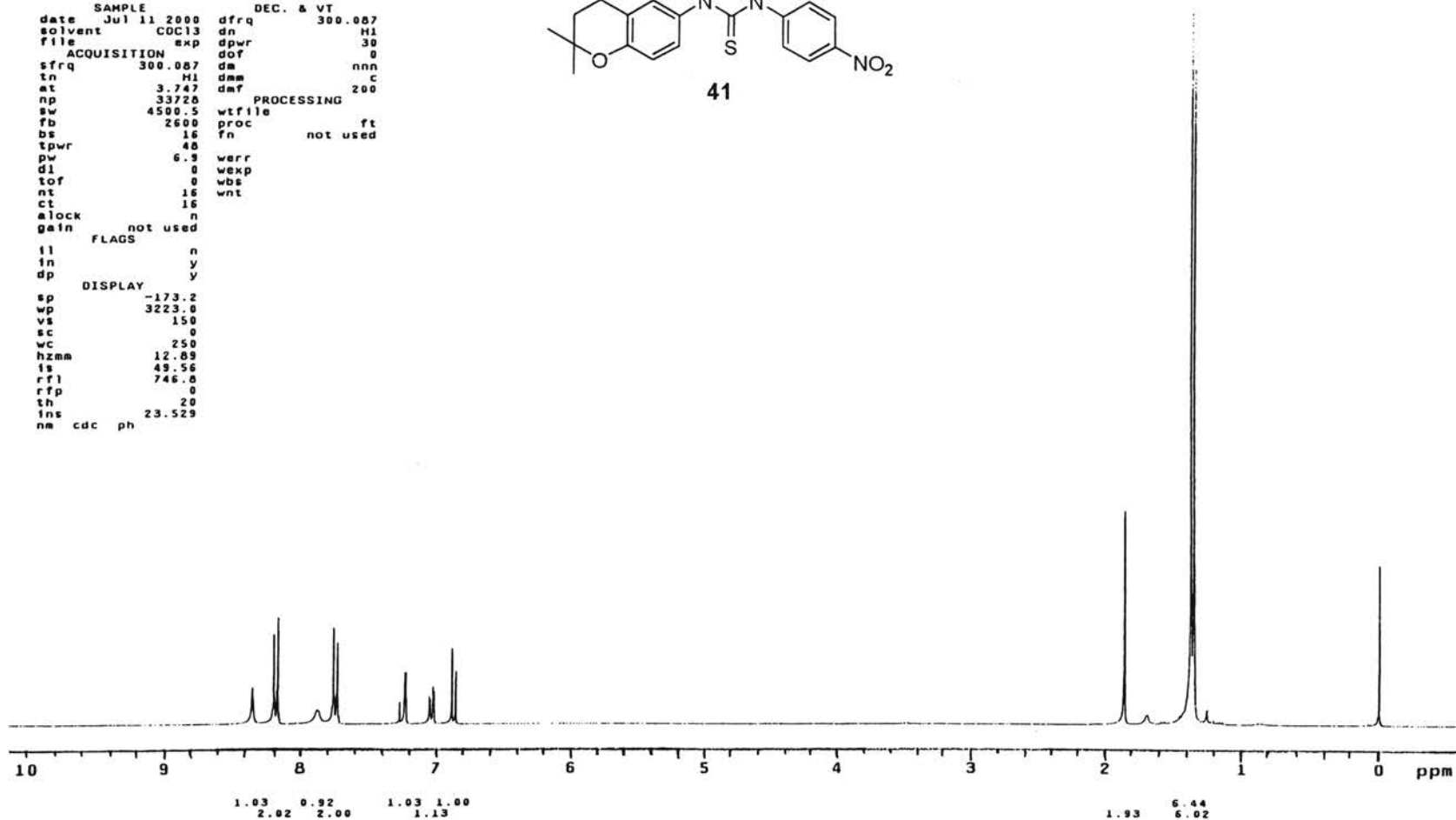
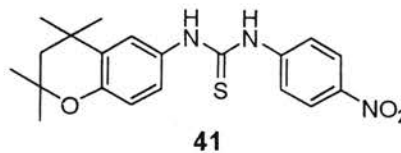
IR Spectrum of 41

Plate XXIX

STANDARD 1H OBSERVE

```

expt stdih
SAMPLE
date Jul 11 2000 dfrq DEC. & VT 300.007
solvent CDCl3 dn H1
file exp dpwr 30
ACQUISITION dof 0
sfrq 300.007 dm nnn
tn H1 dmm c
at 3.747 dmf 200
np 33726
sw 4500.5 wtfile PROCESSING
fb 2600 proc ft
bs 16 fn not used
tpwr 40
pw 6.3 werr
d1 0 wexp
tof 0 wbs
nt 16 wnt
ct 16
alock n
gain not used
FLAGS
fl n
fn y
dp y
DISPLAY
sp -173.2
wp 3223.0
vs 150
sc 0
wc 250
hzmm 12.89
is 49.56
rfl 746.0
rfp 0
th 20
ins 23.529
nm cdc ph
    
```



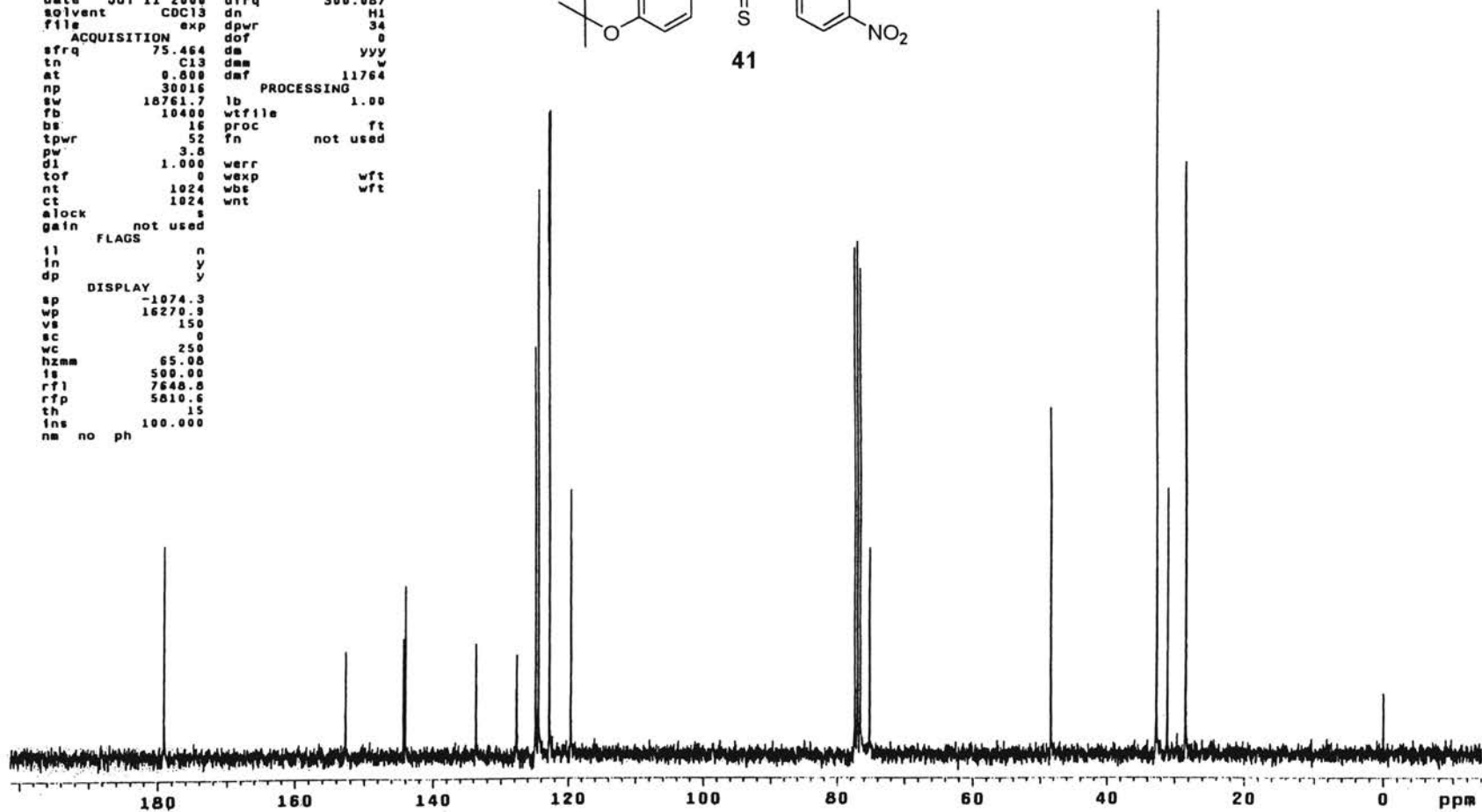
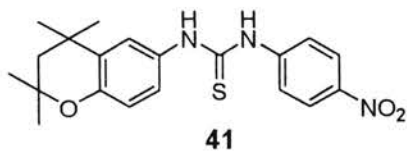
¹H NMR Spectrum of 41

Plate XXX

13C OBSERVE

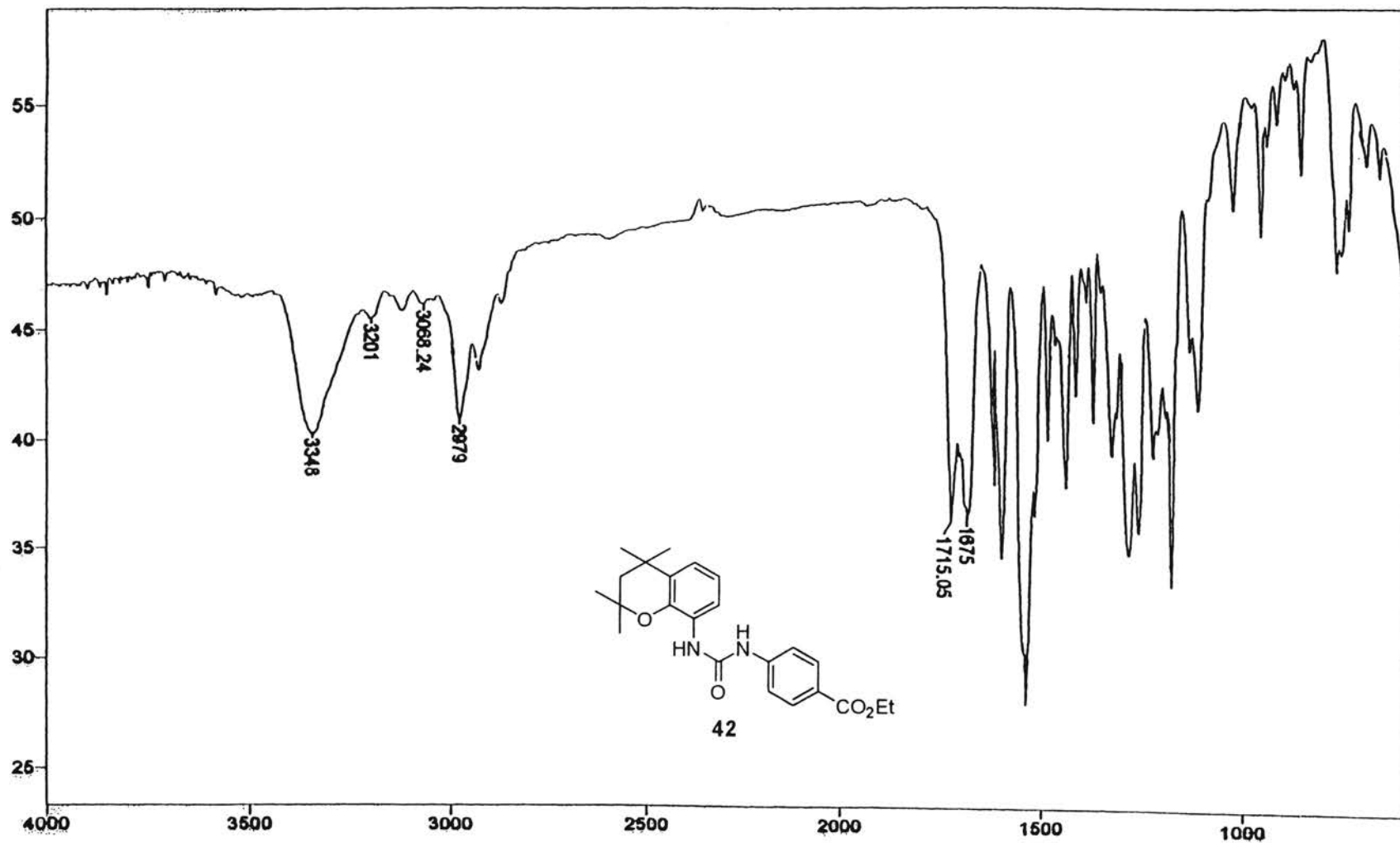
```

expl std13c
SAMPLE
date Jul 11 2000 dfrq DEC. & VT 300.087
solvent CDC13 dn H1
file exp dpwr 34
ACQUISITION dof 0
sfrq 75.464 da yyy
tn C13 dam w
at 0.800 daf 11764
np 30016 PROCESSING
sw 18761.7 lb 1.00
fb 10400 wtfile
bs 16 proc ft
tpwr 52 fn not used
pw 3.8
dl 1.000 werr
tof 0 wexp wft
nt 1024 wbs wft
ct 1024 wnt
alock s
gain not used
FLAGS
fl n
in y
dp y
DISPLAY
sp -1074.3
wp 16270.9
vs 150
sc 0
wc 250
hzmm 65.00
fs 500.00
rfl 7648.8
rfp 5810.6
th 15
ins 100.000
nm no ph
    
```



¹³C NMR Spectrum of 41

Plate XXXI



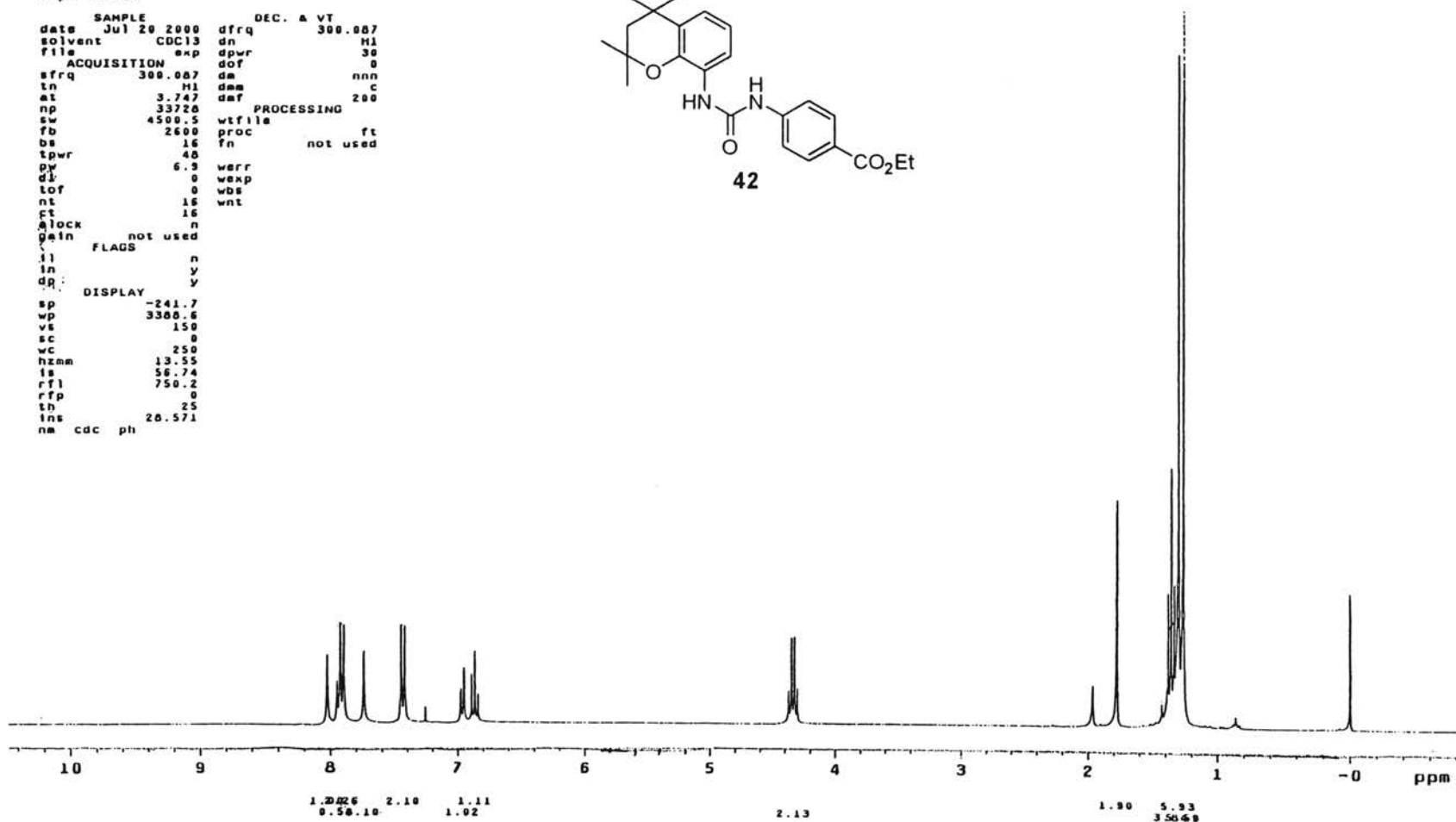
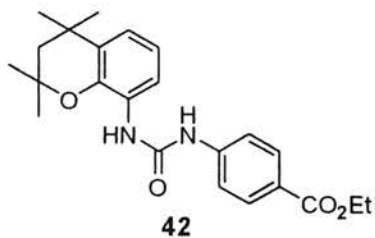
IR Spectrum of 42

Plate XXXII

STANDARD IN OBSERVE

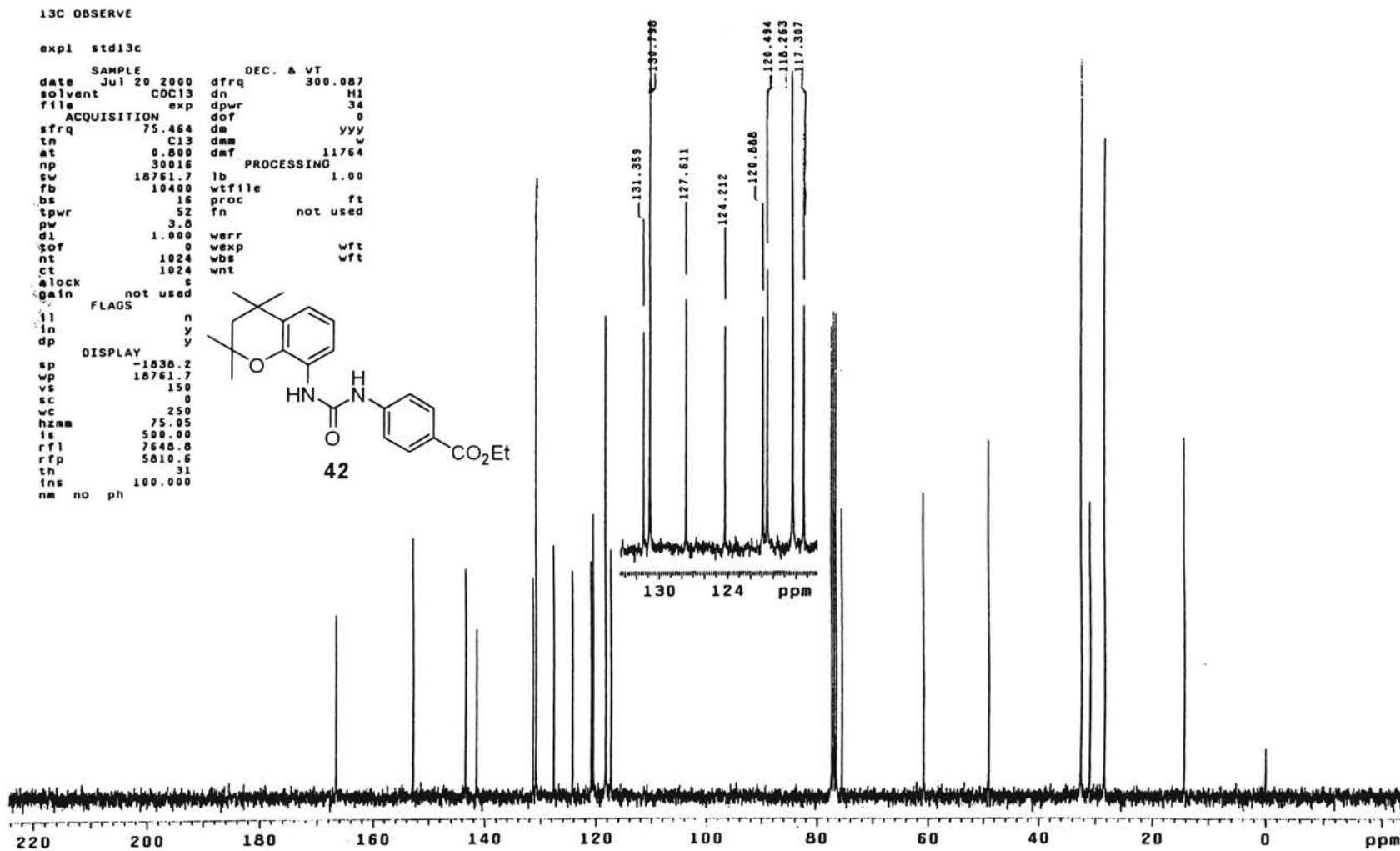
```

expl stdih
SAMPLE DEC. A VT
date Jul 20 2000 dfrq 300.007
solvent CDC13 dn H1
file exp dpwr 30
ACQUISITION dof 0
sfrq 300.007 dm nnn
tn H1 dmw C
at 3.747 daf 200
np 33728 PROCESSING
sw 4500.5 wlf1la
fb 2000 proc ft
bs 16 fn not used
tpwr 40
py 6.3 werr
dl 0 wexp
lof 0 wbs
nt 16 wnt
ct 16
clock n
gain not used
FLAGS
il n
in y
dq y
DISPLAY
sp -241.7
wp 3300.6
vs 150
sc 0
wc 250
hzmm 13.55
is 56.74
rf1 750.2
rfp 0
eb 25
ins 20.571
nm cdc ph
    
```



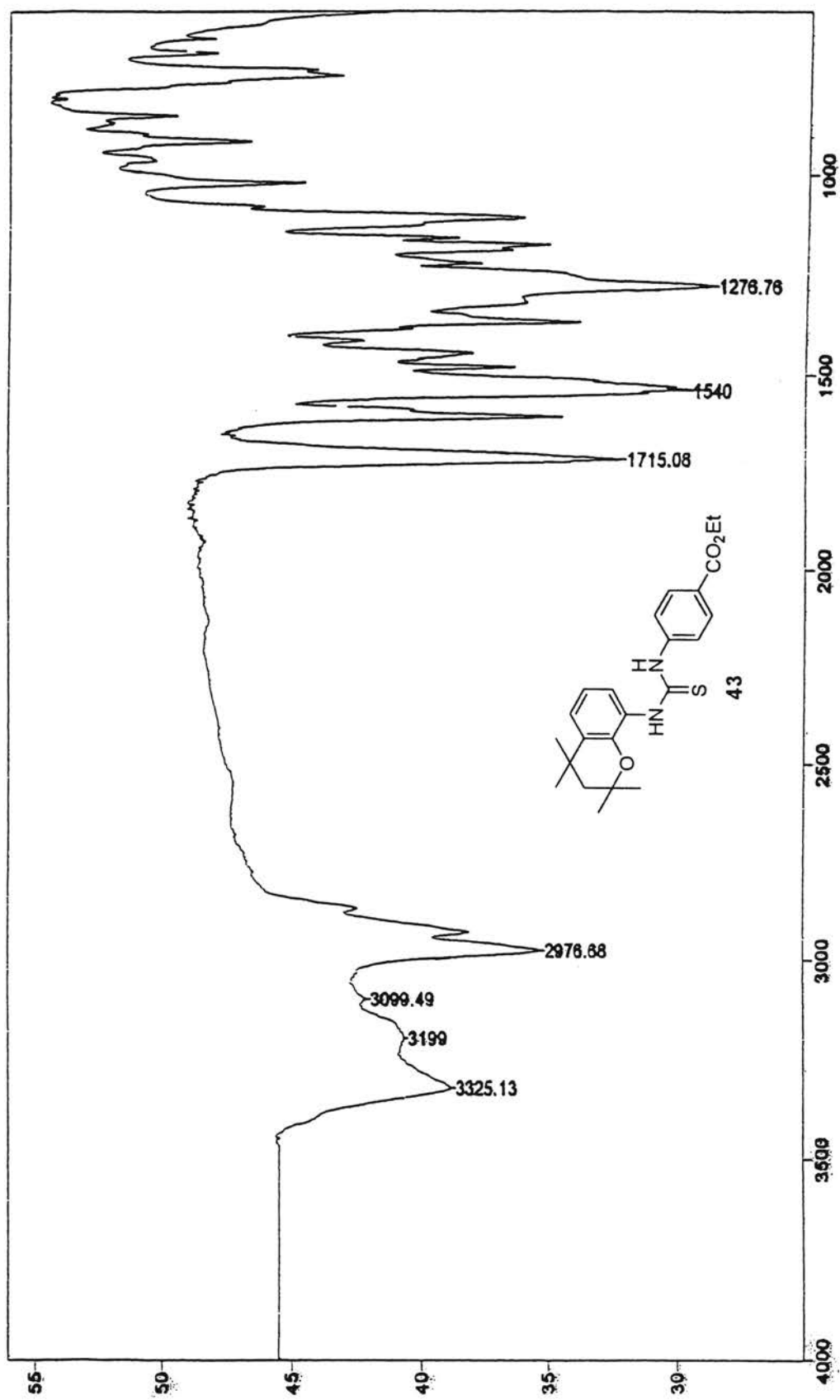
¹H NMR Spectrum of 42

Plate XXXIII



¹³C NMR Spectrum of 42

Plate XXXIV



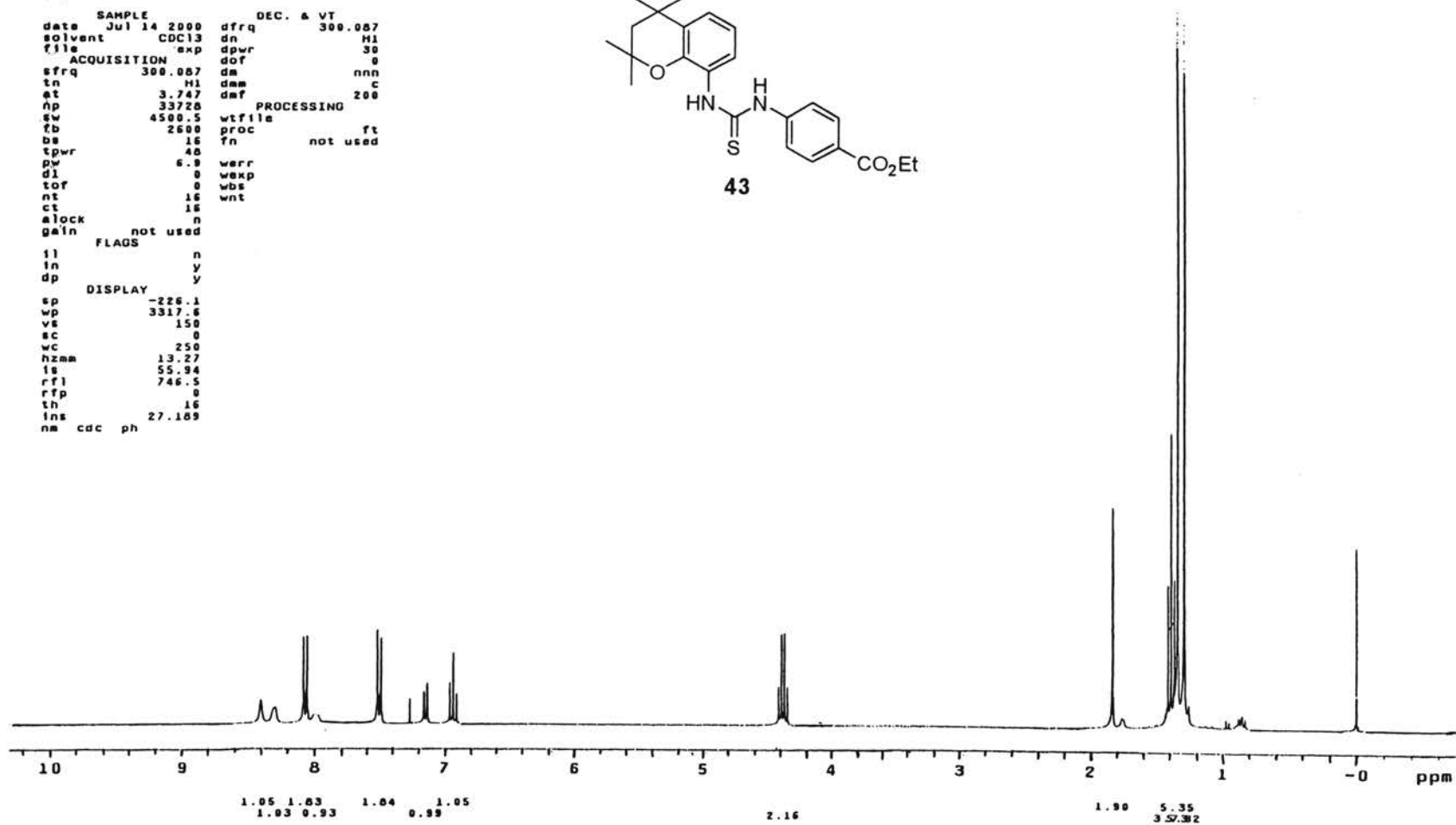
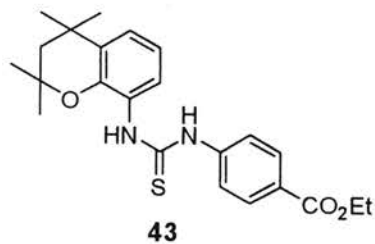
IR Spectrum of 43

Plate XXXV

STANDARD 1H OBSERVE

```

expt std1h
SAMPLE
date Jul 14 2000 dfrq DEC. & VT 300.087
solvent CDC13 dn M1
file exp dpwr M1
ACQUISITION dm 0
sfrq 300.087 dnm nnn
tn M1 dmf C
at 3.747 dmf 200
np 33728 PROCESSING
sw 4500.5 wtfile
fb 2500 proc ft
bs 15 fn not used
tpwr 40
pw 6.9 werr
dl 0 wexp
tof 0 wbs
nt 16 wnt
ct 15
alock n
gain not used
FLAGS
ll n
ln y
dp y
DISPLAY
sp -226.1
wp 3317.6
vs 150
sc 0
wc 250
hzam 13.27
fs 55.94
rfl 746.5
rtp 0
th 16
ins 27.189
nm cdc ph
    
```



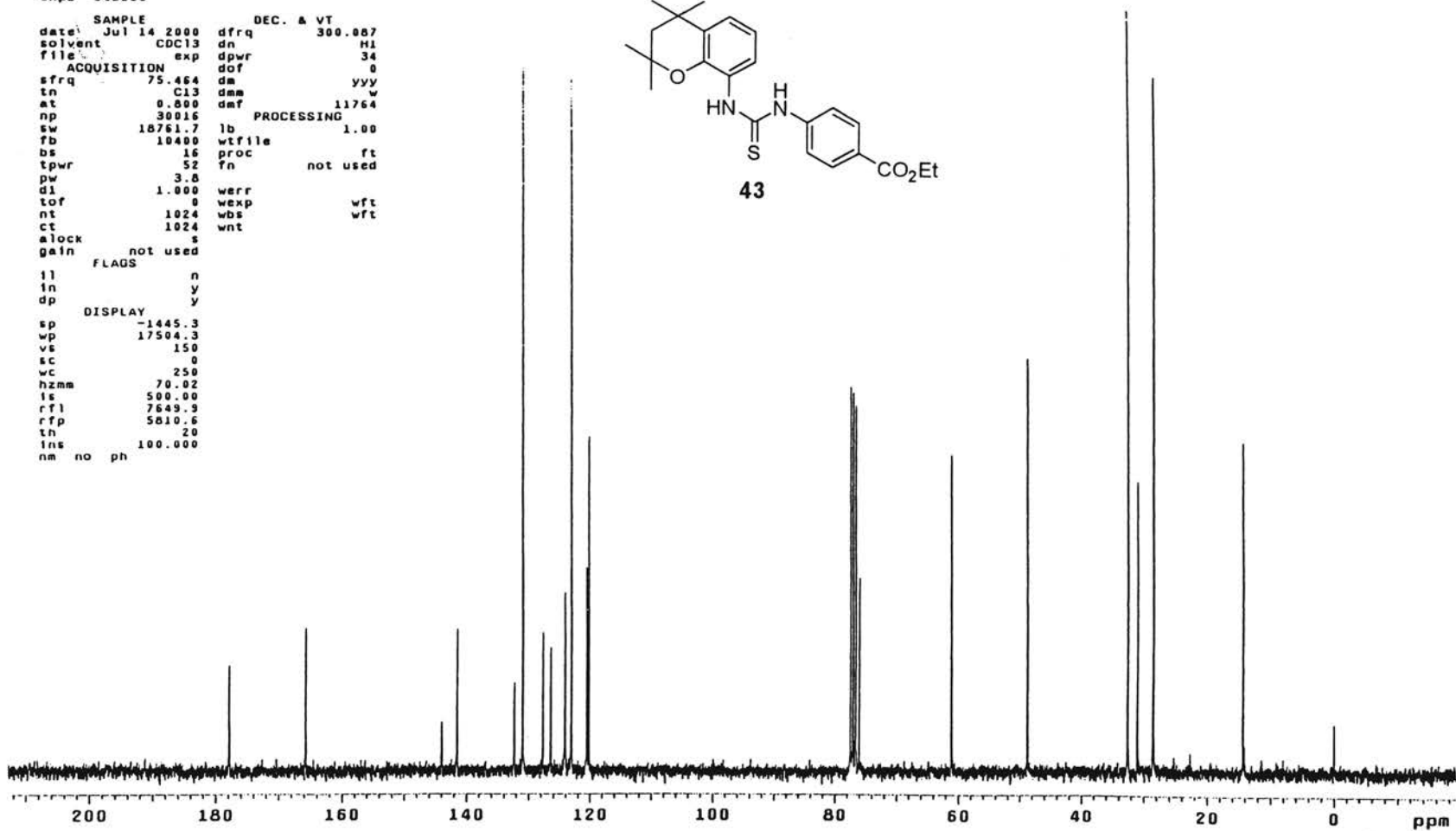
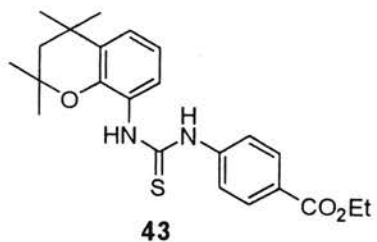
¹H NMR Spectrum of 43

Plate XXXVI

¹³C OBSERVE

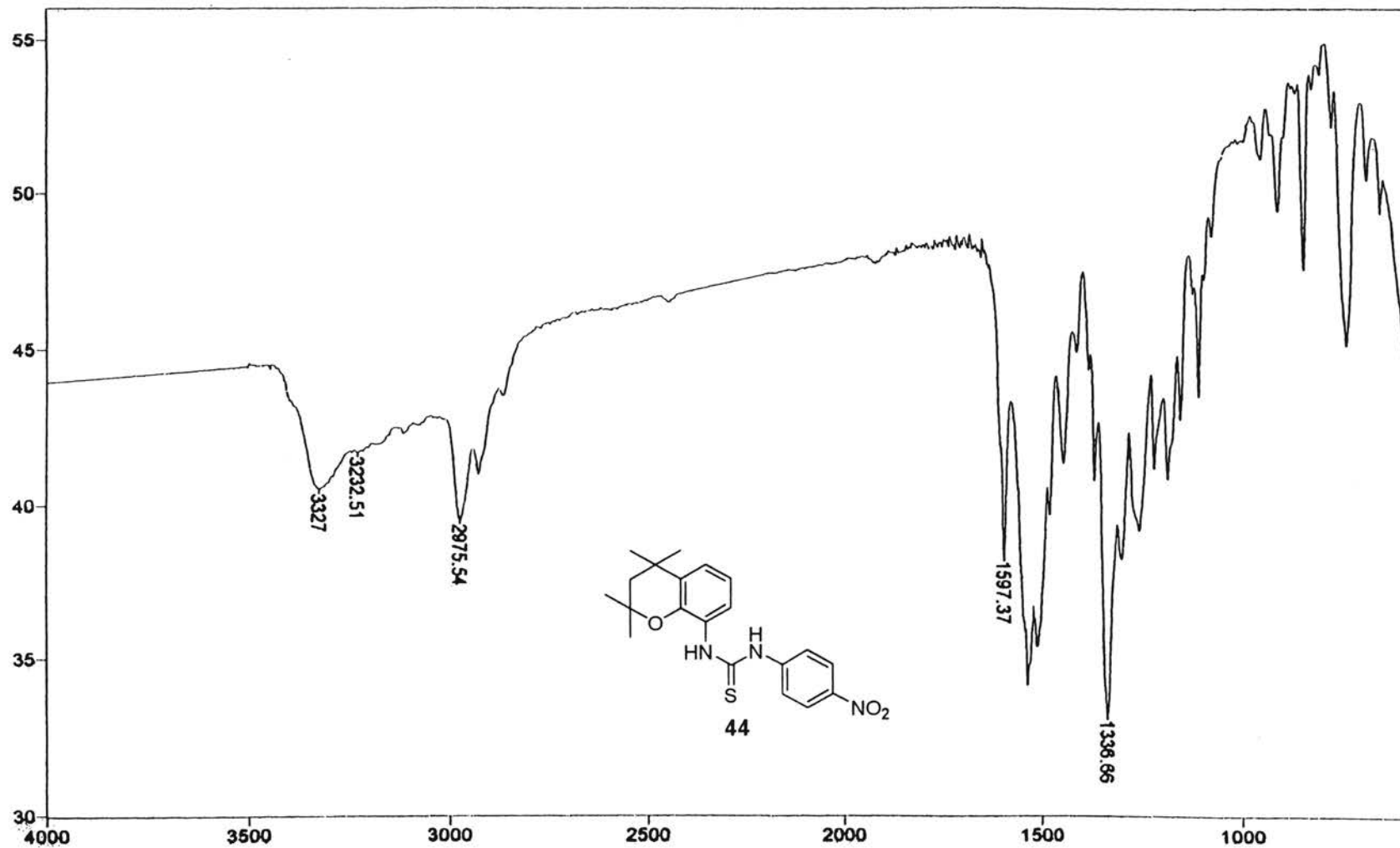
```

NAME: 13013C
SAMPLE
date: Jul 14 2000 dfrq DEC. & VT 300.887
solvent CDC13 dn H1
file exp dpwr 34
ACQUISITION dof 0
sfrq 75.464 dm yyy
tn C13 dm w
at 0.800 dmf 11764
np 30016 PROCESSING
sw 18761.7 lb 1.00
fb 10400 wfile
bs 16 proc ft
tpwr 52 fn not used
pw 3.8
dl 1.000 werr
tof 0 wexp wft
nt 1024 wbs wft
ct 1024 wnt
alock s
gain not used
FLAGS
il n
in y
dp y
DISPLAY
sp -1445.3
wp 17504.3
vs 150
sc 0
wc 250
hzmm 70.02
ls 500.00
rf1 7649.9
rfp 5810.6
th 20
ins 100.000
nm no ph
    
```



¹³C NMR Spectrum of 43

Plate XXXVII



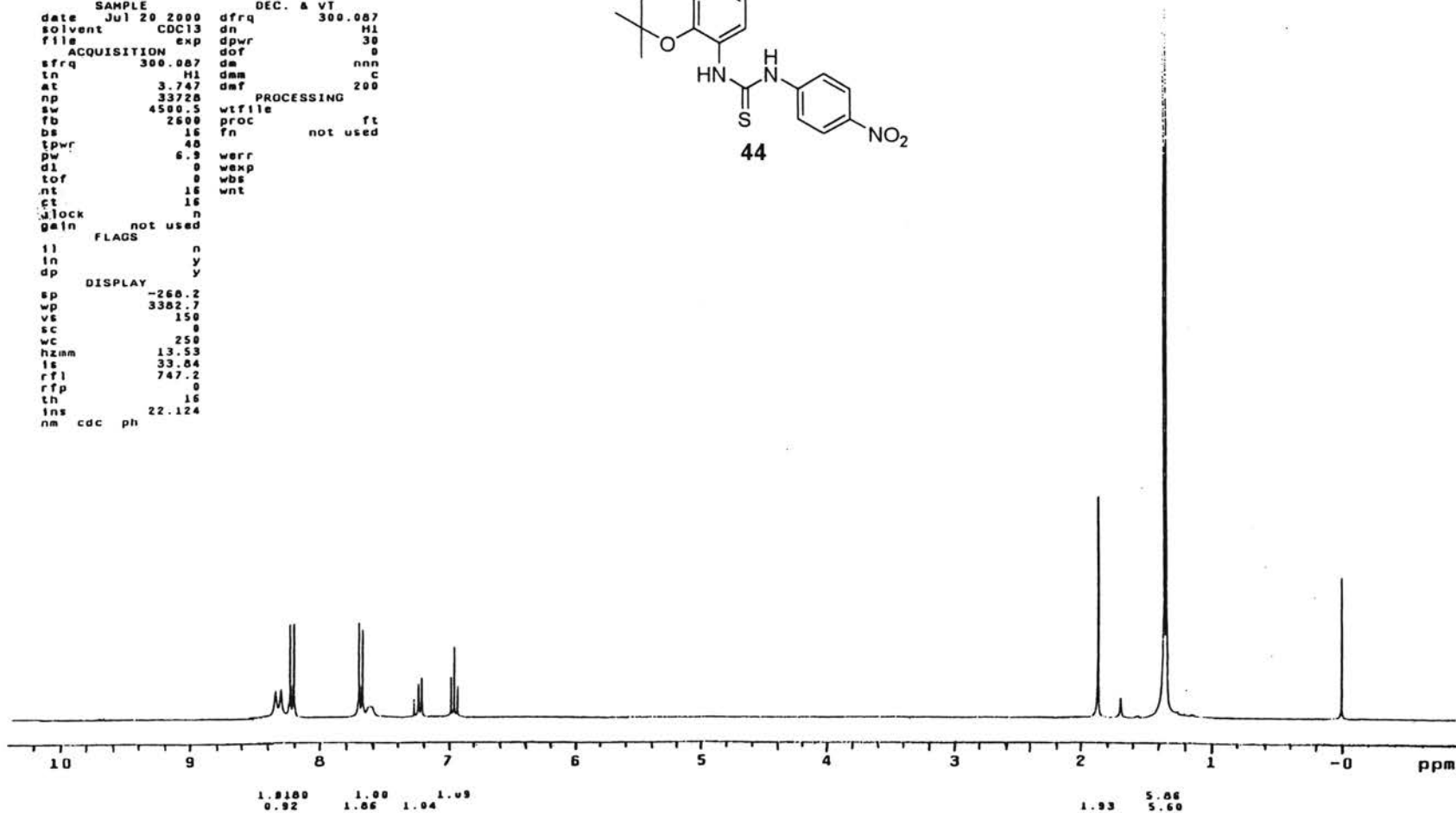
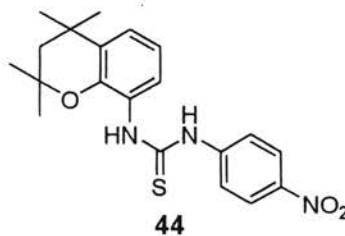
IR Spectrum of 44

Plate XXXVIII

STANDARD 1H OBSERVE

```

expt stdih
SAMPLE
date Jul 20 2000 dfrq DEC. & VT 300.007
solvent CDCl3 dn H1
file exp dpwr 30
ACQUISITION dof 0
sfrq 300.007 dm nnn
tn H1 dm C
at 3.747 dmf 200
np 33720 PROCESSING
sw 4500.5 wtfile
fb 2600 proc ft
ds 15 fn not used
tpwr 40
pw 6.9 werr
d1 0 wexp
tof 0 wbs
nt 16 wnt
ct 16
clock n
gain not used
FLAGS
ll n
ln y
dp y
DISPLAY
sp -260.2
wp 3382.7
vs 150
sc 0
wc 250
Hzimm 13.53
ls 33.04
rf1 747.2
rfp 0
th 16
ins 22.124
nm cdc ph
    
```



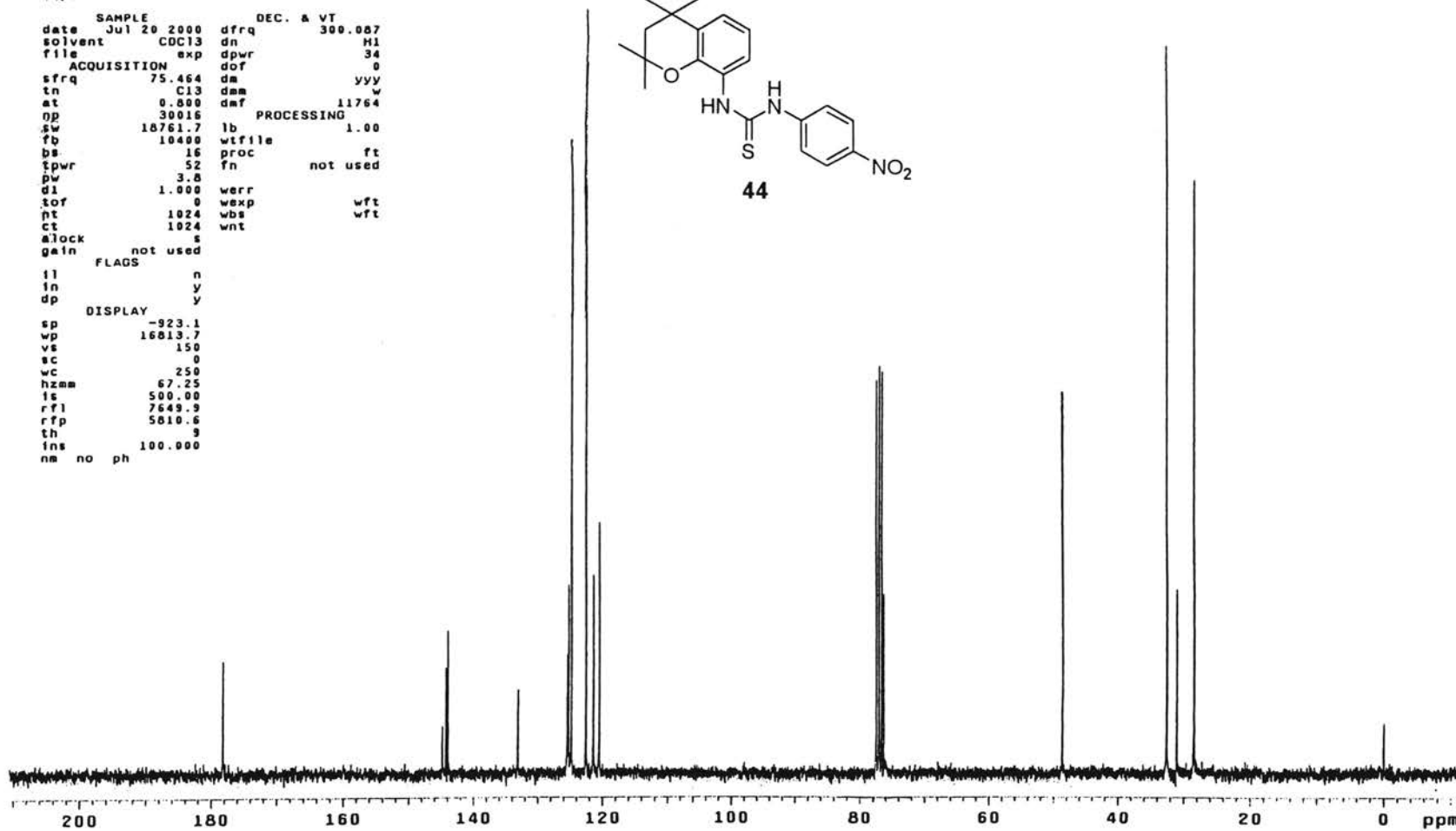
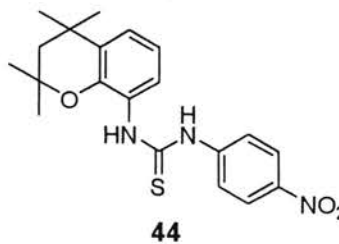
¹H NMR Spectrum of 44

Plate XXXIX

13C OBSERVE

expl std13c

date	Jul 20 2000	dfrq	DEC. & VT	300.057
solvent	CDC13	dn		H1
file	exp	dpwr		34
ACQUISITION				
sfrq	75.464	dof		0
tn	C13	dm		yyy
at	0.800	dsm		w
op	30016	daf	PROCESSING	11764
sw	18761.7	lb		1.00
fb	10400	wffile		
bs	16	proc		ft
tpwr	52	fn		not used
pw	3.8	werr		
d1	1.000	wexp		wft
tof	0	wbs		wft
nt	1024	wnt		
ct	1024			
alock	s			
gain	not used			
FLAGS				
il		n		
in		y		
dp		y		
DISPLAY				
sp	-923.1			
wp	16813.7			
vs	150			
sc	0			
wc	250			
hzmm	67.25			
lc	500.00			
rfl	7649.9			
rfp	5810.6			
th	9			
ins	100.000			
nm	no	ph		



¹³C NMR Spectrum of 44

Plate XL

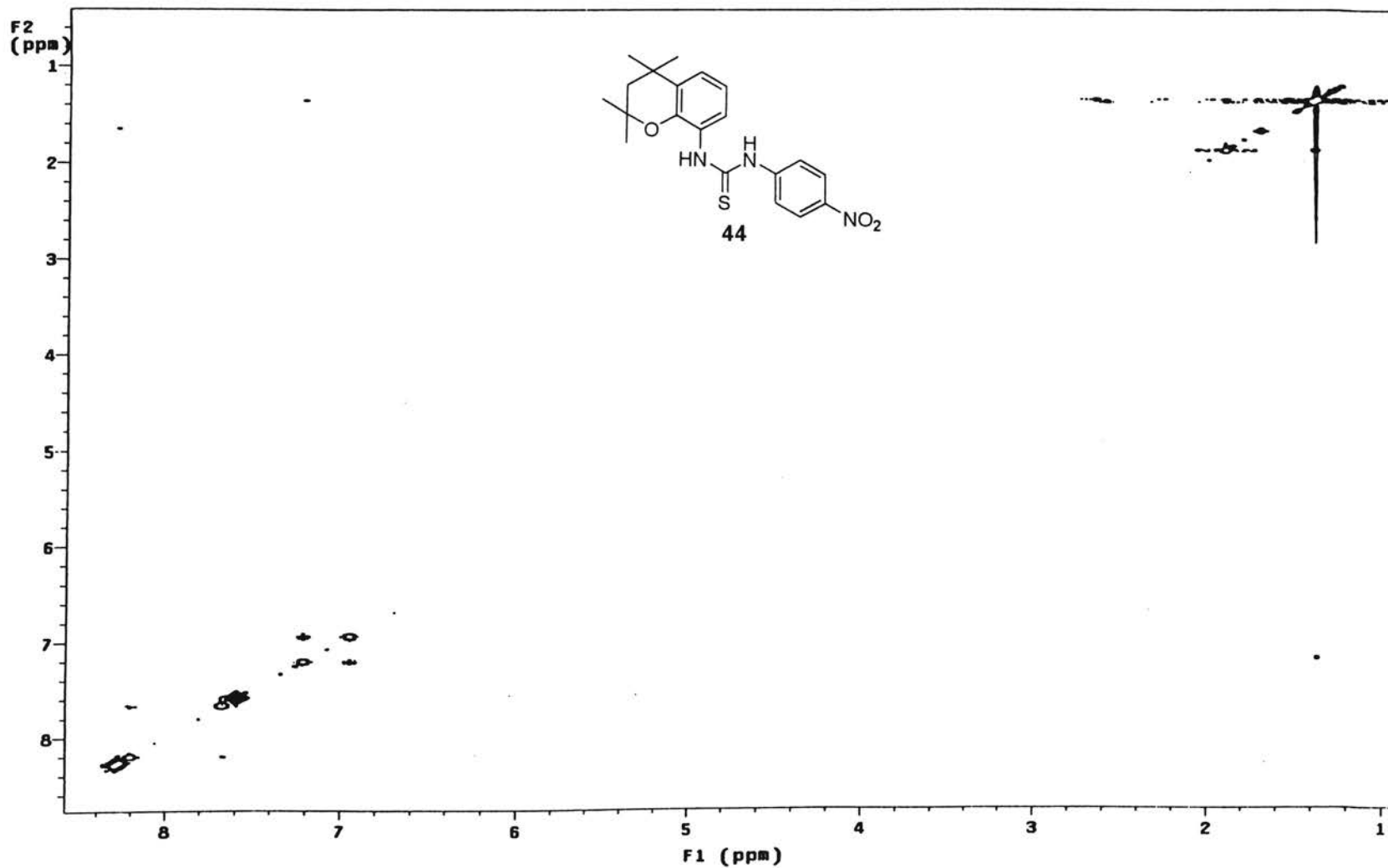
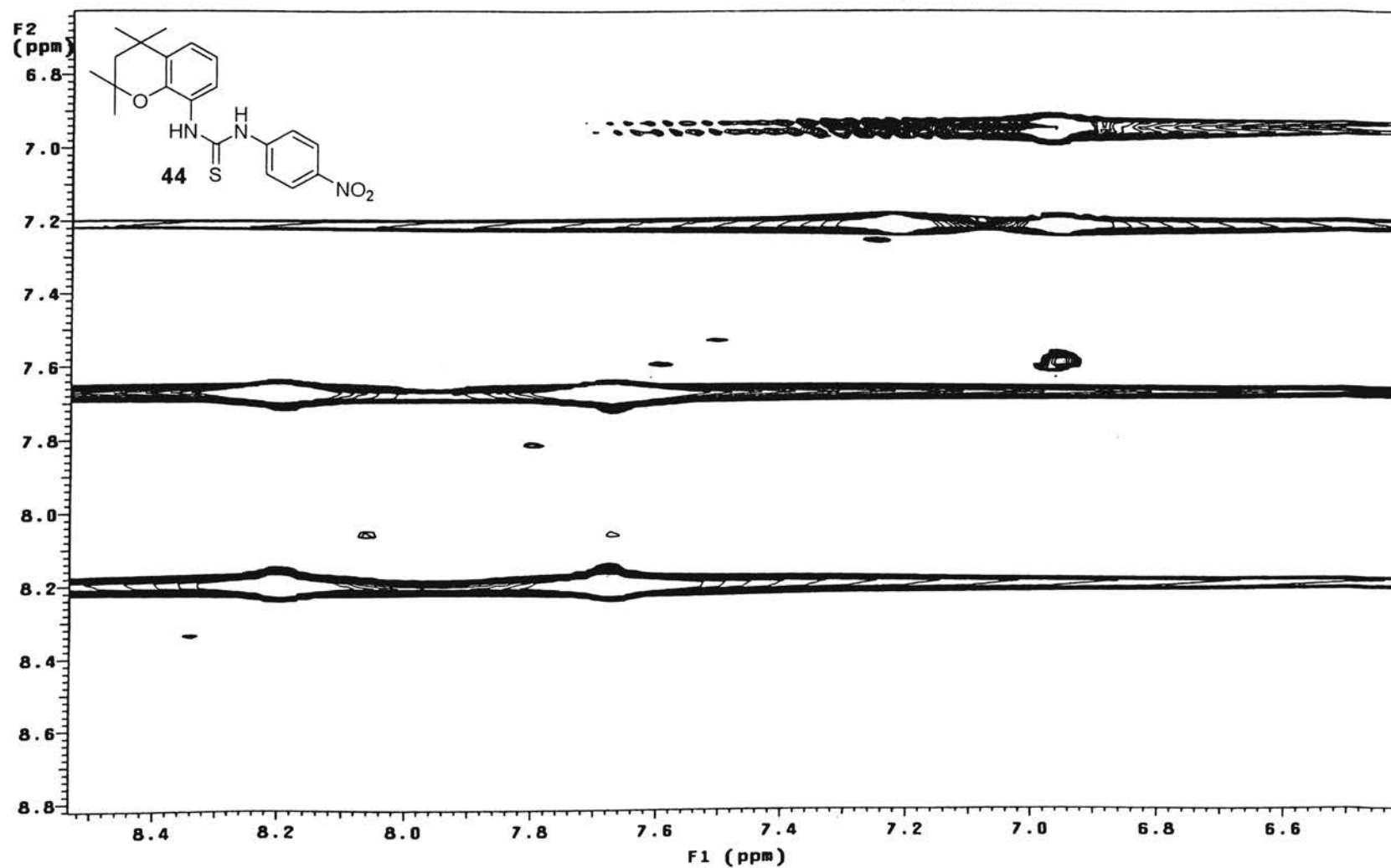
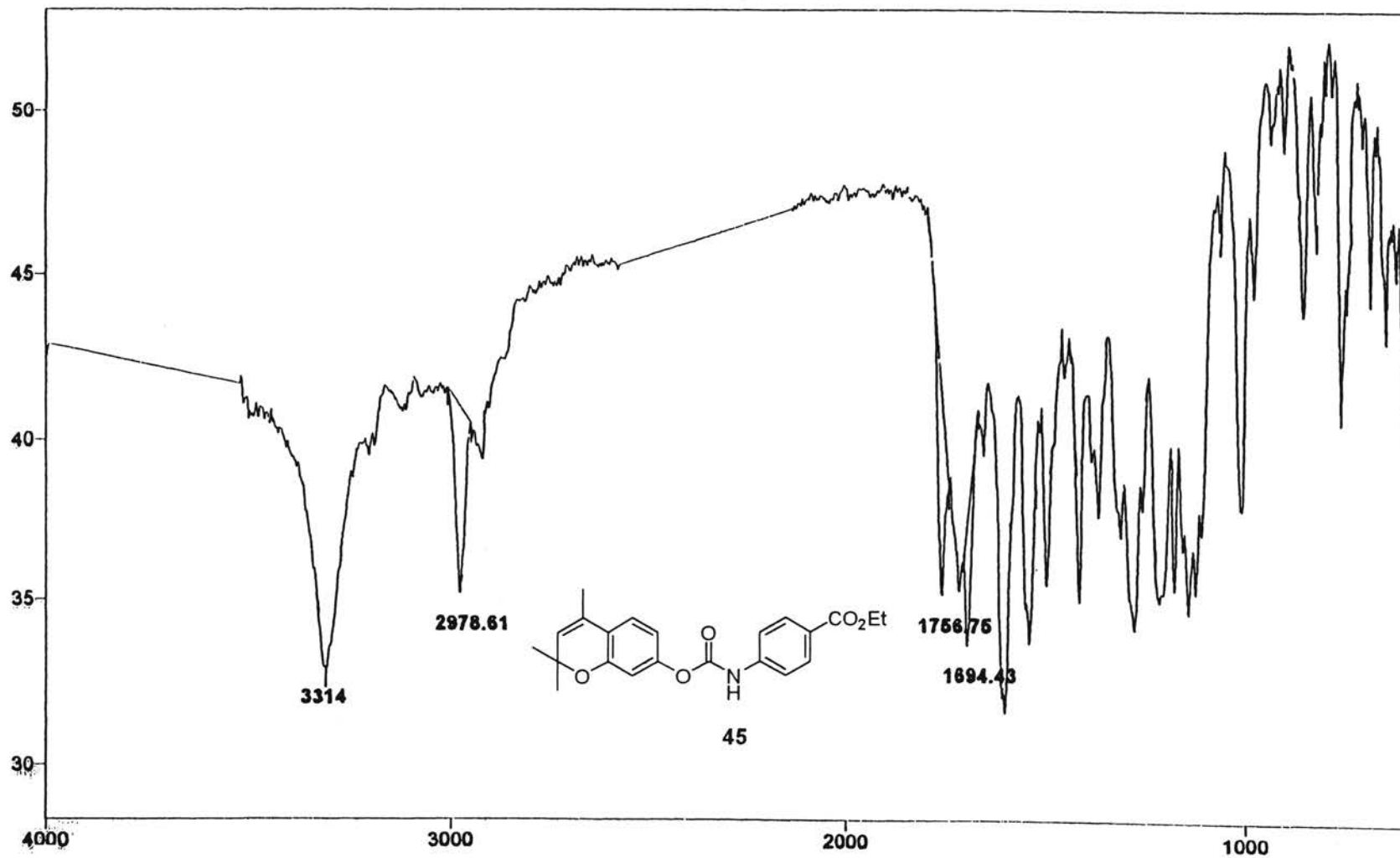


Plate XLI



2D DQCOSY NMR Spectrum of 44

Plate XLII



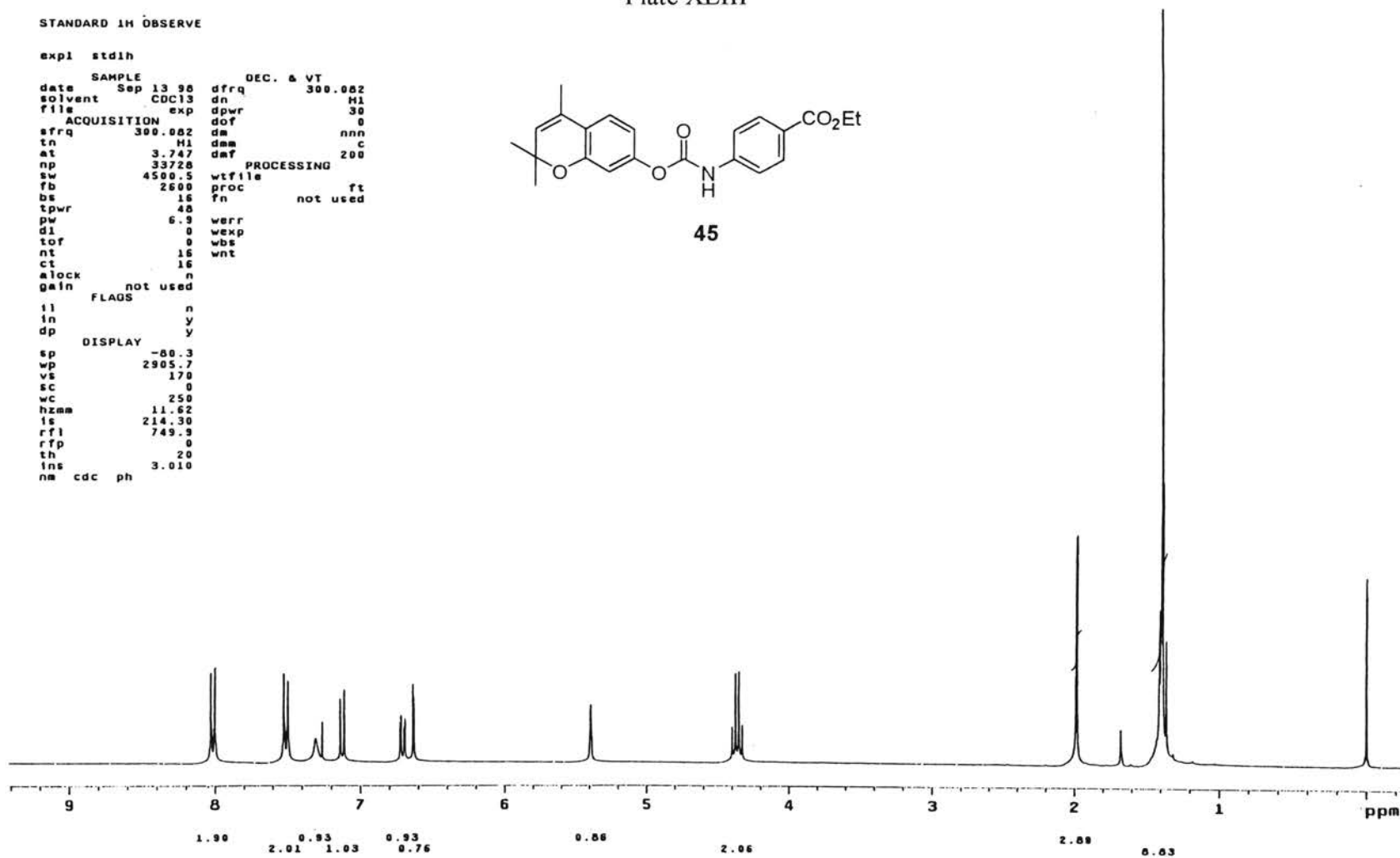
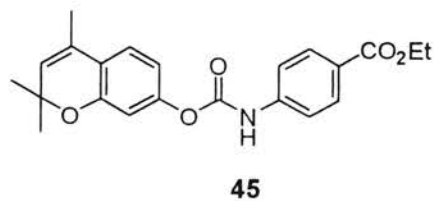
IR Spectrum of 45

Plate XLIII

STANDARD 1H OBSERVE

```

expl stdih
SAMPLE
date Sep 13 98 dfrq DEC. & VT 300.082
solvent CDC13 dn H1
file exp dpwr 30
vs ACQUISITION dof 0
sfrq 300.082 dm nnn
tn H1 dsm c
at 3.747 dmf 200
np 33728 PROCESSING
sw 4500.5 wtfile
fb 2600 proc ft
bs 16 fn not used
tpwr 48
pw 6.9 werr
di 0 wekp
tof 0 wbs
nt 16 wnt
ct 16
alock n
gain not used
FLAOS n
il n
in y
dp y
DISPLAY
sp -80.3
wp 2905.7
vs 170
sc 0
wc 250
hzma 11.62
fs 214.30
rfl 749.9
rfd 0
th 20
ins 3.010
nm cdc ph
    
```



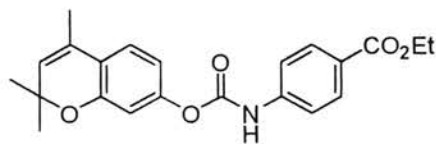
¹H NMR Spectrum of 45

Plate XLIV

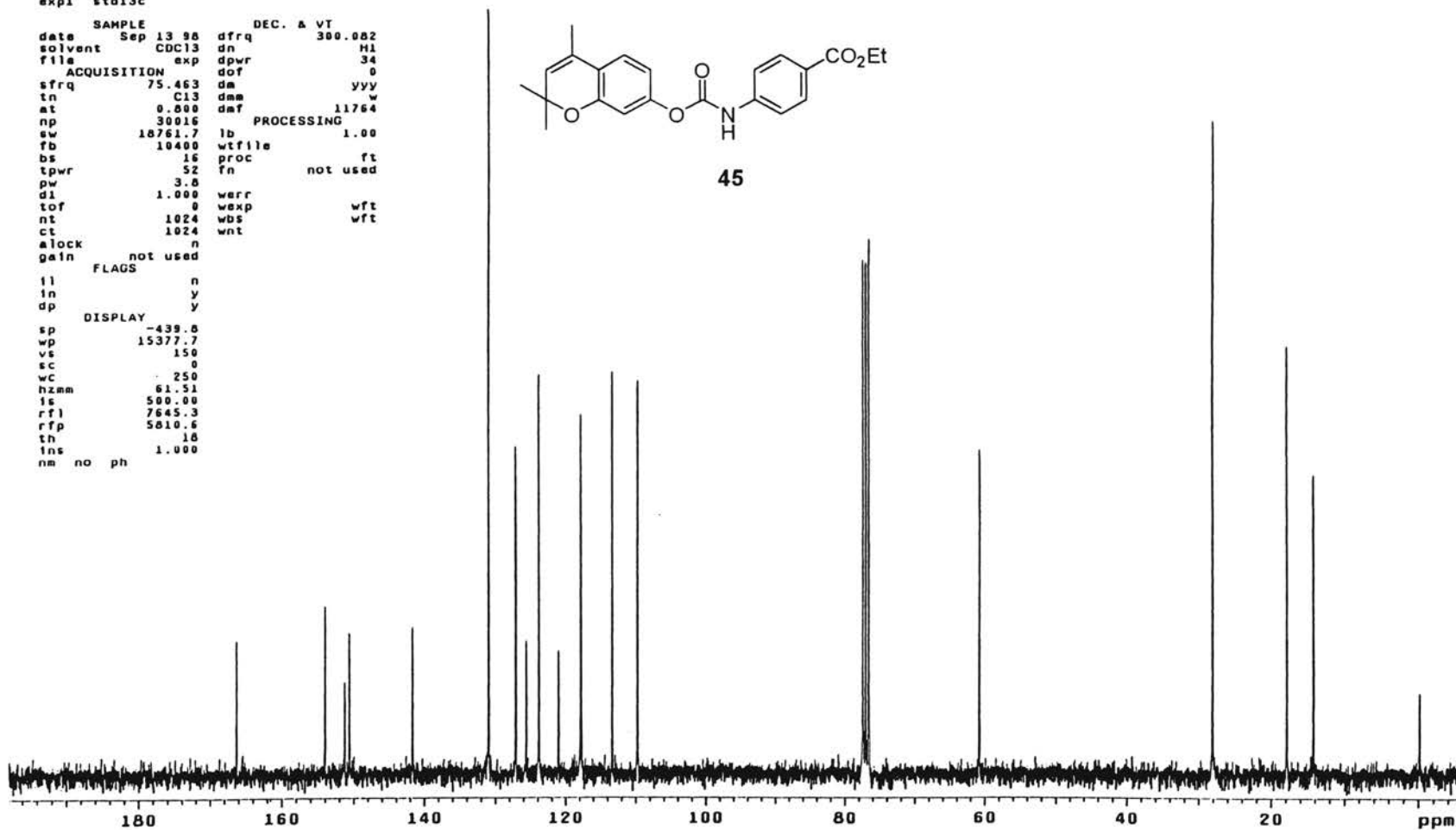
¹³C OBSERVE

exptl std13c

date	Sep 13 98	dfrq	300.082
solvent	CDC13	dn	H1
file	exp	dpwr	34
ACQUISITION			
sfrq	75.463	dof	0
tn	C13	dm	yyy
at	0.800	dmm	w
np	30016	daf	11764
sw	18761.7	lb	PROCESSING 1.00
fb	10400	wtfile	
bs	16	proc	ft
tpwr	52	fn	not used
pw	3.8		
d1	1.000	werr	
tof	0	wexp	wft
nt	1024	wbs	wft
ct	1024	wnt	
alock	n		
gain	not used		
FLAGS			
il	n		
in	y		
dp	y		
DISPLAY			
sp	-439.8		
wp	15377.7		
vs	150		
sc	0		
wc	250		
hzmm	61.51		
is	500.00		
rfl	7645.3		
rfp	5810.6		
tn	16		
ins	1.000		
nm	no	ph	

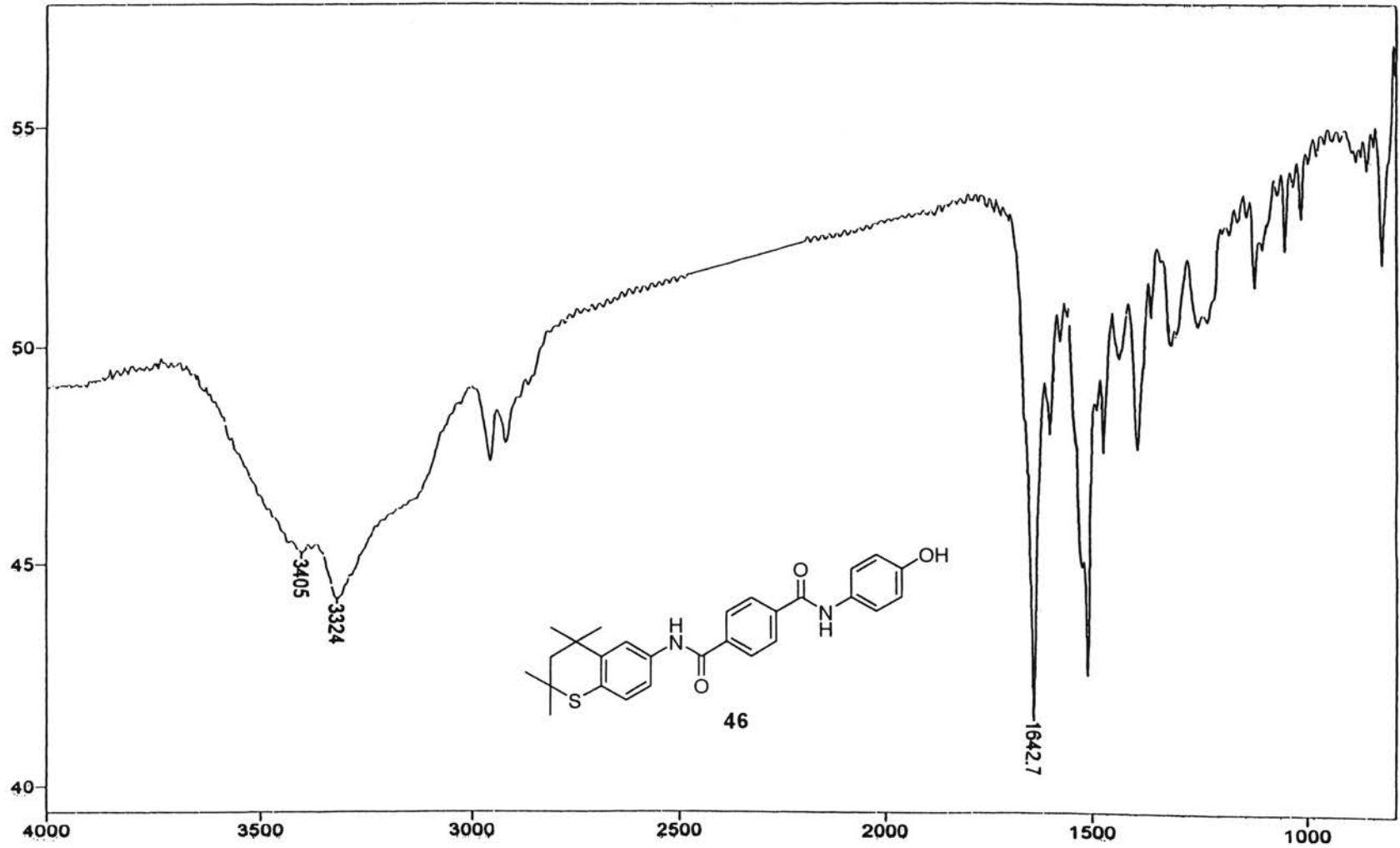


45



¹³C NMR Spectrum of 45

Plate XLV



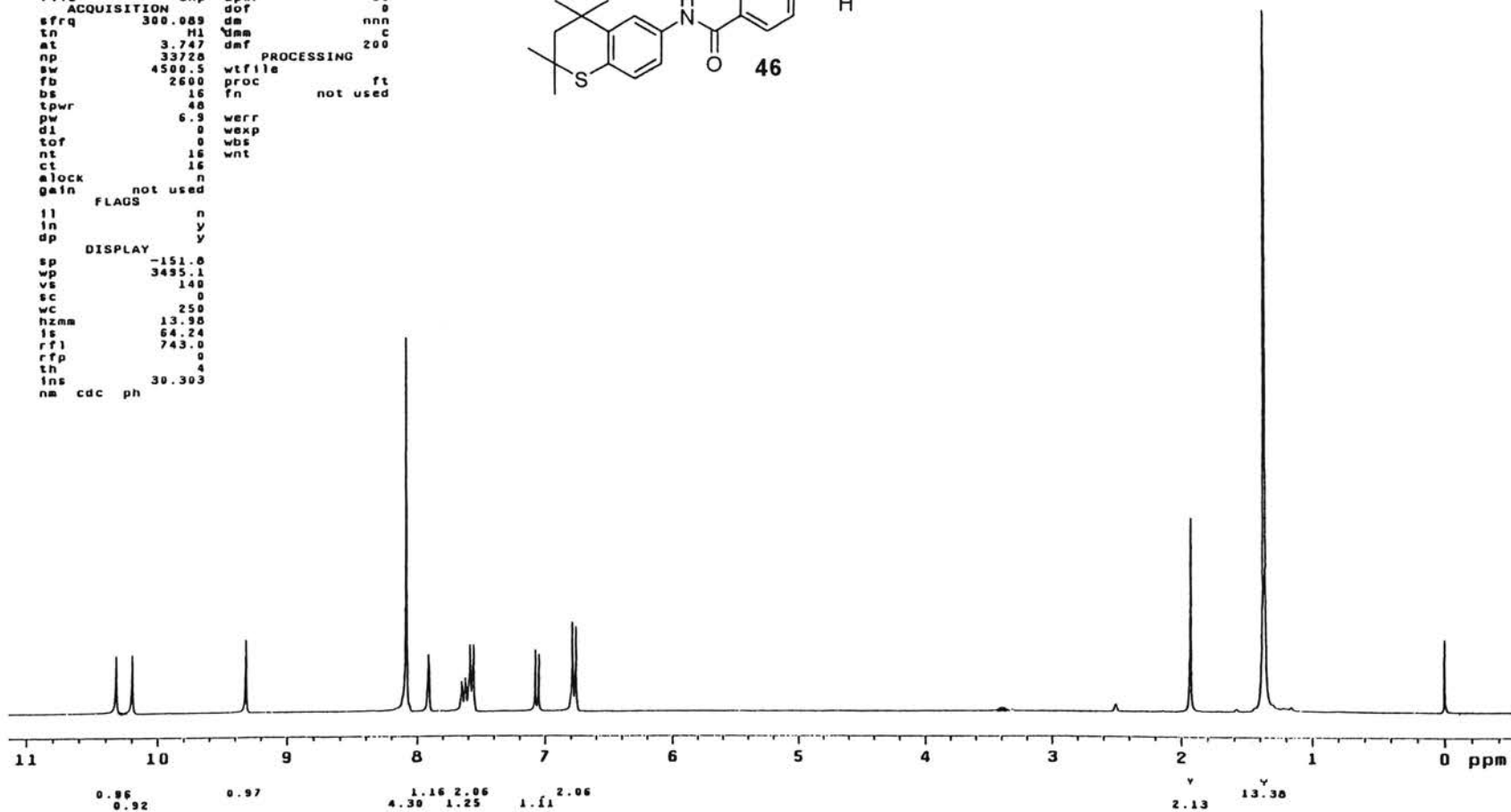
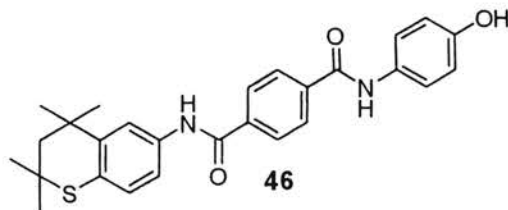
IR Spectrum of 46

Plate XLVI

4-hydroxyphenyl-thio

expl std1h

SAMPLE		DEC. & VT	
date	Feb 28 2001	dfrq	300.009
solvent	DMSO	dn	H1
file	exp	dpr	30
ACQUISITION		dot	0
sfrq	300.009	dm	nnn
tn	H1	dmm	C
at	3.747	dmf	200
np	33720	PROCESSING	
sw	4500.5	wtfile	
fb	2600	proc	ft
bs	16	fn	not used
tpwr	48		
pw	6.3	werr	
d1	0	wexp	
tof	0	wbs	
nt	16	wnt	
ct	16		
alock	n		
gain	not used		
FLAGS			
il	n		
in	y		
dp	y		
DISPLAY			
sp	-151.0		
wp	3495.1		
vs	140		
sc	0		
wc	250		
hzm	13.90		
ls	64.24		
rfl	743.0		
rtp	0		
th	4		
ins	30.303		
nm	cdc ph		



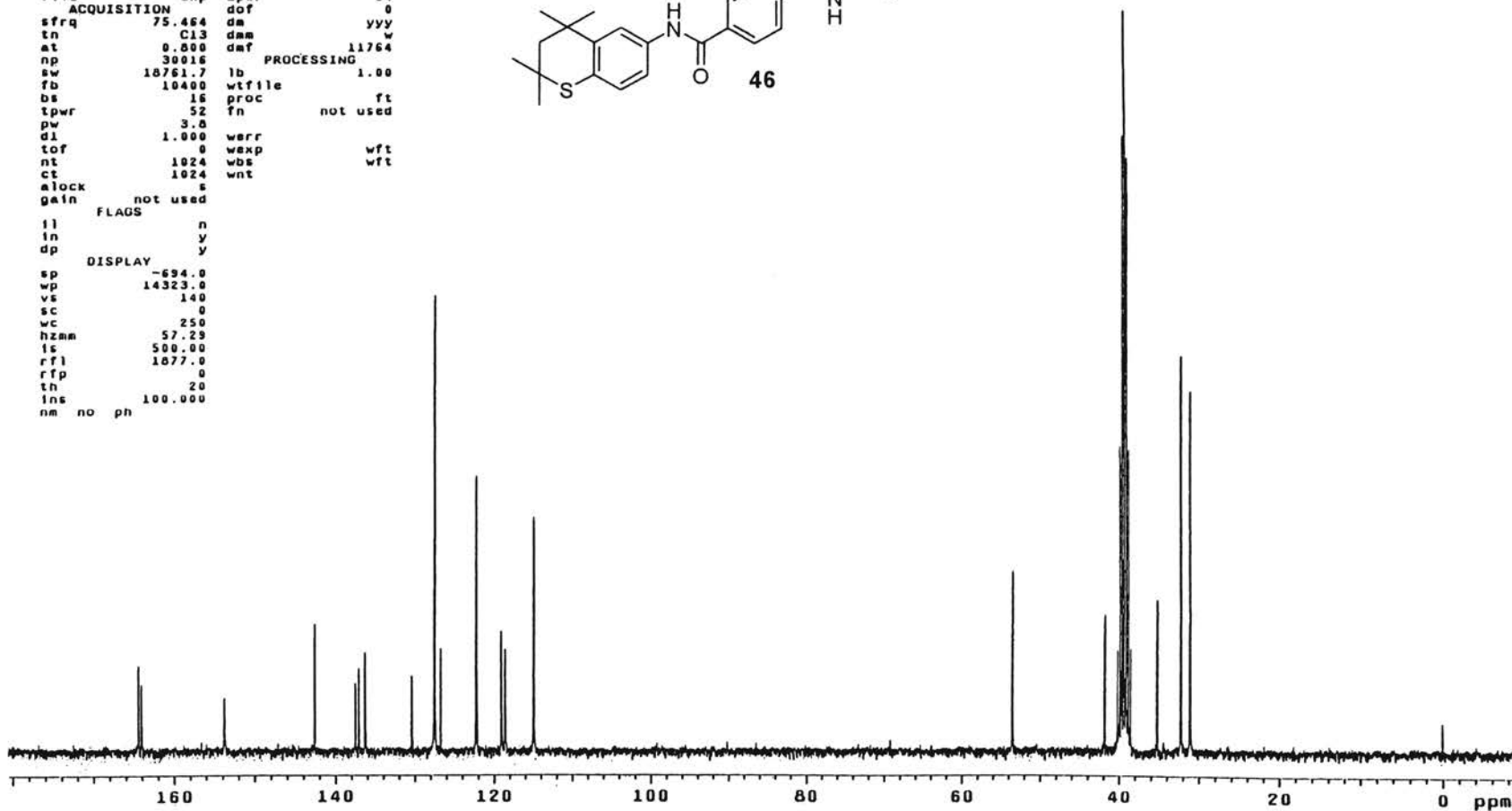
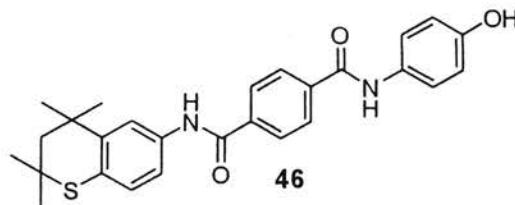
¹H NMR Spectrum of 46

Plate XLVII

4-hydroxyphenyl-thio

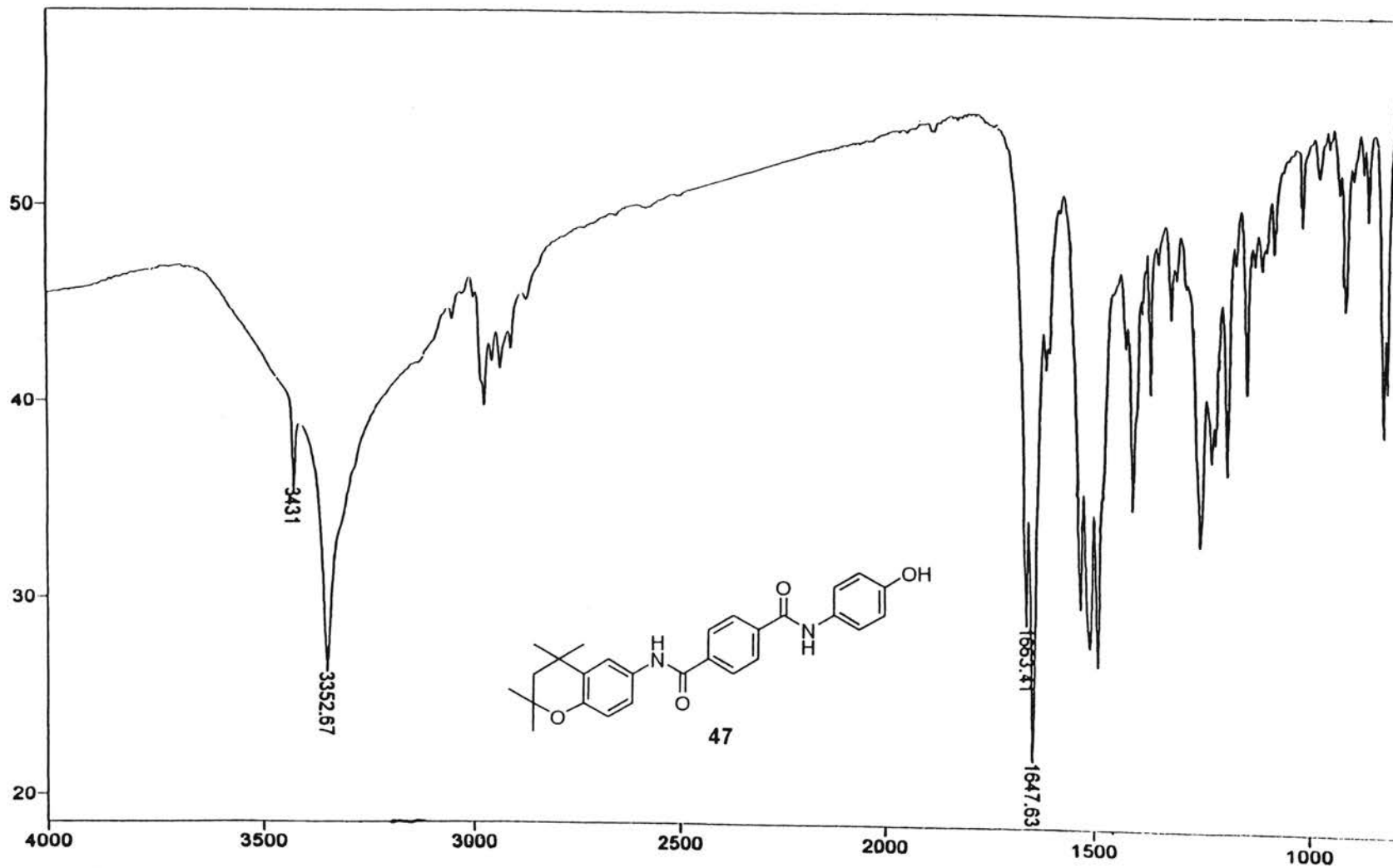
expl std13c

date	FEB 28 2001	dfrq	DEC. & VT	300.089
solvent	DMSO	dn		M1
file	exp	dpwr		34
ACQUISITION		dof		0
sfrq	75.464	dm		yyy
tn	C13	dsm		w
at	0.000	daf		11764
np	30018	PROCESSING		
sw	18761.7	lb		1.00
fb	10400	wffile		
bs	16	proc		ft
tpwr	52	fn		not used
pw	3.0			
dl	1.000	werr		wft
tof	0	wexp		wft
nt	1024	wbs		wft
ct	1024	wnt		
clock	s			
gain	not used			
FLAGS				
fl		n		
ln		y		
dp		y		
DISPLAY				
sp	-694.0			
wp	14323.0			
vs	140			
sc	0			
wc	250			
hzmm	57.29			
fs	500.00			
rfl	1877.0			
rfp	0			
th	20			
lrs	100.000			
nm	no	ph		



¹³C NMR Spectrum of 46

Plate XLVIII



IR Spectrum of 47

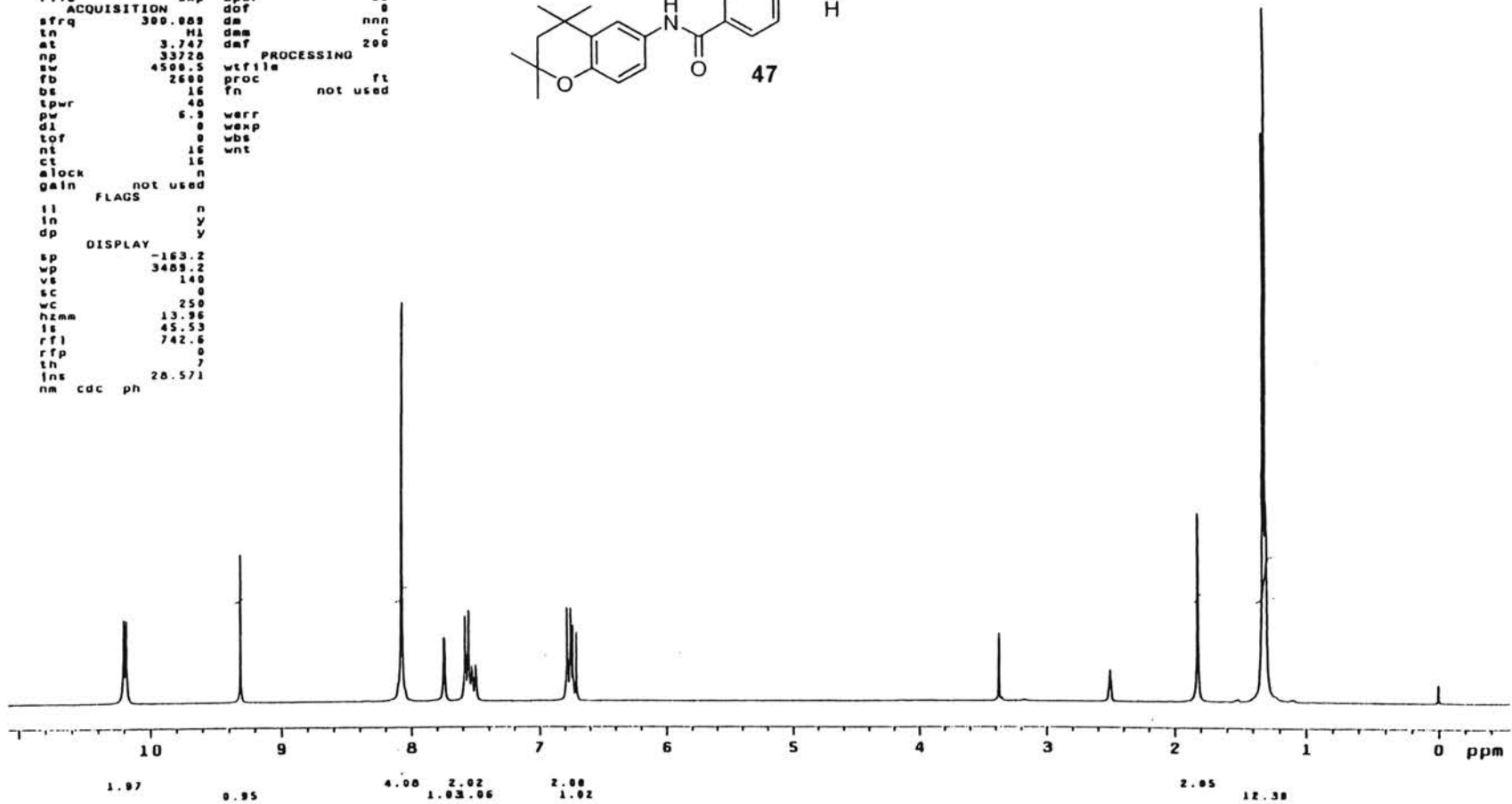
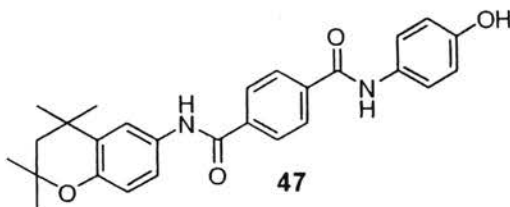
Plate XLIX

4-hydroxyphenyl-0

exptl stdin

```

SAMPLE          DEC. & VT
date   Jan 19 2001  dfrq   300.003
solvent DMSO      dn      H1
file    exp      dpwr   30
ACQUISITION    exp      dof    0
sfrq   300.003  dm      nnn
tn      H1      dnm      C
at     3.747    dmf     200
np     33720    wtfile
sw     4508.5  proc
fb     2600    fn      not used
bs     15
tpwr   40
pw     6.9    werr
d1     0      wexp
tof    0      wbs
nt     15    wnt
ct     15
alock  n
gain  not used
FLAGS
tl     n
ln     y
dp     y
DISPLAY
sp     -163.2
wp     3409.2
vs     140
sc     0
wc     250
hzmm   13.96
ls     45.53
rf1    742.6
rfp    0
th     7
ins    20.571
nm cdc ph
    
```



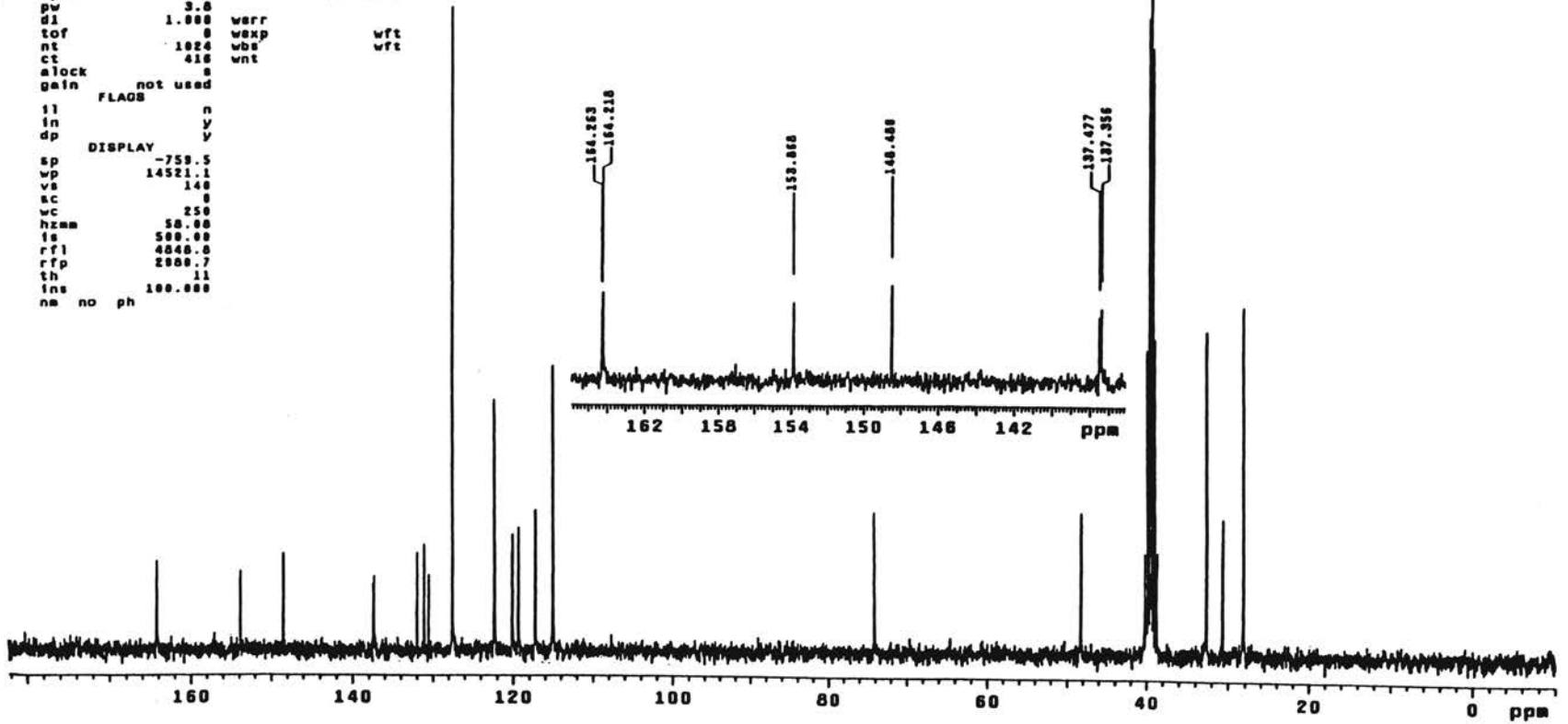
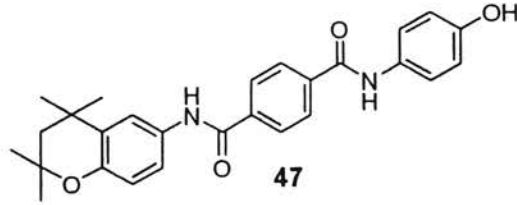
¹H NMR Spectrum of 47

Plate L

4-hydroxyphenyl-O

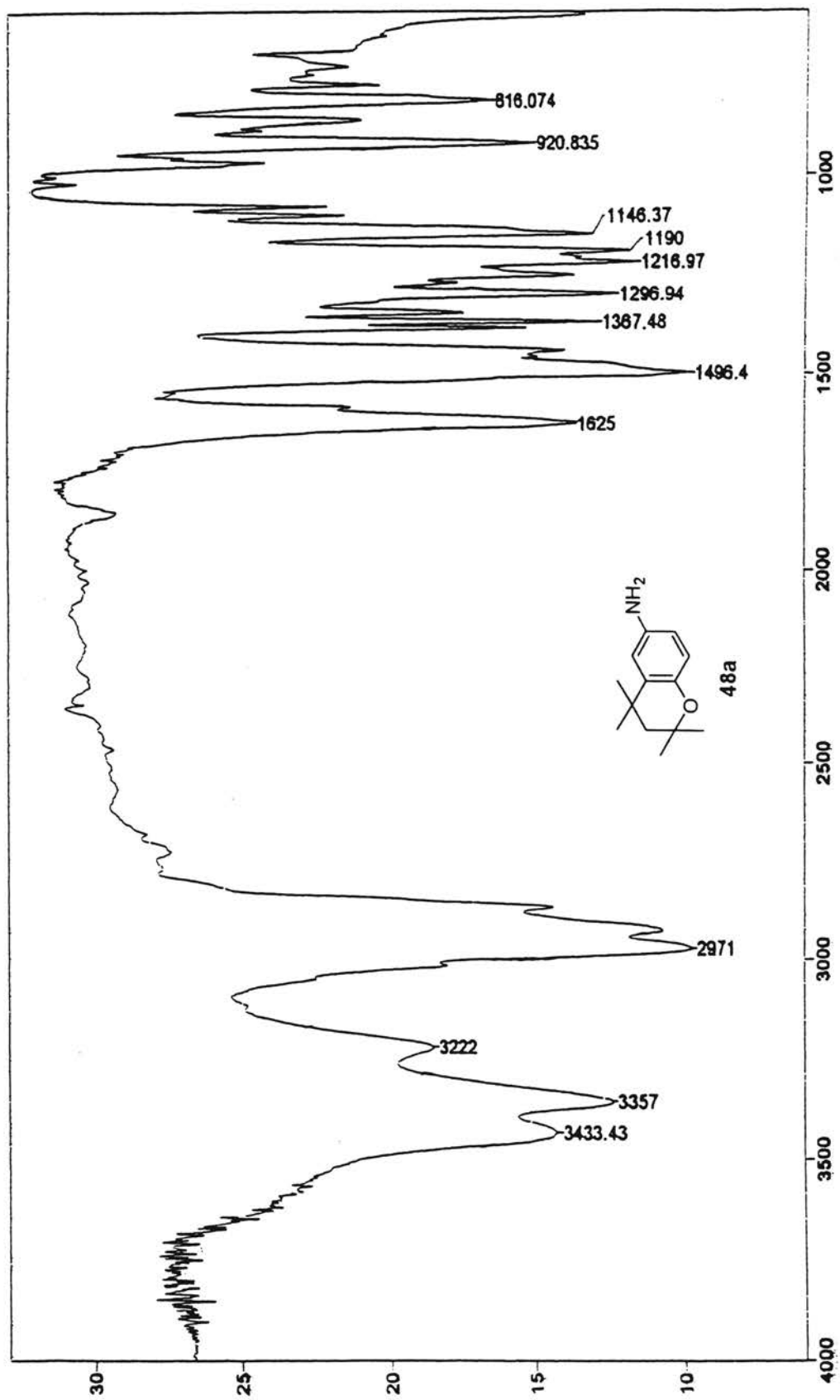
expl std13C

date	Jan 18 2001	dfrq	300.000
solvent	DMSO	dn	H1
file	exp	dpwr	34
ACQUISITION			
strq	75.464	ds	0
tn	C13	dsf	yyy
at	0.600	daf	11764
np	30016	PROCESSING	
sw	10751.7	lb	1.00
fb	10400	wtfile	
bs	16	proc	ft
tpwr	52	fn	not used
pv	3.0		
d1	1.000	warr	
tof	0	wexp	wft
nt	1024	wbs	wft
ct	416	wnt	
alock	0		
gain	not used		
FLAGS			
fl		n	
in		y	
dp		y	
DISPLAY			
sp	-759.5		
wp	14521.1		
vs	140		
sc	0		
uc	250		
hzam	50.00		
fs	500.00		
rfl	4040.0		
rtp	2000.7		
th	11		
ins	100.000		
na	no	ph	



¹³C NMR Spectrum of 47

Plate LI



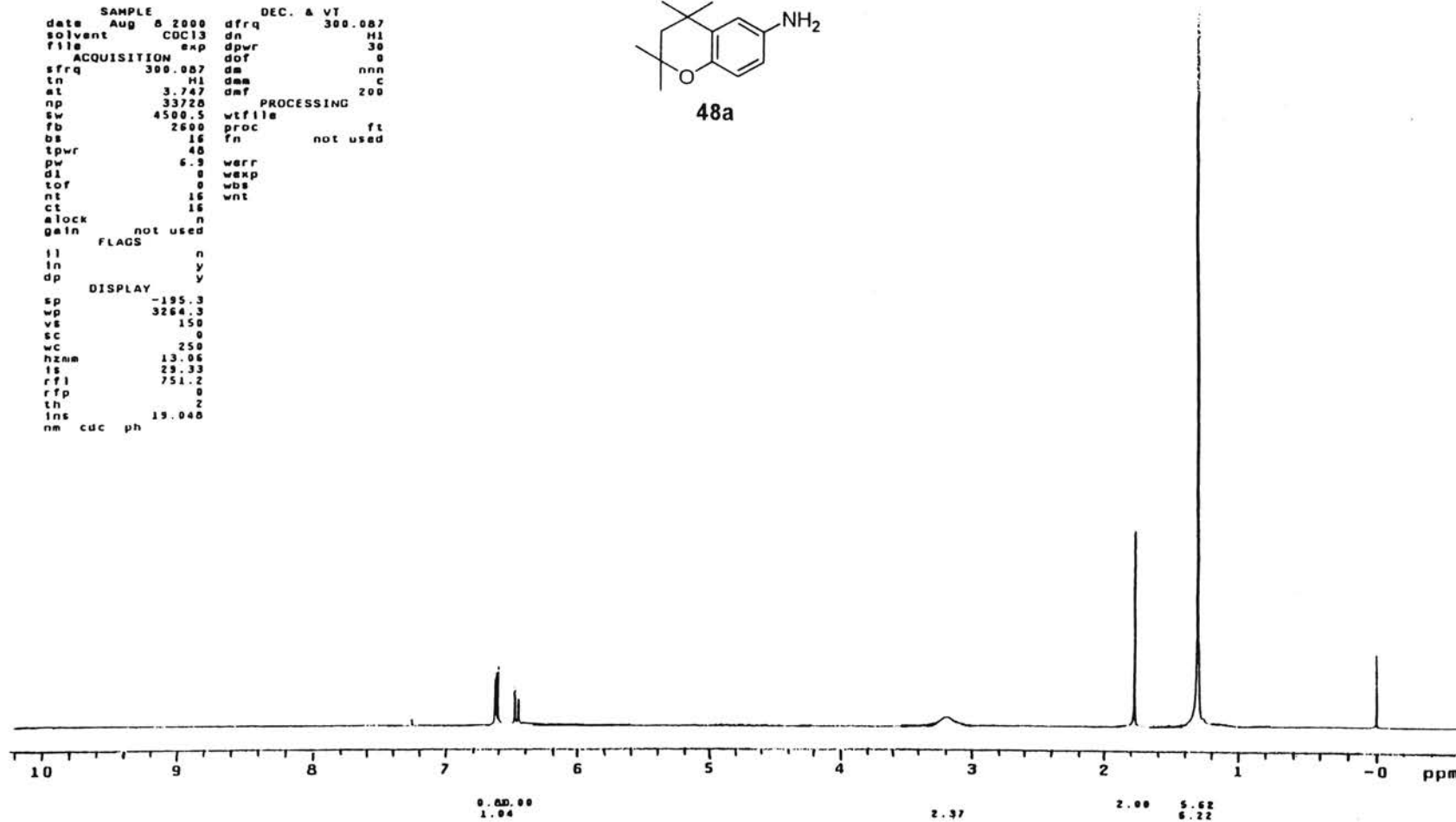
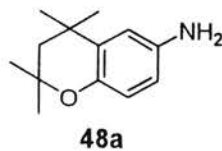
IR Spectrum of 48a

Plate LII

STANDARD IN OBSERVE

```

expl stidh
SAMPLE
date Aug 6 2000 dfrq DEC. & VT 300.087
solvent CDCl3 dn H1
file exp dpwr 30
ACQUISITION dof 0
sfrq 300.087 da nnn
tn H1 dam C
at 3.747 dmf 200
np 33728 PROCESSING
sw 4500.5 wtf file
fb 2500 proc ft
ds 16 fn not used
tpwr 40
pw 6.9 werr
d1 0 wexp
tof 0 wbs
nt 16 wnt
ct 16
alock n
gain not used
FLAGS
il n
in y
dp y
DISPLAY
sp -195.3
wp 3264.3
vs 150
sc 0
wc 250
hznm 13.06
is 29.33
rf1 751.2
rfp 0
th 2
ins 19.040
nm cdc ph
    
```

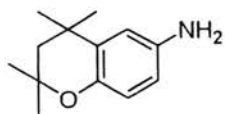


¹H NMR Spectrum of 48a

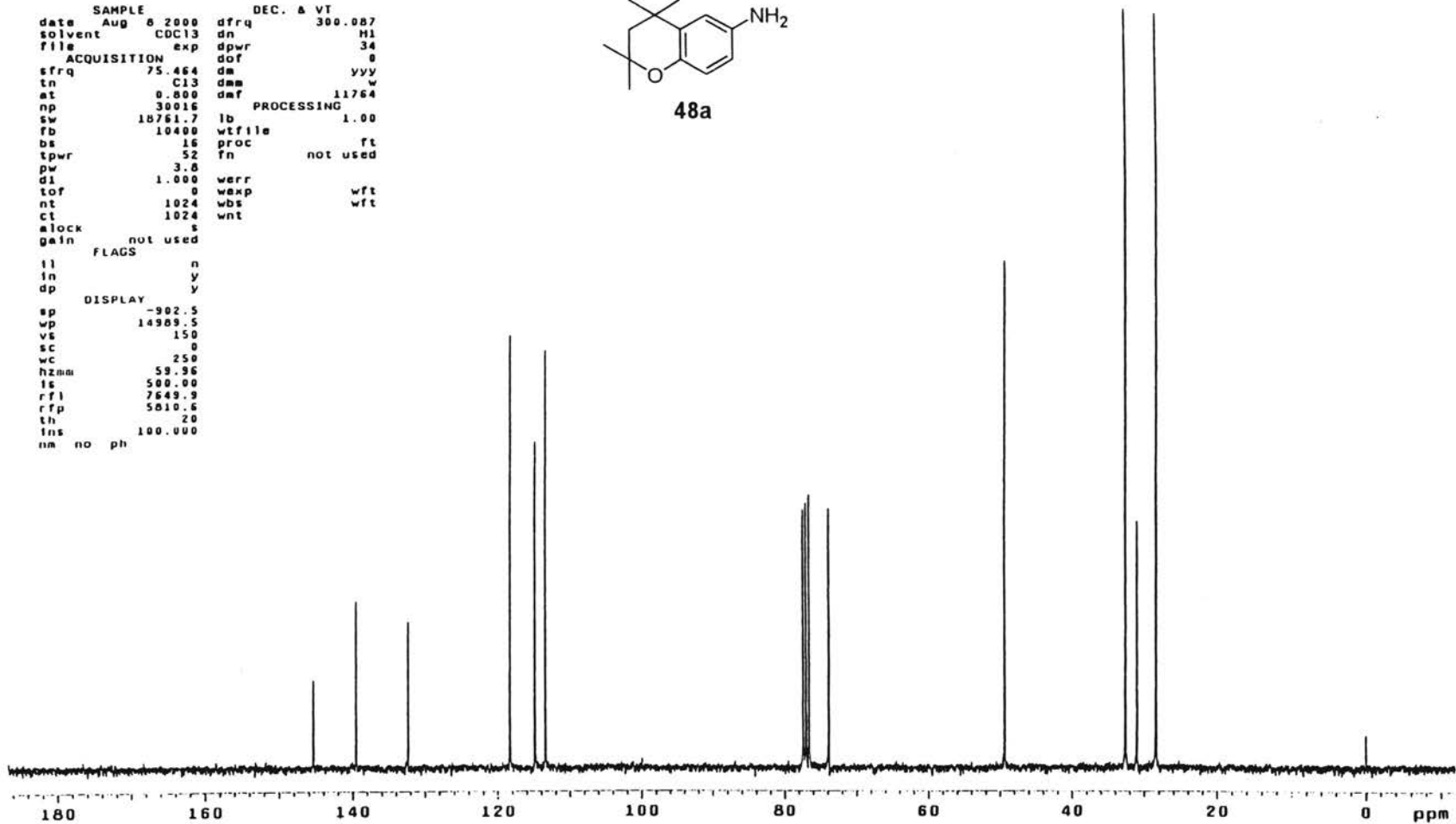
Plate LIII

```

Samine
expi std13c
SAMPLE DEC. & VT
date Aug 8 2000 dfrq 300.087
solvent CDC13 dn M1
file exp dpwr 34
ACQUISITION dof 0
sfrq 75.464 dm yyy
tn C13 dnm w
at 8.800 daf 11764
np 30016 PROCESSING 1.00
sw 18761.7 lb wtfile
fb 10400 proc ft
bs 16 fn not used
tpwr 52
pw 3.8
dl 1.000 werr
tof 0 wexp
nt 1024 wbs
ct 1024 wnt
alock s
gain not used
FLAGS
il n
in y
dp y
DISPLAY
sp -902.5
wp 14989.5
vs 150
sc 0
wc 250
hzmm 59.96
ls 500.00
rf1 7649.9
rfp 5810.6
th 20
ins 100.000
nm no ph
    
```

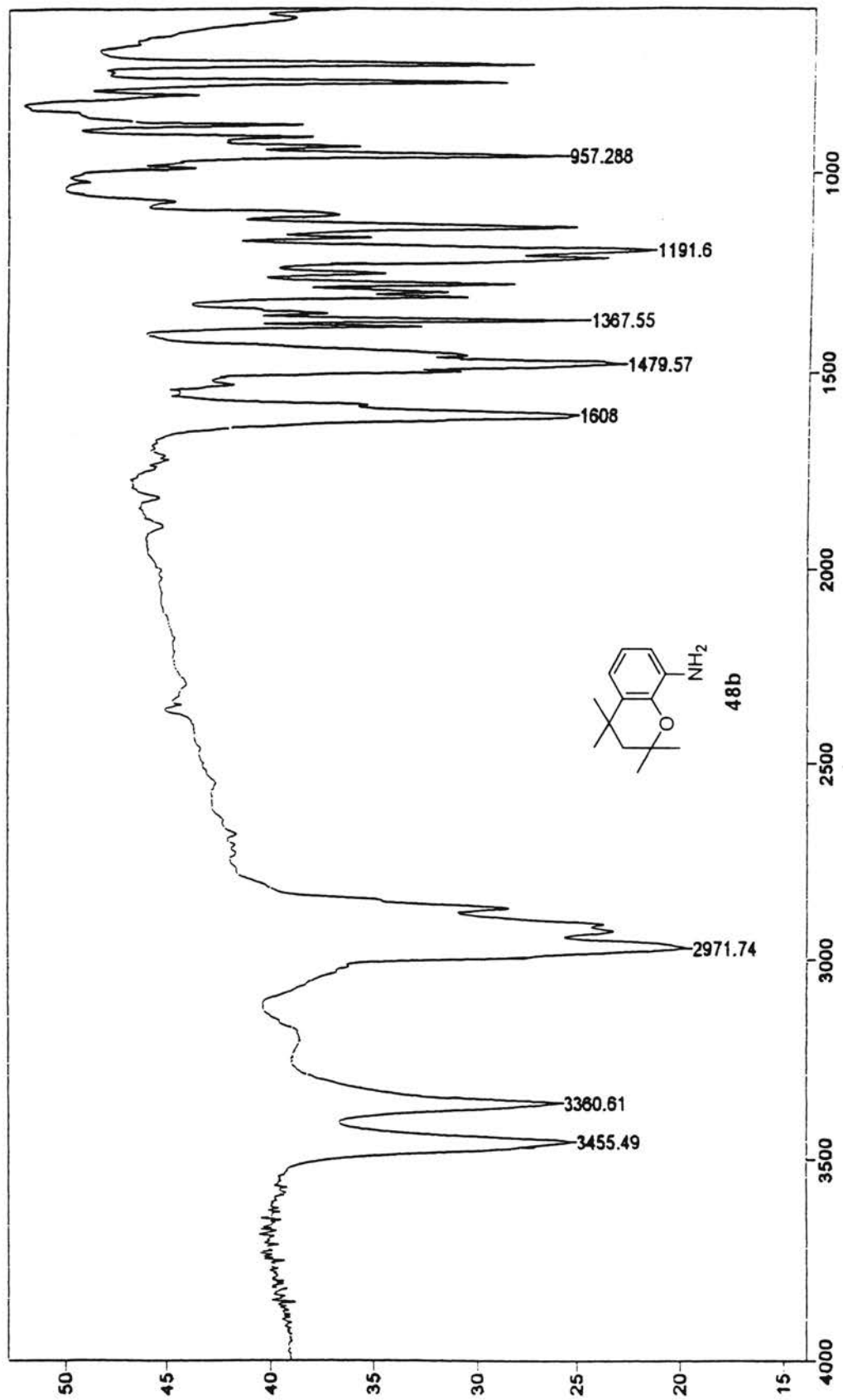


48a



¹³C NMR Spectrum of 48a

Plate LIV

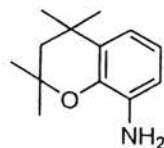


IR Spectrum of 48b

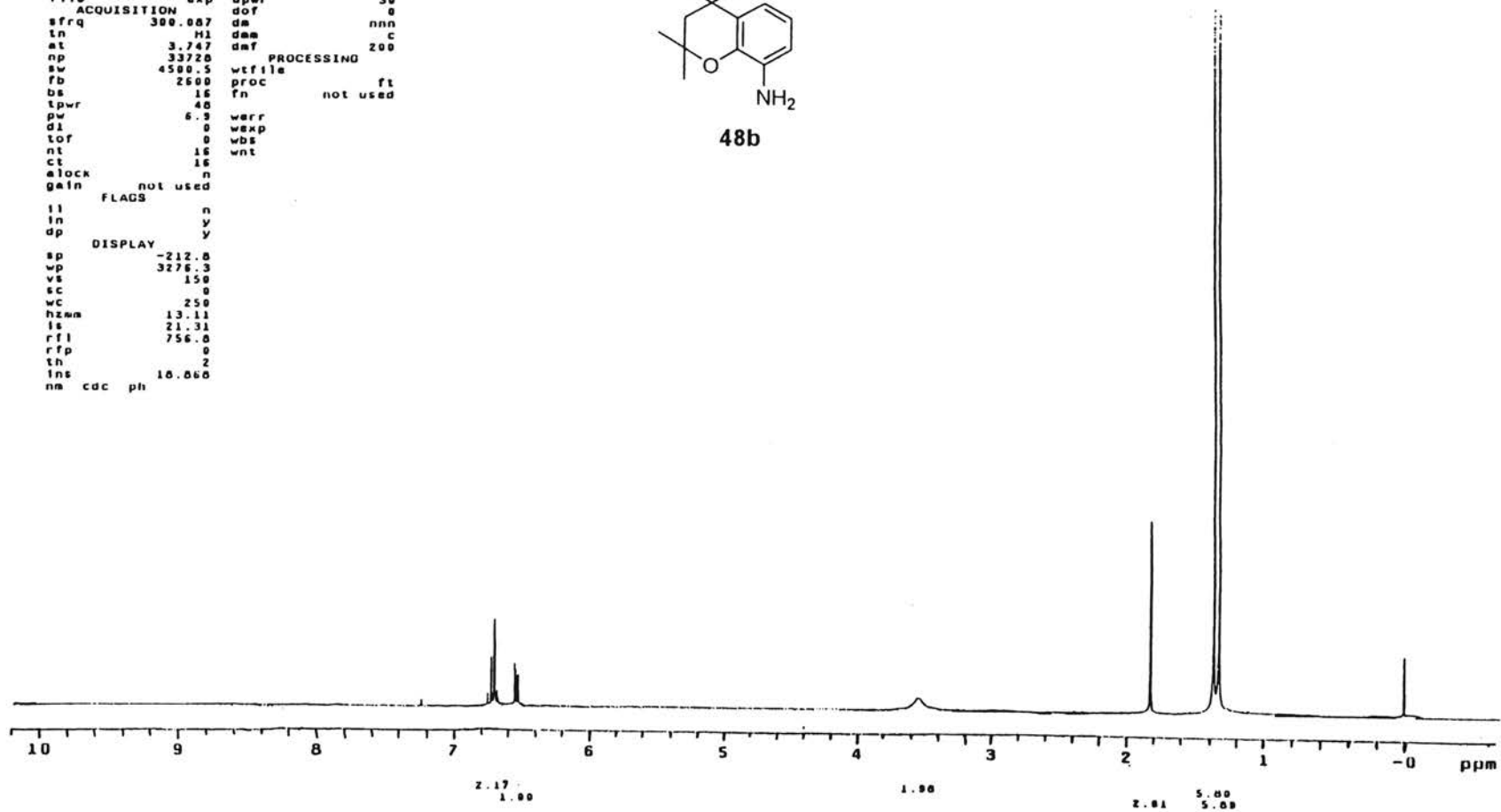
Plate LV

```

damine
expl stdih
SAMPLE
date Aug 8 2000 dfrq DEC. & VI 300.007
solvent CDC13 dn H1
file exp dpwr 30
ACQUISITION dof 0
sfrq 300.007 dm nnn
in H1 dsm c
at 3.747 dmf 200
np 33720 PROCESSING
sw 4500.5 wtfile
fb 2600 proc ft
bs 16 fn not used
tpwr 40 verr
pw 6.0 wexp
di 0 wbs
tof 0 wnt
nt 16
ct 16
elock n
gain not used
FLAGS
ii n
in y
dp y
DISPLAY
sp -212.0
wp 3276.3
vs 150
sc 0
wc 250
hznm 13.11
ls 21.31
rfi 756.0
rfp 0
th 2
ins 10.000
nm cdc ph
    
```



48b

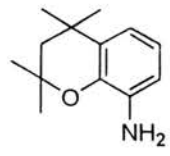


¹H NMR Spectrum of 48b

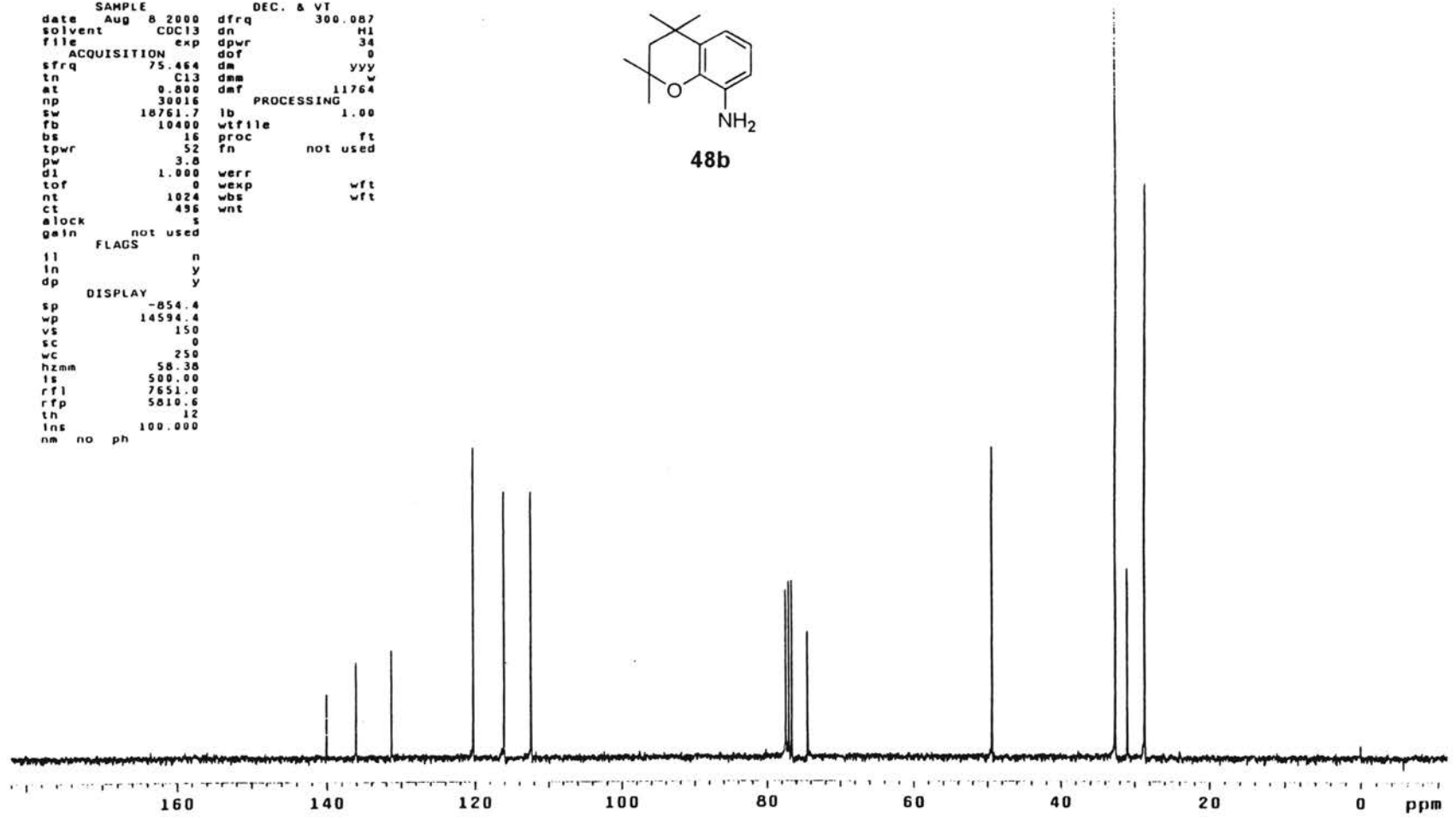
Plate LVI

```

8amine
expl std13c
SAMPLE DEC. & VT
date Aug 8 2000 dfrq 300.087
solvent COC13 dn HI
file exp dpwr 34
ACQUISITION exp dof 0
sfrq 75.464 dm vvy
tn C13 dmm w
at 0.800 dmf 11764
np 30016 PROCESSING
sw 18761.7 lb 1.00
fb 10400 wtf file
bs 16 proc ft
tpwr 52 fn not used
pw 3.0
d1 1.000 verr
tof 0 wexp wft
nt 1024 wbs wft
ct 456 wnt
a1ock s
gain not used
FLAGS
il n
in y
dp y
DISPLAY
sp -854.4
wp 14594.4
vs 150
sc 0
wc 250
hzmm 58.38
ts 500.00
rf1 7651.0
rfp 5810.6
th 12
ins 100.000
nm no ph
    
```

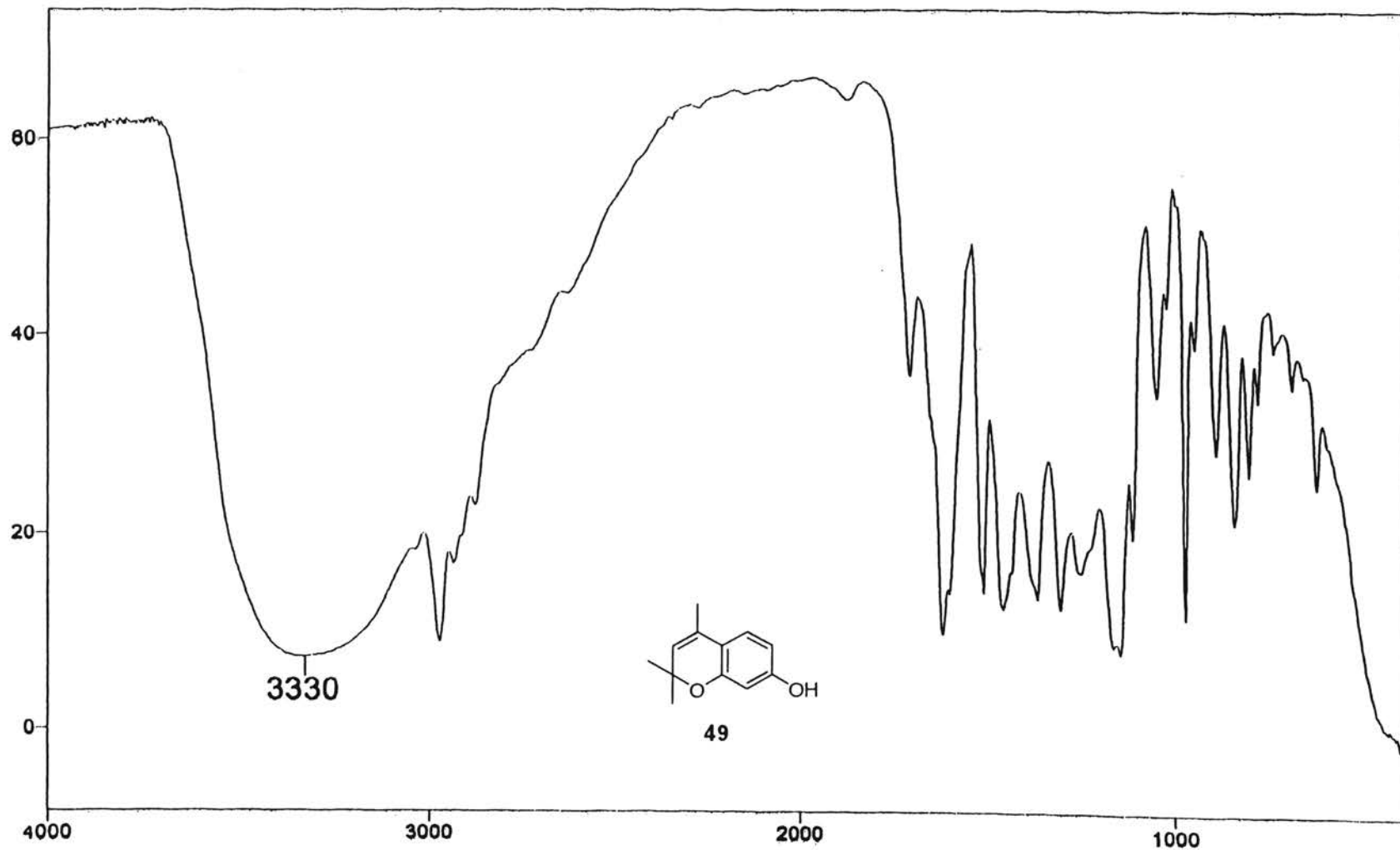


48b



¹³C NMR Spectrum of 48b

Plate LVII



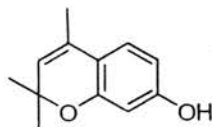
IR Spectrum of 49

Plate LVIII

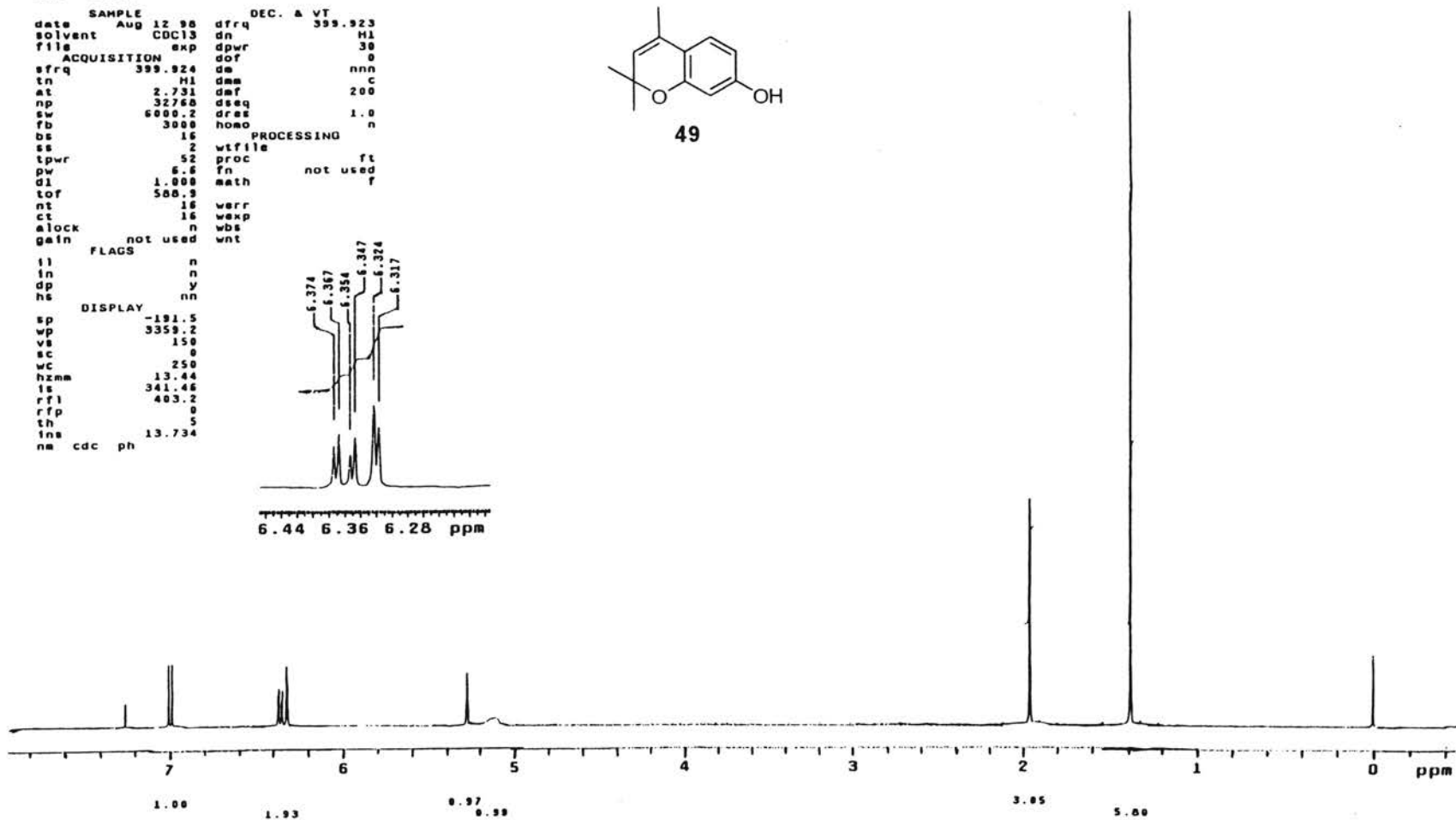
Std. 1H Inova400

expl stdih

date	AUG 12 98	dfrq	DEC. & VT	399.923
solvent	CDCl3	dn		H1
file		dpwr		38
ACQUISITION				
sfrq	399.924	de		nnn
tn	H1	dsm		c
at	2.731	daf		200
np	32760	dseq		
sw	6000.2	dres		1.0
fb	3000	homo		n
bs	16	PROCESSING		
ss	2	wtfile		ft
tpwr	52	proc		not used
pw	6.6	fn		f
ql	1.000	math		
tof	500.9			
nt	16	verr		
ct	16	wexp		
alock		wbs		
gain	not used	wnt		
FLAGS				
il		n		
in		n		
dp		y		
hs		nn		
DISPLAY				
sp	-181.5			
wp	3359.2			
vs	150			
sc	0			
wc	250			
hzma	13.44			
ls	341.46			
rfl	403.2			
rfp	0			
th	5			
ins	13.734			
na	cdc ph			



49



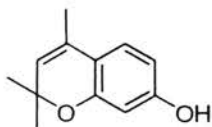
¹H NMR Spectrum of 49

Plate LIX

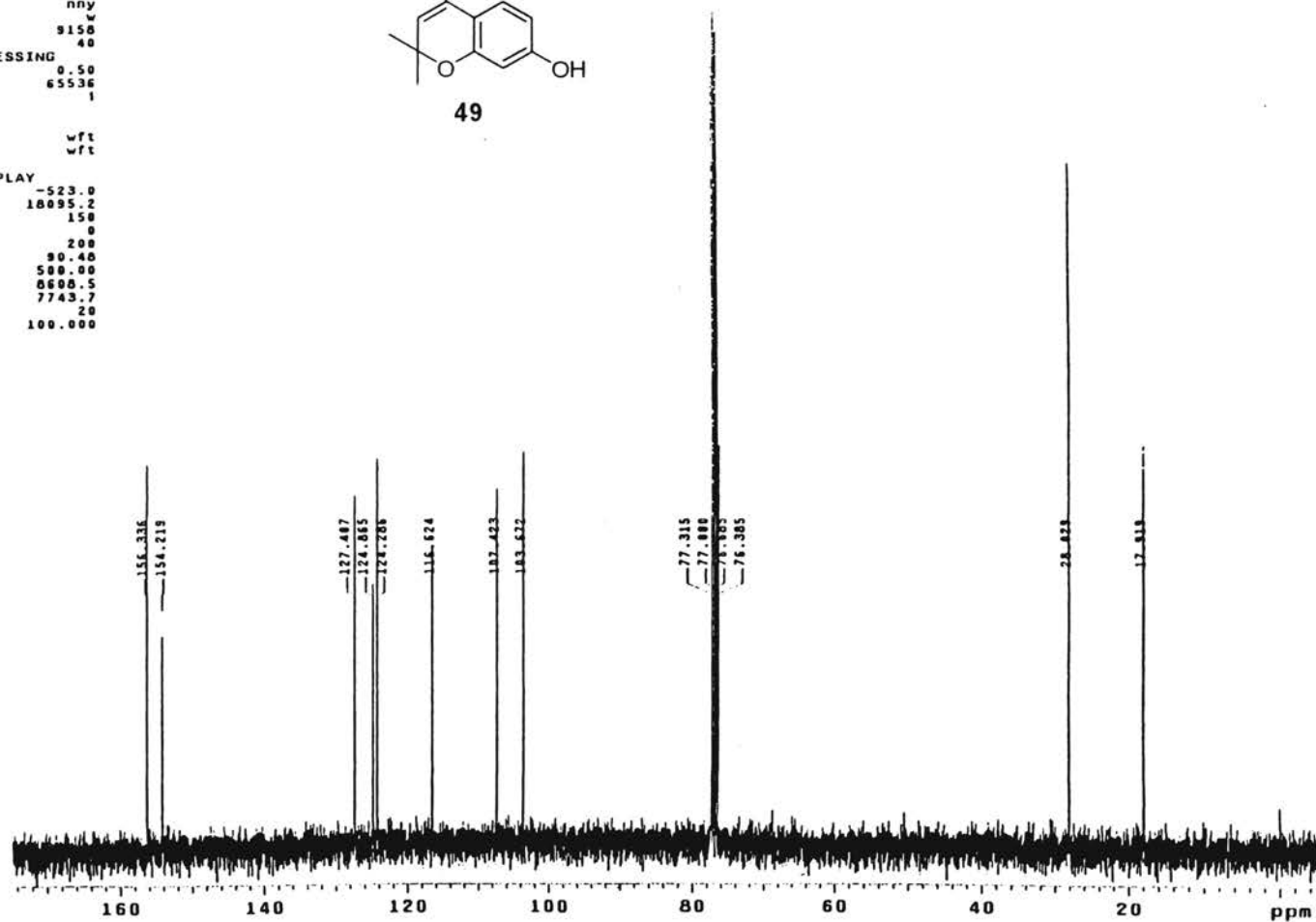
GAMMA-H2 TEST
USE 1 WAIT DECOUPLING

expl s2pu1

date	SAMPLE	Aug 9 88	dn	UEC. & VT	H1
solvent	Aug	CDC13	dof		0
file	exp		dm	nny	w
ACQUISITION					
sfrq	100.571	dma	9158		
tn	C13	dpwr	40		
at	1.903	PROCESSING			
np	95744	lb	0.50		
sw	24140.0	fn	65536		
fb	13000	math	1		
bs	16				
pw	4.9	werr		wft	
pw	4.9	wexp		wft	
tpwr	51	wbs			
d1	1.000	wnt			
tof	1711.4	DISPLAY			
nt	256	sp	-523.0		
ct	256	wp	18095.2		
alock		n	150		
gain	44	sc	0		
FLAGS					
ll	n	wc	200		
ln	n	nzmm	90.40		
dp	y	ls	500.00		
ns	nn	rfl	8600.5		
		rfp	7743.7		
		th	20		
		ins	100.000		
		nm	ph		

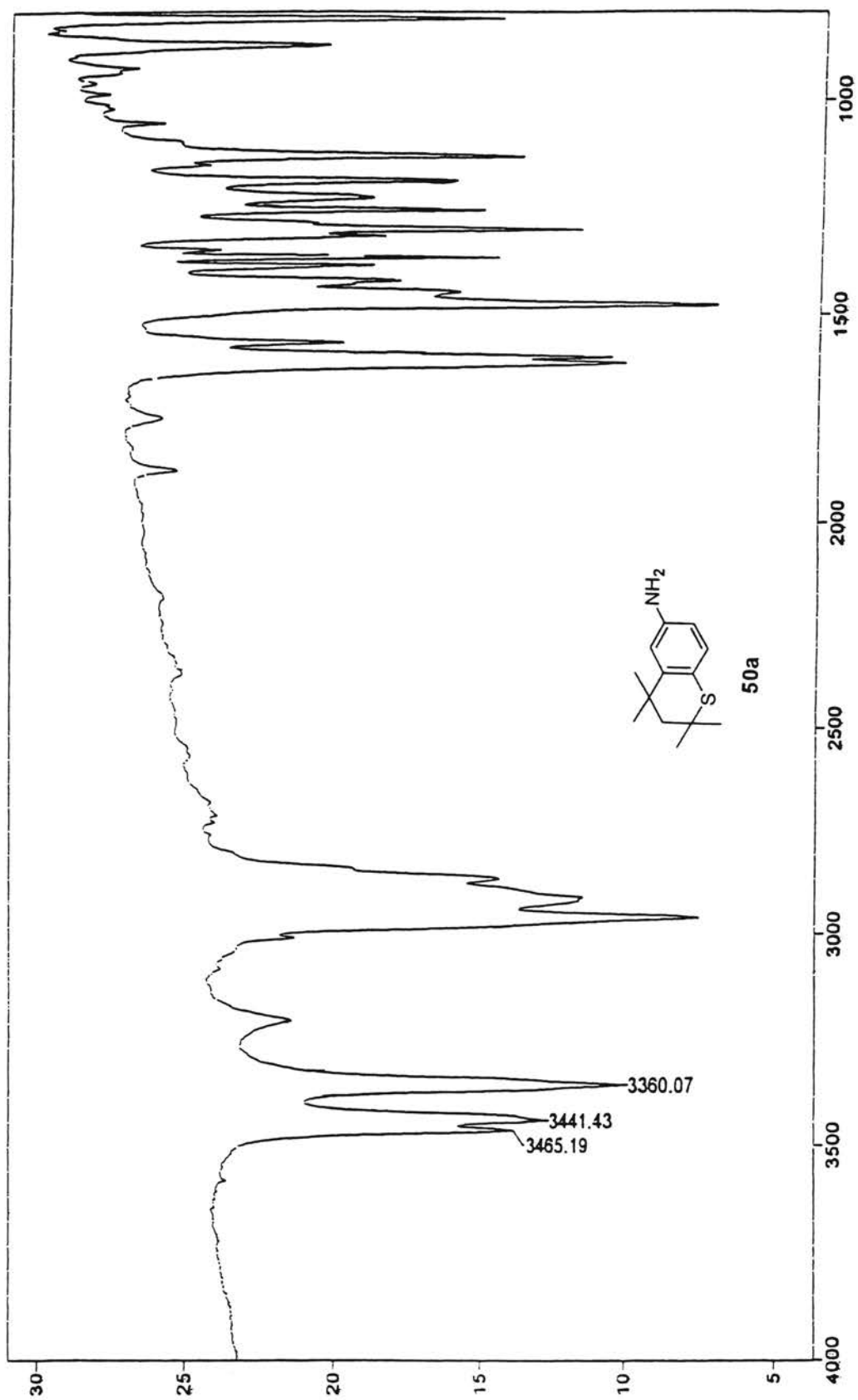


49



¹³C NMR Spectrum of 49

Plate LX



IR Spectrum of 50a

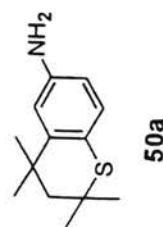
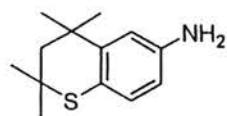


Plate LXI

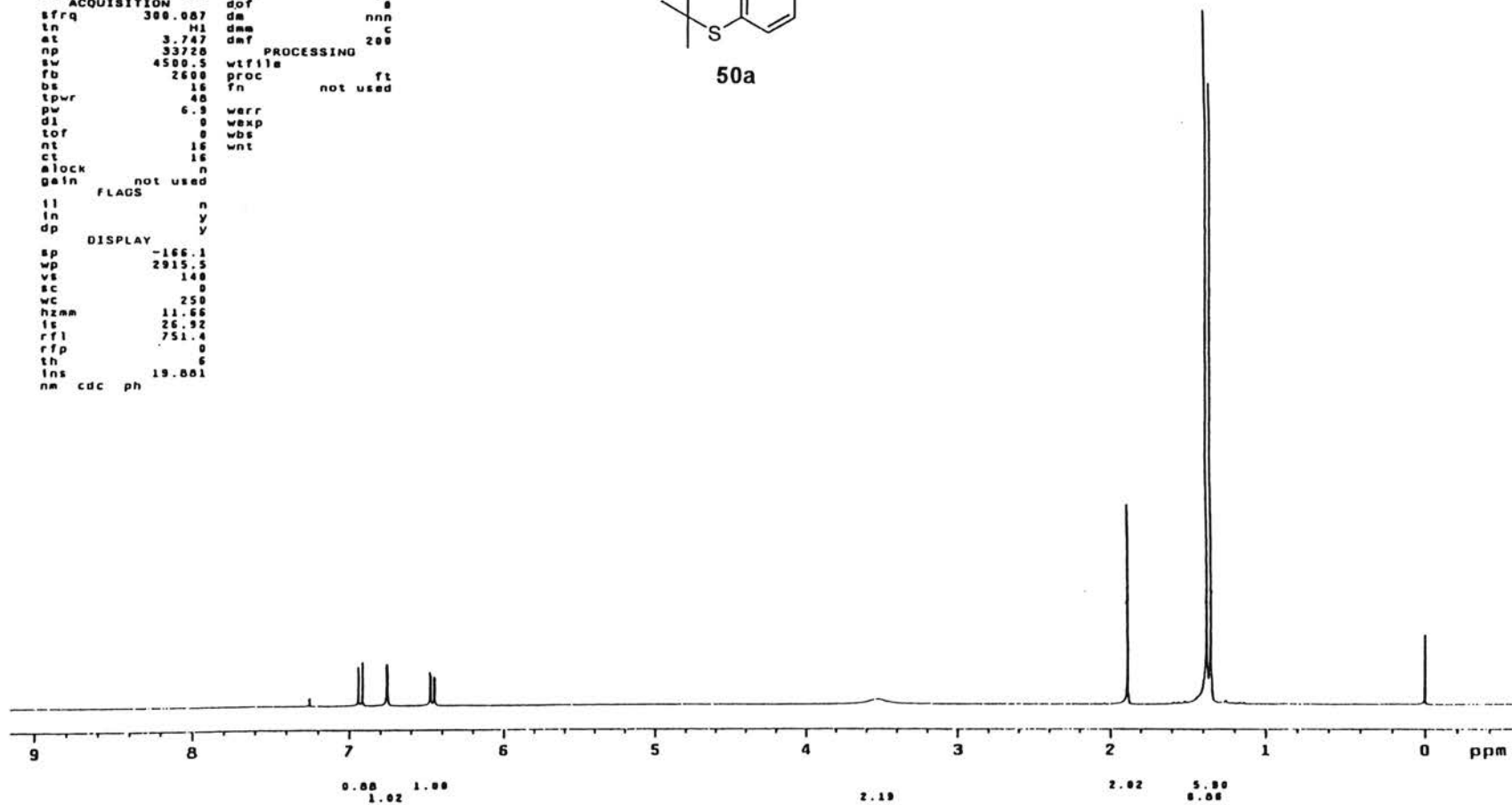
6-aminothiochroman

```

expl stdih
SAMPLE
data Feb 7 2001 dfrq DEC. & VT 300.007
solvent CDC13 dn H1
file exp dpwr 30
ACQUISITION dot 8
sfrq 300.007 da nnn
tn H1 dm c
at 3.747 dmf 200
np 33720
sw 4500.5 wflie
fb 2000 proc ft
bs 16 fn not used
tpwr 40
pw 6.9 werr
d1 0 wexp
tof 0 wbs
nt 16 wnt
ct 16
alock n
gain not used
FLAGS
il n
in y
dp y
DISPLAY
sp -166.1
wp 2915.5
vs 140
sc 0
wc 250
hzmm 11.66
is 26.92
rfl 751.4
rfp 0
th 6
lrs 19.001
nm cdc ph
    
```



50a

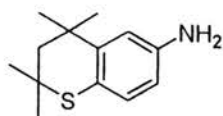


¹H NMR Spectrum of 50a

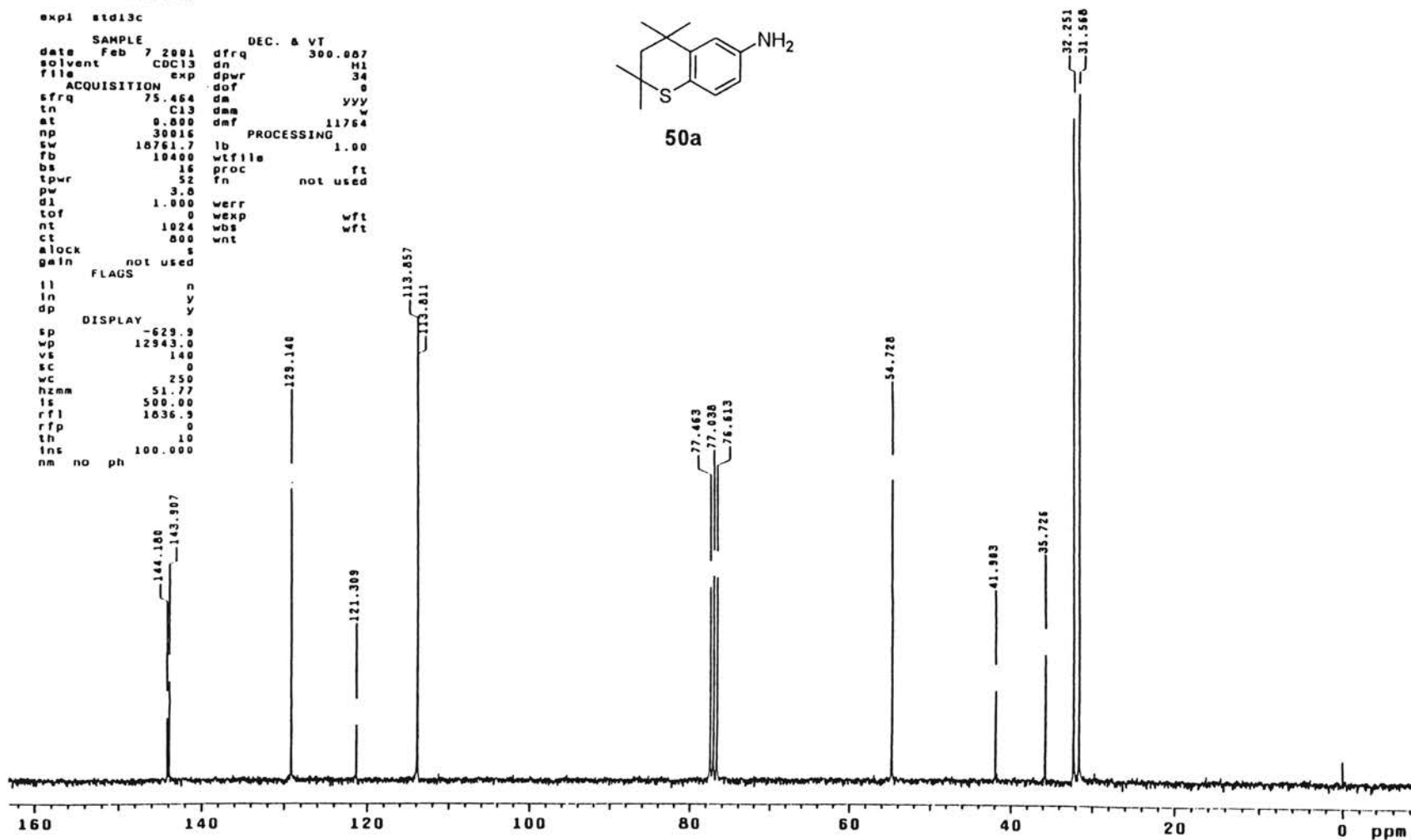
Plate LXII

```

6-aminothiochroman
expt  std13c
SAMPLE
date  Feb 7 2001  dfrq  300.087
solvent  CDC13  dn  H1
file  exp  dpwr  34
ACQUISITION  dof  0
sfrq  75.464  da  yyy
tn  C13  dam  w
at  8.800  dmf  11764
np  30916  PROCESSING
sw  18761.7  lb  1.00
fb  10400  wtfile
bs  16  proc  ft
tpwr  52  fn  not used
pw  3.8
d1  1.000  werr
tof  0  wexp  wft
nt  1024  wbs
ct  800  wnt
alock  s
gain  not used
FLAGS
il  n
in  y
dp  y
DISPLAY
sp  -629.9
wp  12943.0
vs  140
sc  0
wc  250
hzmm  51.77
ls  500.00
rfl  1636.9
rfp  0
th  10
ins  100.000
nm  no  ph
    
```



50a



¹³C NMR Spectrum of 50a

Plate LXIII

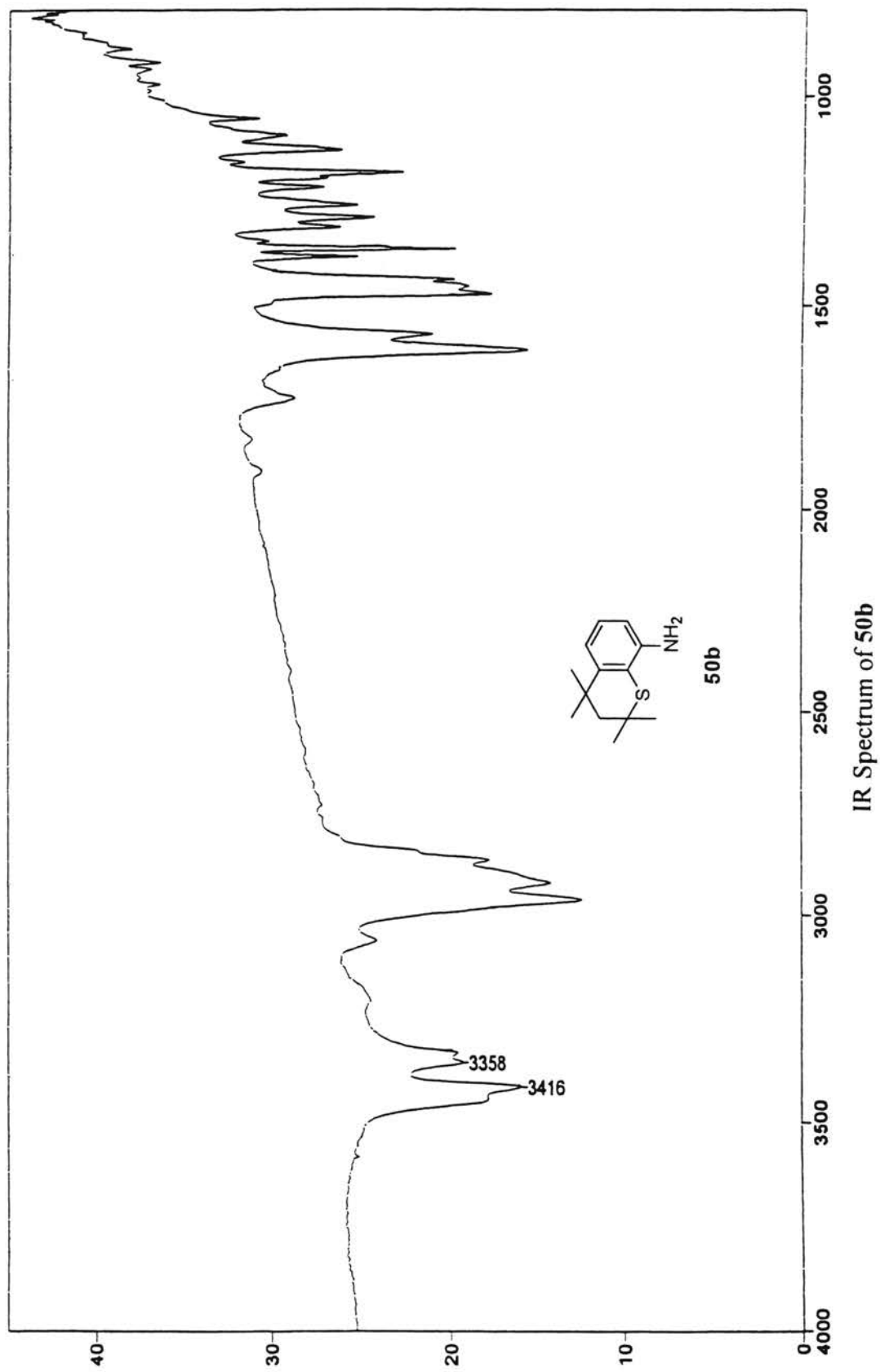


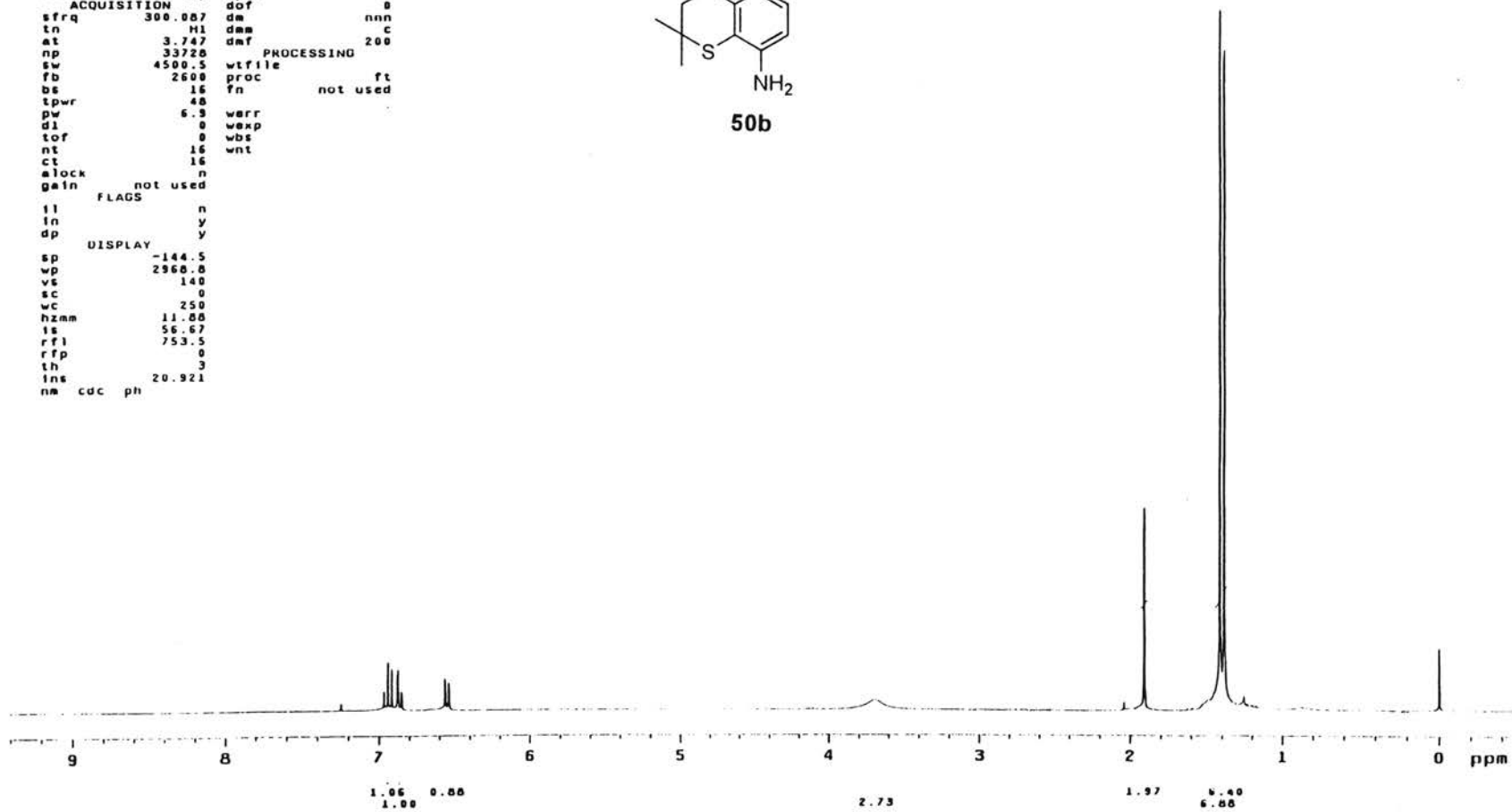
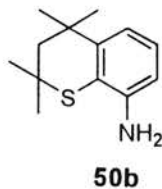
Plate LXIV

8-aminothiochroman

expl stdih

```

SAMPLE          DEC. & VT
date Apr 11 2001 dfrq          300.087
solvent CDC13          dn          H1
file          exp      dpwr          30
ACQUISITION    sfrq          300.087 dof          0
tn          H1          dm          nnn          C
at          3.747      dmf          200
np          33728      PROCESSING
sw          4500.5     wtfile
fb          2600      proc          ft
bs          16        fn          not used
tpwr          48
pw          6.3      warr
d1          0        wexp
tof          0        wbs
nt          16      wnt
ct          16
slock          n
gain          not used
FLAGS
ll          n
ln          y
dp          y
DISPLAY
sp          -144.5
wp          2968.8
vs          140
sc          0
wc          250
hzm          11.88
is          56.67
rf          753.5
rfp          0
th          3
ins          20.921
nm          cdc ph
    
```



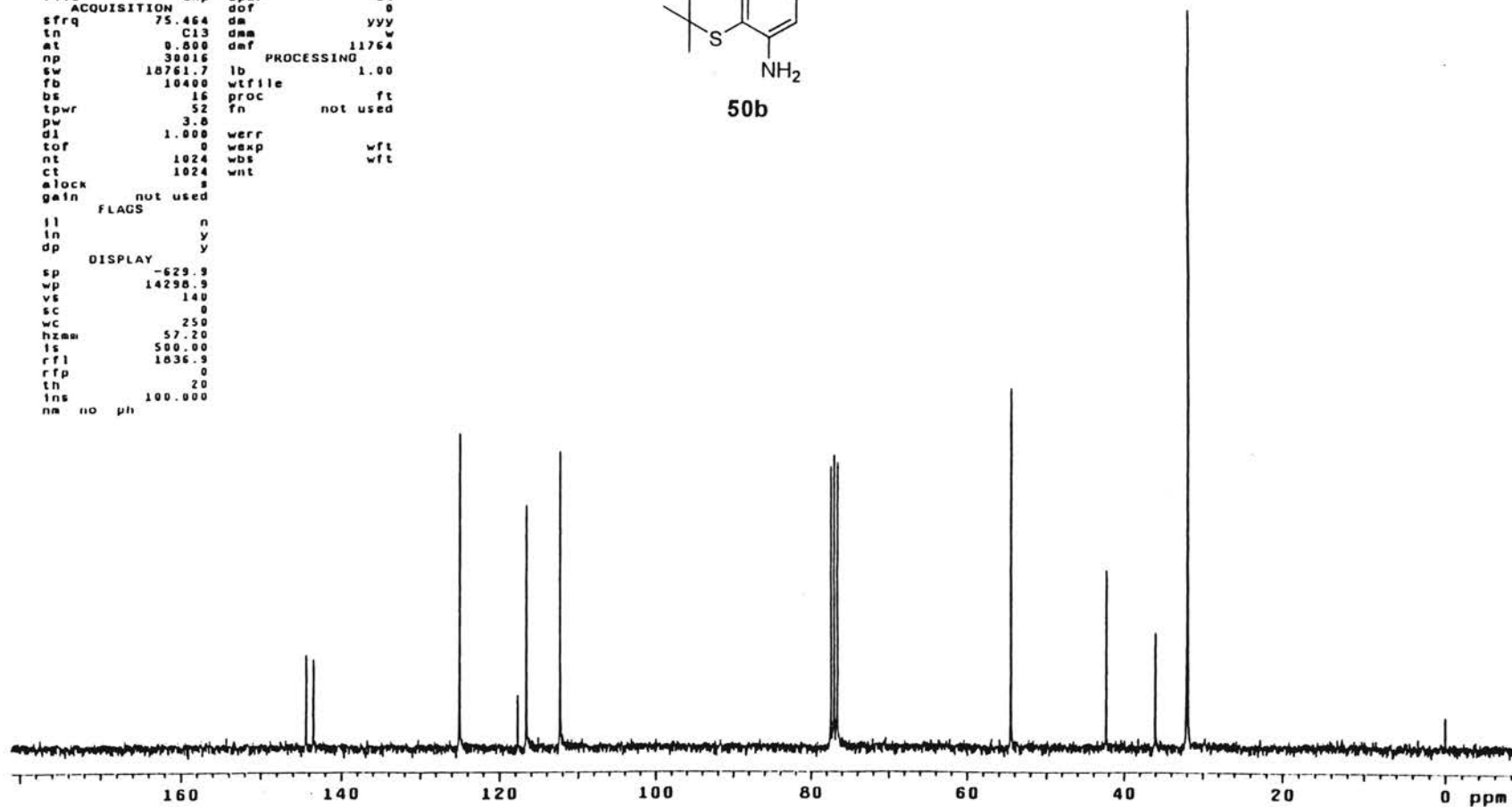
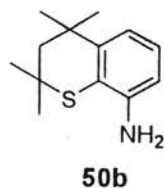
¹H NMR Spectrum of 50b

Plate LXV

5-aminothiochroman

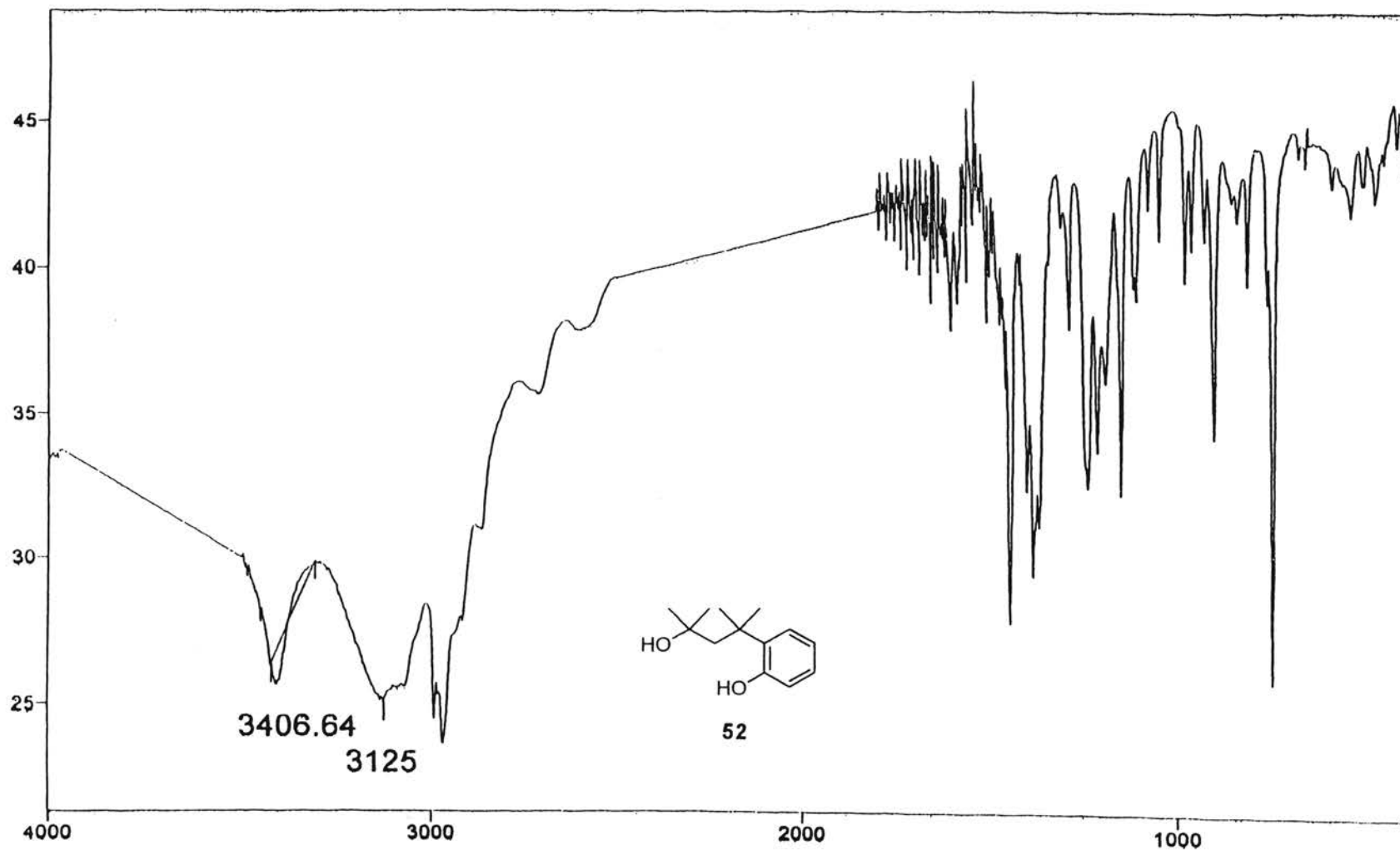
exptl std13c

SAMPLE		DEC. & VT	
date	Apr 11 2001	dfrq	300.087
solvent	CDCl3	dn	M1
file	exp	dpwr	34
ACQUISITION		dof	0
sfrq	75.464	dm	yyy
tn	C13	dsm	w
at	0.800	daf	11764
np	30016	PROCESSING	
sw	18761.7	lb	1.00
fb	10400	wtfile	
bs	16	proc	ft
tpwr	52	fn	not used
pw	3.8	werr	
d1	1.000	wexp	wft
tof	0	wbs	wft
nt	1024	wnt	
ct	1024		
alock	s		
gain	not used		
FLAGS			
il	n		
ln	y		
dp	y		
DISPLAY			
sp	-629.9		
wp	14298.9		
vs	140		
sc	0		
wc	250		
hzmm	57.20		
ls	500.00		
rfl	1836.9		
rfp	0		
th	20		
lms	100.000		
nm	no	ph	



¹³C NMR Spectrum of 50b

Plate LXVI

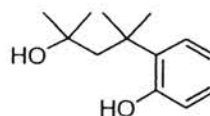


IR Spectrum of 52

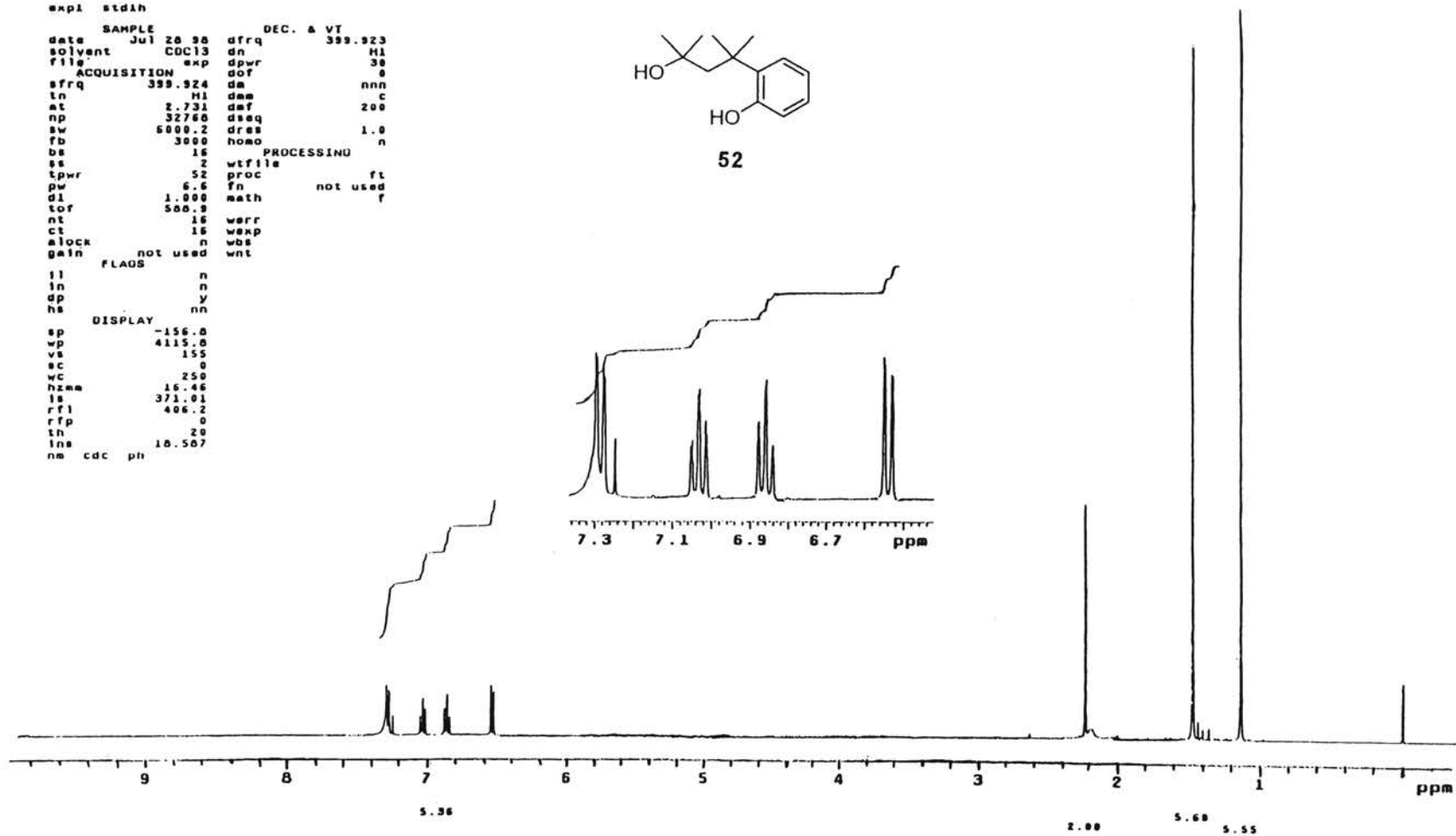
Plate LXVII

```

Std. 1H Inova400
expl std1h
SAMPLE
date Jul 20 98
solvent CDCl3
file exp
ACQUISITION
sfrq 399.924
ln H1
at 2.731
np 32760
aw 5000.2
fb 3000
bs 16
ss 2
tpwr 52
pw 6.6
dl 1.000
tor 500.8
nt 16
ct 15
alock n
gain not used
wnt
DEC. & VT
dfrq 399.923
dn H1
dpwr 30
dof 0
dm nnn
dmf 200
dseq
dres 1.0
homo n
PROCESSING
wtfile
proc ft
fn not used
math f
werr
wexp
wbs
wnt
FLAGS
ij n
ln n
dp y
hs nn
DISPLAY
sp -156.0
wp 4115.0
vs 155
sc 0
wc 250
hzmm 16.46
ls 371.01
rf1 406.2
rfp 0
lh 20
lms 18.507
nm cdc pli
  
```



52



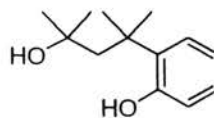
¹H NMR Spectrum of 52

GAMMA-H2 TEST
USE 1 WATT DECOUPLING

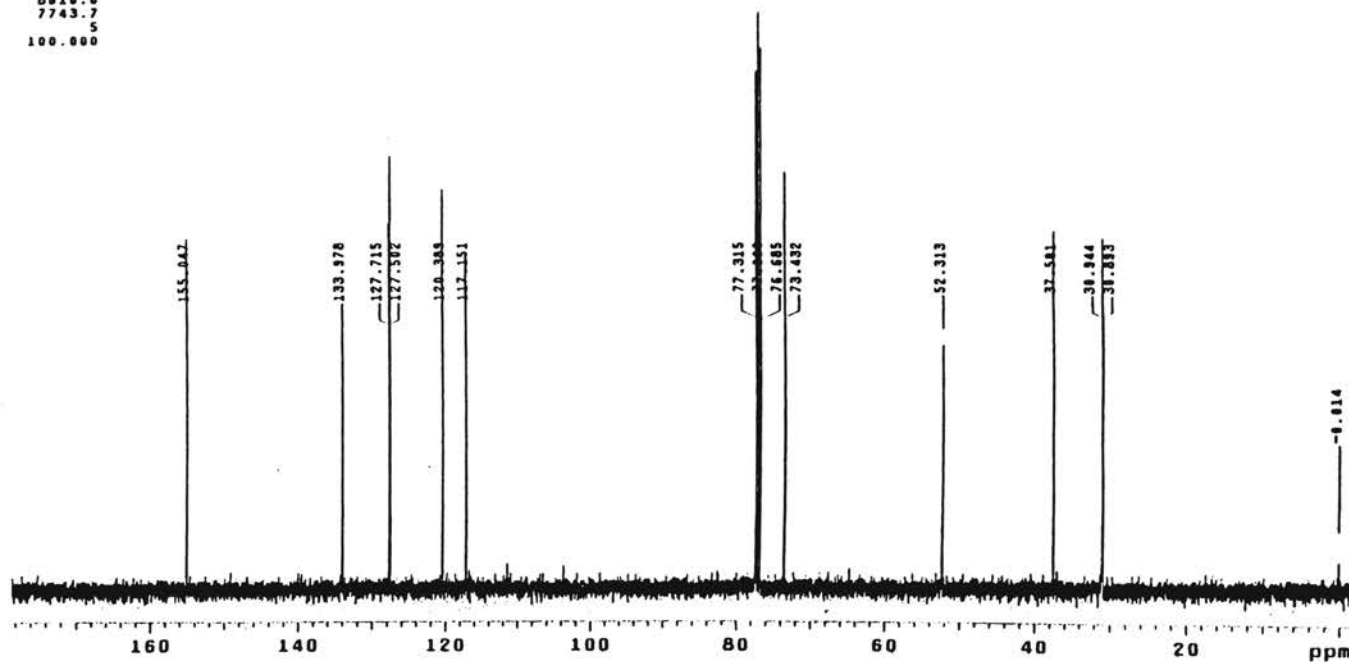
```

expl s2pul
SAMPLE
date Jul 28 98 dn H1
solvent CDCl3 dof 0
file exp dm nny
ACQUISITION dmw w
sfrq 100.571 dmf 9150
tn C13 dpwr 40
at 1.983 PROCESSING
np 95744 lb 0.50
sw 24140.0 fn 65536
fb 13000 math 1
bs 16
pw 4.9 verr
px 4.9 wexp wft
tpwr 51 wbs wft
d1 1.000 wnt
tof 1711.4 DISPLAY
nt 256 sp -250.5
ct 256 wp 10209.4
alock n vs 100
gain 44 sc 0
FLAGS wc 200
il n hzmm 91.05
in n ls 500.00
dp y rfl 8618.0
hs nn rfp 7743.7
th 5
ins 100.000
na ph
  
```

Plate LXVIII

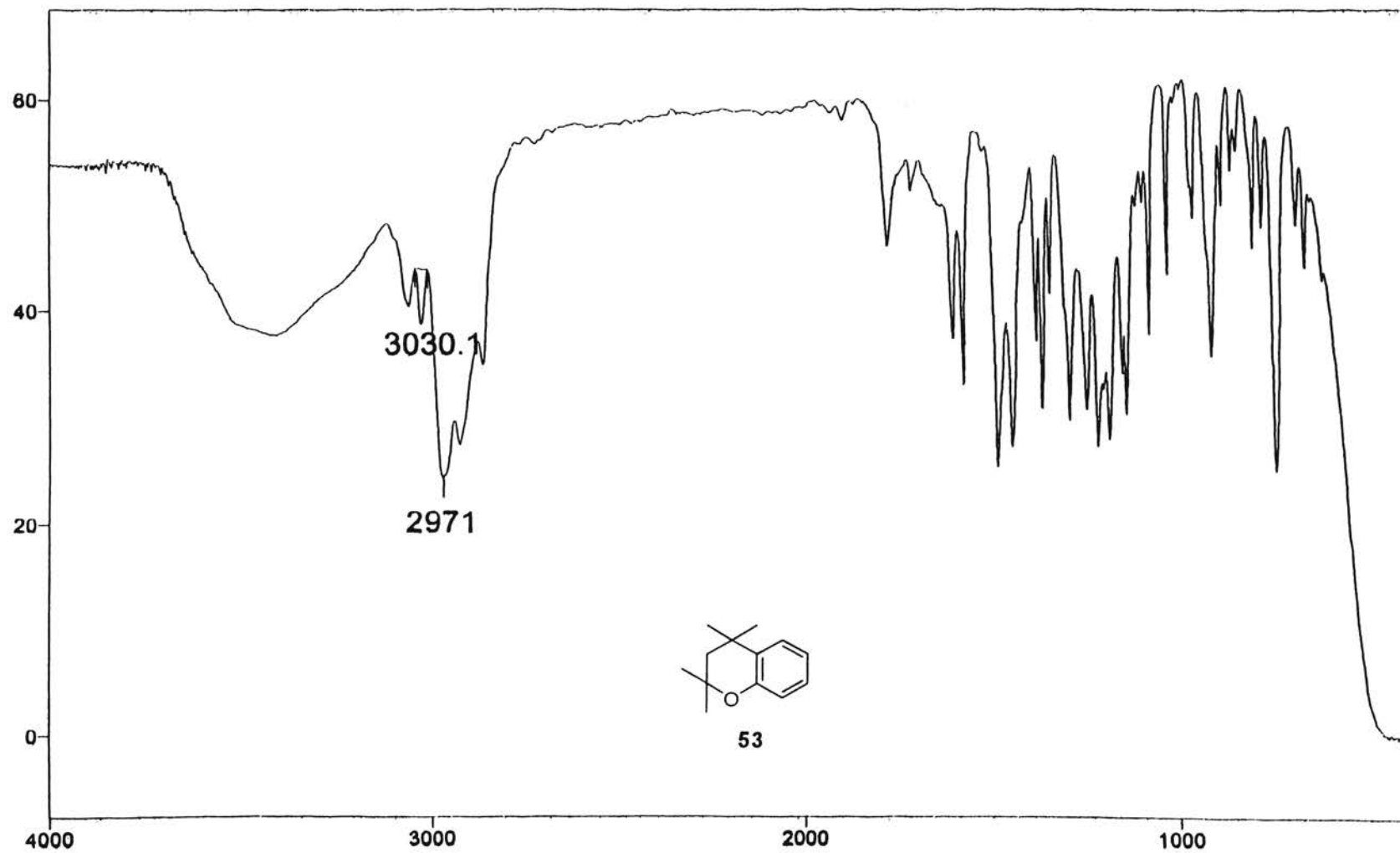


52



¹³C NMR Spectrum of 52

Plate LXIX



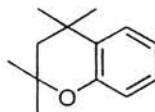
IR Spectrum of 53

Plate LXX

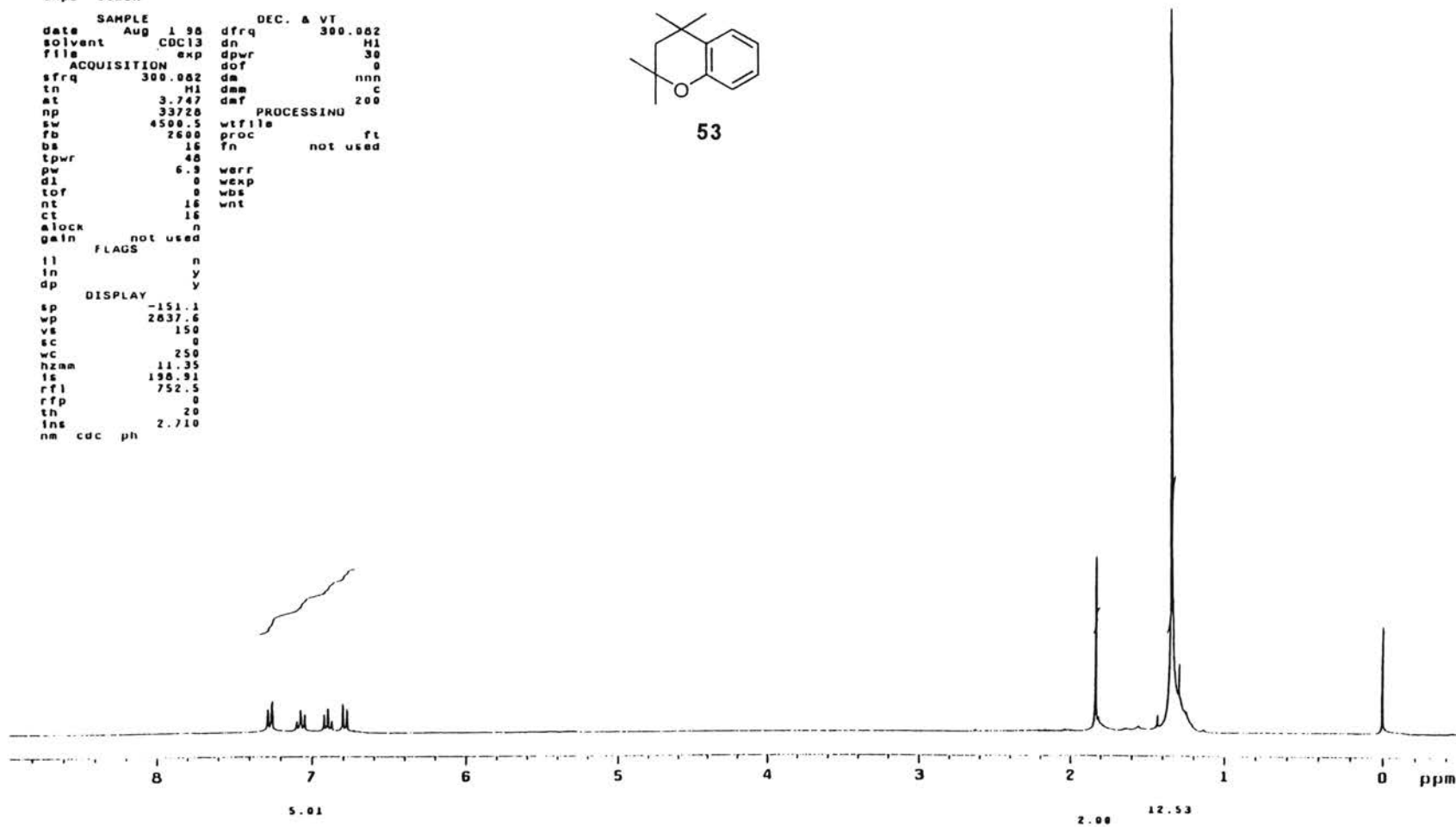
STANDARD IN OBSERVE

```

expl stdih
SAMPLE
date Aug 1 98 dfrq 300.082
solvent CDC13 dn H1
file exp dpwr 30
ACQUISITION dof 0
sfrq 300.082 dm nnn
tn H1 dm c
at 3.747 dmf 200
np 33728 PROCESSING
sw 4500.5 wf file
fb 2600 proc ft
bs 16 fn not used
tpwr 48
pw 6.3 werr
dl 0 wexp
tof 0 wds
nt 16 wnt
ct 16
alock n
gain not used
FLAGS
ll n
ln y
dp y
DISPLAY
sp -151.1
wp 2837.6
vs 150
sc 0
wc 250
hzmm 11.35
ls 198.91
rtl 752.5
rfp 0
th 20
lms 2.710
nm cdc ph
    
```



53



¹H NMR Spectrum of 53

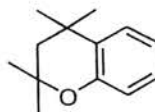
Plate LXXI

13C OBSERVE

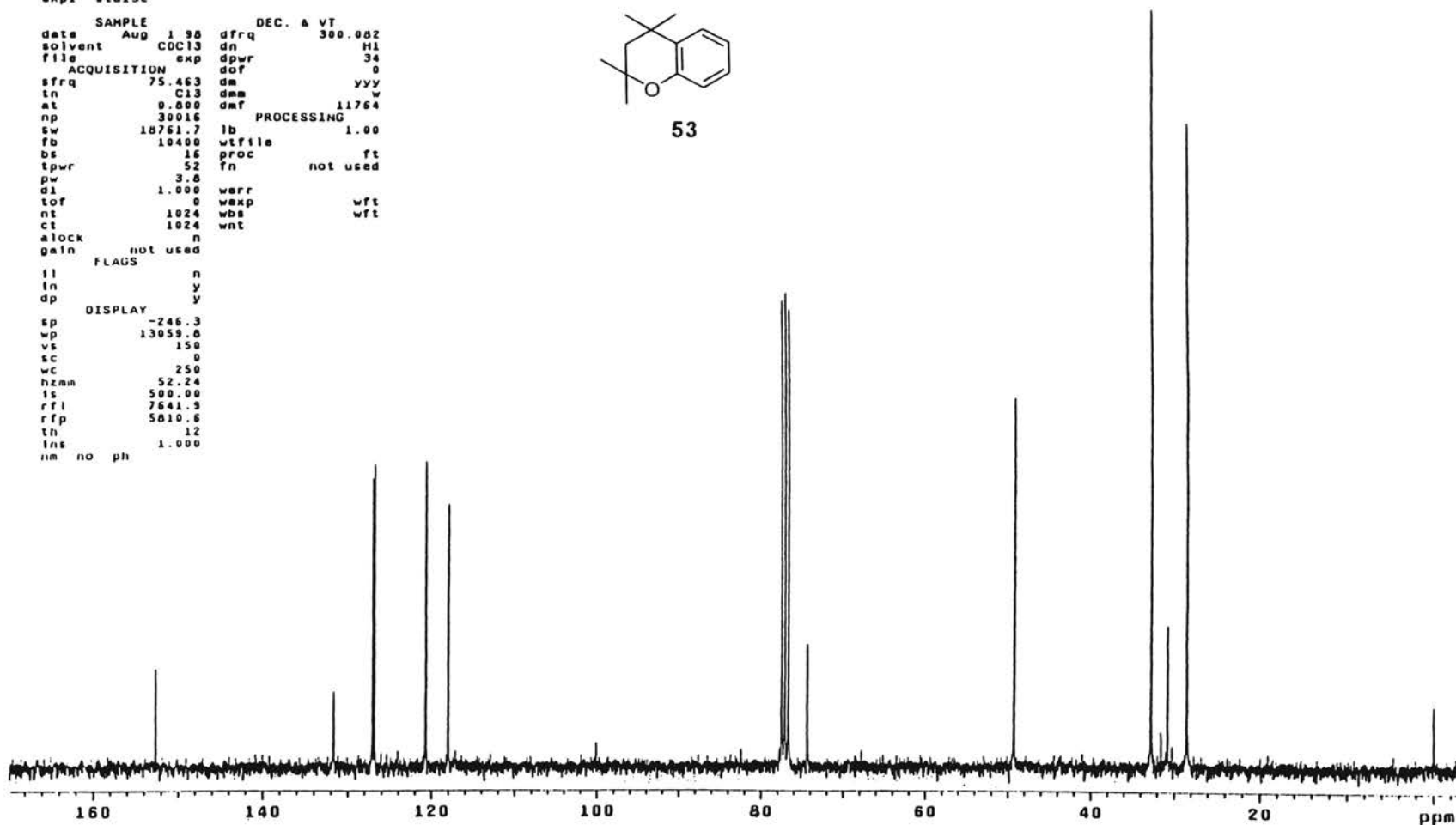
expl std13c

```

SAMPLE          DEC. & VT
date Aug 1 98   dfrq 300.082
solvent CDC13   dn      H1
file exp       dpwr 34
ACQUISITION    dof 0
sfrq 75.463    dm  yyy
in C13         dm  w
at 0.000       dmf 11764
np 30016       PROCESSING
sw 18761.7     lb 1.00
fb 10400       vlfile
ds 16          proc ft
tpwr 52        fn  not used
pw 3.0
d1 1.000       verr
tof 0          wexp wft
nt 1024        wbs wft
ct 1024        wnt
alock n
gain not used
FLAGS n
il n
in y
dp y
DISPLAY
sp -246.3
wp 13053.0
vs 150
sc 0
wc 250
hzmn 52.24
is 500.00
rfl 7641.3
rfp 5810.6
th 12
ins 1.000
nm no ph
    
```

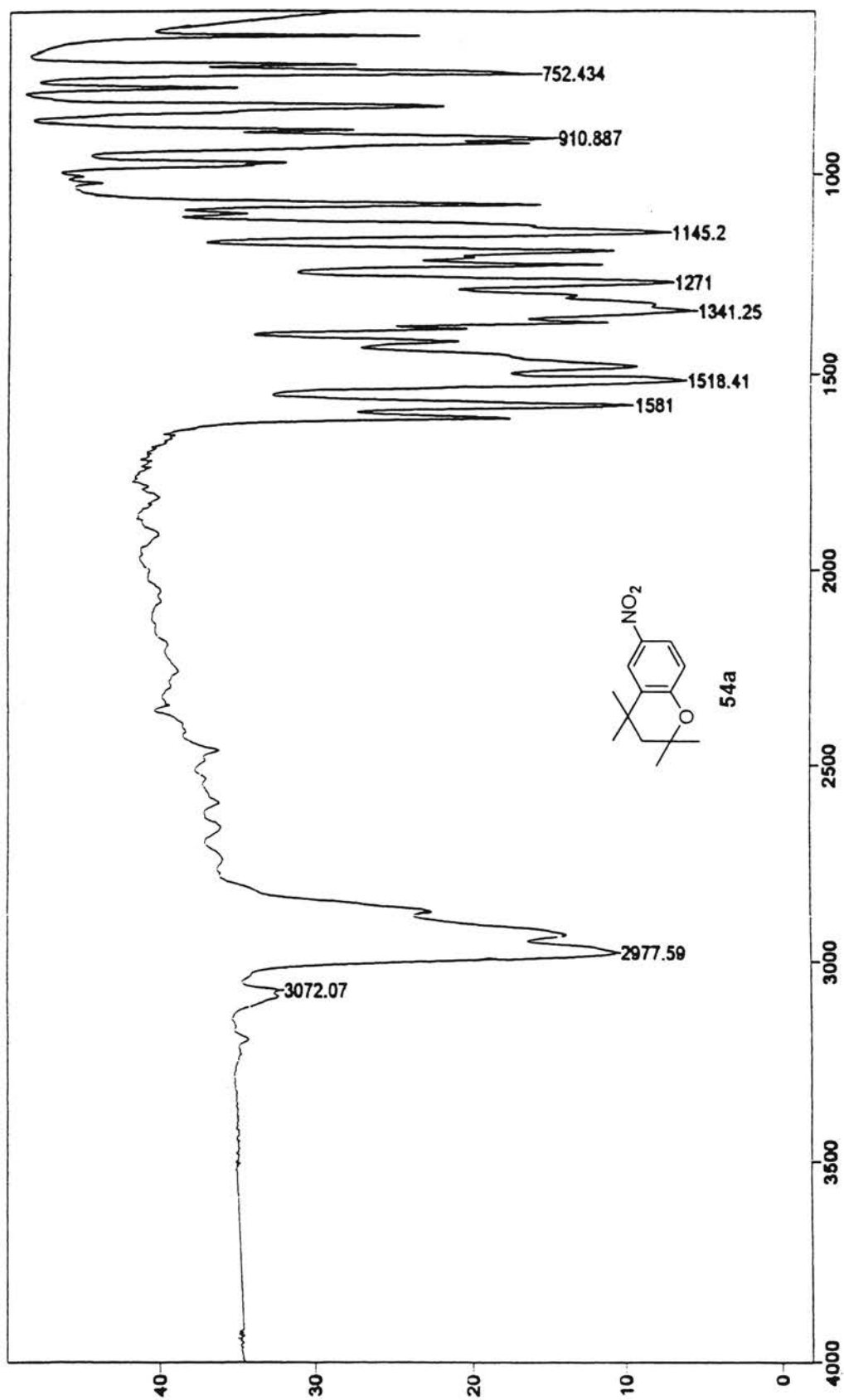


53



¹³C NMR Spectrum of 53

Plate LXXII



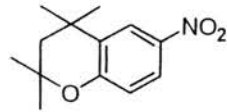
IR Spectrum of 54a

Plate LXXIII

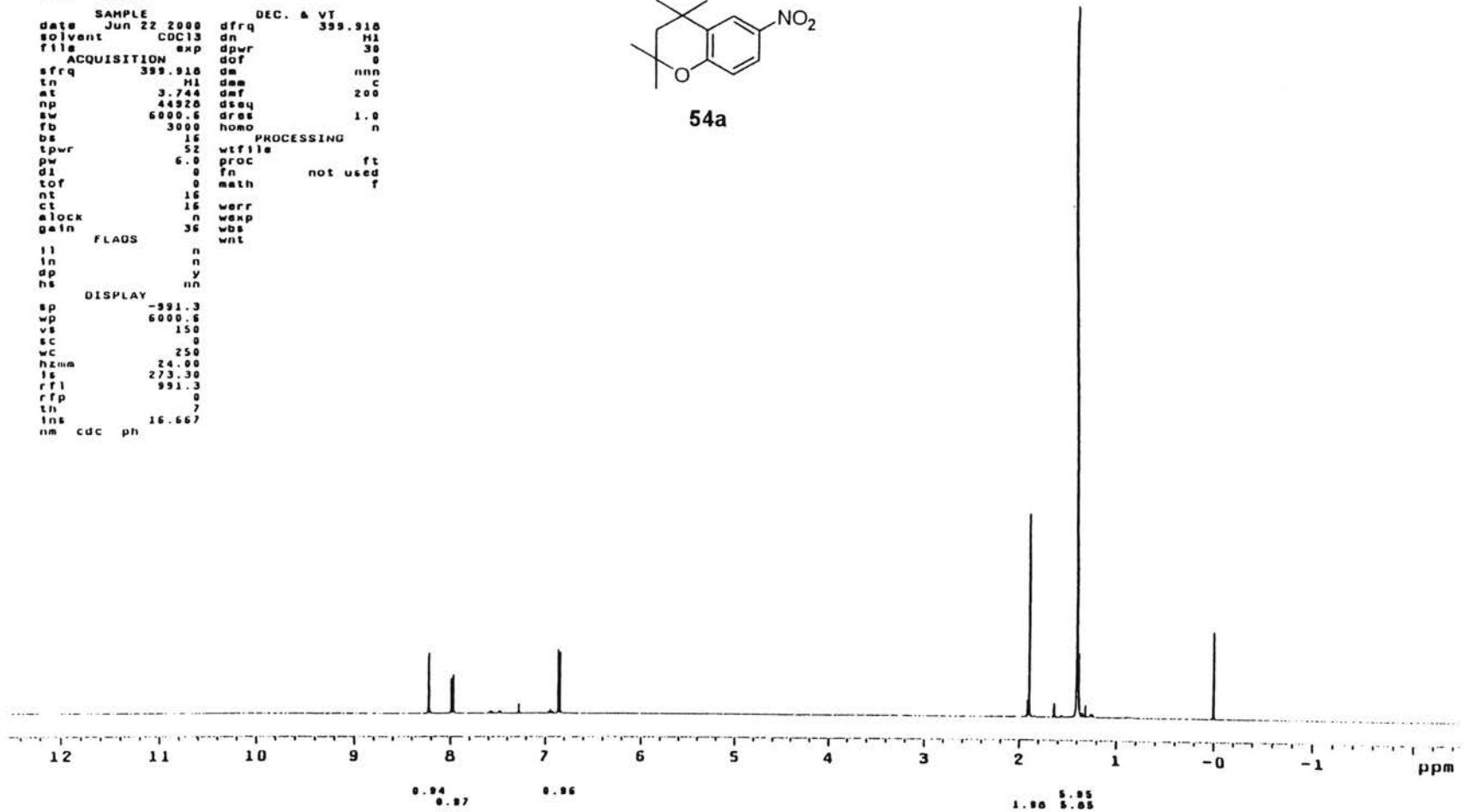
STANDARD 1H OBSERVE

```

expt std1h
SAMPLE
date Jun 22 2000 dfrq DEC. & VT 399.916
solvent CDC13 dn H1
file exp dpwr 30
ACQUISITION dof 9
sfrq 399.916 dm nnn
tn H1 dam c
at 3.744 daf 200
np 44926 dseq 1.0
aw 6000.6 drss
fb 3000 homo n
bs 16 PROCESSING
tpwr 52 wtfile
pw 6.0 proc ft
dl 0 fn not used
tof 0 math f
nt 16
ct 16 werr
alock n wexp
gain 36 vbs
          vnt
          n
          n
          y
          nn
DISPLAY
sp -991.3
wp 6000.6
vs 150
sc 0
wc 250
hzmm 24.00
ls 273.30
rf1 991.3
rfp 0
th 7
ins 16.667
nm cdc ph
  
```



54a



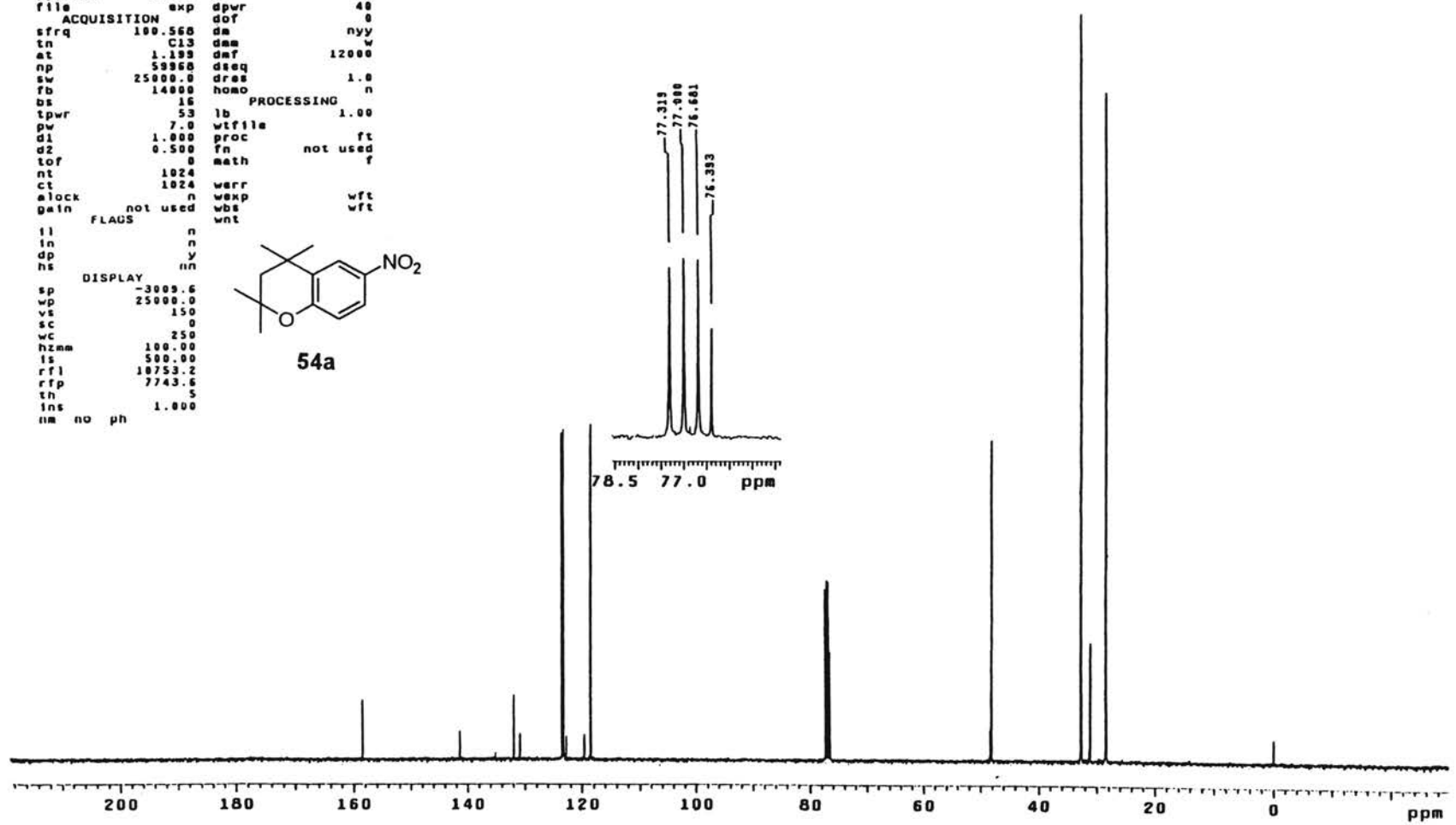
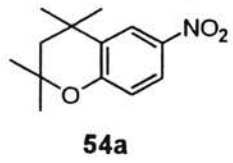
¹H NMR Spectrum of 54a

Plate LXXIV

13C OBSERVE

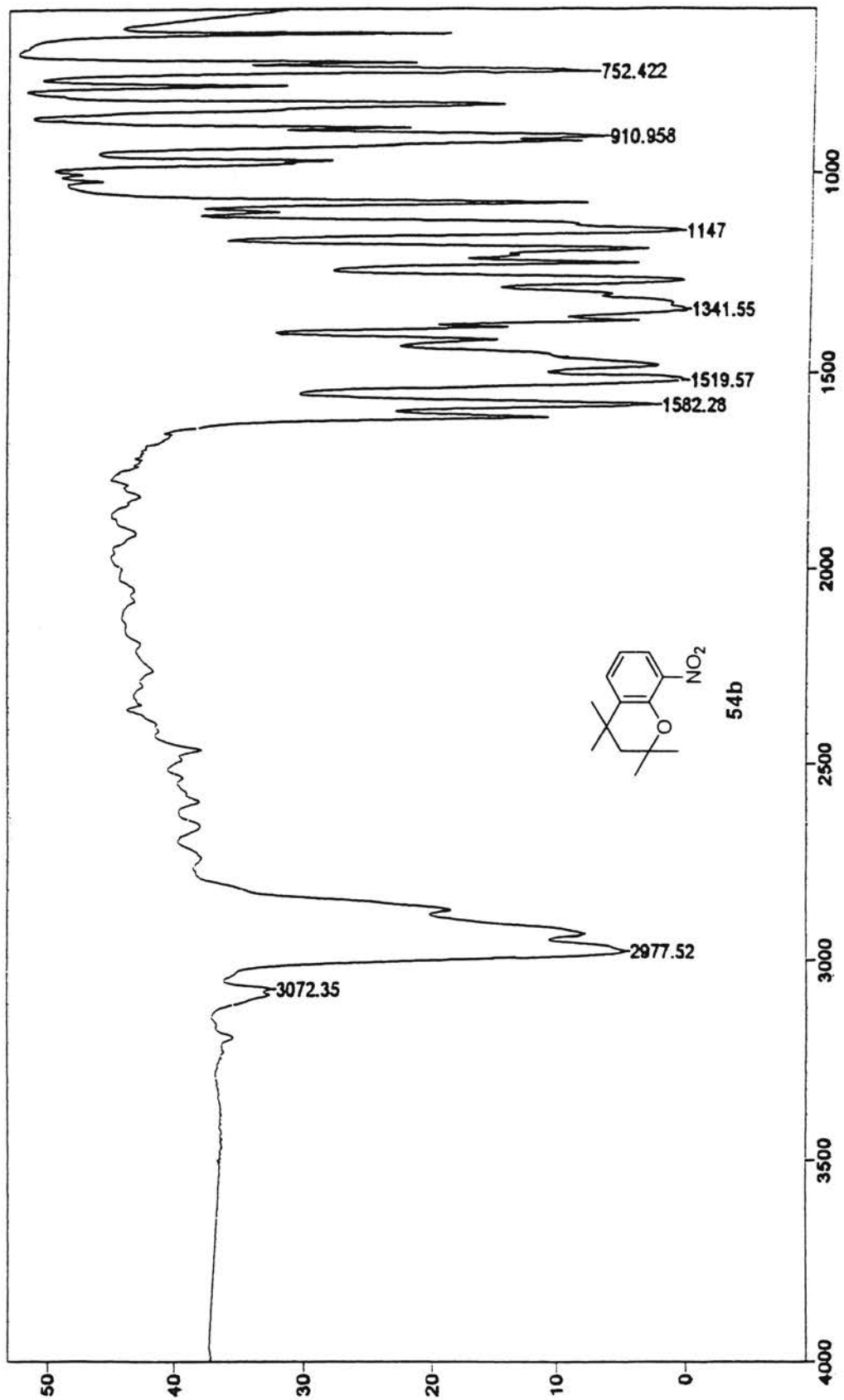
```

expl std13c
SAMPLE
data Jun 22 2000 dfrq DEC. & VT 399.910
solvent CDC13 dn M1
file exp dpwr 40
ACQUISITION
sfrq 100.560 dm nuy
tn C13 dsm w
at 1.199 dmf 12000
np 59960 dseq
sw 25000.0 dres 1.0
fb 14000 homo n
bs 16
tpwr 53 lb PROCESSING 1.00
pw 7.0 wf file
d1 1.000 proc ft
d2 0.500 fn not used f
tof 0 math
nt 1024
ct 1024
alock n werr wft
gain not used wexp wft
wbs wft
wnt
FLAGS n
in n
dp y
hs nn
DISPLAY
sp -3009.6
wp 25000.0
vs 150
sc 0
wc 250
hzmm 100.00
ls 500.00
rfl 10753.2
rfp 7743.6
th 5
ins 1.000
nm no ph
    
```



¹³C NMR Spectrum of 54a

Plate LXXV



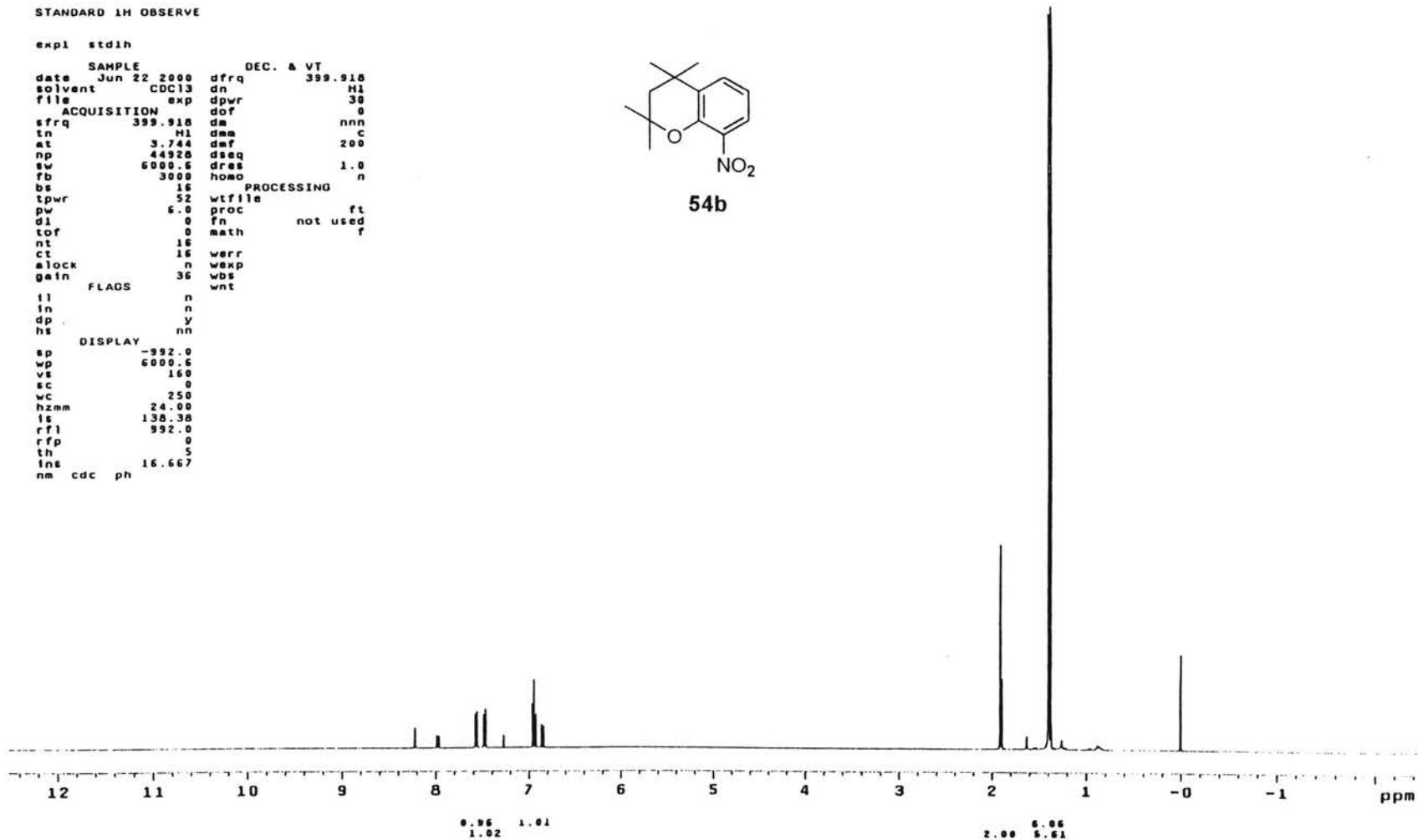
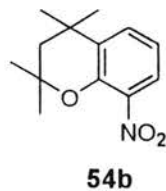
IR Spectrum of 54b

Plate LXXVI

STANDARD 1H OBSERVE

```

expl stdih
SAMPLE
date Jun 22 2000 dfrq DEC. & VT 399.918
solvent CDC13 dn H1
file exp dpwr 30
ACQUISITION dof 0
sfrq 399.918 dm nnn
tn H1 dsm C
at 3.744 daf 200
np 44928 dseq
sw 6000.6 dres 1.0
fb 3000 homo n
bs 16 PROCESSING
tpwr 52 wtfila
pw 6.0 proc ft
d1 0 fn not used
tof 0 math f
nt 16
ct 16 werr
alock n wexp
gain 36 wbs
FLAGS wnt
il n
in n
dp y
hs nn
DISPLAY
sp -992.0
wp 6000.6
vs 160
sc 0
wc 250
hzmm 24.00
fs 138.38
rfl 992.0
rfp 0
th 5
lnE 16.667
nm cdc ph
    
```



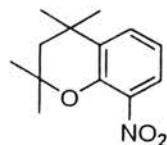
¹H NMR Spectrum of 54b

Plate LXXVII

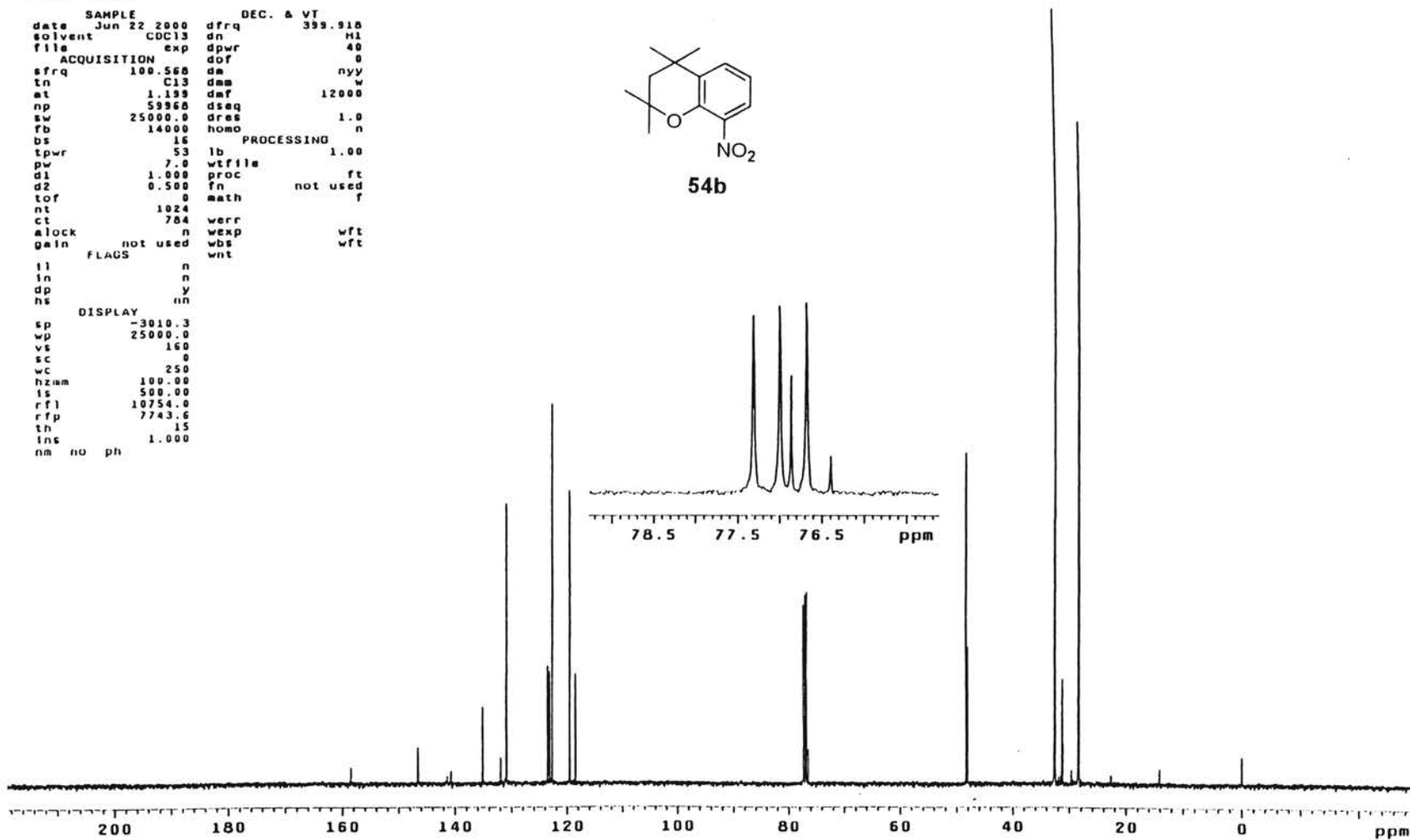
¹³C OBSERVE

expl std13c

date	SAMPLE	DEC. & VT	
Jun 22 2000		399.918	
solvent	CDC13	dn	H1
file	exp	dpwr	40
	ACQUISITION	dof	0
sfrq	100.568	dm	nyy
tn	C13	dmm	w
at	1.139	daf	12000
np	59368	dseq	
sw	25000.0	dres	1.0
fb	14000	homo	n
bs	16	PROCESSING	
tpwr	53	lb	1.00
pw	7.0	wtfile	
d1	1.000	proc	ft
d2	0.500	fn	not used
tof	0	math	f
nt	1024		
ct	784	verr	
alock	n	wexp	wft
gain	not used	wbs	wft
	FLAGS	wnt	
il	n		
in	n		
dp	y		
hs	nn		
	DISPLAY		
sp	-3010.3		
wp	25000.0		
vs	160		
sc	0		
wc	250		
hz/mm	100.00		
is	500.00		
rfl	10754.0		
rfp	7743.6		
th	15		
ins	1.000		
nm	no	ph	

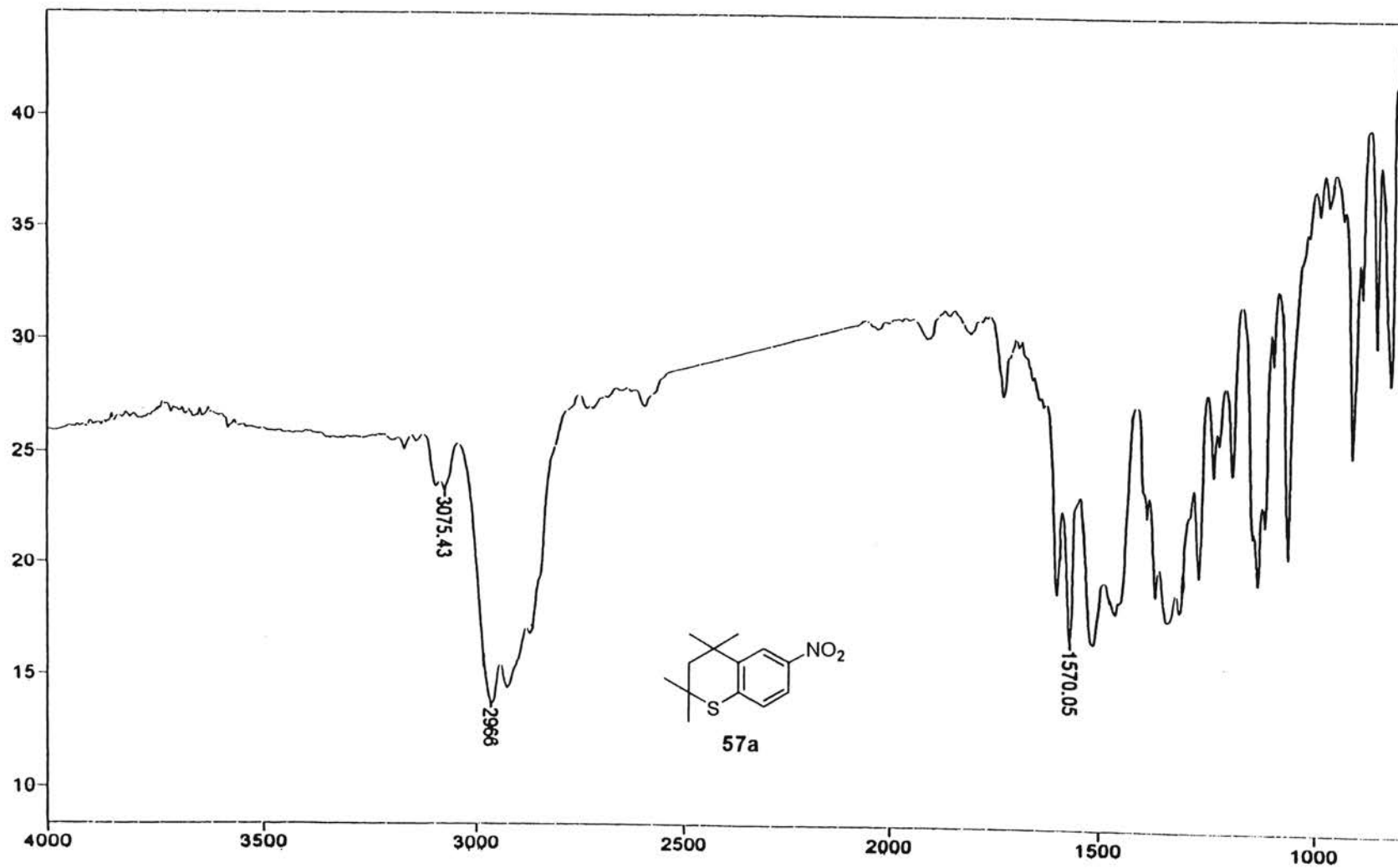


54b



¹³C NMR Spectrum of 54b

Plate LXXVIII



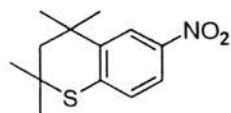
IR Spectrum of 57a

Plate LXXIX

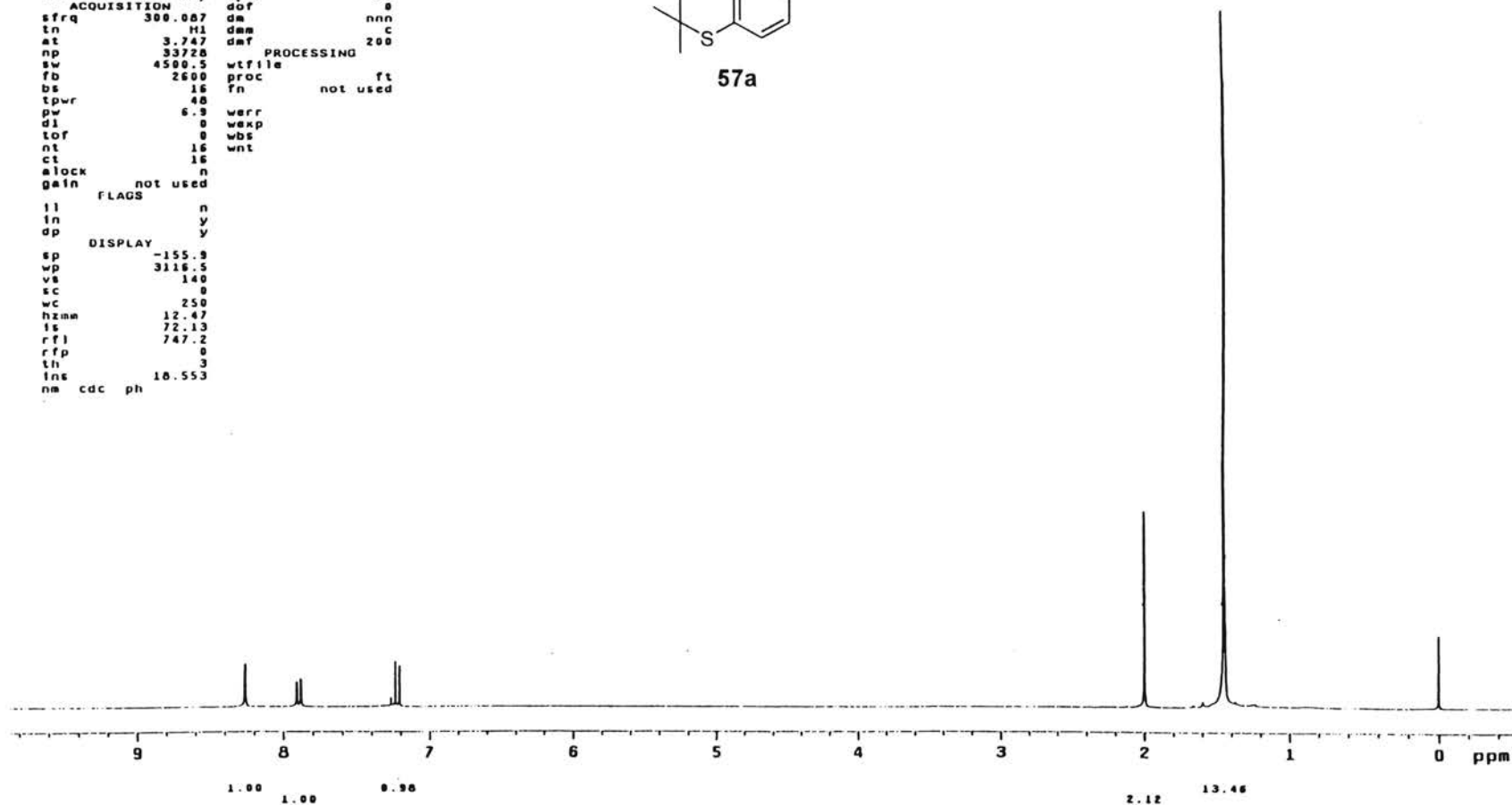
6-nitrothiophene

expl stdih

date	Apr 16 2001	dfrq	DEC. & VT	300.087
solvent	CDC13	dn	H1	
file	exp	dpwr	30	
ACQUISITION				
sfrq	300.087	da	0	
tn	H1	dsm	nnn	
at	3.747	dwt	200	
np	33728	PROCESSING		
sw	4500.5	wtfile		
fb	2600	proc	ft	
bs	16	fn	not used	
tpwr	48	warr		
pw	6.9	wexp		
dl	0	wbs		
tof	0	wnt		
nt	16			
ct	16			
alock	n			
gain	not used			
FLAGS				
ll	n			
ln	y			
dp	y			
DISPLAY				
sp	-155.8			
wp	3116.5			
vs	140			
sc	0			
wc	250			
hzmm	12.47			
ls	72.13			
rfl	747.2			
rtp	0			
th	3			
lms	18.553			
nm	cdc	ph		



57a



¹H NMR Spectrum of 57a

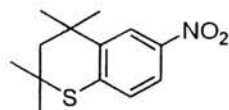
Plate LXXX

6-nitrothiochroman

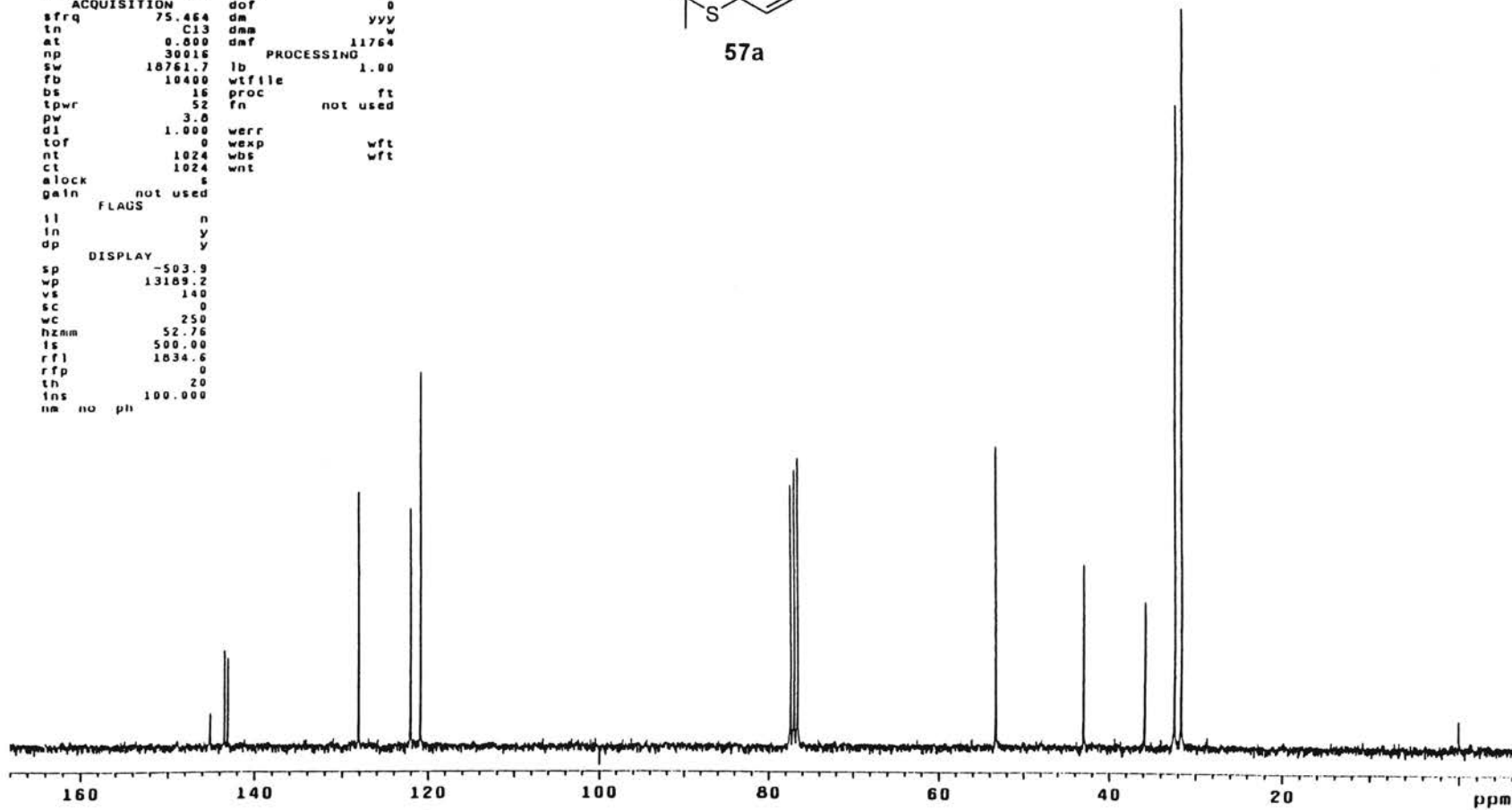
expt std13c

```

SAMPLE          DEC. & VT
date Apr 16 2001 dfrq      300.087
solvent CDC13    dn        M1
file          exp dpwr      34
ACQUISITION    dof        0
sfrq          75.464  dm      yyy
ln            C13  dnm      w
at           0.800  daf      11764
np           30015  PROCESSING
sw          18761.7 lb        1.00
fb           10400  wifile
bs           16    proc      ft
tpwr         52    fn        not used
pw           3.8
d1           1.000  werr
tof          0     wexp      wft
nt           1024  wds      wft
cl           1024  wnt
elock        s
gain         not used
FLAUS
ll           n
ln           y
dp           y
DISPLAY
sp          -503.9
wp          13109.2
vs           140
sc           0
wc           250
hznm        52.76
ls           500.00
rf1         1834.6
rfp          0
th           20
ins         100.000
nm no ph
    
```

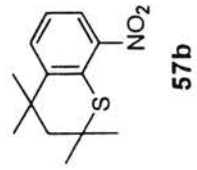
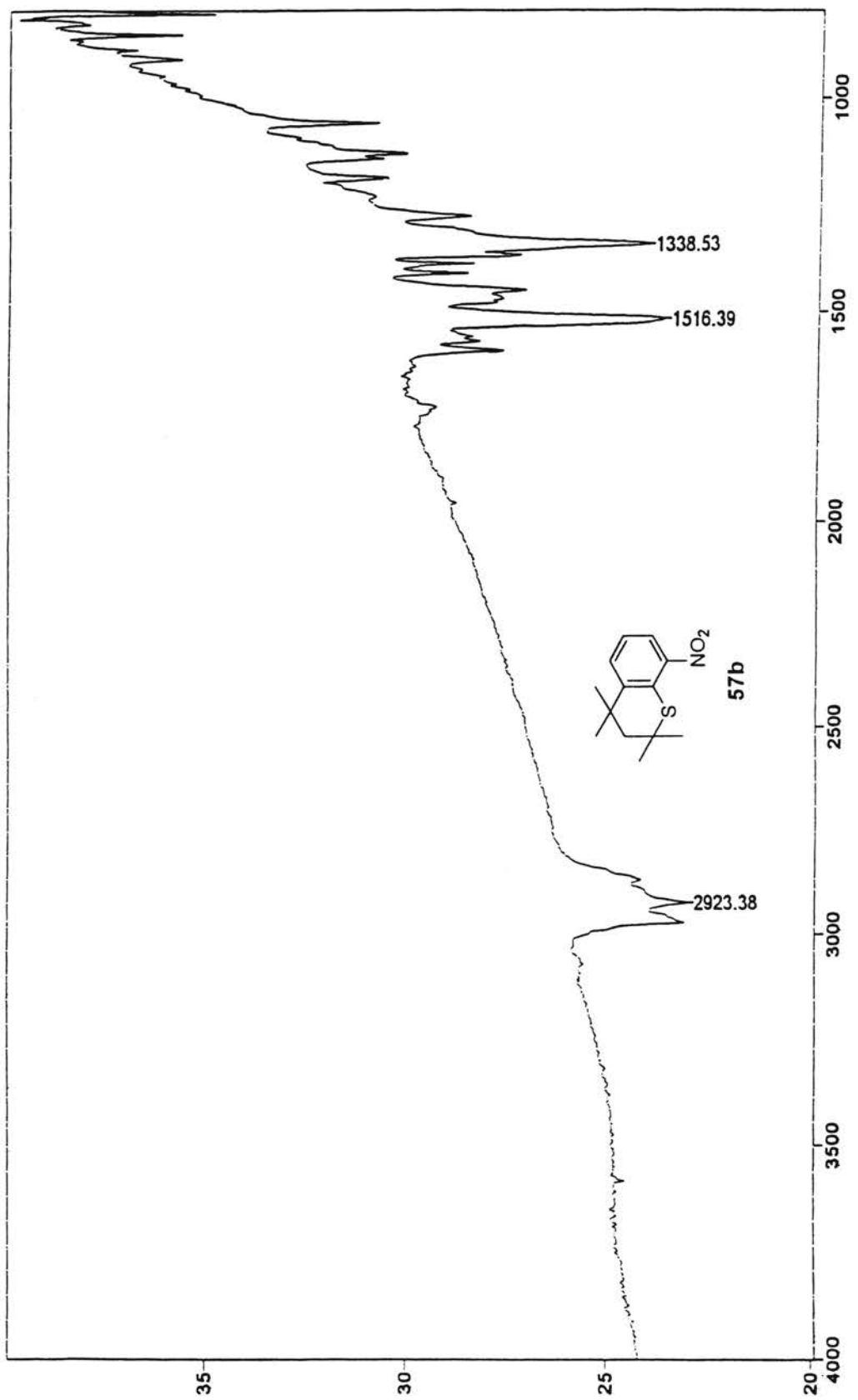


57a



¹³C NMR Spectrum of 57a

Plate LXXXI



IR Spectrum of 57b

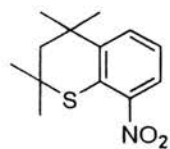
Plate LXXXII

8-nitrothiochroman

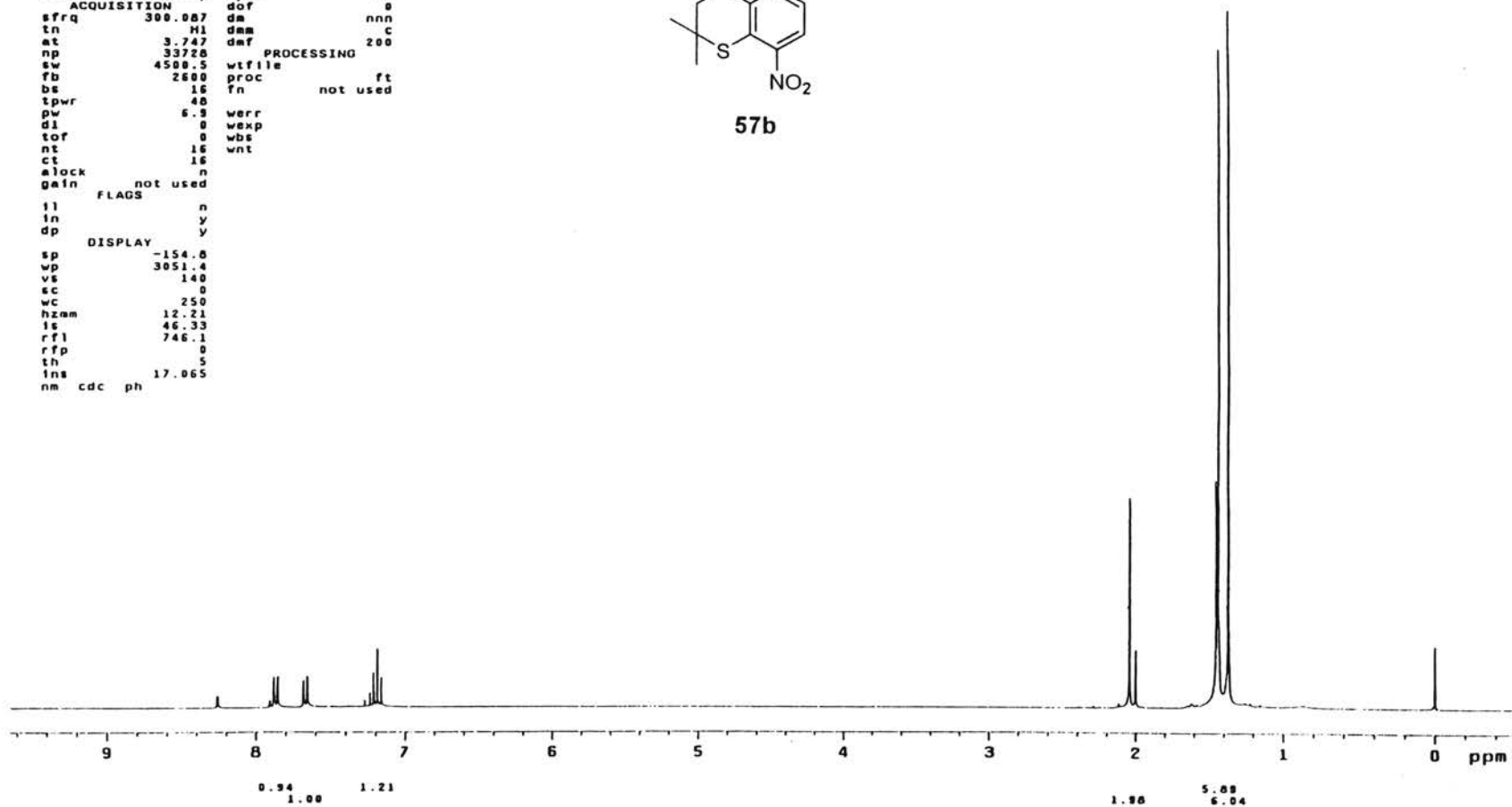
expl stdih

```

SAMPLE          DEC. & VT
date Apr 16 2001 dfrq          300.087
solvent CDCl3   dn             H1
file          exp dpwr         30
ACQUISITION    dof            0
sfrq          300.087 dm         nnn
tn            H1  dam          200
at            3.747 dmf
np            33728
sw            4588.5 wtfila
fb            2600  proc        ft
bs            16    fn         not used
tpwr          48
pw            6.9  werr
di            0    wexp
tof           0    wbs
nt            16  wnt
ct            16
alock         n
gain          not used
FLAGS
il            n
in            y
dp            y
DISPLAY
sp            -154.8
wp            3051.4
vs            140
sc            0
wc            250
hzm          12.21
ls            46.33
rf1           746.1
rfp           0
th            5
fns           17.065
nm cdc ph
    
```



57b



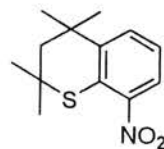
¹H NMR Spectrum of 57b

Plate LXXXIII

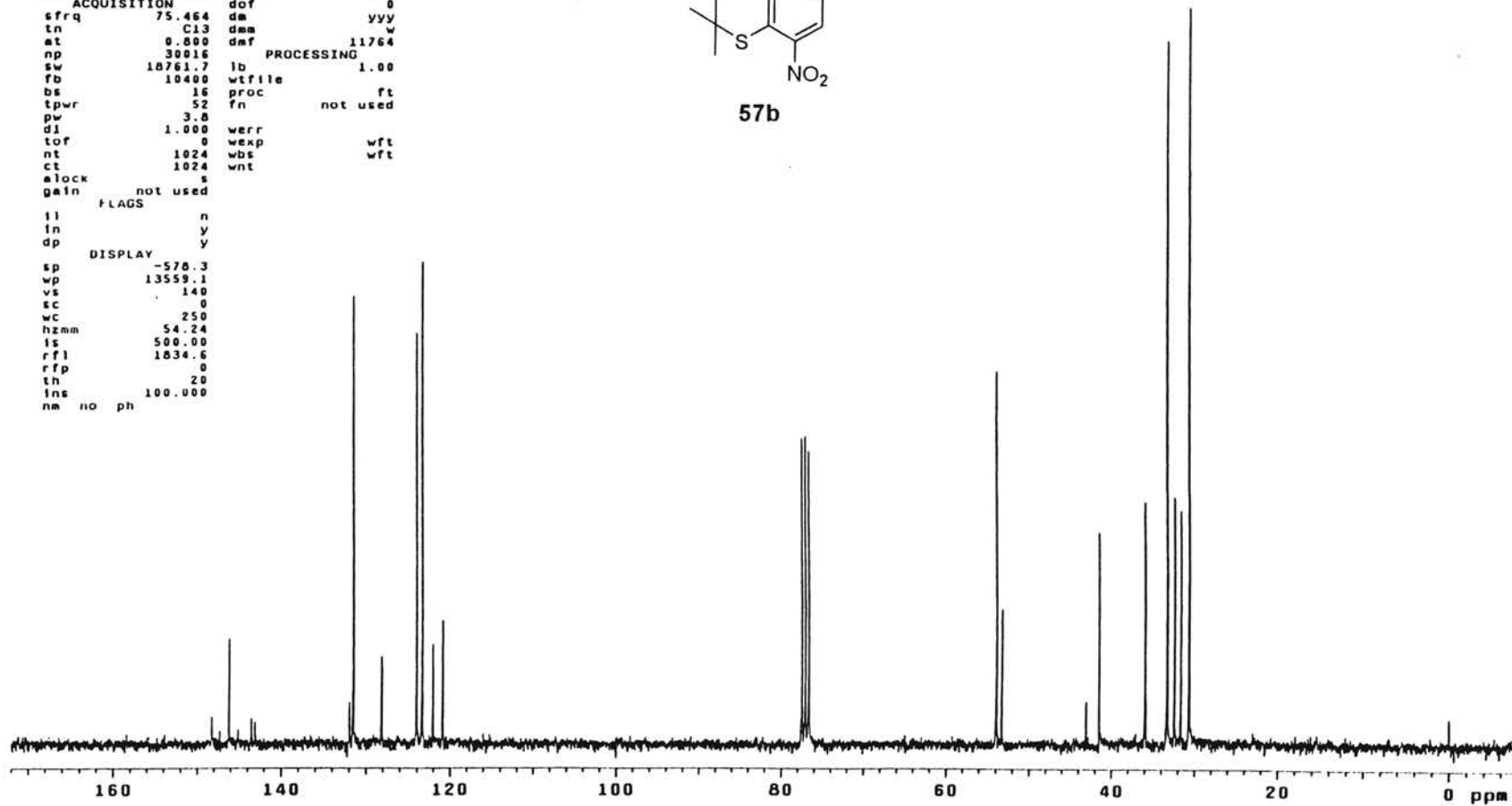
8-nitrothiochroman

exptl std13c

SAMPLE		DEC. & VT	
date	Apr 16 2001	dfrq	300.087
solvent	CDC13	dn	H1
file	exp	dpwr	34
ACQUISITION		dot	0
sfrq	75.464	dm	yyy
tn	C13	dma	w
at	0.800	dmf	11764
np	30016	PROCESSING	
sw	18761.7	lb	1.00
fb	10400	wfile	
bs	16	proc	ft
tpwr	52	fn	not used
pw	3.8		
d1	1.000	werr	
tof	0	wexp	wft
nt	1024	wbs	wft
ct	1024	wnt	
alock	s		
gain	not used		
FLAGS			
ll	n		
ln	y		
dp	y		
DISPLAY			
sp	-576.3		
wp	13559.1		
vs	140		
sc	0		
wc	250		
hzmm	54.24		
ls	500.00		
rfl	1834.6		
rfp	0		
th	20		
ins	100.000		
nm	no ph		

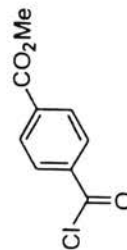
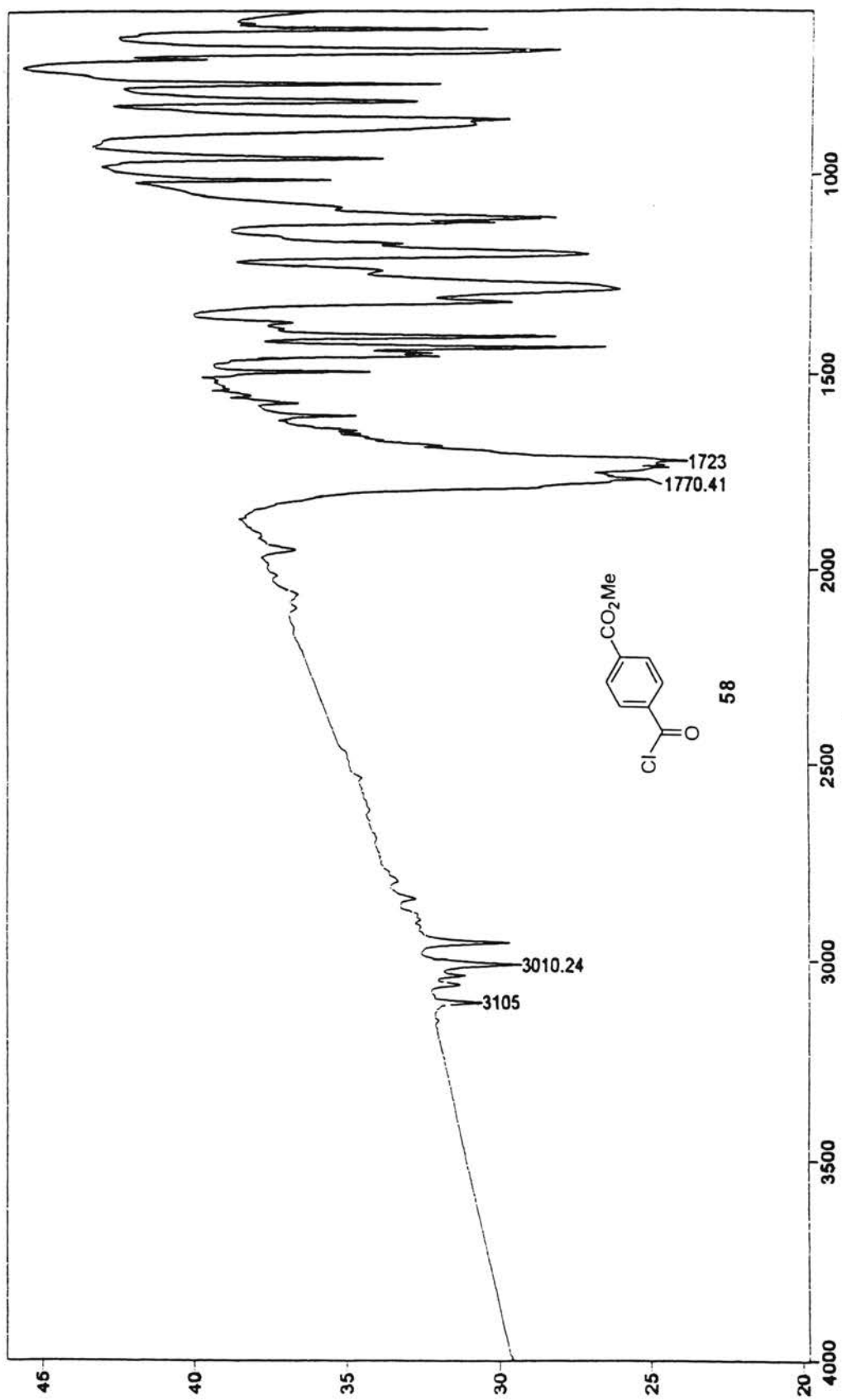


57b



¹³C NMR Spectrum of 57b

Plate LXXXIV



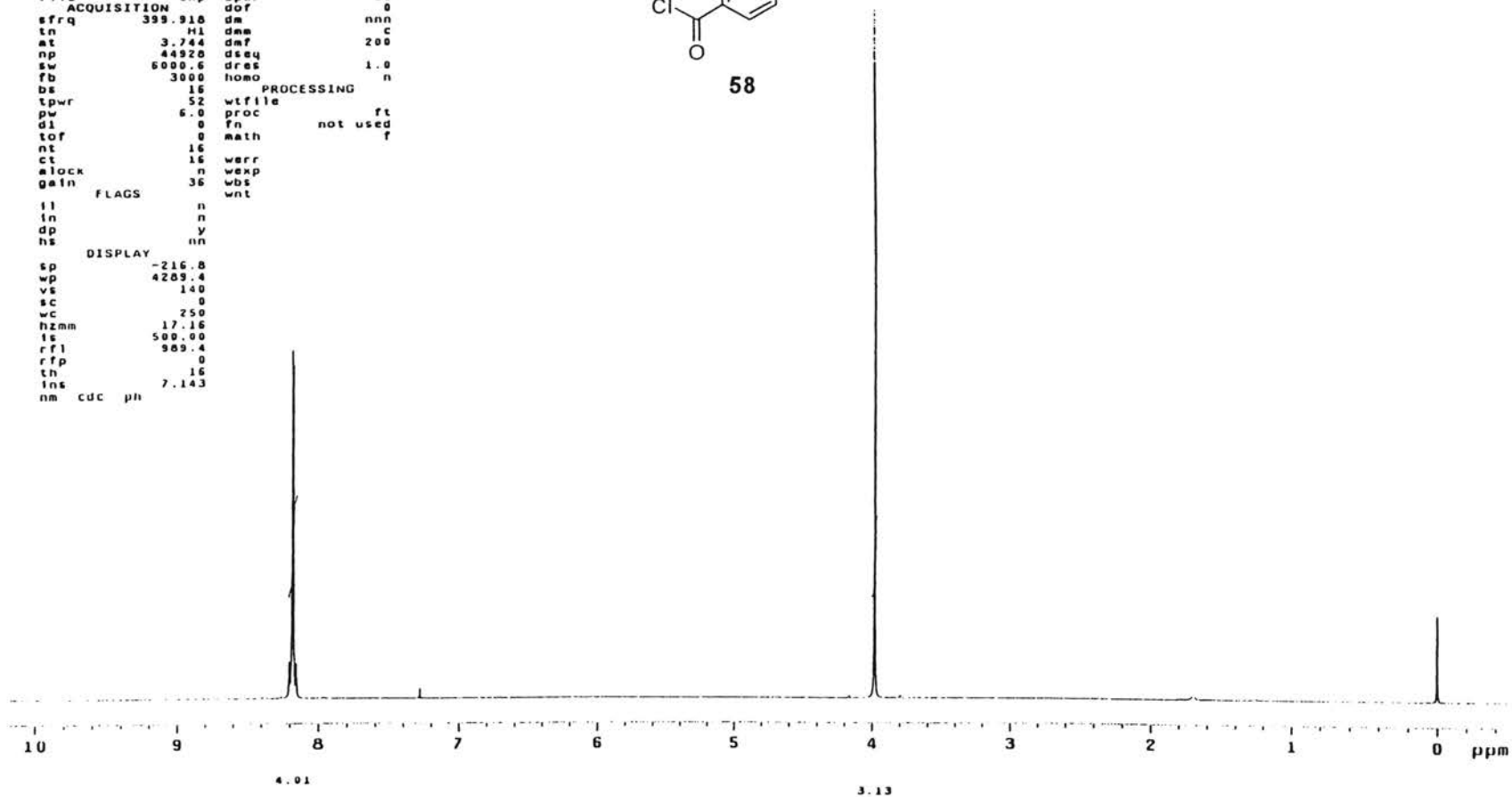
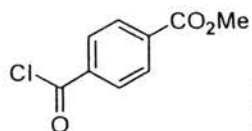
58

IR Spectrum of 58

Plate LXXXV

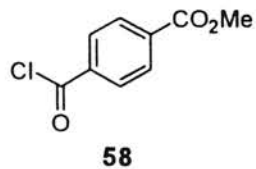
```

actlchlor ide
expl stdin
SAMPLE
date Dec 14 2000 dfrq DEC. & VT 399.918
solvent CDCl3 dn M1
file exp dpwr 30
ACQUISITION
sfrq 399.918 dm nnn
tn H1 dam C
at 3.744 dmf 200
np 44920 dseq 1.0
sw 6000.6 dres n
fb 3000 homo
DS 16
PROCESSING
tpwr 52 wfile
pw 6.0 proc ft
d1 0 fn not used
tof 0 math f
nt 16
ct 16 werr
alock n wexp
gain 36 wbs
wnt
FLAGS
il n
in n
dp y
hs nn
DISPLAY
sp -216.8
wp 4209.4
vs 140
sc 0
wc 250
hzmm 17.16
is 500.00
rfl 909.4
rfp 0
th 16
ins 7.143
nm cdc ph
    
```



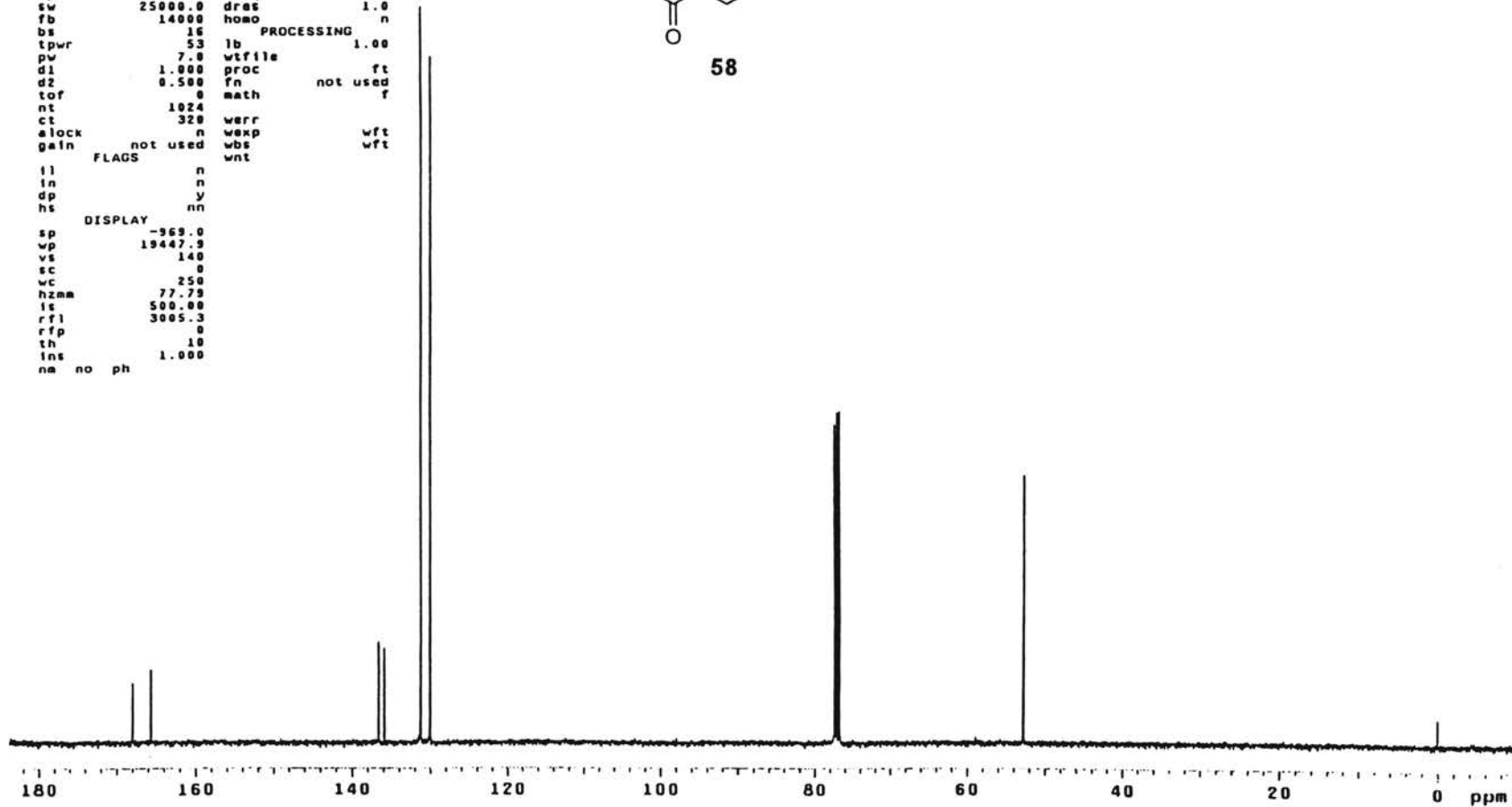
¹H NMR Spectrum of 58

Plate LXXXVI



```

expl std13c
SAMPLE
date Dec 14 2000 dfrq DEC. & VT 300.110
solvent CDCl3 dn HI
file exp dpwr 40
ACQUISITION
sfrq 100.568 dm nvy
tn C13 dnm w
at 1.199 dmf 12000
np 59368 dseq
sw 25000.0 dret 1.0
fb 14000 homo n
bs 16 PROCESSING
tpwr 53 lb 1.00
pw 7.0 wtfile
d1 1.000 proc ft
d2 0.500 fn not used
tof 0 math f
nt 1024
ct 320 werr
alock n wexp wft
gain not used wbs wft
FLAGS wnt
il n
in n
dp y
hs nn
DISPLAY
sp -969.0
wp 19447.9
vs 140
sc 0
wc 250
hzma 77.79
is 500.00
rfl 3005.3
rfp 0
th 10
ins 1.000
na no ph
    
```



¹³C NMR Spectrum of 58

BIBLIOGRAPHY

1. Sporn, M. B.; Roberts, A. B. In *The Retinoids-Biology, Chemistry, and Medicine*, 2nd Ed., Raven Press Ltd.: New York, 1994, pp 1-3.
2. Budd, G. Disorders Resulting from Defective Nutriment. *London Med. Gazette* **1842**, 2, 632-749.
3. (a) Saffiotti, U.; Montesano, R.; Sellakumar, A. R.; Borg, S. A. Experimental Cancer of the Lung. *Cancer* **1967**, 20, 857-864. (b) Chu, E. W.; Malmgren, R. A. An Inhibitory Effect of Vitamin A on the Induction of Tumors of Forestomach and Cervix in the Syrian Hamster by Carcinogenic Polycyclic Hydrocarbons. *Cancer Res.* **1965**, 25, 884-895.
4. Bollag, W.; Ruegg, R.; Ryser, G. (Hoffmann-La Roche, F. und Co., A.-G.)(1974): Polyene Compounds. German Patent 2,414,619 (October 17, 1974); *Chem. Abstr.* **1975**, 82, 111778.
5. Loeliger, P.; Bollag, W.; Mayer, H. Arotinoids, A New Class of Highly Active Retinoids. *Eur. J. Med. Chem.-Chim. Ther.* **1980**, 15, 9-15.
6. (a) Kastner, P.; Mark, M.; Chambon, P. Non Steroid Nuclear Receptors: What are Genetic Studies Telling Us About Their Role in Real Life? *Cell* **1995**, 83, 859-869. (b) Means, A. L.; Gudas, L. J. The Roles of Retinoids in Vertebrate Development. *Annu. Rev. Biochem.* **1995**, 64, 201-233.
7. Wolbach, S. D.; Howe, P. R. Tissue Changes Following Deprivation of Fat Soluble Vitamin A. *J. Exp. Med.* **1925**, 42, 753-761.
8. Lasnitzki, I. The Influence of a Hyper-vitaminosis on the Effect of 3-Methylcholanthrene on Mouse Prostate Glands Grown In Vitro. *Br. J. Cancer* **1955**, 9, 434-441.
9. Itri, L. M.; Moon, R. C. Retinoids and Cancer. *The Retinoids-Biology, Chemistry, and Medicine*, 2nd Ed., Raven Press Ltd.: New York, 1994, pp 357-386.
10. Orfanos, C. E.; Zouboulis, C. C.; Almod-Roesler, B.; Geilen, C. C. Current Use and Future Potential Role of retinoids in Dermatology. *Drugs* **1997**, 53, 358-388.
11. Kligman, D. E.; Kligman, A. M. Use of High Dose Retinoids for the Treatment of Skin Disorders. PCT Int. Appl., 28 pp, WO 9850023 A1 19981112; *Chem. Abstr.* **1998**, 130, 524.

12. Lachgar, S.; Charveron, M.; Gall, Y.; Bonafe, J. L. Inhibitory Effects of Retinoids on Vascular Endothelial Growth Factor Production by Cultured Human Skin Keratinocytes. *Dermatology* (Basel) **1999**, *199* (Suppl. 1), 25-27.
13. Takeuchi, M.; Yano, T.; Omoto, E.; Takahashi, K.; Kibata, M.; Shudo, K.; Harada, M.; Ueda, R.; Ohno, R. Relapsed Acute Promyelocytic Leukemia Previously Treated with All-Trans-Retinoic Acid: Clinical Experience with a New Synthetic Retinoid, Am-80. *Leuk. Lymphoma* **1998**, *31*, 441-451.
14. Munker, R.; Koeffler, P.; Haas, R.; Wilmanns, W. Modulation of CD95 in Leukemia and Lymphoma Cells by Retinoids. *Eur. J. Med. Res.* **2000**, *5*, 273-276.
15. Westarp, M. E. Retinoids in the Management of Central Nervous System (CNS) Tumors. *Adv. Organ Biol.* **1997**, *3*, 231-260.
16. Walmsley, S.; Northfelt, D. W.; Melosky, B.; Conant, M.; Friedman-Kien, A. E.; Wagner, B. Treatment of AIDS-Related Cutaneous Kaposi's Sarcoma with Topical Alitretinoin (9-*cis*-Retinoic Acid) Gel. *J. Acquired Immune Defic. Syndr.* **1999**, *22*, 235-246.
17. Hayes, C. E.; Nashold, F. E.; Gomez, F. E.; Hoag, K. A. Retinoids and Immunity. *Handb. Exp. Pharmacol.* **1999**, *139*, 589-610.
18. Zusi, F. C.; Reczek, P. R.; Ostrowski, J. Preparation of Retinoid-like Compounds as Antitumor and Antiinflammatory Agents. (Bristol-Myers Squibb Company, USA), U. S., 8 pp, US 6008251 A 19991228; *Chem. Abstr.* **1999**, *132*, 35518.
19. Giembycz, M. Retinoids Offer Hope for the Treatment of Emphysema. *Trends Pharmacol. Sci.* **2000**, *21*, 292.
20. (a) Benbrook, D. M.; Subramanian, S.; Gale, J. B.; Liu, S.; Brown, C. W.; Boehm, M. F.; Berlin, K. D. Synthesis and Characterization of Heteroarotinoids Demonstrate Structure Specificity Relationships. *J. Med. Chem.* **1998**, *41*, 3753-3757. (b) See (1), pp 319-321. (c) Dawson, M. I. *Burger's Medicinal Chemistry and Drug Discovery*, 5th Edition, Wolff, M. E., Ed.; John Wiley & Sons, Inc.: New York, 1996, p 579. (d) Jong, L.; Lehmann, J. M.; Hobbs, P. D.; Harlev, E.; Huffman, J. C.; Pfahl, M.; Dawson, M. I. Conformational Effects on Retinoid Receptor Selectivity. 1. Effect of 9-Double Bond Geometry on Retinoid X Receptor Activity. *J. Med. Chem.* **1993**, *36*, 2605-2613. (e) Lehmann, J. M.; Jong, L.; Fanjul, A.; Cameron, J. F.; Lu, X. P.; Haefner, P.; Dawson, M. I.; Pfahl, M. Retinoids Selective for Retinoid X Receptor Response Pathways. *Science* **1992**, *258*, 1944-1946.
21. (a) Petkovich, M.; Brand, N. J.; Krust, A.; Chambon, P. A Human Retinoic Acid Receptor which Belongs to the Family of Nuclear Receptors. *Nature* **1987**, *330*,

- 444-450. (b) Mangelsdorf, D. J.; Umesono, K.; Evans, R. M. The Retinoid Receptors. In *The Retinoids-Biology, Chemistry, and Medicine*, 2nd Ed., Sporn, M. B.; Roberts, A. B.; Goodman, D. S.; Eds., Raven Press: New York, 1994, pp 319-350. (c) Gale, J. B. Recent Advances in the Chemistry and Biology of Retinoids. *Progress Med. Chem.* **1993**, *30*, 1-55.
22. (a) Giguere, V. M.; Shago, R.; Zirngibl, P.; Tate, P.; Rossant, J.; Varmuza, S. Identification of a Novel Isoform of the Retinoic Acid Receptor Gamma Expressed in the Mouse Embryo. *Mol. Cell. Biol.* **1990**, *10*, 2335-2340. (b) See (20c), pp 579-583. (c) See (1), pp 322-323. (d) Giguere, V.; Ong, E. S.; Segui, P.; Evans, R. M. Identification of a New Class of Steroid Hormone Receptors. *Nature* **1987**, *330*, 624-629.
23. (a) Mangelsdorf, D.J.; Borgmeyer, U.; Heyman, R. A.; Zhou, J. Y.; Ong, E. S.; Oro, A. E.; Kakizuka, A.; Evans, R. M. Characterization of Three RXR Genes that Mediate the Action of 9-cis-Retinoic Acid. *Genes Dev.* **1992**, *6*, 329-344. (b) See (20c), pp 579-583. (c) See (1), pp 323-324. (d) Leid, M.; Kastner, P.; Lyons, R.; Nakshatri, H.; Saunders, M.; Zacharewski, T.; Chen, J.-Y.; Staub, A.; Garnier, J.-M.; Mader, S.; Chambon, P. Purification, Cloning, and RXR Identity of the HeLa Cell Factor with which RAR or TR Heterodimerizes to Bind Target Sequences Efficiently. *Cell* **1992**, *68*, 377-395.
24. Marchio, A.; Tiollais, P.; Dejean, A.; de The, H. A Novel Steroid Thyroid Hormone Receptor-Related Gene Inappropriately Expressed in Human Hepatocellular Carcinoma. *Nature* **1987**, *330*, 667-670.
25. (a) Brand, N.; Petkovich, M.; Krust, A.; Chambon, P.; de The, H.; Marchio, A.; Tiollais, P.; Dejean, A. Identification of a Second Human Retinoic Acid Receptor. *Nature* **1988**, *332*, 850-853. (b) Benbrook, D.; Lernhardt, E.; Pfahl, M. A New Retinoic Acid Receptor Identified from a Hepatocellular Carcinoma. *Nature* **1988**, *333*, 669-672.
26. Chambon, P.; Krust, A.; Petkovich, M.; Kastner, P.; Zelent, A. Cloning of Murine α and β Retinoic Acid Receptors and a Novel Receptor γ Predominately Expressed in Skin. *Nature* **1989**, *339*, 714-717.
27. (a) Ishikawa, T.; Umesono, K.; Mangelsdorf, D. J.; Aburatani, H.; Stanger, B. Z.; Shibasaki, Y.; Imawari, M.; Evans, R. M.; Takaku, F. A Functional Retinoic Acid Receptor Encoded by the Gene on Human Chromosome 12. *Mol. Endocrinol.* **1990**, *4*, 837-844. (b) Mattei, M.-G.; Petkovich, M.; Mattei, J.-F.; Brand, N. Chambon, P. Mapping of the Human Retinoic Acid Receptor to the q21 Band of Chromosome 17. *Hum. Genet.* **1988**, *80*, 186-188. (c) Mattei, M.-G.; de The, H.; Mattei, J. F.; Marchio, A.; Tiollais, P.; Dejean, A. Assignment of the Human *Hap* Retinoic Acid Receptor RAR β Gene to the p24 Band of Chromosome 3. *Hum. Genet.* **1988**, *80*, 189-190.

28. (a) Krust, A.; Kastner, P.; Petkovich, M.; Zelent, A.; Chambon, P.; Leroy, P.; Garnier, J. Murine Isoforms of Retinoic Acid Receptor γ with Specific Pattern of Expression. *Proc. Natl. Acad. Sci. U. S. A.* **1990**, *87*, 2700-2704. (b) Leroy, P.; Krust, A.; Zelent, A.; Mendelsohn, C.; Garnier, J. M.; Kastner, P.; Dierich, A.; Chambon, P. Multiple Isoforms of Mouse Retinoic Acid Receptor α are Generated by Alternative Splicing and Differential Induction by Retinoic Acid. *EMBO J.* **1991**, *10*, 59-69. (c) Zelent, A.; Leroy, P.; Krust, A.; Mendelsohn, C.; Garnier, J.M.; Kastner, P.; Chambon, P. Differentially Expressed Isoform of the Mouse Retinoid Acid Receptor β are Generated by Usage of Two Promoters and Alternative Splicing. *EMBO J.* **1991**, *10*, 71-81.
29. Evans, R. M. The Steroid and Thyroid Hormone Receptor Superfamily. *Science* **1988**, *240*, 889-895.
30. Mitchell, P. J.; Tijian R. Transcriptional Regulation in Mammalian Cells by Sequence-Specific DNA Binding Protein. *Science* **1989**, *245*, 371-378.
31. (a) Freedman, L. P.; Luisi, B. F.; Korzsun, R.; Basavapa, R.; Sigler, P. B.; Yamamoto, K. R. The Function and Structure of Metal Coordination Sites within the Glucocorticoid Receptor DNA Binding Domain. *Nature* **1988**, *334*, 543-546. (b) Rastinejad, F.; Perlmann, T.; Evans, R. M.; Sigler, P. B. Structural Determinants of Nuclear Receptor Assembly on DNA Direct Repeats. *Nature* **1995**, *375*, 203-211.
32. Evans, R. M.; Hollenberg, S. M. Zinc Fingers: Guilt by Association. *Cell* **1988**, *52*, 1-3.
33. (a) Perlmann, T.; Rangarajan, P. N.; Umesono, K.; Evans, R. M. Determinants for Selective RAR and TR Recognition of Direct Repeat HREs. *Genes Dev.* **1993**, *7*, 1411-1422. (b) Valee, B. L.; Coleman, J. E.; Ault, D. S. Zinc Fingers, Zinc Clusters, and Zinc Twists in DNA-Binding Protein Domains. *Proc. Natl. Acad. Sci. U. S. A.* **1991**, *88*, 999-1003.
34. Green, S.; Kumar, V.; Theulas, I.; Wahli, W.; Chambon, P. The N-Terminal DNA-Binding 'Zinc-Finger' of the Estrogen and Glucocorticoid Receptors Determines Target Gene Specificity. *EMBO J.* **1988**, *7*, 3037-3044.
35. Tsai, S. Y.; Tsai, M. J.; O'Malley, B. W. Cooperative Binding of Steroid Hormone Receptors Contributes to Transcriptional Synergism at Target Enhancer Element. *Cell* **1989**, *57*, 1139-1146.
36. Hard, T.; Kellembach, E.; Boelens, R.; Maler, B. A.; Dahler, K.; Freedman, L. P.; Carlstedt-Duke, J.; Yamamoto, K. R.; Gustafonn, J. A.; Kaptein, R. Solution Structure of the Glucocorticoid Receptor DNA-Binding Domain. *Science* **1990**, *249*, 157-160.

37. Umesono, K.; Evans, R. M. Determination of Target Gene Specificity for Steroid/Thyroid Hormone Receptor. *Cell* **1988**, *57*, 1139-1146.
38. (a) Laudet, V.; Hanni, C.; Coll, J.; Catzeflis, F.; Stehelin, D. Evolution of the Nuclear receptor Gene Superfamily. *EMBO J.* **1992**, *11*, 1003-1013. (b) Napoli, J. L. Biochemical Pathways of Retinoid Transport, Metabolism, and Signal Transduction. *Clin. Immun. Immunopath.* **1996**, *80*, S52-S62.
39. Gaub, M. P.; Lutz, Y.; Ruberte, E.; Petkovich, M.; Brand, M.; Chambon, P. Antibodies Specific to the Retinoic Acid Human Nuclear Receptors α and β . *Proc. Natl. Acad. Sci. U. S. A.* **1989**, *86*, 3089-3093.
40. Renaud, J. P.; Rochel, N.; Ruff, M.; Vivat, V.; Chambon, P.; Gromemeyer, H.; Moras, D. Crystal Structure of the RAR- γ Ligand-Binding Domain Bound to all-*trans*-Retinoic Acid. *Nature* **1995**, *378*, 681-689.
41. (a) Bourget, W.; Ruff, M.; Chambon, P.; Gronemeyer, G.; Moras, D. Crystal Structure of the Ligand-Binding Domain of the Human Nuclear Receptor RXR α . *Nature* **1995**, *375*, 377-382. (b) Egea, P. F.; Mitschler, A.; Rochel, N.; Ruff, M.; Chambon, P.; Moras, D. Crystal Structure of the Human RXR α Ligand-Binding Domain Bound to its Natural Ligand: 9-*cis*-Retinoic Acid. *EMBO J.* **2000**, *19*, 2592-2601.
42. Leid, M.; Kastner, P.; Chambon, P. Multiplicity Generates Diversity in the Retinoic Acid Pathways. *Trends Biochem. Sci.* **1992**, *17*, 427-433.
43. Fawell, S. E.; Lees, J. A.; White, R.; Parker, M. G. Characterization and Co-localization of Steroid Binding and Dimerization Activities. *Cell* **1990**, *60*, 953-962.
44. Manglesdorf, D. J.; Ong, E. S.; Dyck, J. A.; Evans, R. M. Nuclear Receptor that Identifies a Novel Retinoic Acid Response Pathway. *Nature* **1990**, *345*, 224-229.
45. Cheng, L.; Norris, A. W.; Tate, B. F.; Rosenberger, M.; Grippo, J. F.; Li, E. Characterization of the Ligand Binding Domain of Human Retinoid X Receptor α Expressed in Escherichia Coli. *J. Biol. Chem.* **1994**, *269*, 18662-18667.
46. Giguere, V. Retinoic Acid Receptors and Cellular Retinoid Binding Proteins: Complex Interplay in Retinoid Signaling. *Endocr. Rev.* **1994**, *15*, 61-79.
47. Hoopes, C. W.; Taketo, M.; Ozato, K.; Liu, Q.; Howard, T. A.; Linney, E., Seldin, M. F. Mapping of the RXR Loci Encoding Nuclear Retinoid X Receptors RXR- α , RXR- β , and RXR- γ . *Genomics* **1992**, *14*, 611-617.

48. Mangelsdorf, D. J.; Borgmeyer, U.; Heyman, R. A.; Zhou, J. Y.; Ong, E. S.; Oro, A. E.; Kikazuka, A.; Evans, R. M. Characterization of Three RXR Genes that Mediate the Action of 9-*cis*-Retinoic Acid. *Genes Dev.* **1992**, *6*, 329-344.
49. Heyman, R. A.; Mangelsdorf, D. J.; Dyck, J. A.; Stein, R. B.; Eichele, G.; Evans, R. M.; Thaller, C. 9-*cis*-Retinoic Acid is a High Affinity Ligand for the Retinoid X Receptor. *Cell* **1992**, *68*, 397-406.
50. Dhar, A.; Liu, S.; Klucik, J.; Berlin, K. D.; Madler, M. M.; Lu, S.; Ivey, T. R.; Zacheis, D.; Brown, C. W.; Nelson, E. C.; Birckbichler, P. J.; Benbrook, D. M. Synthesis, Structure-Activity Relationships, and RAR γ -Ligand Interactions of Nitrogen Heteroarotinoids. *J. Med. Chem.* **1999**, *42*, 3602-3614.
51. Giguere, V.; Tini, M.; Flock, G.; Ong, E.; Evans, R. M.; Otulakowski, G. Isoform-Specific Amino-Terminal Domains Dictate DNA-Binding Properties of ROR α , a Novel Family of Hormone Nuclear Receptors. *Genes Dev.* **1994**, *8*, 538-553.
52. (a) Smirnov, A. N. Nuclear Melatonin Receptors. *Biochemistry* **2001**, *66*, 19-26. (b) Becker-Andre, M.; Wiesenberg, I.; Scaeren-Wiemers, N.; Andre, E.; Missbach, M.; Saurat, J. H.; Carlberg, C. Pineal Gland Hormone Melatonin Binds and Activates an Orphan of the Nuclear Receptor Superfamily. *J. Biol. Chem.* **1994**, *269*, 28531-28534. (c) Wiesenberg, I.; Missbach, M.; Kahlen, J. P.; Schrader, M.; Carlberg, C. Transcriptional Activation of the Nuclear Receptor RZR α by the Pineal Gland Hormone Melatonin and Identification of CGP 52608 as a Synthetic Ligand. *Nucl. Acids Res.* **1995**, *23*, 327-333.
53. Repa, J. J.; Mangelsdorf, D. J. The Role of Orphan Nuclear receptors in the Regulation of Cholesterol Homeostasis. *Annu. Rev. Cell Dev. Biol.* **2000**, *16*, 459-481.
54. Meyer, T.; Kneissel, M.; Mariani, J.; Fournier, B. In Vitro and in Vivo Evidence for Orphan Nuclear Receptor ROR α Function in Bone Metabolism. *Proc. Natl. Acad. Sci. U. S. A.* **2000**, *97*, 9197-9202.
55. Kurebayashi, S.; Ueda, E.; Sakaue, M.; Patel, D. D.; Medvedev, A.; Zhang, F.; Jetten, A. M. Retinoid-Related Orphan Receptor γ (ROR γ) is Essential for Lymphoid Organogenesis and Controls Apoptosis During Thymopoiesis. *Proc. Natl. Acad. Sci. U. S. A.* **2000**, *97*, 10132-10137.
56. Becker, A. M.; Delamarter, J. F.; Staple, J. K.; Hooft, H.; Carlberg, C. RZR, a New Family of Retinoid-Related Orphan Receptors that Function as Both Monomers and Homodimers. *Mol. Endocrin.* **1994**, *8*, 757-770.

57. Greiner, E. F.; Kirfel, J.; Greschik, H.; Dorflinger, U.; Becker, P.; Mercep, A.; Schule, R. Functional Analysis of Retinoid Z Receptor, a Brain-Specific Nuclear Orphan Receptor. *Proc. Natl. Acad. Sci. U. S. A.* **1996**, *93*, 10105-10110.
58. Missbach, M.; Jagher, B.; Sigg, I.; Nayeri, S.; Carlberg, C.; Wiesenberg, I. Thiazolidine Diones, Specific Ligand of the Nuclear Z Receptor/Retinoic Acid Related Orphan Receptor α with Potent Antiarthritic Activity. *J. Biol. Chem.* **1996**, *271*, 13515-13522.
59. Morriss-Kay, G. M.; Sokolova, N. Embryonic Development and Pattern Formation. *FASEB J.* **1996**, *10*, 961-968.
60. Joore, J.; Gerald, B. L. J.; Lans, P.; Lanser, J.; Vervaart, J. M. A.; Zitkovic, D.; Kruijer, W. Effect of Retinoic Acid on the Expression of Retinoic Acid Receptors during Zebrafish Embryogenesis. *Mechanism of Development* **1994**, *46*, 137-150.
61. (a) Budowski, P.; Gross, J. Conversion of Carotinoids to 3-Dihydroretinol (Vitamin A₂) in the Mouse. *Nature* **1965**, *206*, 1254-1255. (b) Goodman, D. S.; Huang, H. S. Biosynthesis of Vitamin A with Rat Intestinal Enzymes. *Science* **1965**, *149*, 879-880. (c) Olson, J. A.; Hayaishi, O. The Enzymatic Cleavage of β -Carotene into Vitamin A by Soluble Enzymes of rat Liver and Intestine. *Proc. Natl. Acad. Sci. U. S. A.* **1965**, *54*, 164-1369. (d) Buck, J.; Myc, A.; Garbe, A.; Cathomas, G. Differences in the Action and Metabolism Between Retinol and Retinoic Acid in B-Lymphocytes. *Cell Biol.* **1991**, *115*, 851-859.
62. Kakkad, B.; Ong, D. E. Reduction of Retinaldehyde Bound to Cellular Retinol-Binding Protein (Type II) by Microsomes from Rat Small Intestine. *J. Biol. Chem.* **1988**, *263*, 12916-12919.
63. Ong, D. E.; Kakkad, B.; MacDonald, P. N. Acyl-CoA-Independent Esterification of Retinol in Rat Liver Bound to Cellular Retinol-Binding Protein (Type II) by Microsomes from Rat Small Intestine. *J. Biol. Chem.* **1987**, *262*, 2729-2736.
64. Quick, T. C.; Ong, D. E. Vitamin A Metabolism in the Human Intestinal Caco-2 Cell Line. *Biochemistry* **1990**, *29*, 11116-11123.
65. Blomhoff, R.; Green, M. H.; Green, J. B.; Berg, T.; Norum, K. R. Vitamin A Metabolism: New Perspective on Absorption, Transport, and Storage. *Physiol. Rev.* **1991**, *71*, 951-990.
66. Goodman, D. S.; Blaner, W. S. Biosynthesis, Absorption, and Hepatic Metabolism of Retinol. In *The Retinoids*, Vol. 2, Sporn, M. B.; Roberts, A. B.; Goodman, D. S.; Eds., Academic Press: Orlando, FL, 1984, pp 1-40.

67. (a) Blaner, W. S.; Hendriks, H. F. J.; Brouwer, A.; de Leeuw, A. M.; Knook, D. L.; Goodman, D. S. Retinoids, Retinoid-Binding Proteins, and Retinyl Palmitate Hydrolase Distributions in Different Types of Rat Liver Cells. *J. Lipid Res.* **1985**, *26*, 1241-1251. (b) Blomhoff, R.; Rasmussen, M.; Nilsson, A.; Norum, K. R.; Berg, T.; Peterson, P. A. Hepatic Retinol Metabolism: Distribution of Retinoids, Enzymes and Binding Proteins in Isolated Rat Liver Cells. *J. Biol. Chem.* **1985**, *260*, 13560-13565. (c) Hendriks, H. F. J.; Brekelmans, P. J. A. M.; Buytenhek, R.; Brouwer, A.; de Leeuw, A. M.; Knook, D. L. Liver Parenchymal Cells Differ from the Fat-Storing Cells in Their Lipid Composition. *Lipids* **1987**, *22*, 266-273. (d) Batres, R.O.; Olson, J. A. A Marginal Vitamin A Status Alters the Distribution of Vitamin A Among Parenchymal and Stellate Cells in Rat Liver. *J. Nutr.* **1987**, *117*, 874-879.
68. (a) Gad, M. Z.; Harrison, E. H. Neutral and Acid Retinyl Ester Hydrolases Associated with Rat Liver Microsomes: Relationships to Microsomal Cholesteryl Ester Hydrolases. *J. Lipid Res.* **1991**, *32*, 685-693. (b) Harrison, E. H.; Gad, M. Z. Hydrolysis of Retinyl Palmitate by Enzymes of Rat Pancreas and Liver. *J. Biol. Chem.* **1989**, *264*, 17142-17147.
69. Yamada, M.; Blaner, W. S.; Soprano, D. R.; Dixon, J. L.; Kjeldbye, H. M.; Goodman, D. S. Biochemical Characteristics of Isolated Rat Liver Stellate Cells. *Hepatology* **1987**, *7*, 1224-1229.
70. Soprano, D. R.; Blaner, W. S. Plasma Retinol-Binding Protein. In *The Retinoids, Biology, Chemistry, and Medicine*, 2nd Ed., Sporn, M. B.; Roberts, A. B.; Goodman, D. S.; Eds., Raven Press, Ltd.: New York, 1994, pp 257-281.
71. Levin, M. S. Cellular Retinol-Binding Proteins are Determinants of Retinol Uptake and Metabolism in Stably Transfected Caco-2 Cells. *J. Biol. Chem.* **1993**, *268*, 8267-8276.
72. Boerman, M. H. E.; Napoli, J. L. Cholate-Independent Retinyl Ester Hydrolysis: Stimulation by Apo-Retinol Binding Protein. *J. Biol. Chem.* **1991**, *266*, 22273-22278.
73. Herr, F. M.; Ong, D. E. Differential Interaction of Lecithin-Retinol Acyltransferase with Cellular Retinol Binding Protein. *Biochemistry* **1992**, *31*, 6748-6755.
74. Posch, K. C.; Boerman, M. H. E.; Burns, R. D.; Napoli, J. L. Holo-Cellular Retinol Binding Protein as a Substrate for Microsomal Retinal Synthesis. *Biochemistry* **1991**, *30*, 6224-6230.
75. Posch, K. C.; Burns, R. D.; Napoli, J. L. Biosynthesis of All-*Trans*-Retinoic Acid from Retinal: Recognition of Retinal Bound to the Cellular Retinol Binding

- Protein (type I) as a Substrate by Purified Cytosolic Dehydrogenase. *J. Biol. Chem.* **1992**, *267*, 19676-19682.
76. (a) Boylan, J. F.; Gudas, L. J. The level of CRABP-I Expression Influences the Amounts and Types of All-*Trans*-Retinoic Acid in F9 Teratocarcinoma Stem Cells. *J. Biol. Chem.* **1992**, *267*, 21486-21491. (b) Norris, A. W.; Cheng, L.; Giguere, V.; Rosenberg, M.; Li, E. Measurements of Subnanomolar Retinoic Acid Binding Affinities for Cellular Retinoic Acid Binding Proteins by Fluorometric Titration. *Biochem. Biophys. Acta* **1994**, *109*, 10-18.
77. Fiorella, P. D.; Napoli, J. L. Microsomal Retinoic Acid Metabolism: Effects of Cellular Retinoic Acid Binding Protein (Type I) and C18-Hydroxylation as an Initial Step. *J. Biol. Chem.* **1994**, *269*, 10538-10544.
78. (a) Stahl, W.; Sundquist, A. R.; Hanusch, M.; Schwarz, W.; Sies, H. Separation of β -Carotene and Lycopene Geometrical Isomers in Biological Samples. *Clin. Chem.* **1993**, *39*, 810-814. (b) Canada, F. J.; Law, W. C.; Rando, R. R.; Yamamoto, T.; Derguini, F.; Nakanishi, K. Substrate Specificities and Mechanism in the Enzymatic Processing of Vitamin A into 11-*cis*-Retinol. *Biochemistry* **1990**, *29*, 9690-9697. (c) Horst, R. L.; Reinhardt, T. A.; Goff, J. P.; Nonnecke, B. J.; Gambhir, V. K.; Fiorella, P. D.; Napoli, J. L. Identification of 9,13-di-*cis*-Retinoic Acid as a Major Circulating Retinoid in Plasma. *Biochemistry* **1995**, *34*, 1203-1209.
79. Levin, A. A.; Sturzenbecker, L. J.; Kazmer, S.; Bosakowski, T.; Huselton, C.; Alenby, G.; Speck, J.; Kratzeisen, C. L.; Rosenberger, M.; Lovey, A.; Grippo, J. F. 9-*Cis*-Retinoic Acid Stereoisomer Binds and Activates the Nuclear Receptor RXR α . *Nature* **1992**, *355*, 359-361.
80. Chambon, P. The Retinoid Signaling Pathway: Molecular and Genetic Analysis Semin. *Cell. Biol.* **1994**, *5*, 115-125.
81. Kersten, S.; Pan, L.; Noy, N. The Role of Ligand in Retinoid Signaling: Positive Cooperativity in the Interaction of 9-*cis*-Retinoic Acid with Tetramers of the Retinoid X Receptor. *Biochemistry* **1995**, *34*, 14263-14269.
82. Meyer, M. E.; Gronemeyer, H.; Turcotte, B.; Bocquel, M. T.; Tasset, D.; Chambon, P. Steroid Hormone, Receptors Compete for Factors that Mediate Their Enhancer Function. *Cell*, **1989**, *57*, 433-442.
83. Minucci, S.; Ozato, K. Retinoid Receptors in Transcriptional Regulation. *Curr. Opinions Genet. Dev.* **1996**, *6*, 567-574.
84. Predki, P. F.; Zamble, D.; Sarkar, B.; Giguere, V. Ordered Binding of Retinoic Acid and Retinoid X Receptors to Asymmetric Response Elements Involves

- Determinants Adjacent to the DNA-Binding Domain. *Mol. Endocrin.* **1994**, *8*, 31-39.
85. Mangelsdorf, D. J.; Evans, R. M. The RXR Heterodimers and Orphan Receptors. *Cell* **1995**, *83*, 841-850.
86. Forman, B. M.; Umesono, K.; Chen, J.; Evans, R. M. Unique Response Pathway Established by Allosteric Interaction Among Nuclear Hormone Receptors. *Cell*, **1995**, *81*, 541-550.
87. Halachmi, S.; Merden, E.; Martin, G.; MacKay, H.; Abbodanza, C.; Brown, M. Oestrogen Receptor-Associated Proteins: Possible Mediation of Hormone-Induced Transcription. *Science* **1994**, *264*, 1455-1458.
88. Cuvailles, V.; Dauvois, S.; L'Horset, F.; Lopez, G.; Hoare, S.; Kusner, P. J.; Parker, M. G. Nuclear Factor RIP 140 Modulates Transcription Activation. *EMBO J.* **1996**, *16*, 3741-3751.
89. Cooper, R. J.; von Baur, E.; Zachel, C.; Heery, D.; Heine, M. J.; Garnier, J. M.; Vivat, V.; Le Douarin, B.; Gronemeyer, H.; Chambon, P.; Losson, R. Differential Ligand-Dependent Interaction Between the AF-2 Activating Domain of Nuclear Receptors and the Putative Transcriptional Intermediary Factors mSUG1 and TIF 1. *EMBO J.* **1996**, *16*, 3241-3247.
90. Le Dourin, B.; Zechel, C.; Garnier, J. M.; Lutz, Y.; Tora, L.; Pierrat, P.; Heery, D.; Gronemeyer, H.; Chambon, P.; Losson, R. The N-Terminal Part of TIF 1, a Putative Mediator of the Ligand-Dependent Activation Function (AF-2) of Nuclear Receptor is Fused to B-raf in the Oncogenic Protein T18. *EMBO J.* **1995**, *14*, 2020-2033.
91. Lee, J. W.; Ryan, F.; Swafield, J. C.; Johnston, S. A.; Moore, D. A. Interaction of Thyroid Hormone Receptor with a Conserved Transcriptional Mediator. *Nature* **1995**, *374*, 91-94.
92. Schulman, I. G.; Chakravarti, D.; Juguilon, H.; Romo, A.; Evans, R. M. Interaction Between the Retinoid X Receptor and a Conserved Region of the TATA-Binding Protein Mediates Hormone Dependent Transactivation. *Proc. Natl. Acad. Sci. U. S. A.* **1995**, *92*, 8288-8292.
93. Horlein, A. J.; Naar, A. M.; Heinzl, T.; Gloss, B.; Kurokawa, R.; Ryan, A.; Glass, C. K. Ligand-Independent Repression by the Thyroid Hormone Receptor Mediated by Nuclear Receptor Co-repressor. *Nature* **1995**, *377*, 397-404.
94. Kurokawa, R.; Soderstrom, M.; Horlein, A.; Halachni, S.; Brown, M.; Rosenfeld, M. G.; Glass, C. K. Polarity-Specific Activities of Retinoic Acid Receptors Determined by a Co-repressor. *Nature* **1995**, *377*, 451-454.

95. Chen, J. D.; Evans, R. M. A Transcriptional Co-repressor that Interacts with Nuclear Hormone Receptors. *Nature* **1995**, *377*, 454-457.
96. Glass, C. K. Differential Recognition of Target Genes by Nuclear Receptor Monomers, Dimers, and Heterodimers. *Endocr. Rev.* **1994**, *15*, 391-407.
97. (a) Klein, E. S.; Wang, J. W.; Khalifa, B.; Gavigan, S. A.; Chandraratna, R. A. S. Recruitment of Nuclear Receptor Corepressor and Coactivator to the Retinoic Acid Receptor by Retinoid Ligands. *J. Biol. Chem.* **2000**, *275*, 19401-19408. (b) Foster, R. H.; Brogden, Rex. N.; Benfield, P. Tazarotene. *Drugs* **1998**, *55*, 705-711. (c) Nagpal, S.; Chandraratna, R. A. S. New Dermatological Agents for the Treatment of Psoriasis. In *Annual Reports in Medicinal Chemistry*, Bristol, J. A.; Ed., Academic Press: San Diego, CA, 1997, pp 201-210.
98. Klaholtz, B. P.; Renaud, J. P.; Mitschler, A.; Zusi, C.; Gronemeyer, H.; Chambon, P.; Moras, D. Conformational Adaptations of Agonists in the Nuclear Receptor RAR Gamma. *Nat. Struct. Biol.* **1998**, *5*, 100-202.
99. Gehin, M.; Vivat, V.; Wurtz, J. M.; Losson, R.; Chambon, P.; Moras, D.; Gronemeyer, H. Structural Basis for Engineering of Retinoic Acid Receptor Isotype-Selective Agonists and Antagonists. *Chem. Biol.* **1999**, *6*, 519-529.
100. Wurtz, J. M.; Bourget, W.; Renaud, J. P.; Vivat, V.; Chambon, P.; Moras, D.; Gronemeyer, H. A Conical Structure for the Ligand-Binding Domain of Nuclear Receptors. *Nat. Struct. Biol.* **1996**, *3*, 87-94.
101. Fisher, G. J.; Voorhees, J. J. Molecular Mechanism of Retinoids in Skin. *FASEB J.* **1996**, *10*, 1002-1013.
102. Li, Y.; Hashimoto, Y.; Agador, A.; Kagechika, H.; Zhang, X. Identification of a Novel Class of Retinoic Acid Receptor β -Selective Retinoid Antagonists and Their Inhibitory Effects on AP-1 Activity and Retinoic Acid-Induced Apoptosis in Human Breast Cancer Cells. *J. Biol. Chem.* **1999**, *274*, 15360-15366.
103. Klein, E. S.; Pino, M. E.; Johnson, A. T.; Davies, P. J. A.; Nagpal, S.; Thacher, S.; M.; Krasinski, G.; Chandraratna, R. A. S. Identification and Functional Separation of Retinoic Acid receptor Neutral Antagonists and Inverse Agonists. *J. Biol. Chem.* **1996**, *271*, 22692-22696.
104. Yoshimura, H.; Nagai, M.; Hibi, S.; Kikuchi, K.; Abe, S.; Hida, T.; Higashi, S.; Hishinuma, I.; Yamanaka, T. A Novel Type of Retinoic Acid Receptor Antagonist: Synthesis and Structure-Activity Relationships of Heterocyclic Ring-Containing Benzoic Acid Derivatives. *J. Med. Chem.* **1995**, *38*, 3163-3173.

105. Johnson, A. T.; Klein, E. S.; Wang, L.; Song, T. K.; Pino, M. E.; Chandraratna, R. A. S. Synthesis and Characterization of a Highly Potent and Effective Antagonist of Retinoic Acid Receptors. *J. Med. Chem.* **1995**, *38*, 4764-4767.
106. Standeven, A. M.; Johnson, A. T.; Escobar, M.; Chandraratna, R. A. S. Specific Antagonist of Retinoid Toxicity in Mice. *Tox. Appl. Pharm.* **1996**, *138*, 169-175.
107. (a) Mario, J.; Brown, F. Regulation of Expression Driven by Human Immunodeficiency Virus Type I and Human T-Cell Leukemia Virus Type I Long Terminal Repeats in Pluripotential Human Embryonic Cells. *J. Virol.* **1988**, *62*, 1398-1407. (b) Turpin, J.; Vargo, M.; Meltzer, M. Enhanced HIV-1 Replication in Retinoid-Treated Monocytes. Retinoid Effects Mediated Through Mechanisms Related Cell Differentiation and to a Direct Transcriptional Action on Viral Gene Expression. *J. Immunol.* **1992**, *148*, 2539-2546. (c) Zeichner, S.; Kirka, G.; Andrews, P.; Alwine, J. Differentiation-Dependent Human Immunodeficiency Virus Long Terminal Repeat Regulatory Elements Active in Human Teratocarcinoma Cells. *J. Virol.* **1992**, *66*, 2268-2273.
108. Koch, S. S. C.; Dardashti, L. J.; Hebert, J. J.; White, S. K.; Croston, G. E.; Flatten, K. S.; Heyman, R. A.; Nadzan, A. M. Identification of the First Retinoid X Receptor Homodimer Antagonist. *J. Med. Chem.* **1996**, *39*, 3229-3234.
109. (a) Ameisen, J. C. The Origin of Programmed Cell Death. *Science* **1996**, *272*, 1278-1279. (b) Miller, D. K. Regulation of Apoptosis by Members of the ICE Family and the Bcl-2 Family. *Annu. Repts. Med. Chem.* **1996**, *31*, 249-268.
110. Horn, V.; Minucci, S.; Orgyzko, V. V.; Adamson, E. D.; Howard, B. H.; Levin, A. A.; Ozato, K. RAR and RXR Selective Ligands Cooperatively Induce Apoptosis and Neuronal Differentiation in P19 Embryonal Carcinoma Cells. *FASEB J.* **1996**, *10*, 1071-1077.
111. Nagy, L.; Thomazy, V. A.; Siple, G. L.; Fesus, L.; Lamph, W.; Heyman, R. A.; Chandraratna, R. A. S.; Davies, P. J. A. Activation of Retinoid X Receptors Induces Apoptosis in HL-60 Cell Lines. *Mol. Cell. Biol.* **1995**, *15*, 3540-3551.
112. (a) Wang, T. T. Y.; Phang, J. M. Effect of *N*-(4-Hydroxyphenyl)retinamide on Apoptosis in Human Breast Cancer Cells. *Cancer Lett.* **1996**, *107*, 65-71. (b) Fanjul, A. N.; Delia, D.; Peiriotti, M. A.; Rideout, D.; Qiu, J.; Pfahl, M. 4-Hydroxyphenyl Retinamide is a Highly Selective Activator of Retinoid Receptors. *J. Biol. Chem.* **1996**, *271*, 22441-22446.
113. (a) Montaldo, P. G.; Pagnan, G.; Postorino, F.; Chiesa, V.; Raffaghello, L.; Kirchmeier, M.; Allen, T. M.; Ponzoni, M. *N*-(4-Hydroxyphenyl)retinamide is cytotoxic to Melanoma Cells *in vitro* through the Induction of Programmed Cell Death. *Int. J. Cancer* **1999**, *81*, 262-267. (b) Scher, R. L.; Saito, W.; Dodge, R. K.; Richtsmeier, W. J.; Fine, R. L. Fenretinide-Induced Apoptosis in Human

- Head and Neck Squamous Carcinoma Cell Lines. *Otolaryngol. Head Neck Surg.* **1998**, *118*, 464-471. (c) Hsieh, T. C.; Wu, J. M. Effects of Fenretinide (4-HPR) on Prostate LNCaP Cell Growth, Apoptosis, and Prostate-Specific Gene Expression. *Prostate* **1997**, *33*, 97-104. (d) Deliaq, D.; Aiello, A.; Formelli, F.; Fontanella, E.; Costa, A.; Miyashita, T.; Reed, J. C.; Pierotti, M. A. Regulation of Apoptosis Induced by the Retinoid *N*-(4-Hydroxyphenyl)retinamide and Effect of Deregulated Bcl-2. *Blood* **1995**, *85*, 359-367. (e) Guruswamy, S.; Lightfoot, S.; Gold, M. Hassan, R.; Berlin, K. D.; Ivey, T. R.; Benbrook, D. M. Effects of Retinoids on Cancerous Phenotype and Apoptosis in Organotypic Cultures of Ovarian Carcinoma. *J. Natl. Cancer Inst.* **2001**, *93*, 516-525.
114. (a) Merritt, G.; Aliprandis, E. T.; Prada, F.; Rigas, B.; Kashfi, K. The Retinoid Fenretinide Inhibits Proliferation and Downregulates Cyclooxygenase-2 Gene Expression in Human Colon Adenocarcinoma Cell Lines. *Cancer Lett.* **2001**, *164*, 15-23. (b) Formelli, F.; Cleris, L. Therapeutic Effects of the Combination of Fenretinide and All-*trans*-Retinoic Acid and of the Two Retinoids with Cisplatin in a Human Ovarian Carcinoma Xenograft and in a Cisplatin-Resistant Sub-line. *Eur. J. Cancer* **2000**, *36*, 2411-2419. (c) Pollard, M.; Luckert, P. H.; Sporn, M. B. Prevention of Primary Prostate Cancer in Lobund-Wistar Rats by *N*-(4-Hydroxyphenyl)retinamide. *Cancer Res.* **1991**, *51*, 3610-3611.
115. (a) Lippman, S. M.; Lotan, R. Advances in the Development of Retinoids as Chemopreventive Agents. *J. Nutr.* **2000**, *130*, 479S-482S. (b) Hsieh, T.-C.; Wu, J. M. Apoptosis and Restriction of G₁/S Cell Cycle by Fenretinide in Burkitt's Lymphoma Mutu I Cell Line Accessed with Bcl-6 Down Regulation. *Biochem. Biophys. Res. Commun.* **2000**, *276*, 1295-1301. (c) Kitareewa, S.; Spinella, M. J.; Allopenna, J.; Reczek, P. R.; Dmitrovsky, E. 4HPR Triggers Apoptosis but not Differentiation in Retinoid Sensitive and Resistant Human Embryonal Carcinoma Cells through an RAR γ Independent Pathway. *Oncogene* **1999**, *18*, 5747-5755. (d) Sheikh, M. S.; Shao, Z.-M.; Li, X.-S.; Ordonez, J. V.; Conley, B. A.; Wu, S.; Dawson, M. I.; Han, Q.-X.; Chao, W.-R. *N*-(4-Hydroxyphenyl)retinamide (4-HPR)-Mediated Biological Actions Involve Retinoid Receptor-Independent Pathways in Human Breast Carcinoma. *Carcinogenesis* **1995**, *16*, 2477-2486.
116. (a) Clifford, J. L.; Menter, D. G.; Wang, M.; Lotan, R.; Lippman, S. M. Retinoid Receptor-Dependent and Receptor-Independent Effects of *N*-(4-Hydroxyphenyl)-retinamide in F9 Embryonal Carcinoma Cells. *Cancer Res.* **1999**, *59*, 14-18. (b) Liu, G.; Wu, M.; Levi, G.; Ferrari, N. Inhibition of Cancer Cell Growth by All-*trans*-Retinoic Acid and its Analog *N*-(4-Hydroxyphenyl)retinamide: A Possible Mechanism of Action Via Regulation of Retinoid Receptors Expression. *Int. J. Cancer* **1998**, *78*, 248-254. (c) Sabichi, A. L.; Hendricks, D. T.; Bober, M. A.; Birrer, M. J. Retinoic Acid Receptor β Expression and Growth Inhibition of Gynecologic Cancer Cells by the Synthetic Retinoid *N*-(4-Hydroxyphenyl)retinamide. *J. Natl. Cancer Inst.* **1998**, *90*, 597-605.

117. Madler, M. M. Ph. D. Dissertation. Flexible Heteroarotinoids as Potential Anticancer Agents. Oklahoma State University, 1997.
118. Klucik, J. Ph. D. Dissertation. Modification of Heteroarotinoids to Enhance Their Retinoic Acid Receptor Binding Specificity and Anti-Cancer Activity. Oklahoma State University, 2000.
119. Wagner, M. In *Retinoid Protocols: Methods in Molecular Biology*, Redfern, C. P. F.; Ed., Humana Press: Totowa, NJ, 1998, vol. 89, pp. 41-53.
120. Armstrong, R. B.; Ashenfelter, K. O.; Eckhoff, C.; Levin, A. A.; Shapiro, S. S. General and Reproductive Toxicology of Retinoids. In *The Retinoids-Biology, Chemistry, and Medicine*, 2nd Ed., Sporn, M. B.; Roberts, A. B.; Goodman, D. S., Eds., Raven Press Ltd.: New York, 1994, pp 545-572.
121. Pignatello, M. A.; Kauffman, F. C.; Levin, A. A. Multiple Factors Contributing to the Toxicity of the Aromatic Retinoid TTNPB: Interaction with Retinoic Acid Receptors. *Tox. Appl. Pharm.* **1999**, *159*, 109-116.
122. Hani, R.; Bigler, F. Isolation and Identification of Three Major Metabolites of Retinoic Acid from Rat Feces. *Helv. Chim. Acta.* **1977**, *60*, 881-887.
123. Zacheis, D.; Dhar, A.; Lu, S.; Madler, M. M.; Klucik, J.; Brown, C. W.; Liu, S.; Clement, F.; Subramanian, S.; Weerasekare, G. M.; Berlin, K. D.; Gold, M. A.; Houck, Jr., J. R.; Fountain, K. R.; Benbrook, D. M. Heteroarotinoids Inhibit Head and Neck Cancer Cell Lines in Vitro and in Vivo Through Both RAR and RXR Retinoic Acid Receptors. *J. Med. Chem.* **1999**, *42*, 4434-4445.
124. Klaholz, B. P.; Mitschler, A.; Moras, D. Structural Basis for Isotype Selectivity of the Human Retinoic Acid Nuclear Receptor. *J. Biol. Chem.* **2000**, *302*, 155-170.
125. Benbrook, D. M.; Madler, M. M.; Spruce, L. W.; Birckbichler, P. J.; Nelson, E. C.; Subramanian, S.; Weerasekare, G. M.; Gale, J. B.; Patterson, Jr., M. K.; Wang, B.; Wang, W.; Lu, S.; Rowland, T.; DiSivestro, P.; Lindamood III, C.; Hill, D. L.; Berlin, K. D. Biologically Active Heteroarotinoids Exhibiting Anticancer Activity and Decreased Toxicity. *J. Med. Chem.* **1997**, *40*, 3567-3583.
126. (a) Spruce, L. W.; Gale, J. B.; Berlin, K. D.; Verma, K. A.; Breitman, T. R.; Ji, X.; van der Helm, D. Novel Heteroarotinoids: Synthesis and Biological Activity. *J. Med. Chem.* **1991**, *34*, 430-439. (b) Spruce, L. W.; Rajadhyaksha, S. N.; Berlin, K. D.; Gale, J. B.; Miranda, E. T.; Ford, W. T.; Blossey, E. C.; Verma, A. K.; Hossain, M. B.; van der Helm, D.; Breitman, T. R. Heteroarotinoids. Synthesis, Characterization, and Biological Activity in Terms of an Assessment of These Systems to Inhibit Induction of Ornithine Decarboxylase Activity and to

- Induce Terminal Differentiation of HL-60 Cells. *J. Med. Chem.* **1987**, *30*, 1474-1482. (c) Waugh, K. M.; Berlin, K. D.; Ford, W. T.; Holt, E. M.; Carroll, J. P.; Schomber, P. R.; Schiff, L. J. Synthesis and Characterization of Selected Heteroarotinoids. Pharmacological Activity as Assessed in Vitamin A Deficient Hamster Tracheal Organ Cultures. Single-Crystal X-ray Diffraction Analysis of 4,4-Dimethylthiochroman-6-yl Methyl Ketone 1,1-Dioxide and Ethyl(*E*)-4-[2-(4,4-Dimethylthiochroman-6-yl)-1-propenyl]benzoate. *J. Med. Chem.* **1985**, *27*, 116-124.
127. Bernard B. A.; Bernardon, J.-M.; Delescluse, C.; Martin, B.; Lenoir, M.-C.; Maigan, J.; Charpentier, B.; Pilgrim, W. R.; Reichert, U.; Shroot, B. Identification of Synthetic Retinoids with Selectivity for Human Nuclear Retinoic Acid Receptor Gamma. *Biochem. Biophys. Res. Commun.* **1992**, *186*, 977-983.
128. (a) Klaholz, B. P.; Mitschler, A.; Belema, M.; Zusi, C.; Moras, D. Enantiomer Discrimination Illustrated by High Resolution Crystal Structures of the Human Nuclear Receptor hRAR γ . *Proc. Natl. Acad. Sci. USA* **2000**, *97*, 6322-6327. (b) Yu, K.-L.; Spinazze, P.; Ostrowski, J.; Currier, S. J.; Pack, E. J.; Hammer, L.; Roalsvig, T.; Honeyman, J. A.; Tortolani, D. R.; Reczek, P. R.; Mansuri, M. M.; Starrett Jr., J. E. Retinoic Acid Receptor Beta, Gamma-Selective Ligands: Synthesis and Biological Activity of 6-Substituted 2-Napthoic Acid Retinoids. *J. Med. Chem.* **1996**, *39*, 2411-2421.
129. Kato, S.; Mano, H.; Kumazawa, T.; Yoshizawa, Y.; Kojima, R.; Masushige, S. Effect of Retinoid Status on Alpha, Beta, and Gamma Retinoic Acid Receptors mRNA in Various Rat Tissues. *Biochem. J.* **1992**, *286*, 755-760.
130. Dawson, M. I.; Hobbs, P. D.; Derdzinski, K.; Chan, R. L.-S.; Gruber, J.; Chao, W.; Smith, S.; Thies, R. W.; Schiff, L. J. Conformationally Restricted Retinoids. *J. Med. Chem.* **1984**, *27*, 1516-1531.
131. Sparks, A. K. Solvent Effects in Aromatic Nitration. Nitration by Acyl Nitrates. *J. Org. Chem.* **1966**, *31*, 2299-2302.
132. Schroter, R. In Houben-Weyl, *Methoden der Organischen Chemie*, 4th Edition, Vol. X1, Muller, E., Ed., Georg Thieme Verlag: Stuttgart, 1957, pp. 422-436.
133. Owsley, D. C.; Bloomfield, J. J. The Reduction of Nitroarenes with Iron/Acetic Acid. *Synth. Comm.* **1977**, 118-120.
134. Kappe, J.; Ziegler, E. Modification of the Pechmann Reaction. *Org. Prep. Proc.* **1969**, *1*, 61-62.
135. Subramanian, S. Ph. D. Dissertation. Modified Heteroarotinoids: Potential Anti-Cancer Agents. Oklahoma State University, 1993.

136. Yli-Kauhahuoma, J. T.; Ashley, J. A.; Lo, C. H.; Tucker, L.; Wolfe, M. M.; Janda, K. D. Anti-Metallocene Antibodies: A New Approach to Enantioselective Catalysis of the Diels-Alder Reaction. *J. Am. Chem. Soc.* **1995**, *117*, 7041-7047.
137. Wolfe, S.; Godfrey, J. C.; Holdrege, C. T.; Perron, Y. G. Rearrangement of Penicillins to Anhydropenicillins. *Can. J. Chem.* **1968**, *46*, 2549-2559.
138. Barstow, L. E.; Hruby, V. J. A Simple Method for the Synthesis of Amides. *J. Org. Chem.* **1971**, *36*, 1305-1306.
139. (a) Wei, Z.-Y.; Brown, W.; Takasaki, B.; Plobeck, N.; Delorme, D.; Zhou, F.; Yang, H.; Jones, P.; Gawell, L.; Gagnon, H.; Schmidt, R.; Yue, S.-Y.; Walpole, C.; Payza, K.; St-Onge, S.; Labarre, M.; Godbout, C.; Jakob, A.; Butterworth, J.; Kamassah, A.; Morin, P.-E.; Pjean, D.; Ducharme, J.; Roberts, E. *N,N*-Diethyl-4-(phenylpiperidin-4-ylidenemethyl)benzamide: A Novel Exceptionally Selective, Potent δ Opioid Receptor Agonist with Oral Bioavailability and Its Analogues. *J. Med. Chem.* **2000**, *43*, 3895-3905. (b) Deady, L. W.; Kaye, A. J.; Finlay, G. J.; Baguley, B. C.; Denny, W. A. Synthesis and Antitumor Properties of *N*-[2-(Dimethylamino)ethyl]carboxamide Derivatives of Fused Tetracyclic Quinolines: A new Class of Putative Topoisomerase Inhibitors. *J. Med. Chem.* **1997**, *40*, 2040-2046. (c) Walter, M. Substituted Phenyl Esters of PGA2. (Upjohn Co., USA), U. S., 8 pp, US 4042606 19770816; *Chem. Abstr.* **1977**, *88*, 6404.
140. Galabov, B.; Vassilev, G.; Koleva, V.; Ilieva, M. Spectra and Conformations of Substituted Thioureas. *J. Mol. Struct.* **1982**, *82*, 35-41.
141. (a) Lindamood, III, C.; Dillehay, D. L.; Lamon, E. W.; Giles, H. D.; Shealy, Y. F.; Sani, B. P.; Hill, D. L. Toxicologic and Immunologic Evaluations of *N*-(All-*trans*-Retinoyl)-*d,l*-Leucine and *N*-(All-*trans*-Retinoyl)glycine. *Toxicol. Appl. Pharmacol.* **1988**, *96*, 279-295. (b) Lindamood, III, C.; Giles, H. D.; Hill, D. L. Preliminary Profile of Arotinoids SMR-2 and SMR-6 in Male B6D2F1 Mice. *Fundam. Appl. Toxicol.* **1987**, *8*, 517-530.
142. Kagechika, H.; Kawachi, E.; Hashimoto, Y.; Himi, T.; Shudo, K. Retinobenzoic Acids. 1. Structure-Activity Relationships of Aromatic Amides with Retinoidal Activity. *J. Med. Chem.* **1988**, *31*, 2182-2192.
143. Van de Waterbeemd, H.; Smith, D. A.; Beaumont, K.; Walker, D. K. Property-Based Design: Optimization of Drug Absorption and Pharmacokinetics. *J. Med. Chem.* **2001**, *44*, 1312-1333.
144. (a) Rouhi, A. M. Tuberculosis: A Tough Adversary. *Chem. Eng. News* **1999**, *77*, 52-69. (b) Dolin, P. J.; Raviglione, M. D.; Kochi, A. Global Tuberculosis Incident and Mortality During 1990-2000. *Bull. World Health Org.* **1994**, *72*, 213-220.

145. Li, R.; Sirawaraporn, R.; Chitnumsub, P.; Sirawaraporn, W.; Wooden, J.; Athappilly, F.; Turley, S.; Hol, W. G. Three-Dimensional Structure of *M. Tuberculosis* Dihydrofolate Reductase Reveals Opportunities for the Design of Novel Tuberculosis Drugs. *J. Biol. Chem.* **2000**, *295*, 307-323.
146. Nunn, P.; Kochi, A. A Deadly Duo – TB and AIDS. *World Health* **1993**, *46*, 7-8.
147. (a) Bass, J. B.; Farer, L. S.; Hopewell, P. C.; O'Brien, R.; Jacobs, R. F.; Ruben, F.; Dixie, E.; Snider, J.; Thornton, G. Treatment of Tuberculosis Infection in Adults and Children. *Am. J. Respir. Crit. Care Med.* **1994**, *149*, 1359-1374. (b) Bloom, B. R.; Murray, C. J. L. Tuberculosis: Commentary on a Reemergent Killer. *Science* **1992**, *257*, 1055-1064.
148. Nakahima, H. Tuberculosis: A Global Emergency. *World Health* **1993**, *46*, 3.
149. (a) Kuyper, L. F.; Baccanari, D. P.; Jones, M. L.; Huner, R. N.; Tansik, R. L.; Joyner, S. S.; Boytos, C. M.; Rudolph, S. K.; Knick, V.; Wilson, H. R.; Caddell, J. M.; Friedman, H. S.; Comley, J. C.; Stables, J. N. High-Affinity Inhibitors of Dihydrofolate Reductase: Antimicrobial and Anticancer Activities of 7,8-Dialkyl-1,3-diaminopyrrolo[3,2-*f*]quinazolines with Small Molecular Size. *J. Med. Chem.* **1996**, *39*, 892-903. (b) Blakeley, R. L. Eukaryotic Dihydrofolate Reductase. *Advan. Enzymol. Relat. Areas Mol. Biol.* **1995**, *70*, 23-102.
150. (a) Zuccotto, F.; Martin, A. C.; Laskowski, R. A.; Thornton, J. M.; Gilbert, I. H. Dihydrofolate Reductase: A Potential Drug Target in Trypanosomes and Leishmania. *J. Comput. Aided Mol. Des.* **1998**, *12*, 241-257. (b) Roth, B.; Stammers, D. K. Drug Interactions with Target Enzymes of Known Structure. In *The Design of Drugs to Macromolecular Targets*, Beddell, C. R.; Ed., Wiley: Chichester, 1992, pp 85-118.
151. Wiktor, S. Z.; Sassan-Morokro, M.; Grant, A. D.; Abouya, L.; Karon, J. M.; Marice, C.; Djomand, G.; Ackah, A.; Domoua, K.; Kadio, A.; Yapi, A.; Cobe, P.; Tossou, O.; Roels, T. H.; Lackritz, E. M. Efficacy of Trimethoprim-sulphamethoxazole Prophylaxis to Decrease Morbidity and Mortality in HIV-1-Infected Patients with Tuberculosis in Abijian Cote d'Ivoire: A Randomized Controlled Trial. *Lancet* **1999**, *353*, 1469-1475.
152. Schweitzer, B. I.; Dicker, A. P.; Bertino, J. R. Dihydrofolate Reductase as a Therapeutic Target. *FASEB J.* **1990**, *4*, 2441-2452.
153. Phetsuksiri, B.; Baulard, A. R.; Cooper, A. M.; Minnikin, D. E.; Douglas, J. D.; Besra, G. S.; Brennan, P. J. Antimycobacterial Activities of Isoxyl and New Derivatives Through the Inhibition of Mycolic Acid Synthesis. *Antimicrob. Agents Chemother.* **1999**, *43*, 1042-1051.

154. Nudelman, A.; Raphaeli, A. Novel Mutual Prodrug of Retinoic and Butyric Acids with Enhanced Anticancer Activity. *J. Med. Chem.* **2000**, *43*, 2962-2966.
155. Raphaeli, A.; Nordenberg, J.; Aviram, A.; Rabizadeh, E.; Zimrah, Y.; Nudelman, A.; Novogrodsky, A.; Shaklai, M. Butyrate Induced Differentiation in Leukemic Myeloid Cells in Vitro and in Vivo Studies. *Oncol. Rep.* **1994**, *1*, 481-487.
156. (a) Kruh, J. Effects of Sodium Butyrate, A New Pharmacological Agent, On Cells in Culture. *Mol. Cell. Biochem.* **1982**, *42*, 65-82. (b) Candido, E. P.; Reeves, R.; Davie, J. R. Sodium Butyrate Inhibits Histone Deacetylation in Cultured Cells. *Cell* **1978**, *14*, 105-113.
157. (a) Lin, R. J.; Nagy, L.; Inoue, S.; Shao, W.; Miller, W. H., Jr.; Evans, R. M. Role of Histone Deacetylase Complex in Acute Promyelocytic Leukemia. *Nature* **1998**, *39*, 811-814. (b) Fenrick, R.; Hiebert, S. W. Role of Histone Deacetylases in Acute Leukemia. *J. Cell. Biochem. Suppl.* **1998**, *30-31*, 194-202. (c) Wolffe, A. A Sinful Repression. *Nature* **1997**, *387*, 16-17.
158. (a) Warrell, R. P., Jr.; He, L. Z.; Richon, V.; Calleja, E.; Pandolfi, P. P. Therapeutic Targeting of Transcription in Acute Promyelocytic Leukemia by Use of an Inhibitor of Histone Deacetylase. *J. Natl. Cancer Inst.* **1999**, *90*, 1621-1625. (b) Grignani, F.; De Matteis, S.; Nervi, C.; Tomassoni, L.; Gelmetti, V.; Cioce Fanelli, M.; Ruthardt, M.; Ferrara, F. F.; Zamir, I.; Seiser, C.; Grignani, F.; Lazer, M. A.; Minucci, S.; Pelicci, P. G. Fusion Proteins of the Retinoic Acid Receptor- α Recruit Histone Deacetylase in Promyelocytic Leukemia. *Nature* **1998**, *391*, 815-816.
159. (a) Chen, T. A.; Allfrey, V. G. Rapid and Reversible Changes in Nucleosome Structure Accompany the Activation, Repression, and Superinduction of Murine Fibroblast Protooncogenes c-fos and c-myc. *Proc. Natl. Acad. Sci. U. S. A.* **1987**, *84*, 5252-5256. (b) Thorne, A. W.; Kmiecik, D. K.; Mitchelson, K.; Sautiere, P.; Crane-Robinson, C. Patterns of Histone Acetylation. *Eur. J. Biochem.* **1990**, *193*, 701-713.
160. Miller, A. A.; Kurschel, E.; Osieka, R.; Schmidt, C. Clinical Pharmacology of Sodium Butyrate in Patients with Acute Leukemia. *Eur. J. Cancer Clin. Oncol.* **1987**, *23*, 1283-1287.
161. Cologne, J.; Le Sech, E.; Marey, R. Recherches sur les Dihydrocoumarines et sur les Chromannes. *Bull. Soc. Chim. Fr.* **1957**, 776-779.
162. McClatchy, J. K. Antimycobacterial Drugs: Mechanism of Action, Drug Resistance, Susceptibility Testing, and Assay of Activity in Biological Fluids. In *Antibiotics in Laboratory Medicine*, Lorian, V.; Ed., The Williams and Wilkins Company: Baltimore, MD, 1986, pp 181-222.

2

VITA

Chad Wayne Brown

Candidate for the Degree of

Doctor of Philosophy

Thesis: HETEROAROTINOIDS WITH TWO- AND THREE-ATOM LINKERS
AS POTENTIAL ANTICANCER AGENTS

Major Field: Chemistry

Biographical:

Personal Data: Born in Ardmore, Oklahoma, on September 9, 1972, as the son of Glen D. and Holly J. Brown.

Education: Received primary education from Fox High School, Fox, Oklahoma, and received a Bachelor of Science degree from the University of Central Oklahoma, Edmond, Oklahoma, in December, 1996. Completed requirements for the Doctor of Philosophy degree at Oklahoma State University in August, 2001.

Experience: Teaching Assistant, Department of Chemistry, Oklahoma State University, January, 1997, through August, 1997; Graduate Research Assistant, Department of Chemistry, Oklahoma State University, September, 1997, to present.

Honors: Graduate Research Fellow in the NIH Biomedical Research Program, Department of Biochemistry and Molecular Biology, Oklahoma State University, September, 1997, through August, 1999; NIH MARC Fellow, September, 1999, to present.

Professional Memberships: American Chemical Society, Sigma Xi Scientific Research Society.